Series: TRENDS IN MECHANICS OF MATERIALS

OPTICAL BEAMS AT DIELECTRIC INTERFACES – fundamentals

WOJCIECH NASALSKI

IPPT PAN
Institute of Fundamental Technological Research
Polish Academy of Sciences

SERIES: TRENDS IN MECHANICS OF MATERIALS

OPTICAL BEAMS AT DIELECTRIC INTERFACES – fundamentals

Wojciech Nasalski

Institute of Fundamental Technological Research
Polish Academy of Sciences

➤ Institute of Fundamental Technological Research
Polish Academy of Sciences

Series: **TRENDS IN MECHANICS OF MATERIALS**

ISBN 978-83-89687-26-5

Contents

Preface

The content of this book presents a comprehensive review of my recent work on optical beams at dielectric interfaces. Some indication of results published on this topic by other authors the reader may find in the lists of references enclosed. The same concerns experimental verifications and possible applications of reflection and transmission of narrow beams at dielectric interfaces.

I have tried to be as rigorous as possible. However, when rigor might disturb clarity of the presentation, clarity has won out. The book is aimed at the level of the graduate or Ph.D. students in physics and electronics. It should also appeal to the wider audience of researches and engineers working within the range of optics. I hope that the material presented in this book will appear helpful for anyone who works on the theory or applications of various phenomena of optical beam interactions with planar dielectric interfaces and multilayers.

WOJCIECH NASALSKI

Warszawa, May 2007

CHAPTER 1

Introduction

Optical beam interactions with a planar dielectric interface, understood as the plane boundary between two semi-infinite dielectric media of different values of a refractive index, have been under continuing interests of many researches even since Newton's time. For incidence of narrow beams the reflected and refracted beams suffer from several distortions of their spatial shape. These beam distortions are commonly understood as geometrical modifications - the shifts or displacements - of the beams and these beam shifts have been primarily under intense studies in early research on the beam-interface interactions. Later on, it has been gradually recognised that the geometrical effects of beam reflection and transmission were accompanied by other effects, those related to amplitude, polarization and spatial distribution of intensity and phase of the incident beam.

The existence of a spatial shift at total internal reflection of an optical beam incident on a plane interface was suggested by Newton [1] in XVIII century on the grounds of his corpuscular theory. Two centuries later Pitch (1929) [2] reported results of his theoretical studies on energy flux inside evanescent waves caused by total internal reflection. He also predicted a lateral spatial shift of the reflected beam and related this shift with a finite transverse cross-section of the beam. The lateral shift was next experimentally observed in 1947 by Goos and Hänchen [3] and called after their names as the Goos-Hänchen shift. Analytical expressions for this shift were derived by Artmann in 1948 [4], on the grounds of a stationary-phase approach, and by Fragstein in 1949 [5], who used energy-flux conservation principles. These reports were followed by further publications on this topic of Schilling (1961) [6], Renard (1964) [7] and many others. Detailed

overview of early studies on this problem was published by Lotsch in a series of his papers in 1970 [8].

Reflected and refracted or transmitted beams are usually described by spatial changes of their field amplitude and polarization. The changes in the beam spatial structure and polarization are evaluated with respect to predictions of geometrical optics governed by the well-known Fresnel and Snell laws of plane wave reflection and refraction. They are known as effects of nonspecular reflection and refraction or as nonspecular effects of reflection and refraction. Essentially two basic approximate approaches have been primarily used in their evaluation - the first approach based on the stationary-phase arguments and the second one based on the energy-flux conservation arguments. More recently other, more accurate methods have been devised, based mainly on analytical beam field evaluation and mode expansion techniques.

The spatial changes in the beam field spatial distribution can be described up to the second-order approximation by real displacements of a beam internal coordinate frame and scaling of the beam coordinates dependent on a beam width. All of these spatial effects can be defined in two mutually orthogonal planes: the incidence plane that contains a beam axis and a normal to the interface, and the transverse plane, understood as the plane that contains a beam axis and is transverse to the incidence plane. In each of these two planes there are one lateral (transverse to the beam axis), one longitudinal (along the beam axis) and one angular (a change of the beam axis direction) displacements of the beam frame. In addition, there are also changes of a beam width in each of the two orthogonal planes. Moreover, each displacement is specific to one of two orthogonal states of beam polarization, say of the TM and TE type. Therefore one has sixteen parameters of beam geometrical reconfiguration, four for each of two orthogonal planes and for each of two orthogonal polarizations.

From all the nonspecular phenomena the longitudinal shifts of beams, that is the shifts observed in the incidence plane, are known the most. They were mainly analysed in the two-dimensional configuration, as they are common to two-dimensional and three-dimensional models of beams. Besides the Goos-Hänchen shift of a beam waist position along the axis orthogonal to the beam axis [1-9], the angular shift equal to the angle of rotation of the beam axis has

been found to exist by Ra, Bertoni, and Felsen in 1973 [10]. The beam focal shift, understood as the shift of a beam waist position along the beam axis, has been predicted by McGuirk, Carniglia and Brownstein in 1977 [11,12]. Studies on the nonspecular phenomena continued further [13-20] and, finally, the fourth effect, called the beam waist modification or the increment of a beam cross-section radius, has been reported by Tamir in 1986 [21]. It was also shown that the first three composite geometric longitudinal effects: the lateral, focal and angular beam shifts, contribute together to the net longitudinal shift of the beam in the interface plane [22-24].

The lateral shifts have been commonly considered in two-dimensional configurations, where the beam field and the reflecting/transmitting structure were assumed to be independent of the coordinate transverse to the incidence plane of the beam. However, the transverse shifts, that is the shifts observed in the plane transverse to the incidence plane, disappear in two-dimensional approximate models of beams. These shifts are specific only to real three-dimensional beams and as such they have been analysed in the three-dimensional configurations. Among these effects the transverse lateral shift has been predicted first by Fedorov in 1955 [25] and experimentally confirmed by Imbert in 1972 [26], who also derived pertinent analytical expressions and compared them with previous theoretical predictions of Costa de Beauregard (1965) [27], Schilling (1965) [28] and Ricard (1970) [29]. Next studies treated the three-dimensional beams in detail, with their profiles displaced by both, transverse and longitudinal, shifts at the same time [30-34]. In general, besides some special cases like that of the beam TM or TE polarization, both types, longitudinal and transverse, geometrical nonspecular effects exist together for three-dimensional narrow beam reflection and transmission.

In spite of the geometrical parameters of the longitudinal and transverse beam spatial deformations, other four additional parameters on the beam reflection and transmission problem also exist for arbitrary beam polarization (Nasalski (1989) [35]). Two of them are attributed to changes of beam complex on-axis amplitude and the next two are attributed to changes of beam polarization. It was shown that the amplitude modifications could be quite strong, especially at layered structures [36]. The longitudinal and transverse nonspecular effects of the geometrical, amplitude and polarization

type exist in general altogether during reflection and transmission of narrow beams. Therefore, for interactions of three-dimensional beams with the interface, one has to consider at least twenty independent parameters of the nonspecular beam deformations for arbitrary beam shape and polarization, and for arbitrary type of the interface, including interfaces composed of nonlinear or inhomogeneous media (Nasalski (1996) [37]).

All these parameters depend on the spatial structure of the beam incident upon the interface, mainly on the beam width and direction of an incident beam axis with respect to the normal to the interface. In addition, they depend on the polarization state of the incident beam. They depend also on parameters characteristic of the two media of which the interface is composed; for instance, on dielectric contrast in the simplest case of the two lossless, isotropic, linear media [37-39] and, in addition, on the strength of a nonlinear coefficient in nonlinear media of Kerr type [40-43]. Theoretical predictions of the nonspecular effects and beam deformations have been subsequently followed by advanced experimental measurements [26], [31] and [44-54].

Still, the story on enumerating the parameters of the beam-interface interactions does not seem to be finished yet. The above list of the parameters may be regarded as complete only under the fundamental assumption, common for paraxial beams propagating in free space, according to which their amplitude spatial distribution can be treated independently of their (transversely uniform) polarization. However, the polarization of beams of finite cross-section can be considered as transversely uniform only approximately and even this approximation does not seem to be always justified in vicinity of singular points of the beam field.

The separation of the beam amplitude distribution from the beam polarization is not valid at medium discontinuities like the interface is in the first place. Therefore, for singular points of the beam field, the amplitude-polarization coupling may become dominant over other effects of nonspecular reflection and transmission, especially for very narrow (nonparaxial) beams of diameter comparable with a beam field wavelength or less. Recently, however, the beams with singularities present in their field-amplitude spatial distribution, for example in a form of optical vortices, are now in frontiers of optical research [55,56]. Considering temporal variations of optical wave packets and, in addition, their partial coherence, instead of

relatively simpler cases of monochromatic or quasi-monochromatic beams, complicates the problem under consideration even further.

The author does not intend to go too far with relaxing approximations convenient for analysis presented in this book. Thus, the beams are considered monochromatic or completely coherent with their polarization being spatially uniform in any transverse plane of the beam. Moreover, numerical simulations presented will not go below the one-wavelength limit in the incident-beam cross-section diameter. Still the beams of this limiting width are very close to the range of nonparaxial beams. That makes problems concerning convergence and accuracy of numerical procedures rather demanding.

In the beam field evaluation, the results of which are presented in this book, the field is expressed first in spectral domain as a composition of plane waves. Two complex quantities called the complex lateral and focal shifts [11,12,18,21] are defined, real and imaginary parts of which correspond to the geometrical effects of nonspecular reflection and refraction. Next, the results are converted analytically into configuration domain, where a beam coordinate frame, together with their on-axis complex amplitude and polarization parameter, are redefined [24,37]. Note that the beam shifts obtained in the configuration domain are of finite values for all angles of incidence. A number of beam field representations, leading to this otherwise rather obvious feature of beam reflection and refraction, have been devised and discussed in the past [9,20,23,24].

The theoretical approach to the beam-interface interactions presented in the book basically employs the plane wave (spectral) decomposition of the beam field and in this respect corresponds to the earlier approach proposed by Schilling (1965) [28]. Other approaches based on application of conservation principles [5,26,29,57], entropy of optical systems [58] or methods of moments [59], geometrical optics [60] and quantum mechanics [61] are outside the scope of this book. Most numerical procedures applied here have rather a semi-analytical character and have been devised by the author especially for treatment of narrow, three-dimensional beams at linear and nonlinear interfaces. The methods start with parameterisation of beam field distribution and next, with beam parameters evaluated, mimic dynamics of beam

field rearrangements during beam propagation and interactions with planar interfaces.

One method, known as the method of Monotonic Iteration of Gaussians (MIG) [40-41], iterates the beam field distribution at the interface using the nonspecular effects evaluated in subsequent steps of the iteration. The MIG method has been devised primarily to treat three-dimensional reflection and refraction nonlinear problems [40-43] and generalises previous author's work on the two-dimensional linear problems of the same type [24]. The second semi-analytical method, called the scaled complex ray tracing (SCRT) [62], has been devised especially for treatment of the beam propagation in nonlinear media. The SCRT method converts a nonlinear propagation problem into a problem of linear propagation, augmented by specified evolution of beam parameters.

Effects of beam field rearrangements, similar to the effects of nonspecular reflection or transmission, are observed during beam propagation in nonlinear media of Kerr type [62-64]. These effects, called as aberrationless effects of nonlinear propagation [63], have been derived analytically within parabolic approximation to the nonlinear Schrödinger equation (NLSE). They can be described in terms of beam parameters like: a beam waist position, beam radius and phase front curvature, a beam on-axis complex amplitude and a nonlinearly modified wave number of a beam field. All of them evolve along the propagation distance of the beam.

Within the SCRT method the problem of beam propagation in nonlinear or inhomogeneous media is reformulated into the problem of linear propagation, with the help of an appropriate parabolic approximation to the wave equation and analytical scaling of the beam parameters. The aberrationless effects of the beam-field-distribution rearrangements in nonlinear media result in inhomogeneous distribution of the medium dielectric permittivity. Therefore, in general, the SCRT method [62-64], together with the MIG method [40-43], can be directly applied as well in analysing the problems of beam propagation in inhomogeneous media.

It is pertinent to note that, recently, a method of collective variables (CVs) has been developed to treat pulse nonlinear propagation in dispersion-managed fibres (cf. Refs. [65-67] and references therein). It appears that there is a

close analogy between the pulse parameters considered within the CVs method in temporal domain and the beam parameters analysed within the SCRT method in spatial domain. In fact, the SCRT method has been devised in a form suitable for treatment of monochromatic, one- two- or three-dimensional beams, as well as polychromatic, two-, three- or four-dimensional wave packets in one unified manner.

Note also that the MIG and SCRT methods have been devised primarily to treat beams within the range of paraxial optics. Their results coincide in this range with results of a separate numerical method based on direct integration of the Maxwell equations [68] and with other available numerical data [39,69]. However, the MIG and SCRT methods provide also quite accurate results even for really narrow beams of their transverse radii of the order of one wavelength.

The intention of writing this book is to put the results concerning the beam-interface interactions, recently reported by the author elsewhere [70-74], in one comprehensive publication, and to discuss main features of these interactions in some appropriate order. After a brief introduction into basic definitions of first-order optics given in Chapter 2, next five chapters of this book treat, in some convenient to the reader sequence, several aspects of the problem of three-dimensional beams reflected or refracted at dielectric interfaces. The beam geometrical displacements, the beam amplitude distribution and polarization changes, the cross-polarization coupling between beam components of opposite polarization, as well as effects of vector beam mode switching at linear and nonlinear interfaces and multilayers, will be described and discussed in detail.

Chapters 3-7 follow almost chronologically, somewhere with substantial extensions, author's latest main publications [71], [70] and [72-74] in this field. All chapters are written in a self-contained manner, with the content, notation and references of the respective publications preserved. The beams are considered as three-dimensional with arbitrary polarization and the problem under consideration is inherently of vector nature. This implies that the beam characteristics presented differ substantially from those specific for two-dimensional beams of linear (TM or TE) polarization. The beam-interface characteristics of the two-dimensional scalar case have been already summarised by the author in the past [42].

Introduction into the formalism of first-order optics is given in Chapter 2. Basic definitions, necessary to interpret optical phenomena involving coherent paraxial beams are presented. A link between concepts of optical rays and ray-transfer matrices on the one hand and canonical integral transforms and Lorentz transformations on the other hand is shown. The formalism presented is limited to homogeneous optical transformations because, to the best of the author's knowledge, the formalism of inhomogeneous transformations still is not available in a finite, self-contained and concise form. Although the beam-interface interactions belong to the range of the inhomogeneous first-order optics, the inhomogeneous phenomena that occur at dielectric interfaces are usually, although probably not always, small enough to interpret them as small corrections to the formalism of homogeneous first-order optics. Some other technical issues, which also may provide connections with next chapters of this book, are discussed in comments and conclusions of this chapter.

In Chapter 3, three-dimensional beams reflected at the interface are considered in their general form, with arbitrary transverse distribution of their intensity, phase and polarization [71]. The interface is assumed to be planar and composed of two linear media although some basic results that pertain to nonlinear interfaces are also given. Complex amplitude distribution of the beam field is assumed as being factorised into two spatially orthogonal factors. Roles of paraxial approximation, cross-dimensional coupling and cross-polarization coupling in the beam description are discussed. Analytical expressions for all the first-order and the second-order, longitudinal and transverse, nonspecular effects are derived. Results of their numerical evaluation are given for beam incidence close to the critical incidence of total internal reflection.

It is shown that the transverse effects exist even for linear-diagonal polarization. Expressions showing the symmetry that occurs between linear and circular polarization of beams and transverse lateral and angular displacements of beams are analytically derived. A possibility to achieve a bistable switch of beams at a nonlinear interface is discussed and numerically confirmed, the fact that was unclear or even disputed previously. The interesting problem of the cross-polarization coupling between the beam components of opposite polarization risen in Section 5 has been further under investigation in [49,68,74]. It will be also explicitly shown in Chapter 7 how

this coupling interrelates the beam field distribution in its magnitude and phase and the beam polarization state.

In Chapter 4, a detailed description of the method of treatments beam fields at nonlinear interfaces is presented [70]. A special case of the nonlinear-linear interface with medium nonlinearity of the Kerr local type is analysed. The reduced variational technique is applied that converts a system of nonlinear Schrödinger equations into a system of ordinary differential equations. The beam deformations are described by aberrationless effects of nonlinear propagation and nonspecular effects of reflection. Analytical expressions of these effects are derived and numerical simulations of their rearrangements during the beam-interface interactions are given. It is shown that, for certain sets of incident beam and interface parameters, a bistable switch of the reflected beam is possible to achieve. Characteristic features of this switch appear different from those of plane wave reflection. In the Appendix, a concise summary of the complex ray tracing the nonlinear propagation of a single Gaussian beam is also given. Results of the analysis presented in this chapter confirms, contrary to common opinions on this problem, that the bistable switching of the nonlinear interface could, at least in principle, be obtained by incidence of a single beam.

Definitions of beam amplitude and beam polarization are discussed in Chapter 5 [72]. In this context new definitions of the nonspecular effects of beam reflection and transmission are also introduced. The problem is formulated and solved in such a manner that the beams are obtained with uniquely defined uniform spatial displacements of their axes in a spatial domain and angular displacements of their spectral components in a spectral domain. It is shown that additional modifications of the beam polarization state remain non-uniform throughout the entire beam spectrum, although they are generally rather small. A special role of beam polarization states of linear-diagonal and circular-diagonal types is indicated. The results of this chapter are confronted with results of different approaches presented in this context in the past. The role of beam on-axis phase in the beam field evaluation in this context is indicated.

In Chapter 6, the problem of beam interactions with a single planar discontinuity of the medium is generalised to the case of a planar layered medium [73]. The problem is formulated and solved analytically. Transmis-

sion and reflection matrices are rederived in beam reference frames dependent on a polarization state of the incident beam. Spinor representations of two-by-two polarization matrices, Jones two-vectors and Stokes four-vectors are defined. Scattering and transfer matrices of the layered structure are given with the help of Stokes reciprocity relations for incidence of beams of arbitrary polarization. Factorisation of these matrices results in scalar complex transformations separately for beam polarization and for beam amplitudes. While the transformations of beam polarization describe multilayer action in terms of Lorentz transformations, the amplitude transformations yield spatial beam shaping. Therefore scattering vector problems of three-dimensional beams at multilayers, as well as at a single interface, resolve into two independent transformations of two scalar parameters.

In Chapter 7, an exact description of spatial versus polarization characteristic interrelations of optical beam fields at a planar isotropic interface is given [74]. Three-dimensional monochromatic beams of uniform polarization interacting with a planar boundary between two homogeneous, isotropic and lossless media are analysed in the most general, exact manner. Generalised Fresnel transmission and reflection coefficients for beam spectra are derived. Interrelations induced by cross-polarization coupling between beam profile and phase and beam polarization, or between spin and orbital angular momentum of beams, are derived for normal incidence of the beams. In this case the analysis directly indicates that these interelations exist independently of the beam nonspecular shifts.

It is shown that Hermite-Gaussian beams of linear polarization and Laguerre-Gaussian beams of circular polarization, all projected at the interface and in their complex-valued or elegant version, may be considered as normal modes at this interface. Their creation and annihilation are shown, with total angular momentum being conserved on the total beam field and single photon levels. That results in the beam amplitude-sensitive rearrangements of beam polarization and in the polarization-sensitive rearrangements of beam amplitude spatial distribution even at the plain isotropic interface [74]. In the final appendix of this book, basic relations for the beam shifts at the dielectric interface are collected together and commented.

Let me finally mention on some possible applications of the theory presented in this book. The dielectric interface, or, in general, any planar multi-

layered structure, can be used, for example, as a mean of control the interplay between the beam field distribution, in its magnitude and phase, and the beam field polarization. The control process is based on the cross-polarizarion coupling (XPC) effect acting at the interface [71] and depends on the incident beam parameters like the beam polarization, shape and angle of incidence [49,68,74]. The ability to control the beam shape and polarization may appear useful in many applications in contemporary optics.

In three-dimensional optical imaging the polarimetric passive imaging systems are used to extract three-dimensional information from an object scene. The three-dimensional imaging can be achieved by computing orientation angles of normal vectors of the light-reflecting surface. Values of these angles can be retrieved from Stokes vector parameters of the reflected optical field with the help of the well-known Fresnel equations and Snell's law [75]. The imaging process depends considerably on shape and polarization of the illuminating beam, especially when the elements of the object scene are of a nanometric scale.

In nanoscopic space-time-resolved spectroscopy polarization pulse shaping can be used to control spatial and temporal evolution of optical near field. By appropriate control of two polarization components of an incident femtosecond laser wave-packet, pump and probe excitation occur at different positions and at different times, with nanometer spatial and femtosecond temporal resolution [76]. Narrow or focussed beams are commonly used to trap dielectric or metallic particles in optical tweezers [77,78]. The corresponding field distribution generates a trapping potential, strongly influenced by, for example, a metal nanostructure located in the vicinity of a focus of the beam [79]. In such a trapping configuration the superposition of a non-resonant beam field with a resonant beam or plane wave illumination provides the possibility to modify the trapping potential. The processes of this sort strongly depend on distribution of the optical field intensity, phase and polarization [80,81].

It is well-known that light beams carry, besides the spin angular momentum (SAM) associated with beam polarization, the well-defined orbital angular momentum (OAM) associated with their spiral wave fronts [55]. Both parts of the beam angular momentum can be used to cause trapped particles to rotate [82]. Moreover, as it has been shown here for beam

reflection and transmission, exact relations induced by the XPC effect exist between these two parts of the beam angular momentum at the interface. Both of them can be used in the planar configuration for beam sorting on the basis of SAM and OAM, per analogy to the known methods of encoding and processing optical information that is carried by individual photons [83-85].

It seems that coexistence of the XPC effect with the beam shifts of nonspecular reflection can be also observed for beam fields in optical resonators. Meanwhile the XPC effect determines a transverse pattern of the beam field in an optical cavity the beam shifts should enter into the resonance condition for beam eigenmodes of this cavity. This type of interplay between polarization and shape of nonspecularly reflected beam fields in an optical resonator has been recently reported for the case of a dome cavity [86].

Having in mind the applications mentioned above, as well as many others reported elsewhere, interactions of optical beams with dielectric interfaces are analysed in this book.

References

[1] I. Newton, *Opticks*, fourth edition (London, 1730; republished by Dover, New York, 1952).

[2] J. Picht, "Beitrag zur Theorie der Totalreflexion", Ann. Phys. Leipzig **5**, 433-496 (1929).

[3] F. Goos and H. Hänchen, "Ein neuer and fundamentaler Versuch zur Totalreflexion", Ann. Phys. (Leipzig) **1**, 333-345 (1947).

[4] K. V. Artmann, "Berechnung der Seitenversetzung des totalreflektierten Strahles", Ann. Phys. Leipzig **2**, 87-102 (1948).

[5] C. Fragstein, "Zur Seitenversetzung des totalreflektierten Lichstrahles", Ann. Phys. Leipzig **4**, 271-278 (1949).

[6] H. Schilling, "Die Reflexion von ebenen Wellen und von Kugelwellen an der Trennebene zwischen absorbierenden Medien", Wiss. Zeitschr. TH Magdeburg **4**, 461-473 (1961).

[7] R. H. Renard, "Total reflection: a new evaluation of the Goos-Hänchen shift", J. Opt. Soc. Am. **54**, 1190-1197 (1964).

[8] H. K. V. Lotsch, "Beam displacement at total reflection: The Goos-Hänchen effect", Part I – Part IV, Optic (Stuttgart) **32**, 116-137 (1970); ibid. **32**, 189-204 (1970); ibid. **32**, 299-319 (1970); ibid. **32**, 553-569 (1970).

[9] B. R. Horowitz and T. Tamir, "Lateral displacement of a light beam at dielectric interface", J. Opt. Soc. Am. **61**, 586-594 (1971).

[10] J. W. Ra, H. L. Bertoni, and L. B. Felsen, "Reflection and transmission of beams at a dielectric interface", SIAM J. Appl. Math. **24**, 396-413 (1973).

[11] M. McGuirk and C. K. Carniglia, "An angular spectrum representation approach to the Goos-Hänchen shift", J. Opt. Soc. Am. **67**, 103-107 (1977).

[12] C. K. Carniglia and K. R. Brownstein, "Focal shift and ray model for total internal reflection", J. Opt. Soc. Am. **67**, 121-122 (1977).

[13] Y. M. Antar and W. M. Boerner, "Gaussian beam interaction with a planar dielectric interface", Can. J. Phys. **52**, 962-972 (1974).

[14] I. A. White, A. W. Snyder, and C. Pask, "Directional change of beams undergoing partial reflection", J. Opt. Soc. Am. **67**, 703-705 (1977).

[15] S. Kozaki and H. Sakurai, "Characteristics of a Gaussian Beam at a dielectric interface", J. Opt. Soc. Am. **68**, 508-514 (1978).

[16] C. W. Hsue and T. Tamir, "Lateral displacement and distortion of beams incident upon a transmitting-layer configuration", J. Opt. Soc. Am. A **2**, 978-987 (1985).

[17] C. C. Chan and T. Tamir, "Angular shift of a Gaussian beam reflected near the Brewster angle", Opt. Lett. **10**, 378-380 (1985).

[18] R. P. Riesz and R. Simon, "Reflection of a Gaussian beam at a dielectric slab", J. Opt. Soc. Am., A **2**, 1809-1817 (1985)

[19] A. Puri and J. L. Birman, "Goos-Hänchen beam shift at total internal reflection with application to spatially dispersive media", J. Opt. Soc. Am. A **3**, 543-549 (1986).

[20] H. M. Lai, F. C. Cheng, and W. E. Tang, "Goos-Hänchen effect around and on the critical angle", J. Opt. Soc. Am. A, **3**, 550-557 (1986).

[21] T. Tamir, "Nonspecular phenomena in beam fields reflected by multilayered media", J, Opt. Soc. Am. A **3**, 558-565 (1986).

[22] W. Nasalski and T. Tamir, "Composite beam-shifting effects under critical reflection conditions", J. Opt. Soc. Am. A **3**, P124 (1986).

[23] C. C. Chan and T. Tamir, "Beam phenomena at and near critical incidence upon dielectric interface", J. Opt. Soc. Am. A **4**, 655-663 (1987).

[24] W. Nasalski, T. Tamir and L. Lin, "Displacement of the intensity peak in narrow beams reflected at a dielectric interface", J. Opt. Soc. Am. A **5**, 132-140 (1988).

[25] F. I. Fedorov, "K teorii polnovo otrazenija". Dokl. Akad. Nauk SSSR **105**, 465-467 (1955).

[26] C. Imbert, "Calculation and experimental proof of the transverse shift induced by total internal reflection of a circularly polarized light beam", Phys. Rev. D **5**, 787-796 (1972).

[27] O. Costa de Beauregard, "Translational internal spin effect with photons", Phys. Rev. **139**, B1443-B1446 (1965).

[28] H. Schilling, “Die Strahlversetzung bei dei Reflexion linear oder elliptisch polarisierten ebenen Wellen an der Trennebene zwischen absobierenden Medien” Ann. Physik, **7**, 122-134 (1965).

[29] J. Ricard, “Courbes de flux d'énergie de l'onde évanescente et nouvelle explication du déplacement d'un faisceau lumineux dans la réflexion totale,” Nouv. Rev. Opt. **1**, 275-286 (1970).

[30] O. Costa de Beauregard and C. Imbert, “Quantized longitudinal and transverse shifts associated with total internal reflection”, Phys. Rev. D **7**, 3555-3563 (1972).

[31] J. J. Covan and B. Anicin, Longitudinal and transverse displacements of a bounded microwave beam at total internal reflection”, J. Opt. Soc. Am. **67**, 1307-1314 (1977).

[32] J. P. Hugonin and R. Petit, “Étude générale des déplacements à la réflexion totale”, J. Optics (Paris), **8**, 73-87 (1977).

[33] R. G. Turner, “Shifts of coherent light beams on reflection at plane interfaces between isotropic media”, Aust. J. Phys. **33**, 319-335 (1980).

[34] J.-J. Greffet and C. Baylard, “Nonspecular astigmatic reflection of a 3D gaussian beam on an interface”, Opt. Commun. **93**, 271-276 (1992).

[35] W. Nasalski, "Modified reflectance and geometrical deformations of Gaussian beams at a dielectric interface", J. Opt. Soc. Am. A **6**, 1447-1454 (1989).

[36] F. Falco and T. Tamir, “Improved analysis of nonspecular phenomena in beams reflected from stratified media”, J. Opt. Soc. Am. A **7**, 185-190 (1990).

[37] W. Nasalski, "Longitudinal and transverse effects of nonspecular reflection", J. Opt. Soc. Am. A, **13**, 172-181 (1996).

[38] N. Bonomo and R. A. Depine, “Nonspecular reflection of ordinary and extraordinary beams in uniaxial media”, J. Opt. Soc. Am. A **14**, 3402-3409 (1997).

[39] F. I. Baida, D. Van Labeke, and J.-M. Vigoureux, “Numerical study of the displacement of a three-dimensional Gaussian beam transmitted at total internal reflection. Near-field applications”, J. Opt. Soc. Am. A **17**, 858-866 (2000).

[40] W. Nasalski, “Nonspecular reflection by an electro-optically driven nonlinear interface”, Proc. The 1989 URSI International Symposium on EM Theory, 219-221 (1989).

[41] W. Nasalski, "Nonspecular bistability versus diffraction at nonlinear hybrid interfaces", Optics Commun. **77**, 443-450 (1990).

[42] W. Nasalski, *Nonspecular reflection of electromagnetic field at a dielectric interface* (in Polish), Habilitation Thesis, IFTR Reports **32** (IFTR PAS, Warsaw, 1990).

[43] W. Nasalski, “Nonspecular bistability at a delocalized nonlinear interface”, J. Modern Optics **44**, 1355-1372 (1997).

[44] L. Dutriaux, A. Le Floch, and F. Bretenaker, „Goos-Hänchen effect in the dynamics of laser eigenstates”, J. Opt. Soc. Am. B **9**, 2283-2289 (1992).

[45] E. Pfleghaar, A. Marseille, and A. Weis, „Quantitative investigation of the effect of resonant absorbers on the Goos- Hänchen shift”, Phys. Rev. Lett. **70**, 2281- 2284 (1993).

[46] L. Lévesque and B. E. Paton, „Light switching in a glass-AG-polymer structure using attenuated total reflection (ATR)”, Can, J. Phys. **72**, 651-657 (1994).

[47] B. M. Jost, A-A. R. Al-Rashed, and B. E. A. Saleh, „Observation of the Goos-Hänchen effect in a phase-conjugate mirror”, Phys. Rev. Lett. **81** 2233-2235 (1998).

[48] A. Haibel, G. Nimtz, and A. A. Stahlhofen, “Frustrated total reflection: The double-prism revisited”, Phys. Rev. E **63**, 047601-1-3 (2001).

[49] A. Köházi-Kis, „Cross-polarization effects of light beams at interfaces of isotropic media”, Opt. Commun. **253**, 28-37 (2005).

[50] R. Dasgupta, P. K. Gupta, „ Experimental observation of spin-independent transverse shift of the centre of gravity of a reflected Laguerre-Gaussian light beam”, Opt. Commun. **257**, 91-96 (2006).

[51] D. Müller, D. Tharanga, A. A. Stahlhofen and G. Nimtz, „Nonspecular shift of microwaves in partial reflection”, Europhys. Lett., **73**, 526-532 (2006).

[52] V. Delaubert, N. Treps, C. C. Harb, P. K. Lam, and H.-A. Bachor, „Quantum measurements of spatial conjugate variables: displacement and tilt of a Gaussian beam", Opt. Lett. **31**, 1537-1539 (2006).

[53] H. Okuda and H. Sasada, „Huge transverse deformation in nonspecular reflection of a light beam possessing orbital angular momentum near critical incidence", Opt. Express **14**, 8393-8402 (2006).

[54] X. Yin, L. Hesselink, H. Chin, and D. A. B. Miller, „Temporal and spectral nonspecularities in reflection at surface plasmon resonance", Appl. Phys. Lett. **89**, 041102-1-3 (2006).

[55] L. Allen, M. J. Padgett and M. Babiker, "The orbital angular momentum of light", Progress in Optics **39**, 291-372 (1999).

[56] M. S. Soskin and M. V. Vasnetsov, "Singular optics", Progress in Optics **42**, 220-276 (2001).

[57] V. G. Fedoseyev, "Energy motion on total internal reflection of an electromagnetic wave packet", J. Opt. Soc. Am. A **3**, 826-829 (1986).

[58] M. Lehman, "An entropic foundation of the angular change in the reflected beam from a planar interface", Optik **107**, 73-78 (1997).

[59] M. A. Porras, "Nonspecular reflection of general light beams at a dielectric interface", Optics Commun. **135**, 369-377 (1997).

[60] M. Onoda, S. Murakami, and N. Nagaosa, "Hall effect of light", Phys. Rev. Lett. **93**, 083901-1-4 (2004).

[61] M. T. L. Hsu, W. P. Bowen, N. Treps, and P. K. Lam, "Continuous-variable spatial entaglement for bright optical beams", Phys. Rev. A **72**, 013802-1-7 (2005).

[62] W. Nasalski, "Complex ray tracing of nonlinear propagation", Opt. Commun. **119**, 218-226 (1995).

[63] W. Nasalski, "Aberrationless effects of nonlinear propagation", J. Opt. Soc. Am. B **13**, 1736-1747 (1996).

[64] W. Nasalski, "Scale formulation of first-order nonlinear optics", Opt. Commun. **137**, 107-112 (1997).

[65] P. T. Dinda, A. B. Moubissi and K. Nakkeeran, "A collective variable approach for dispersion-managed solitons", J. Phys. A: Math. Gen. **34**, L103-L110 (2001).

[66] P. K. A. Wai, K. Nakkeeran, "On the uniqueness of Gaussian ansatz parameters equations: generalized projection operator method", Phys. Lett. A **332**, 239-243 (2004).

[67] S. I. Fewo, J. Atangana, A. Kenfack-Jiotsa, T. C. Kofane, "Dispersion-managed solitons in the cubic complex Ginzburg-Landau equation as perturbations of nonlinear Schrödinger equation", Opt. Commun. **252**, 138-149 (2005).

[68] W. Nasalski and Y. Pagani, "Excitation and cancellation of higher-order beam modes at isotropic interfaces", J. Opt. A: Pure Appl. Opt. **8**, 21-29 (2006).

[69] F. I. Baida, D. Van Labeke, and J.-M. Vigoureux, "Near-field surface plasmon microscopy: A numerical study of plasmon excitation, propagation and edge interaction using a three-dimensional Gaussian beam", Phys. Rev. B **60**, 7812-78-15 (1999).

[70] W. Nasalski, "Modelling of beam reflection at a nonlinear-linear interface", J. Opt. A: Pure Appl. Opt. **2**, 433-441 (2000).

[71] W. Nasalski, "Three-dimensional beam reflection at dielectric interfaces", Opt. Commun. **197**, 217-233 (2001).

[72] W. Nasalski, "Amplitude-polarization representation of three-dimensional beams at a dielectric interface", J. Opt. A: Pure Appl. Opt. **5**, 128-136 (2003).

[73] W. Nasalski, "Three-dimensional beam scattering at multilayers: formulation of the problem", J. Tech. Phys. **45**, 121-139 (2004).

[74] W. Nasalski, "Polarization versus spatial characteristics of optical beams at a planar isotropic interface", Phys. Rev. E **74**, 056613-1-16 (2006).

[75] F. A. Sadjadi, " Passive three-dimensional imaging using polarimetric diversity", Opt. Lett. **32**, 229-231 (2007).

[76] T. Brixner, F. J. García de Abajo, J. Schneider, and W. Pfeiffer, "Nanoscopic ultrafast space-time-resolved spectroscopy", Phys. Rev. Lett. **95**, 093901-1-4 (2005).

[77] L. Novotny, R. X. Bian, and X. S. Xie, “Theory of nanometric optical tweezers”, Phys. Rev. Lett. **79**, 645-648 (1997).

[78] G. Volpe, R. Quidant, G. Badenes, and D. Petrov, “Surface plasmon radiation forces”, Phys. Rev. Lett. **96**, 238101-1-4 (2006).

[79] P. C. Chaumet, A. Rahmani, and M. Nieto-Vesperinas, “Optical trapping and manipulation of nano-objects with an apertureless probe”, Phys. Rev. Lett. **88**, 123601-1-4 (2002).

[80] A. S. Zelenina, R. Quidant, and G. Badenes, “ Tunable optical sorting and manipulation of nanoparticles via plasmon excitation”, Opt. Lett. **31**, 2054-2056 (2006).

[81] F. J. García de Abajo, T. Brixner, and W. Pfeiffer, “Nanoscale force manipulation in the vicinity of a metal nanostructure”, J. Phys. B: At. Mol. Opt. Phys. **40**, S249-258 (2007).

[82] M. E. Friese, J. Enger, H. Rubinsztein-Dunlop, and N. R. Heckenberg, “ Optical angular-momentum transfer to trapped absorbing particles”, Phys. Rev. A **54**, 1593-1596 (1996).

[83] G. Molina-Terriza, J. P. Torres, and L. Torner, “Management of the angular momentum of light: preparation of photons in multidimensional vector states of angular momentum”, Phys. Rev. Lett. **88**, 013601-1-4 (2002).

[84] A. Vaziri, G. Weihs, and A. Zeilinger, “Experimental two-photon, three-dimensional entanglement for quantum communication”, Phys. Rev. Lett. **89**, 240401-1-4 (2002).

[85] J. Leach, J. Courtial, K. Skeldon, S. M. Barnett, S. Franke-Arnold, and M. J. Padgett, “Interferometric methods to measure orbital and spin, or the total angular momentum of a single photon”, Phys. Rev. Lett. **92**, 013601-1-4 (2004).

[86] D. H. Foster, A. K. Cook, and J. U. Nöckel, “Goos-Hänchen induced vector eigenmodes in a dome cavity”, Opt. Lett. **32**, 1764-1766 (2007).

CHAPTER 2

Basic framework of first-order optics

This chapter provides a brief overview of basic definitions of first-order optics concerning propagation of three-dimensional paraxial beams in centred optical systems. Parallel descriptions of beam propagation in terms of ray-transfer matrices and canonical transforms of optical systems are outlined. Relations between transformations of amplitude and polarization of beam fields and homogeneous Lorentz transformations are shown. The formalism presented yields basic framework within which the beam-interface interactions will be analysed in next chapters.

2.1 Introduction

Any optical system acts on amplitude and polarization of beams propagating through this system. When the system is of first-order type and the beams are treated approximately as paraxial of uniform polarization in their transverse planes, then the transformations of beam amplitude and beam polarization can be treated independently. The analysis of beam propagation phenomena usually employs expansions of the beam amplitude distribution in terms of Hermite-Gaussian or Laguerre-Gaussian functions on the one hand and Jones vectors, polarization matrices and Stokes parameters of the beam polarization on the other hand. Transformations of the beam amplitude can be expressed by ray-transfer symplectic matrices or, equivalently, in terms of linear canonical transformations and integral transforms associated with them. Similarly, unimodular Jones matrices represent linear transforma-

tions of polarization states of beams. Basic content of this formalism will be outlined in this chapter.

There are a number of textbooks devoted to certain aspects of, linear and nonlinear, first-order optics. A few examples of them [1-12] can be found in the reference list enclosed to this chapter. However, the sequence of definitions given below follows rather the approach that has been gradually developed in several separate publications [13-28] over a few last decades and has not been commonly regarded as a unified formalism of first-order optics yet. The formalism translates the conventional description of optical transformations in terms of rays and matrices [13-15] into the language of canonical operator transforms and homogeneous Lorentz transformations [16-28]. The set of definitions given in this introductory chapter should be regarded only as a short guide through fundamentals of first-order optics. Most equations will be given without proofs and mathematical details. The material presented may serve as a convenient self-contained theoretical tool for interpretation of several aspects of beam propagation in first-order optical systems.

2.2 Paraxial wave equation

First-order optical systems are understood as optical systems composed of medium or media with quadratic variation of their, generally complex, refractive indices. This quadratic variation occurs in planes $x-y$ transverse to an optical axis of the system, assumed here along the z-axis of a Cartesian coordinate frame $Oxyz$. The optical systems will be considered as an isotropic, lossless, dispersion-free bulk nonmagnetic medium or as a stratified structure that consists of several layers of media of this type. Therefore, the magnetic permeability is equal to that of free space and in each layer the medium is specified by the, uniform (constant) in space, scalar electric permittivity ε.

Let us assume first that the medium is linear and homogeneous. The optical field will be analysed in a source-free range of this structure. In each layer of the structure, transverse E_x, E_y and longitudinal E_z components of the propagating beam field $\underline{\mathrm{E}}=(E_x,E_y,E_z)$ satisfy the homogeneous wave equation

$$\left[\underline{\nabla}^2 - c^{-2}\partial_t^2\right]\underline{\mathrm{E}}(\underline{r},t) = 0\,, \tag{2.1}$$

where $c = c_v/n$ is the phase speed of light in the medium, related to the phase speed c_v in a vacuum by a relative refractive index n. We will use interchangeably the notation $Oxyz$ and (x,y,z) to indicate coordinate frames, as well as $\underline{r} \equiv (\underline{r}_\perp, z) = (x,y,z)$ and $\underline{\nabla} \equiv (\underline{\nabla}_\perp, \partial_z) = (\partial_x, \partial_y, \partial_z)$ to indicate, where necessary, the planes $x-y$ transverse to the optical axis z.

Any solution to the wave equation in a homogeneous medium of the uniform permittivity ε should also fulfil the Gauss law

$$\nabla \cdot \left[\underline{E}(\underline{r})\right] = 0\,, \tag{2.2}$$

which interrelates, through their derivatives, the longitudinal component E_z with the transverse components E_x and E_y of the optical beam field. However, for the case of dielectric inhomogenous or nonlinear media, each layer of the structure is specified by the nonuniform electric permittivity $\varepsilon \equiv \varepsilon(r)$. Therefore, in this case, $c \equiv c(\underline{r})$ and $n \equiv n(\underline{r})$ are also nonuniform and the Gauss law reads:

$$\nabla \cdot \left[\varepsilon(\underline{r})\underline{E}(\underline{r})\right] = 0\,. \tag{2.3}$$

Moreover, it can be proved that the wave equation (2.1) still approximately holds even in each inhomogeneous layer if the increment $\Delta\varepsilon$ of ε does not vary significantly within a range of one wavelength λ in this layer, that is when $(2\pi\varepsilon)^{-1}\Delta\varepsilon << 1$ in this range [2,7]. Only the cases of such weakly inhomogeneous media, together with homogeneous media, will be considered in this book.

The beam field will be considered as monochromatic,

$$\underline{\mathrm{E}}(\underline{r},t) = \underline{E}(\underline{r})\exp(-ikct)\,, \tag{2.4}$$

with the wave number $k \equiv k(\underline{r})$ and the wave vector $\underline{k} \equiv \underline{k}(\underline{r})$, $\underline{k} = (\underline{k}_\perp, k_z) = (k_x, k_y, k_z)$, in the medium related, through the refractive index n, to the wave number in the vacuum k_v, that is with $\underline{k}(\underline{r}) = \underline{k}_v n(\underline{r})$. In this chapter, we will be interested only in the transverse electric field components E_x, E_y and $\widetilde{E}_x$, $\widetilde{E}_y$ in the configuration $x-y$ and spectral $k_x - k_y$ transverse planes, respectively. They form two two-dimensional vectors

$$\underline{E}_{\perp}(\underline{r}_{\perp},z)=\begin{bmatrix}E_x(\underline{r}_{\perp},z)\\ E_y(\underline{r}_{\perp},z)\end{bmatrix}, \tag{2.5}$$

$$\underline{\widetilde{E}}_{\perp}(\underline{k}_{\perp},z)=\begin{bmatrix}\widetilde{E}_x(\underline{k}_{\perp},z)\\ \widetilde{E}_y(\underline{k}_{\perp},z)\end{bmatrix}, \tag{2.6}$$

in these transverse planes, interrelated by the two-dimensional Fourier transform in the transverse coordinates $\underline{r}_{\perp}$ and $\underline{k}_{\perp}$:

$$\underline{E}_{\perp}(\underline{r}_{\perp},z)=(2\pi)^{-2}\iint d\underline{k}_{\perp}\,\underline{\widetilde{E}}_{\perp}(k_{\perp},z)\exp[i(k_{\perp}\cdot r_{\perp})]. \tag{2.7}$$

The transverse field vectors $\underline{E}_{\perp}(\underline{r}_{\perp},z)$ and $\underline{\widetilde{E}}_{\perp}(k_{\perp},z)$ obey the homogeneous Helmholtz (reduced wave) equation in the configuration space and its counterpart in the spectral or momentum space:

$$\left[\partial_z^2+\underline{\nabla}_{\perp}^2+k^2\right]\underline{E}_{\perp}(r_{\perp},z)=0, \tag{2.8}$$

$$\left[\partial_z^2-\underline{k}_{\perp}^2+k^2\right]\underline{\widetilde{E}}_{\perp}(k_{\perp},z)=0, \tag{2.9}$$

respectively.

Let us assume that the optical system is centred, where the beam axis coincides with the axis of the system and the refractive index takes its extreme values at this axis:

$$(\partial n^2/\partial x)(z)\,|_{x=0,\,y=0}=0,$$

$$(\partial n^2/\partial y)(z)\,|_{x=0,\,y=0}=0. \tag{2.10}$$

Then, the quadratic approximation of the refractive index in any transverse plane of this system results in the parabolic form of the transverse increment $\Delta n^2=1-n^2/n_0^2$ of the refractive index squared:

$$n_0^2\Delta n^2\equiv n_0^2\Delta n^2(x,y,z)\cong-(\Delta_{x^2}n^2)(z)\,x^2-(\Delta_{y^2}n^2)(z)\,y^2, \tag{2.11}$$

$$\Delta_{x^2}n^2\equiv\Delta_{x^2}n^2(z)=\tfrac{1}{2}(\partial^2n^2/\partial x^2)(z)\,|_{x=0,\,y=0},$$

$$\Delta_{y^2}n^2\equiv\Delta_{y^2}n^2(z)=\tfrac{1}{2}(\partial^2n^2/\partial y^2)(z)\,|_{x=0,\,y=0}, \tag{2.12}$$

where on the beam axis $x = 0 = y$ and at the beam waist centre $x = y = z = 0$ we have, respectively:

$$n_0 \equiv n_0(z) = n(0,0,z),$$

$$k_0 \equiv k_0(z) = k(0,0,z), \tag{2.13}$$

$$n_w \equiv n_0(0) = n(0,0,0),$$

$$k_w \equiv k_0(0) = k(0,0,0). \tag{2.14}$$

The above quantities still may be dependent on z:

$$n^2 \equiv n^2(x,y,z) \cong n_0^2(z)[1-\Delta n^2(x,y,z)], \tag{2.15}$$

$$k^2 \equiv k^2(x,y,z) \cong k_0^2(z)[1-\Delta n^2(x,y,z)]. \tag{2.16}$$

Equations (2.11)-(2.16) describe the fundamental parabolic approximation usually taken for centred optical first-order systems. For example, in cases of the square-law in lens-like media [3] $\Delta n^2 > 0$ ($\Delta n^2 < 0$) correspond to a focusing (defocusing) medium.

Let us define the slowly varying amplitude (SVA) of the beam:

$$\underline{E}_\perp(\underline{r}_\perp, z) \to \underline{E}_\perp(\underline{r}_\perp, z)\exp\left[i\int_0^z dz' k_0(z')\right], \tag{2.17}$$

by factoring out the beam on-axis phase accumulated along the beam axis. Note in Equation (2.17) the convention taken in this chapter that preserves notation of quantities redefined by their factoring or scaling. Under the paraxial approximation of the wave equation (2.8), the second derivatives with respect to z can be neglected with respect to the terms proportional to the first derivatives:

$$\left|\partial_z^2 E_x\right| << \left|k_0 \partial_z E_x\right|,$$

$$\left|\partial_z^2 E_y\right| << \left|k_0 \partial_z E_y\right|, \tag{2.18}$$

and the wave equation (2.8) converts into the equation of the parabolic type

$$\left[2ik_0\partial_z + \partial_x^2 + \partial_y^2 - k_0^2\Delta n^2\right]\underline{E}_\perp(\underline{r}) = 0\,. \tag{2.19}$$

The form of Equation (2.19) is identical to the Schrödinger equation of a particle with z replacing time, the wave number k_0 playing the role of $m/\hbar$ and the term $k_0^2\Delta n^2$ corresponding to the particle potential.

Next, the reduction of the z-dependent refractive index $n_0(z)$ at the beam axis with respect to the refractive index n_w at the centre $(x,y,z) = (0,0,0)$ of the beam waist:

$$n_w \int_0^z dz'/n_0(z') \to z\,, \tag{2.20}$$

yields the paraxial wave equation,

$$\left[2ik_w\partial_z + \partial_x^2 + \partial_y^2 - k_w^2(n_0^2/n_w^2)\Delta n^2\right]\underline{E}_\perp(\underline{r}) = 0\,, \tag{2.21}$$

in the form dependent on the wave number k_w at the beam waist centre regarded as the beam parameter. This is the paraxial wave equation in the non-normalised form. As k_w does not depend on z, the reduction (2.20) considerably simplifies further definitions.

The coordinates in Equation (2.21) are not dimensionless and some appropriate scaling of them seems necessary. To this end, let us introduce the beam parameter w_w, as the radius of the beam cross-section at the beam waist placed here at $z = 0$, with its value common in both transverse dimensions. For a fundamental Gaussian beam of cylindrical symmetry, for example, this parameter has such clear geometrical meaning. Introduction of two other beam parameters: the diffraction length z_D and the scaled wave number κ:

$$z_D = k_w w_w^2\,, \qquad \kappa = k_w w_w\,, \tag{2.22}$$

leads to the scaled parabolic equation for the SVA of the beam:

$$\left[2i\partial_{z/z_D} + \partial_{x/w_w}^2 + \partial_{y/w_w}^2 - \kappa^2(n_0^2/n_w^2)\Delta n^2\right]\underline{E}_\perp(\underline{r}) = 0\,. \tag{2.23}$$

Note that the presence of the transverse field $\underline{E}_\perp$ in (2.8), (2.21) and (2.23) is not accidental. Rigorous derivation of the paraxial equation (2.23) from the Maxwell equations yields the electric field expansion in powers of κ^{-1} [29]:

$$\underline{E} = \underline{E}_\perp + \underline{E}_z = \underline{E}_\perp^{(0)} + \kappa^{-1}\underline{E}_z^{(1)} + \kappa^{-2}\underline{E}_\perp^{(2)} + \kappa^{-3}\underline{E}_z^{(3)} + \kappa^{-4}\underline{E}_\perp^{(4)} + \ldots, \quad (2.24)$$

valid for $\kappa >> 1$. The subsequent even and odd terms in (2.24) approximate the transverse $\underline{E}_\perp$ and longitudinal $\underline{E}_z$ field components, respectively. The first, zero-order, field term is purely transverse indeed, $\underline{E} \cong \underline{E}_\perp \equiv \underline{E}_\perp^{(0)}$, and exactly this term appears in the paraxial equation (2.23).

Further, in this chapter, we will use the coordinates scaled in the configuration domain and the spectral domain, respectively:

$$x/w_w \to x, \qquad y/w_w \to y,$$

$$z/z_D \to z, \quad (2.25)$$

$$k_x w_w \to k_x, \qquad k_y w_w \to k_y,$$

$$k_w w_w \to k_w \equiv \kappa. \quad (2.26)$$

Then, after the additional replacement:

$$\kappa^2 (n_0^2/n_w^2)\Delta_{x^2} n^2 \to \Delta_{x^2} n^2,$$

$$\kappa^2 (n_0^2/n_w^2)\Delta_{y^2} n^2 \to \Delta_{y^2} n^2,$$

$$\kappa^2 (n_0^2/n_w^2)\Delta n^2 \to \Delta n^2, \quad (2.27)$$

the scaled parabolic equation (2.23) is obtained in the in dimensionless form:

$$\left[2i\partial_z + \partial_x^2 + \partial_y^2 - \Delta n^2\right]\underline{E}_\perp(\underline{r}) = 0. \quad (2.28)$$

In the transversely homogeneous ($\Delta n^2 = 0$) media this equation resolves into the well-known Fock equation [3]:

$$\left[2i\partial_z + \partial_x^2 + \partial_y^2\right]\underline{E}_\perp(\underline{r}_\perp, z) = 0, \quad (2.29)$$

in its scaled version with constant coefficients. Note that in the scaled coordinates Eqs. (2.28) and (2.29) do not depend now on the field wave number k_w and the beam half-width w_w. Therefore, they describe a general case of paraxial beam propagation with arbitrary values of the spatial

frequency and the beam half-width, provided that the scaled wave number $k_w w_w$ is small enough to fulfil the conditions (2.18).

In isotropic and homogeneous medium both field components E_x and E_y of the three-dimensional beam satisfy separately the same scalar Helmhotz equation (2.8). The same happens if the homogeneous medium is replaced by weakly inhomogeneous medium of cylindrical symmetry with respect to the z-axis. Therefore, when the structure is axially symmetric and stratified with respect to the z-axis, the field components E_x and E_y in each weakly inhomogeneous layer may be treated as independent scalar quantities for TM polarization ($E_x = E$, $E_y = 0$) and for TE polarization ($E_y = E$, $E_x = 0$). The decomposition of the electromagnetic field in each layer into its TM and TE components can be rigorously derived with the help of two scalar Hertz potentials. The derivation follows that for the case of isotropic and homogeneous medium and can be found, for example, in [30] or in [31]. Note also that, in spite of the TM-TE decomposition of the beam field within each layer, the TM and TE beam field components are coupled at plane boundaries (interfaces) of the layers.

Still, however, one should be aware that for three-dimensional beams the TM and TE beam field components still depend on the longitudinal (z-) coordinate and on the two transverse (x-) and (y-) coordinates, that is on $E_x \equiv E_x(x,y,z)$ and $E_y \equiv E_y(x,y,z)$, respectively. However, in each layer of the optical system filled by the weakly inhomogeneos medium, the three-dimensional scalar problems (in x, y and z), governed in the paraxial approximation by (2.28) or (2.29), reduce into two independent two-dimensional scalar problems (in x and z or in y and z) [3]. Then, the beam field amplitude $E \equiv E(x,y,z)$ is factorised into two-dimensional field amplitudes $E(x,z)$ and $E(y,z)$ in two planes $x-z$ and $y-z$ and these amplitudes are governed by two independent two-dimensional parabolic equations, respectively [3]:

$$E(x,y,z) \cong E(x,z)\,E(y,z), \tag{2.30}$$

$$\left[2i\partial_z + \partial_x^2 - \Delta_{x^2} n^2 x^2\right] E(x,z) = 0, \tag{2.31}$$

$$\left[2i\partial_z + \partial_y^2 - \Delta_{y^2} n^2 y^2\right] E(y,z) = 0 . \tag{2.32}$$

Once the two-dimensional solutions (2.31) and (2.32) are obtained within the paraxial approximation, the three-dimensional paraxial solution is given by Equation (2.30).

The scaling procedure can be also applied in the transverse coordinates x and y independently, with different scale parameters w_{wx} and w_{wy}. Such a scaling is conventionally applied in the case of, for example, a fundamental Gaussian beam with elliptic cross-section. However, and only to avoid unnecessary complication of the notation, we will use below in this chapter the paraxial wave equation in its scaled version (2.28) with $w_{wx} = w_{wy} = w_w$, like for beams of cylindrical symmetry in their fundamental order.

2.3 Beam amplitude and polarization

Any spectral constituent of the electric field of the paraxial beam takes the form of a plane wave $\underline{\widetilde{E}}(\underline{k}_\perp, z)\exp(i\underline{k}_\perp \underline{r}_\perp)$ defined by two components $\widetilde{E}_x$ and $\widetilde{E}_y$ of the transverse electric field $\underline{\widetilde{E}}_\perp$. Polarization of the plane wave is parameterised by a complex polarization parameter $\widetilde{\chi}$, given by the ratio of the transverse field components:

$$\widetilde{\chi}(\underline{k}_\perp, z) = \widetilde{E}_x(\underline{k}_\perp, z) \Big/ \widetilde{E}_y(\underline{k}_\perp, z) . \tag{2.33}$$

The field of the plane wave can be also alternatively described as a product two complex, in general, quantities: a scalar complex amplitude $\widetilde{E}$ and a polarization complex vector $\underline{\widetilde{e}}$ of the plane wave:

$$\underline{\widetilde{E}}_\perp(\underline{k}_\perp, z) = \widetilde{E}(\underline{k}_\perp, z)\underline{\widetilde{e}}(\underline{k}_\perp, z) . \tag{2.34}$$

One additional restriction should be imposed on the definitions of the field polarization and amplitude to make this factorisation unique. To this end, let us assume that the polarization vector in the transverse plane $\underline{\widetilde{e}} = \left[\widetilde{e}_x, \widetilde{e}_y\right]^T$ (the superscript T means transpose) satisfies the condition $\widetilde{e}_x \widetilde{e}_y = 1$ instead of the conventional condition to have this vector normalised to unity [32]. That uniquely defines the complex amplitude of the plane wave,

$$\widetilde{E}(\underline{k}_\perp, z) = \left(\widetilde{E}_x(\underline{k}_\perp, z)\widetilde{E}_y(\underline{k}_\perp, z)\right)^{1/2}, \tag{2.35}$$

and the polarization vector of the beam:

$$\underline{\widetilde{e}}(\underline{k}_\perp, z) = \begin{bmatrix} \widetilde{e}_x(\underline{k}_\perp, z) \\ \widetilde{e}_y(\underline{k}_\perp, z) \end{bmatrix} = \begin{bmatrix} \widetilde{\chi}^{+1/2}(\underline{k}_\perp, z) \\ \widetilde{\chi}^{-1/2}(\underline{k}_\perp, z) \end{bmatrix}. \tag{2.36}$$

Both entities are symmetric with respect to the replacement $\widetilde{E}_x \leftrightarrow \widetilde{E}_y$ of transverse field components and to the change $\widetilde{\chi} \leftrightarrow \widetilde{\chi}^{-1}$ of beam polarization, as it should be. It appears that such definition of the base polarization vectors makes the reflection and transmission matrices at the interface unimodular [32].

The same factorisation procedure can be applied as well to the beam field in the configuration domain [32]:

$$\underline{E}_\perp(\underline{r}) = E(\underline{r})\underline{e}(\underline{r}), \tag{2.37}$$

$$E(\underline{r}) = \left[E_x(\underline{r})E_y(\underline{r})\right]^{1/2}, \tag{2.38}$$

$$\underline{e}(\underline{r}) = \begin{bmatrix} e_x(\underline{r}) \\ e_y(\underline{r}) \end{bmatrix} = \begin{bmatrix} \chi^{+1/2}(\underline{r}) \\ \chi^{-1/2}(\underline{r}) \end{bmatrix}, \tag{2.39}$$

$$\chi(\underline{r}) = E_x(\underline{r}) \big/ E_y(\underline{r}). \tag{2.40}$$

Dependence of the quantities $\widetilde{E}_x$, $\widetilde{E}_y$ and $\widetilde{\chi}$ on $\underline{k}_\perp$ and z, as well as the dependence of E_x, E_y and χ on $\underline{r}_\perp$ and z, will be further understood as implicit. In this way the beam polarization and the beam complex amplitude has been uniquely defined in the configuration and spectral domains. For example, $\widetilde{\chi} = \chi = \mp i$ for beams of right-handed (-) and left-handed (+) uniform (constant) circular polarization, respectively. Note that the assumption that the parameters χ and $\widetilde{\chi}$ are equal to each other (i.e. $e_x/e_y = \widetilde{e}_x/\widetilde{e}_y$) for all points of the transverse planes, direct and spectral, implies that these parameters are constant in these planes.

The beam amplitude-polarization factorisation is unique but remains singular in two distinctive cases in the spectral and configuration domains. In

the spectral domain, when one of the transverse field components $\widetilde{E}_x$ or $\widetilde{E}_y$ is zero at one specific spatial transverse frequency $\underline{k}_\perp$, the field is of the TM ($\widetilde{E}_y = 0$, $\widetilde{\chi}^{-1} = 0$) or TE ($\widetilde{E}_x = 0, \widetilde{\chi} = 0$) type at $\underline{k}_\perp$, respectively. Similarly, in the spatial domain, when one of the transverse field components E_x or E_y is zero at one specific point $\underline{r}_\perp$ in the transverse plane, the field is of the TM ($E_y = 0, \chi^{-1} = 0$) or TE ($E_x = 0, \chi = 0$) type at $\underline{r}_\perp$, respectively. Then, at this point:

$$\underline{E}_\perp{}^{(TM)} = E_x \underline{e}_x = E_x \begin{bmatrix} 1 \\ 0 \end{bmatrix},$$

$$\underline{E}_\perp{}^{(TE)} = E_y \underline{e}_y = E_y \begin{bmatrix} 0 \\ 1 \end{bmatrix}, \tag{2.41}$$

for the beam polarization of the TM or TE type, respectively.

Moreover, if in one transverse plane the field TM or TE polarization does not vary from point to point in the spatial and spectral domains, then the field is totally of the TM or TE polarization in any transvese plane. In general, for paraxial beams in free space, when the polarization parameters $\widetilde{\chi}$ and χ are constant and equal $\widetilde{\chi} = \chi$ in the transverse planes, then the beam polarization is independent of the beam field distribution in these planes. Then the complex amplitude (2.38) of the beam field is described by the scalar paraxial wave equation:

$$\left[2i\partial_z + \partial_x^2 + \partial_y^2 - \Delta n^2\right] E(x, y, z) = 0, \tag{2.42}$$

and the problem under consideration becomes a scalar one.

In the next sections of this chapter the beams will be analysed as paraxial, that is for their rays being close to the beam axis and with their angular deviations from the beam axis direction being small. Beam polarization will be assumed constant at any transverse plane. Within this range the beam polarization and the beam complex amplitude are independent of each other and will be treated separately.

2.4 Hamilton's canonical equations

Action of any first-order optical system can be described within the formulation of Hamiltonian optics [1,2]. As a part of this formalism, linear canonical transformations are well suited for the treatment of parabolic differential equations. The transformations of this kind are present in classical and quantum theoretical formulations in optics and are common in many aspects with those one can meet in mechanics. The Hamilton's equations for optical ray data will be given in this section. The issue of canonical operator transforms will be discussed in the next sections.

The paraxial scalar wave equation (2.28) can be recast in the form of the nonrelativistic Schrödinger equation with the Hamiltonian H [21]:

$$i\partial_z E(x,y,z) = \mathrm{H}E(x,y,z),$$

$$\mathrm{H} \equiv \mathrm{H}(x,y,p_x,p_y,z) = \tfrac{1}{2}[p_x^2 + p_y^2 + \Delta n^2(x,y,z)] \tag{2.43}$$

and with the generalized momenta p_x and p_y defined by:

$$p_x E(x,y,z) = -i\partial_x E(x,y,z),$$

$$p_y E(x,y,z) = -i\partial_y E(x,y,z). \tag{2.44}$$

At this level of analysis the eigenvalues p_x and p_y in the differential equations (2.44) depend on the solution $E(x,y,z)$ to the Schrödinger equation, which is not known yet. Therefore p_x and p_y are also not known. They can be found in the paraxial approximation to $E(x,y,z)$ by use of a point-spread function of the optical system and this issue will be discussed below.

For the time being, however, let us assume that $E(x,y,z)$ is known. Then, at arbitrary point (x,y) in any transverse plane $z = const.$ of the optical system, a solution $E(x,y,z)$ to the Schrödinger equation defines a vector normal to a phase front of this solution at this point. Direction of this vector or its tilt with respect to the axis of the optical system is given by the momentum components p_x and p_y. Note that for a plane wave, which may be regarded as an approximate model of a sufficiently wide beam, the momentum vector is equal to the transverse (normalised here) wave vector

$\underline{k}_{\perp}$ of this plane wave, that is $(p_x, p_y) = (k_x, k_y)$ in this case. For beams of finite width, a set of the data (x, y) and (p_x, p_y) in subsequent transverse planes defines optical rays passing from some point (x', y') in an input (transverse) plane to some point (x, y) in an output (transverse) plane. Therefore the data (x, y) and (p_x, p_y) are dependent on z. This pair constitutes, for any ray progressing through the first-order system, the two two-dimensional ray data vectors:

$$\underline{\eta}_x(z) = \begin{bmatrix} x(z) \\ p_x(z) \end{bmatrix},$$

$$\underline{\eta}_y(z) = \begin{bmatrix} y(z) \\ p_y(z) \end{bmatrix}, \tag{2.45}$$

defined in phase space of three-dimensional, paraxial first-order optics. Vectors $\underline{\eta}_x(z)$ and $\underline{\eta}_y(z)$ belong to the phase space of ray data for rays advancing through the optical system. They represent points of intersections $(x(z), y(z))$ of the rays with any transverse plane of this system and directions of these rays, through their generalised momenta $(p_x(z), p_y(z))$ at the intersection points.

To put the definitions (2.45) in a more formal perspective, note that action of any first-order system can be defined by its impulse response function, $g(x, y \mid x', y'; z) \propto \exp[iI(x, y \mid x', y'; z)]$ with quadratic dependence of its point characteristic $I(x, y \mid x', y'; z) \equiv I(z)$ on the transverse coordinates x', y' and x, y in the input and output planes, respectively. Note that linear terms are absent in $I(x, y \mid x', y'; z)$ because misaligned first-order systems are not considered in this chapter. The point characteristic is determined by elements of the ray-transfer *ABCD* matrix specific to this system (see Equation (5.57) in Section 5, as well as Equations (6.91)-(6.92) in Section 6 in the case of the system of cylindrical symmetry). The solution $E(x, y, z)$ to the Schrödinger equation (2.42) can be obtained by use of this function when the initial beam field distribution $E(x', y', 0)$ in the input plane are known. The momenta $p_x(z)$ and $p_y(z)$ are then given by partial derivatives $p_x(z) = \partial_x I(z)$ and $p_y(z) = \partial_y I(z)$ of the point characteristic, and the ray vectors $\underline{\eta}_x(z)$ and

$\underline{\eta}_y(z)$ are obtained, for any value of z, from the solution of the Hamilton-Jacobi partial differential equation and Jacobi's theorem [21]. That results in the Hamilton's canonical equations for the ray data (2.45):

$$\partial \mathrm{H}/\partial p_x = \partial x/\partial z\,,$$

$$\partial \mathrm{H}/\partial x = -\partial p_x/\partial z\,, \tag{2.46}$$

$$\partial \mathrm{H}/\partial p_y = \partial y/\partial z\,,$$

$$\partial \mathrm{H}/\partial y = -\partial p_y/\partial z\,, \tag{2.47}$$

valid at any transverse plane $z = const.$ of the optical system, provided that the initial conditions at the input plane $z = 0$ are known. Therefore, the solution $\underline{\eta}_x(z)$, $\underline{\eta}_y(z)$ of Equations (2.46)-(2.47) in the output plane depends on the initial condition $\underline{\eta}_x(0)$, $\underline{\eta}_y(0)$ for the optical ray in the input plane.

For paraxial beams in the first-order optical system, the refractive index contribution Δn^2 to the Hamiltonian is approximated by its quadratic variation in the transverse coordinates x and y,

$$\mathrm{H} \cong \tfrac{1}{2}[p_x^2 + p_y^2 + \Delta_x n^2 x^2 + \Delta_y n^2 y^2] \tag{2.48}$$

and the canonical equations reduce to the set of the four first-order equations:

$$\partial x/\partial z = p_x\,,$$

$$\partial p_x/\partial z = -\Delta_x n^2 x\,, \tag{2.49}$$

$$\partial y/\partial z = p_y\,,$$

$$\partial p_y/\partial z = -\Delta_y n^2 y\,, \tag{2.50}$$

or, only for the optical ray data $x(z)$ and $y(z)$, to the two second-order differential equations:

$$\partial^2 x/\partial_z^2 + \Delta_x n^2 x = 0\,,$$

$$\partial^2 y/\partial_z^2 + \Delta_y n^2 y = 0\,. \tag{2.51}$$

Note that in the homogeneous medium $\Delta_x n^2 = 0 = \Delta_y n^2$ and the solution of (2.51) consists only of straight rays. In general, however, $\Delta_x n^2 \neq 0 \neq \Delta_y n^2$ and the ray data are determined by the ray-transfer matrix. This issue will be discussed in the next section.

Now let us return to the notion of a canonical transformation. Consider two pairs of the ray data $\underline{\eta}_x^{(1)}(z)$, $\underline{\eta}_y^{(1)}(z)$ and $\underline{\eta}_x^{(2)}(z)$, $\underline{\eta}_y^{(2)}(z)$ representing two optical rays advancing through the optical system from one transverse plane to another plane according to the Hamilton's equations. Then the Poisson (Lagrange) brackets for the optical rays:

$$\{\underline{\eta}_a^{(1)}, \underline{\eta}_a^{(2)}\} = (\underline{\eta}_a^{(1)})^T \underline{\underline{\varepsilon}}\, \underline{\eta}_a^{(2)}\,, \tag{2.52}$$

a=x,y, remain invariant during beam propagation in any first-order system [21]:

$$(d/dz)\{\underline{\eta}_a^{(1)}, \underline{\eta}_a^{(2)}\} = 0\,, \tag{2.53}$$

where the four-by-four antisymmetric matrix

$$\underline{\underline{\varepsilon}} = \begin{bmatrix} \underline{\underline{0}} & \underline{\underline{I}} \\ -\underline{\underline{I}} & \underline{\underline{0}} \end{bmatrix}, \tag{2.54}$$

$\underline{\underline{\varepsilon}} = -\underline{\underline{\varepsilon}}^{-1} = -\underline{\underline{\varepsilon}}^{T}$, $\underline{\underline{\varepsilon}}^2 = -\underline{\underline{1}}$ is composed of the two-dimensional identity $\underline{\underline{I}}$ and null $\underline{\underline{0}}$ matrices [21]. For two pairs of the ray data $x(z)$, $p_x(z)$ and $y(z)$, $p_y(z)$ this invariance explicitly reads:

$$(d/dz)\left[x^{(1)} p_x^{(2)} - x^{(2)} p_x^{(1)}\right] = 0\,, \tag{2.55}$$

$$(d/dz)\left[y^{(1)} p_y^{(2)} - y^{(2)} p_y^{(1)}\right] = 0\,, \tag{2.56}$$

and means that these data are canonically conjugate variables in the first-order system. Then the optical transformation described by them is understood as canonical.

2.5 Ray-transfer matrices

The transformation performed by optical system transfers the amplitude distribution of the input beam given in the input transverse plane, say at $z = 0$, to the amplitude distribution of the output beam in the output plane taken at some value of z. If the optical system is of the first-order type, its action can be described by a linear transformation represented by four-by-four ray-transfer *ABCD* matrix:

$$\underline{\underline{M}}_{(\perp)} = \begin{bmatrix} \underline{\underline{A}} & \underline{\underline{B}} \\ \underline{\underline{C}} & \underline{\underline{D}} \end{bmatrix}, \tag{2.57}$$

where the elements of the matrix $\underline{\underline{M}}_{(\perp)}$ are viewed with explicit dependence on z not displayed for brevity. The matrix $\underline{\underline{M}}_{(\perp)}$ is composed of the four two-by-two matrices $\underline{\underline{A}}$, $\underline{\underline{B}}$, $\underline{\underline{C}}$ and $\underline{\underline{D}}$ and relates the position $\underline{r}_{\perp}$ and momentum $\underline{p}_{\perp}$ of the incoming ray in the input plane to the position $\underline{r}'_{\perp}$ and momentum $\underline{p}'_{\perp}$ of the outcoming ray in the output plane:

$$\begin{bmatrix} \underline{r}'_{\perp} \\ \underline{p}'_{\perp} \end{bmatrix} = \begin{bmatrix} \underline{\underline{A}} & \underline{\underline{B}} \\ \underline{\underline{C}} & \underline{\underline{D}} \end{bmatrix} \begin{bmatrix} \underline{r}_{\perp} \\ \underline{p}_{\perp} \end{bmatrix}. \tag{2.58}$$

The ray-transfer matrices represent linear canonical transformations of the first-order optical systems, that is the transformations that preserve Poisson brackets and commutation relations during mapping of the canonically conjugate variables given in the input plane into their counterparts in the output plane. To fulfil this condition, the ray-transfer matrices have to be symplectic, that is they have to satisfy the symplecticity condition [21]:

$$\underline{\underline{M}}^{T}_{(\perp)} \underline{\underline{\varepsilon}} \, \underline{\underline{M}}_{(\perp)} = \underline{\underline{\varepsilon}}, \tag{2.59}$$

where $\underline{\underline{\varepsilon}}$ is the four-dimensional antisymmetric matrix (2.54) and $\underline{\underline{M}}^{T}{}_{(\perp)}$ means the matrix transposed of $\underline{\underline{M}}_{(\perp)}$. If the matrix $\underline{\underline{M}}_{(\perp)}$ is symplectic, then its inverse $\underline{\underline{M}}^{-1}_{(\perp)}$ exists and is symplectic as well. Unit matrix $\underline{\underline{1}}$ is symplectic too. The product of two symplectic matrices is also symplectic and associativity holds for this product. Therefore, symplectic matrices form a

group. If the optical system is lossless and without gain, the ray matrix is unitary, i.e. $\underline{\underline{M}}_{(\perp)}\underline{\underline{M}}^{+}{}_{(\perp)} = \underline{\underline{1}}$, where the superscript "$+$" denotes the combined action of transposition and conjugation. However, the symplecticity condition (2.59) remains also valid for any ray-transfer matrix representing transformations of paraxial beams in a first-order system with arbitrary quadratic distribution of the, complex in general, refraction index.

In order to simplify further derivations let us consider now the separable symmetric optical system. Then the field amplitude of a beam can be factorised into two independent factors in two orthogonal transverse coordinates, say in x and y. The beam propagation in such a system is described by two independent two-dimensional vectors $\underline{\eta}_x = [x, p_x]^T$ and $\underline{\eta}_y = [y, p_y]^T$ in two independent two-dimensional phase spaces of the beam field. Next, alternatively to the four-dimensional position-momentum ray vector $[\underline{r}_\perp, \underline{p}_\perp]^T$, (cf. (2.45) and (2.58)), define a new four-dimensional vector, composed of the two two-dimensional position-momentum vectors:

$$\underline{\eta}_\perp(z) = \begin{bmatrix} \underline{\eta}_x(z) \\ \underline{\eta}_y(z) \end{bmatrix}. \tag{2.60}$$

The four-vector ray-data $\underline{\eta}_\perp(z)$ describes also adequately the positions and directions of the optical ray in each transverse plane of the optical system. Its optical transformation is also described by the four-by-four ray-transfer matrix $\underline{\underline{m}}_{(\perp)}$ of the first-order system, with arrangements of its elements different, however, than that of matrix $\underline{\underline{M}}_{(\perp)}$ (2.57). Because the system is assumed now as separable, $\underline{\underline{m}}_{(\perp)}$ is composed of two-by-two *abcd* matrices placed on its diagonal. Further, if this system is also circularly symmetric in any transverse plane $x - y$, then these two two-by-two *abcd* matrices are equal to each other.

In the paraxial approximation the relation between the vector $\underline{\eta}_\perp$, defined in the input plane and the vector $\underline{\eta'}_\perp$, defined in the output plane, is linear and given in terms of the ray-transfer matrix $\underline{\underline{m}}_{(\perp)}$:

$$\underline{\eta}'_{\perp} = \underline{\underline{m}}_{(\perp)}\,\underline{\eta}_{\perp}\,. \tag{2.61}$$

When the optical system is separable, the four-by four ray matrix $\underline{\underline{m}}_{(\perp)}$ decomposes into two identical two-by-two ray transfer matrices $\underline{\underline{m}}_{(x)}$ and $\underline{\underline{m}}_{(y)}$:

$$\underline{\underline{m}}_{(\perp)} = \begin{bmatrix} \underline{\underline{m}}_{(x)} & \underline{\underline{0}} \\ \underline{\underline{0}} & \underline{\underline{m}}_{(y)} \end{bmatrix} \tag{2.62}$$

and acts independently on the two-dimensional ray vectors:

$$\underline{\eta}'_{x} = \underline{\underline{m}}_{x}\,\underline{\eta}_{x}\,,$$

$$\underline{\eta}'_{y} = \underline{\underline{m}}_{y}\,\underline{\eta}_{y}\,. \tag{2.63}$$

In addition, for the system of cylindrical symmetry, these ray matrices are mutually equal:

$$\underline{\underline{m}}_{(x)} = \underline{\underline{m}}_{(y)} = \underline{\underline{m}} = \begin{bmatrix} a & b \\ c & d \end{bmatrix} \tag{2.64}$$

and instead of two ray vectors $\underline{\eta}_{x}$ and $\underline{\eta}_{y}$ we may consider only one of them, say $\underline{\eta}_{x} \equiv \underline{\eta}$.

The matrix $\underline{\underline{m}}$ is unimodular, a feature common to all two-dimensional symplectic transformations:

$$\det \underline{\underline{m}} = ad - cb = 1\,. \tag{2.65}$$

Note that the scaling (2.25)-(2.26) of Cartesian coordinates implies also the scaling

$$a \to a\,, \qquad b/z_D \to b\,,$$

$$c \to c\,, \qquad d\,z_D \to d\,, \tag{2.66}$$

already accounted for in the defintion (2.64) of the *abcd* matrix. The ray-transfer matrix $\underline{\underline{m}}$ describes directly transformations of ray data $\underline{\eta}$ under action of elements of the circularly symmetric optical system [27-28].

For example, refraction of the beam at the dielectric interface at $z = z^{(\mathrm{int})}$, that is at the boundary between two semi-infinite dielectric media, is governed just by the identity matrix $\underline{\underline{m}}^{(I)}$:

$$\underline{\eta}' = \underline{\underline{m}}^{(I)} \underline{\eta} = \underline{\eta},$$

$$\underline{\underline{m}}^{(I)} \equiv \underline{\underline{m}}^{(I)}(z^{(\mathrm{int})}) = \begin{bmatrix} 1 & 0 \\ 0 & 1 \end{bmatrix}, \tag{2.67}$$

due to the reduction (2.20) of the axial coordinate z by the refractive index of the medium. The ray vector $\underline{\eta}'$ in two-dimensional phase space of ray data at the output plane, just behind the interface, equals the ray vector $\underline{\eta}$ in the input plane – just before the interface.

Beam propagation in free space between the input and output planes is described by the matrix $\underline{\underline{m}}^{(F)}$:

$$\begin{bmatrix} x' \\ p' \end{bmatrix} = \underline{\underline{m}}^{(F)} \begin{bmatrix} x \\ p \end{bmatrix} = \begin{bmatrix} x + zp \\ p \end{bmatrix},$$

$$\underline{\underline{m}}^{(F)} \equiv \underline{\underline{m}}^{(F)}(z) = \begin{bmatrix} 1 & z \\ 0 & 1 \end{bmatrix}, \tag{2.68}$$

with the upper off-diagonal term of $\underline{\underline{m}}^{(F)}$ equal to the scaled propagation distance z, positive $z > 0$ for propagation from the waist plane $z = 0$. The position of a ray intersection with the output plane is displaced from its counterpart in the input plane by a product of z and p.

Action of the thin lens of a focal length $f = -\rho^{-1}$, positive $f > 0$ for a convex lens and negative $f < 0$ for a concave lens, is described by the matrix $\underline{\underline{m}}^{(L)}$:

$$\begin{bmatrix} x' \\ p' \end{bmatrix} = \underline{\underline{m}}^{(L)} \begin{bmatrix} x \\ p \end{bmatrix} = \begin{bmatrix} x \\ p + \rho x \end{bmatrix},$$

$$\underline{\underline{m}}^{(L)} \equiv \underline{\underline{m}}^{(L)}(\rho) = \begin{bmatrix} 1 & 0 \\ \rho & 1 \end{bmatrix}, \tag{2.69}$$

with the lower off-diagonal term $\rho = -f^{-1}$ equal to the minus reciprocal of the scaled focal length f of the lens. The generalised momentum or the direction of the optical ray is then angularly displaced or tilted by ρx. Note that, for $f = -2/R$ and $\rho = R/2$, the matrix transformation $\underline{\underline{m}}^{(L)}$ describes also action of a spherical mirror with radius of curvature R.

Other optical transformations commonly encountered in optics are the phase-shift, the magnification and the rotation. The optical phase-shifter introduces relative phase difference μ between the phase-space coordinates and is given by the matrix $\underline{\underline{m}}^{(P)}$:

$$\begin{bmatrix} x' \\ p' \end{bmatrix} = \underline{\underline{m}}^{(P)}(\mu) \begin{bmatrix} x \\ p \end{bmatrix} = \begin{bmatrix} x \exp(-i\mu/2) \\ p \exp(+i\mu/2) \end{bmatrix},$$

$$\underline{\underline{m}}^{(P)} \equiv \underline{\underline{m}}^{(P)}(\mu) = \begin{bmatrix} \exp(-i\mu/2) & 0 \\ 0 & \exp(+i\mu/2) \end{bmatrix}. \tag{2.70}$$

Action of the magnifier that scales x by the factor $w = \exp(+\xi/2)$ and p_x by $w^{-1} = \exp(-\xi/2)$, is given by the matrix $\underline{\underline{m}}^{(M)}$,

$$\begin{bmatrix} x' \\ p' \end{bmatrix} = \underline{\underline{m}}^{(M)}(\xi) \begin{bmatrix} x \\ p \end{bmatrix} = \begin{bmatrix} x \exp(+\xi/2) \\ p \exp(-\xi/2) \end{bmatrix},$$

$$\underline{\underline{m}}^{(M)} \equiv \underline{\underline{m}}^{(M)}(\xi) = \begin{bmatrix} \exp(+\xi/2) & 0 \\ 0 & \exp(-\xi/2) \end{bmatrix}, \tag{2.71}$$

and the rotation in the phase space about the z-axis by an angle $\varphi/2$ is given by the matrix $\underline{\underline{m}}^{(R)}$:

$$\begin{bmatrix} x' \\ p' \end{bmatrix} = \begin{bmatrix} x\cos(\varphi/2) - p\sin(\varphi/2) \\ x\sin(\varphi/2) + p\cos(\varphi/2) \end{bmatrix},$$

$$\underline{\underline{m}}^{(R)} \equiv \underline{\underline{m}}^{(R)}(\varphi) = \begin{bmatrix} \cos(\varphi/2) & -\sin(\varphi/2) \\ \sin(\varphi/2) & \cos(\varphi/2) \end{bmatrix}. \tag{2.72}$$

The angle φ is taken positive when a right-handed screw associated with this rotation (in the x-y plane) is advancing in the positive direction of the z-axis.

An arbitrary first-order optical system may be regarded as composed of several optical elements, represented by such the ray-transfer matrices. A cascade of these elements whose ray-transfer matrices are $\underline{\underline{m}}^{(1)}$, $\underline{\underline{m}}^{(2)}$,…, $\underline{\underline{m}}^{(m)}$ is then equivalent to a single first-order optical element with the ray-transfer matrix $\underline{\underline{m}}$ given by the matrix multiplication in reverse order,

$$\underline{\underline{m}} = \underline{\underline{m}}^{(m)} \ldots \underline{\underline{m}}^{(2)} \underline{\underline{m}}^{(1)} . \tag{2.73}$$

Consider now the reverse problem – having postulated the total ray-transfer matrix $\underline{\underline{m}}$ known, find an optical system composed of optical elements represented by $\underline{\underline{m}}^{(j)}$, j=1,2,…, which yield the total matrix $\underline{\underline{m}}$ according to (2.73). The problem is not unique - there are several equivalent decompositions of an arbitrary unimodular matrix $\underline{\underline{m}}$. For instance, any non-singular matrix can be decomposed into a product of two matrices, one Hermitian and one unitary, what implies that any two-by-two unimodular matrix $\underline{\underline{m}}$ decomposes into the product of one Hermitian matrix and one rotation matrix.

However, the decomposition of other type appeared especially suitable in considerations of the behaviour of optical beams in optical systems. It is the lens-magnifier-rotation decomposition, known also as the Iwasawa three-parameter decomposition [27,33]:

$$\underline{\underline{m}} = \underline{\underline{m}}^{(L)}(\rho)\underline{\underline{m}}^{(M)}(\xi)\underline{\underline{m}}^{(R)}(-\varphi) . \tag{2.74}$$

According to the decomposition (2.74), action of first-order optical systems can be interpreted in terms of successive actions of the basic optical elements - the rotator, the magnifier and the lens - performed in the phase space of positions and tilts of rays of the optical beam fields propagating in these systems.

2.6 Optical canonical transforms

Consider the Hilbert space of square-integrable complex-valued functions $E(x,y,z)$, in any transverse plane $z = \text{constant}$ and define the position $\hat{x}$, $\hat{y}$ and momentum $\hat{p}_x$, $\hat{p}_y$ canonically conjugate operators in the input plane $z = 0$ of the optical system:

$$\hat{x}\,E(x,y,0) = x\,E(x,y,0)\,,$$

$$\hat{p}_x\,E(x,y,0) = -i\partial_x\,E(x,y,0) = p_x\,E(x,y,0)\,, \tag{2.75}$$

$$\hat{y}\,E(x,y,0) = y\,E(x,y,0)\,,$$

$$\hat{p}_y\,E(x,y,0) = -i\partial_y\,E(x,y,0) = p_y\,E(x,y,0)\,, \tag{2.76}$$

where $\iint dxdy|\,E(x,y,z)|^2 < \infty$. The upper hat denotes an operator. These Hermitian operators correspond to the position x, y and momentum p_x, p_y phase-space coordinates of optical rays introduced in Section 4. They satisfy the commutation relations [27]:

$$[\hat{x},\hat{p}_x] = i = \lfloor\hat{y},\hat{p}_y\rfloor, \tag{2.77}$$

$$\lfloor\hat{x},\hat{p}_y\rfloor = 0 = [\hat{y},\hat{p}_x], \tag{2.78}$$

where, for arbitrary operators $\hat{q}$ and $\hat{p}$,

$$[\hat{q},\hat{p}] \equiv \hat{q}\hat{p} - \hat{p}\hat{q} \tag{2.79}$$

stands for a commutator of these operators.

The canonically conjugate position and momentum operators $\hat{x}$, $\hat{y}$, $\hat{p}_x$ and $\hat{p}_y$ (2.75)-(2.76) have been defined in the input plane at $z = 0$. In another transverse plane, say in the output plane, they may take, in general, another form, as it will be explicitly postulated in Equation (2.86). Therefore a form of these operators is changing from one transverse plane to another and thus it depends on z. These changes are induced by a transfer operator of the system $\underline{\underline{\hat{m}}}_\perp$ defined in Equation (2.82) below. The operators $\hat{x}$, $\hat{y}$, $\hat{p}_x$ and $\hat{p}_y$ can be arranged in two two-dimensional column vectors

$$\underline{\hat{\eta}}_x(z) = \begin{bmatrix} \hat{x}(z) \\ \hat{p}_x(z) \end{bmatrix},$$

$$\underline{\hat{\eta}}_y(z) = \begin{bmatrix} \hat{y}(z) \\ \hat{p}_y(z) \end{bmatrix}, \tag{2.80}$$

or in one four-dimensional column vector

$$\underline{\hat{\eta}}_{\perp}(z)=\begin{bmatrix}\underline{\hat{\eta}}_{x}(z)\\ \underline{\hat{\eta}}_{y}(z)\end{bmatrix}, \tag{2.81}$$

now written in an arbitrary transverse plane at $z=const.$

Define a linear transfer operator $\underline{\underline{\hat{m}}}_{\perp}\equiv\underline{\underline{\hat{m}}}_{\perp}(z)$ of the first-order separable optical system, that relates the input beam-field-amplitude $E(x,y,0)$ given in the input transverse plane taken at $z=0$, to the output beam-field-amplitude $E(x,y,z)$ obtained in the output transverse plane at arbitrary $z=const.$:

$$E(x,y,z)=\underline{\underline{\hat{m}}}_{\perp}(z)\,E(x,y,0),$$

$$\underline{\underline{\hat{m}}}_{\perp}=\begin{bmatrix}\underline{\underline{\hat{m}}}_{x} & 0\\ 0 & \underline{\underline{\hat{m}}}_{y}\end{bmatrix}. \tag{2.82}$$

Next, postulate the integral form of $\underline{\underline{\hat{m}}}_{\perp}(z)$,

$$\underline{\underline{\hat{m}}}_{\perp}(z)\,E(x,y,0)=\iint dx'dy'\,g(x,y\,|\,x',y';z)E(x',y',0), \tag{2.83}$$

involving an impulse-transfer (impulse-response) function $g(x,y\,|\,x',y';z)$ of the optical system [2]. Then, the condition $E(x,y,z)=E(x,y,0)$ at $z=0$ implies:

$$g(x,y\,|\,x',y';0)=\delta(x-x')\delta(y-y'). \tag{2.84}$$

The definitions of the canonically conjugate operators (2.75)-(2.76) describe the action of these operators $\underline{\hat{\eta}}_{\perp}(0)$ on the field function $E(x,y,0)$ in the input plane at $z=0$.

Define this action in the output plane at $z=const.$ by the ray-transfer operator $\underline{\underline{\hat{m}}}_{\perp}(z)$ [20],

$$\underline{\hat{\eta}}_{\perp}(z)E(x,y,z)=\underline{\underline{\hat{m}}}_{\perp}(z)\underline{\hat{\eta}}_{\perp}(0)E(x,y,0), \tag{2.85}$$

or equivalently by the self-similar relation:

$$\underline{\hat{\eta}}_{\perp}(z)=\underline{\underline{\hat{m}}}_{\perp}(z)\underline{\hat{\eta}}_{\perp}(0)\underline{\underline{\hat{m}}}_{\perp}^{-1}(z). \tag{2.86}$$

The definition (2.86) states that the operators $\hat{\underline{\eta}}_{\perp}$, one defined in the input plane $z=0$ and one in the output plane $z=const.$, are equivalent or self-similar.

What we expect now is that the self-similar transformation (2.86) of the vector $\hat{\underline{\eta}}_{\perp}$ (2.81) of the conjugated pairs of operators $\hat{x}$, $\hat{p}_x$ and $\hat{y}$, $\hat{p}_y$, induced by the operator transformation $\hat{\underline{\underline{m}}}_{\perp}$ of the beam-field-amplitude $E(x,y,z)$ (2.82) or, equivalently, by the matrix transformation $\underline{\underline{m}}_{\perp}$ (2.61) of the ray-data vector $\underline{\eta}_{\perp}$ (2.60), is canonical. This means that the operators $\hat{x}$, $\hat{p}_x$ and $\hat{y}$, $\hat{p}_y$ given in any transverse plane are (i) linear superposition of these operators given in the input plane and (ii) satisfy the commutation relations (2.77)-(2.78) in any transverse plane of the optical system. The condition (ii) implies that the linear ray-transfer transformation $\underline{\underline{m}}_{\perp}$ should be symplectic (2.59) or, in separable optical systems, unimodular (2.65) ($\det \underline{\underline{m}}_{\perp}=1$). Moreover, in addition to the action of the ray-transfer matrix $\underline{\underline{m}}_{\perp}$ on the ray-data vectors $\underline{\eta}_{\perp}$:

$$\underline{\eta}_{\perp}(z)=\underline{\underline{m}}_{\perp}(z)\underline{\eta}_{\perp}(0), \tag{2.87}$$

the equivalent transformation of the vector $\hat{\underline{\eta}}_{\perp}$ exists [20,27]:

$$\hat{\underline{\eta}}_{\perp}(z)=\underline{\underline{m}}_{\perp}^{-1}(z)\hat{\underline{\eta}}_{\perp}(0). \tag{2.88}$$

The definitions (2.85)-(2.88) display the explicit correspondence between the symplectic matrices $\underline{\underline{m}}_{\perp}$ (2.62) and the canonical transfer operators $\hat{\underline{\underline{m}}}_{\perp}$ (2.83) [20]. It is a homomorphism; an algebraic structure of the group of symplectic matrices is preserved under this correspondence. However globally it is not an isomorphism; this correspondence is not one to one - the two operators $\hat{\underline{\underline{m}}}_{\perp}$ and $-\hat{\underline{\underline{m}}}_{\perp}$ represent the same matrix $\underline{\underline{m}}_{\perp}$. In spite of that, the definitions (2.85)-(2.88) state that the transfer operator $\hat{\underline{\underline{m}}}_{\perp}$, that transforms the beam field amplitude $E(x,y,0)$ from the input plane to the beam field amplitude $E(x,y,z)$ in the output plane of a first-order optical system, is canonical.

For separable optical systems with cylindrical symmetry, the transformation (2.88) is explicitly given by only one two-dimensional *abcd* ray-transfer matrix of the system [20]:

$$\underline{\hat{\eta}}_x(z)=\begin{bmatrix}\hat{x}(z)\\ \hat{p}_x(z)\end{bmatrix}=\begin{bmatrix}d & -b\\ -c & a\end{bmatrix}\begin{bmatrix}\hat{x}(0)\\ \hat{p}_x(0)\end{bmatrix}=\underline{\underline{m}}_x^{-1}(z)\underline{\hat{\eta}}_x(0),$$

$$\underline{\hat{\eta}}_y(z)=\begin{bmatrix}\hat{y}(z)\\ \hat{p}_y(z)\end{bmatrix}=\begin{bmatrix}d & -b\\ -c & a\end{bmatrix}\begin{bmatrix}\hat{y}(0)\\ \hat{p}_y(0)\end{bmatrix}=\underline{\underline{m}}_y^{-1}(z)\underline{\hat{\eta}}_y(0), \tag{2.89}$$

where the equality of the ray-transfer matrices $\underline{\underline{m}}_x=\underline{\underline{m}}_y=\underline{\underline{m}}$ entails the same relation for the transfer operators: $\underline{\underline{\hat{m}}}_x=\underline{\underline{\hat{m}}}_y=\underline{\underline{\hat{m}}}$. It can directly be shown [20] that, for the nonsingular case ($b\neq 0$), the outcome of the action (2.82)–(2.83) of the transfer operator $\underline{\underline{\hat{m}}}_\perp(z)$ on the beam field distribution $E(x,y,0)$ at the transverse input plane at $z=0$ can be described by the beam field distribution $E(x,y,z)$ at the transverse output plane at $z=const.$ This leads to the integral form [20]:

$$E(x,y,z)=\iint dx'dy'\,g(x,y\,|\,x',y';z)E(x',y',0). \tag{2.90}$$

An impulse-response function of the system is given by the kernel $g(x,y\,|\,x',y';z)$ of this integral,

$$g(x,y\,|\,x',y';z)=(i2\pi b)^{-1}\exp[iI(x,y\,|\,x',y';z)], \tag{2.91}$$

with the phase term determined by the *abcd* matrix:

$$I(x,y\,|\,x',y';z)=\tfrac{1}{2}[d(x^2+y^2)-2(xx'+yy')+a(x'^2+y'^2)]/b. \tag{2.92}$$

This phase term is known as a point characteristic of a first-order system [21]. For z=0 $\underline{\underline{m}}=\underline{\underline{I}}$, $a=c=1$, $b\to 0$, as it should be, and the response function converts into the two-dimensional Dirac function, according to the stipulation (2.84),

$$\begin{aligned}&\delta(x-x')\delta(y-y')\\ &=\lim_{b\to 0}(2\pi ib)^{-1}\exp\{-\tfrac{1}{2}(ib)^{-1}[(x-x')^2+(y-y')^2]\}.\end{aligned} \tag{2.93}$$

The beam field representation (2.90)-(2.92) is known as the generalised Huygens integral [20]. For the singular case, that is in the case, when the upper-right non-diagonal element of the *abcd* matrix equals zero ($b = 0$), the integral representation (2.90)-(2.92) is replaced by a simple algebraic relation [27]:

$$E(x, y, 0) = (|a|/a^2)\exp[\tfrac{i}{2}(c/a)(x^2 + y^2)]E(x/a, y/a, 0). \tag{2.94}$$

Any transfer operator $\underline{\underline{\hat{m}}}$ can be decomposed in several ways into basic optical operators, per analogy to decompositions of the ray-transfer matrices $\underline{\underline{m}}$ mentioned in Section 5. For example, the Iwasawa decomposition (2.74) of the transfer matrix $\underline{\underline{m}}$, entails the same decomposition of the transfer operator $\underline{\underline{\hat{m}}}$ and $\underline{\underline{\hat{m}}}_{\perp}$:

$$\underline{\underline{\hat{m}}} = \underline{\underline{\hat{m}}}^{(L)}(\rho)\underline{\underline{\hat{m}}}^{(M)}(w)\underline{\underline{\hat{m}}}^{(R)}(-\varphi),$$

$$\underline{\underline{\hat{m}}}_{\perp} = \underline{\underline{\hat{m}}}_{\perp}^{(L)}(\rho)\underline{\underline{\hat{m}}}_{\perp}^{(M)}(w)\underline{\underline{\hat{m}}}_{\perp}^{(R)}(-\varphi). \tag{2.95}$$

Therefore, action of any first-order optical system can be described by successive actions of three basic transfer operators on the beam field distribution at the input plane, that is the action of the lens $\underline{\underline{\hat{m}}}_{\perp}^{(L)}$,

$$\underline{\underline{\hat{m}}}_{\perp}^{(L)}(\rho)E(x, y, 0) = \exp[\tfrac{i}{2}\rho^{-1}(x^2 + y^2)]E(x, y, 0), \tag{2.96}$$

the magnifier $\underline{\underline{\hat{m}}}_{\perp}^{(M)}$,

$$\underline{\underline{\hat{m}}}_{\perp}^{(M)}(w)E(x, y, 0) = w^{-1}E(xw^{-1}, yw^{-1}, 0), \tag{2.97}$$

where we have changed the argument of this operator from ξ to $w = \exp(\xi/2)$, and the rotator $\underline{\underline{\hat{m}}}_{\perp}^{(R)}$,

$$\underline{\underline{\hat{m}}}_{\perp}^{(R)}(-\varphi)E(x, y, 0) = (i/2\pi\sin(\varphi/2))\iint dx'\,dy'\,E(x', y', 0)$$
$$\exp\left\{-\tfrac{i}{2}[(x^2 + y^2)\cos(\varphi/2) - 2(xx' + yy') + \cos(\varphi/2)(x'^2 + y'^2)]/\sin(\varphi/2)\right\}. \tag{2.98}$$

For $\varphi = -\pi$ one gets $\underline{\underline{m}}^{(R)}(\pi) = \underline{\underline{I}}$ and the rotator induces the Fourier transformation,

$$\hat{\underline{\underline{m}}}^{(R)}(\pi)E(x,y,0) = (i/2\pi)\,\tilde{E}(x,y,0)\,, \tag{2.99}$$

where $\tilde{E}$ means the conventional two-dimensional Fourier transform of E,

$$\tilde{E}(x,y,0) = \iint dx'dy'\,E(x',y',0)\exp[i(xx'+yy')]\,. \tag{2.100}$$

Otherwise, for arbitrary values of φ, the rotator is equivalent to the fractional Fourier transform in two dimensions, of the order $-\varphi/\pi$. For example, if $\varphi/\pi = 1/2$, then the rotator is a square root of the Fourier transformation.

The operators $\hat{\underline{\underline{m}}}_{\perp}^{(L)}(\rho)$, $\hat{\underline{\underline{m}}}_{\perp}^{(M)}(\xi)$ and $\hat{\underline{\underline{m}}}_{\perp}^{(R)}(-\varphi)$ can be explicitly related to the position $\hat{x}$, $\hat{y}$ and momentum $\hat{p}_x$, $\hat{p}_y$ operators by three Hermitian operators [27]:

$$\hat{j}_2 = -\tfrac{1}{4}(\hat{x}^2 + \hat{y}^2 + \hat{p}_x^2 + \hat{p}_y^2)\,, \tag{2.101}$$

$$\hat{k}_1 = -\tfrac{1}{4}(\hat{x}^2 + \hat{y}^2 - \hat{p}_x^2 - \hat{p}_y^2)\,, \tag{2.102}$$

$$\hat{k}_3 = \tfrac{1}{4}(\hat{x}\hat{p}_x + \hat{y}\hat{p}_y + \hat{p}_x\hat{x} + \hat{p}_y\hat{y})\,, \tag{2.103}$$

which, through their exponentials, generate three unitary transformations applied in the Iwasawa decomposition (2.95):

$$\hat{\underline{\underline{m}}}_{\perp}^{(L)}(\rho) = \exp(-i\rho^{-1}(\hat{\underline{\underline{j}}}_2 + \hat{\underline{\underline{k}}}_1))\,, \tag{2.104}$$

$$\hat{\underline{\underline{m}}}_{\perp}^{(M)}(m) = \exp(-i\xi\hat{\underline{\underline{k}}}_3)\,, \tag{2.105}$$

$$\hat{\underline{\underline{m}}}_{\perp}^{(R)}(-\varphi) = \exp(-i\varphi\hat{\underline{\underline{j}}}_2)\,. \tag{2.106}$$

On the ground of the relations (2.86) and (2.88), the action of the transfer operators $\hat{\underline{\underline{m}}}_{\perp}$ is related to the action of the ray-transfer matrices $\underline{\underline{m}}_{\perp}$ by the identity [20,27]:

$$\hat{\underline{\underline{m}}}_{\perp}(z)\hat{\underline{\eta}}_{\perp}(0)\hat{\underline{\underline{m}}}_{\perp}^{-1}(z) = \underline{\underline{m}}_{\perp}^{-1}(z)\hat{\underline{\eta}}_{\perp}(0)\,. \tag{2.107}$$

Hence the canonical transformations $\hat{\underline{\underline{m}}}_{\perp}$ of beam amplitudes distributed across transverse planes of any first-order symmetric optical system

correspond to members of a three-parameter symplectic group represented by unimodular matrices $\underline{\underline{m}}_{\perp}$. We will return to this group representation in the discussion on transformations of beam polarization.

2.7 Hermite-Gaussian beams

There are several families of beams, for instance: Hermite-Gaussian and Laguerre-Gaussian beams [3,6], generalized Gaussian beams [34], Bessel-Gaussian beams [35], [36], spiral Laguerre-Gaussian beams [37] or Hermite-Laguerre-Gaussian beams [38], which propagate through first-order optical systems according to the paraxial wave equation. Their propagation is shape-invariant, that is they do not change their transverse shape in spite of scaling their beam-field parameters and changes of their on-axis amplitude and phase. In this chapter two basic families of such beams will be considered, one of rectangular symmetry and one of cylindrical symmetry in their field amplitude distribution in the transverse planes, namely the standard Hermite-Gaussian (SHG) and the standard Laguerre-Gaussian (SLG) beams, respectively [6]. As they can be generated in standard laser cavities, their features are commonly well known and have been extensively discussed in many textbooks, for example in [3-6]. Here we will show how their field amplitude is determined by the ray-transfer matrix of the paraxial propagation in a dielectric infinite medium.

The ray-transfer matrix of beam propagation in free space:

$$\underline{\underline{m}}_{\perp}^{(F)}(z)=\begin{bmatrix}\underline{\underline{m}}^{(F)}(z) & 0\\ 0 & \underline{\underline{m}}^{(F)}(z)\end{bmatrix}, \tag{2.108}$$

$$\underline{\underline{m}}^{(F)}(z)=\begin{bmatrix}1 & z\\ 0 & 1\end{bmatrix}, \tag{2.109}$$

leads, through the Huygens integral (2.90)-(2.92) to Fresnel integral formula for the field of a optical beam:

$$\begin{aligned}&E(x,y,z)=\hat{\underline{\underline{m}}}_{\perp}^{(F)}(z)\,E(x,y,0)\\&=(-i/2\pi z)\iint dx'dy'E(x',y',0)\exp\left\{\tfrac{i}{2}[(x-x')^2+(y-y')^2]/z\right\}.\end{aligned} \tag{2.110}$$

Assume that in the input plane the beam field has a form of the two-dimensional fundamental Gaussian-beam-function modulated by Hermite polynomials $H_m(x)$ and $H_n(y)$:

$$E(x,y,0) = G_{m,n}^{(SH)}(x,y,0) = c_{m,n} H_m(x) H_n(y) \exp[-\tfrac{1}{2}(x^2+y^2)], \quad (2.111)$$

where the Hermite polynomials are defined as:

$$H_m(x) = (-1)^m \exp(+x^2)(d^m/dx^m)\exp(-x^2). \quad (2.112)$$

The function $G_{m,n}^{(SH)}(x,y,0)$ is exactly the two-dimensional standard Hermite-Gaussian (SHG) function of the order N=m+n [3-6]. It describes the SHG beam at its waist plane, taken here at $z=0$. The SHG beam (2.111), through the amplitude normalisation factor [23]

$$c_{m,n} = (2^{m+n}\pi m!n!)^{-1/2}, \quad (2.113)$$

can be normed in intensity to one:

$$\iint dxdy \left| G_{m,n}^{SH}(x,y,z) \right|^2 = 1. \quad (2.114)$$

This implies that the amplitude of the normed fundamental SHG beam, that is for n=0=m, is equal $\pi^{-1/2}$ at the centre of its waist at $x=y=z=0$.

The SHG function $G_{m,n}^{(SH)}(x,y,0)$ in two dimensions factorises into two one-dimensional SHG functions,

$$G_{m,n}^{(SH)}(x,y,0) = G_m^{(SH)}(x,0) G_n^{(SH)}(y,0), \quad (2.115)$$

$$G_m^{(SH)}(x,0) = \pi^{-1/4}(m!)^{-1/2} H_m(x) \exp(-\tfrac{1}{2}x^2), \quad (2.116)$$

$$G_n^{(SH)}(y,0) = \pi^{-1/4}(n!)^{-1/2} H_n(y) \exp(-\tfrac{1}{2}y^2), \quad (2.117)$$

of the orders m and n, respectively. Note that the left-hand side of Eq. (2.115) is separated in the coordinates x and y and thus the 2D problem can be solved by solving separately two identical 1D problems. Therefore, let us temporarily restrict our considerations only to one 1D problem with one coordinate x. The one-dimensional SHG function $G_m^{(SH)}(x,0)$ is a solution of the differential equation:

$$\tfrac{1}{2}(x^2 - \partial_x^2 - 1)G_m^{(SH)}(x,0) = m\,G_m^{(SH)}(x,0)\,, \tag{2.118}$$

or, equivalently, an eigenfunction of the number operator $\hat{N}_x$, with the eigenvalue m equal to the order m of this function,

$$\hat{N}_x G_m^{(SH)}(x,0) = m\,G_m^{(SH)}(x,0)\,. \tag{2.119}$$

The operator $\hat{N}_x$ can be expressed by the ladder differential operators $\hat{a}_x^{\pm}$:

$$\hat{N}_x = \hat{a}_x^{+}\hat{a}_x^{-}, \tag{2.120}$$

$$\hat{a}_x^{\pm} = 2^{-1/2}(x \mp \partial_x)\,, \tag{2.121}$$

where $\hat{a}_x^{+}$ is Hermitian transpose of $\hat{a}_x^{-}$ [23]. As the ladder operators obey the standard commutation rules:

$$[\hat{a}_x^{-}, \hat{a}_x^{+}] = 1,$$

$$[\hat{a}_x^{-}, \hat{a}_x^{-}] = 0 = [\hat{a}_x^{+}, \hat{a}_x^{+}], \tag{2.122}$$

they lower and rise the order of the SHG functions:

$$\hat{a}_x^{-} G_m^{(SH)}(x,0) = m^{1/2} G_{m-1}^{(SH)}(x,0)\,, \tag{2.123}$$

$$\hat{a}_x^{+} G_m^{(SH)}(x,0) = (m+1)^{1/2} G_{m+1}^{(SH)}(x,0)\,. \tag{2.124}$$

Hence, the higher-order SHG beams $G_m^{(SH)}(x,0)$ can be obtained from the fundamental (of zero order) beam $G(x,0)$ by applying consecutively the raising operator $\hat{a}_x^{+}$,

$$G_m^{(SH)}(x,0) = (n!)^{-1/2}(\hat{a}_x^{+})^m G_0^{(SH)}(x,0) \tag{2.125}$$

to the fundamental Gaussian beam function:

$$G_0^{(SH)}(x,0) = \pi^{-1/4} G(x,0) = \pi^{-1/4} \exp(-\tfrac{1}{2}x^2)\,. \tag{2.126}$$

The higher-order beams $G_m^{(SH)}(x,0)$, m=1,2,…, together with the fundamental beam $G_0^{(SH)}(x,0)$, constitute a complete set of solutions of the one-dimensional paraxial wave equation [23].

With the differential equation (2.118) in its two-dimensional version in mind we may consider the two-dimensional SGH function $G_{m,n}^{(SH)}(x,y,0)$ as an eigenstate of the operator $\underline{\underline{\hat{j}}}_2$:

$$\underline{\underline{\hat{j}}}_2 G_{m,n}^{(SH)}(x,y,0) = -\tfrac{1}{2}(m+n+1) G_{m,n}^{(SH)}(x,y,0), \tag{2.127}$$

where

$$\underline{\underline{\hat{j}}}_2 = -\tfrac{1}{4}(x^2 + y^2 - \partial_x^2 - \partial_y^2). \tag{2.128}$$

In fact, the operator $\underline{\underline{\hat{j}}}_2$ corresponds to the Hamiltonian operator $\underline{\underline{\hat{H}}}$ of a two-dimensional isotropic oscillator with eigenvalues equal m+n+1:

$$\underline{\underline{\hat{H}}} = -2\underline{\underline{\hat{j}}}_2 = \tfrac{1}{2}(x^2 + y^2 - \partial_x^2 - \partial_y^2). \tag{2.129}$$

Moreover, the operator $\underline{\underline{\hat{j}}}_2$ generates, through its exponential $\underline{\underline{\hat{m}}}_{\perp}^{(R)}(\varphi) = \exp(-i\varphi \underline{\underline{\hat{j}}}_2)$, rotation in the phase-space by an angle $\varphi/2$. Therefore, the SHG functions are also eigenstates of the operator $\underline{\underline{\hat{m}}}_{\perp}^{(R)}(-\varphi)$ with eigenvalues $\exp(-i\varphi_{m,n}(z))$:

$$\underline{\underline{\hat{m}}}_{\perp}^{(R)}(-\varphi) G_{m,n}^{(SH)}(x,y,0) = \exp(-\tfrac{i}{2}\varphi_{m,n}(z)) G_{m,n}^{(SH)}(x,y,0),$$

$$\varphi_{m,n}(z) = (m+n+1)\varphi(z). \tag{2.130}$$

The phase $\frac{1}{2}\varphi_{m,n}(z)$ is the well-known Gouy on-axis phase of the SHG beam of the order m+n, [2-7]. The phase function $\varphi(z)$ is still to be found under the condition that $\varphi(0) = 0$ at the input plane $z = 0$, as the beams $G_{m,n}^{(SH)}(x,y,0)$, m, n=1,2,…, have been defined above only in one plane - the input plane at $z = 0$.

Now we are prepared to consider the propagation of the beam field, defined by the distribution (2.111) of the SHG beam in the input plane. Characteristics of this propagation are completely determined by the ray-transfer matrix of this system. To show this let us apply the Iwasawa decomposition (2.74) defined as:

$$\underline{\underline{m}}_{\perp}^{(F)}(z) = \underline{\underline{m}}_{\perp}^{(L)}(\rho)\underline{\underline{m}}_{\perp}^{(M)}(w)\underline{\underline{m}}_{\perp}^{(R)}(-\varphi), \tag{2.131}$$

to the free-space ray-transfer matrix [27], that is solve the algebraic equation

$$\begin{bmatrix} 1 & z \\ 0 & 1 \end{bmatrix} = \begin{bmatrix} 1 & 0 \\ \rho^{-1} & 1 \end{bmatrix} \begin{bmatrix} w & 0 \\ 0 & w^{-1} \end{bmatrix} \begin{bmatrix} \cos(\varphi/2) & \sin(\varphi/2) \\ -\sin(\varphi/2) & \cos(\varphi/2) \end{bmatrix} \tag{2.132}$$

in terms of the beam parameters ρ, w and φ. Note that all these parameters are dependent on the propagation distance z. The solution is:

$$\rho \equiv \rho(z) = z + z^{-1}, \tag{2.133}$$

$$w \equiv w(z) = (1 + z^2)^{1/2}, \tag{2.134}$$

$$\tfrac{1}{2}\varphi \equiv \tfrac{1}{2}\varphi(z) = \arctan(z), \tag{2.135}$$

with the beam waist at $z = 0$ and with the relation

$$\rho(z)\sin\varphi(z) = 2 \tag{2.136}$$

equivalent to the unimodularity of the ray-transfer matrix (2.132); $\det \underline{\underline{m}}_{\perp}^{(F)}(z) = 1$. The Gouy on-axis phase of the fundamental Gaussian beam increases its value by π between $z = -\infty$ and $z = +\infty$.

As it will be evident later, ρ denotes the radius of phase front curvature of the beam, w stands for the radius of the beam cross-section (beam half-width) and the phase $\varphi(z)/2$ is the well-known Gouy on-axis phase of the fundamental SHG beam [2-7]. For further purposes we define also the complex radius of the beam:

$$v \equiv v(z) = (1 + iz)^{1/2}, \tag{2.137}$$

which also yields the radii w and ρ, and the phase φ,

$$v(z)\bar{v}(z) = w(z), \tag{2.138}$$

$$\bar{v}(z)/v(z) = \exp(-i\varphi(z)/2), \tag{2.139}$$

$$v^{-2}(z) = w^{-2}(z) - i\rho^{-1}(z) = w^{-1}(z)\exp[-i\varphi(z)/2]. \tag{2.140}$$

Now, with the beam parameters (2.133) - (2.140) known, let us apply the operator of the beam propagation in free space $\underline{\underline{\hat{m}}}^{(F)}(z)$ in its Iwasawa decomposition (2.131) to the beam field $G_{m,n}^{(SH)}(x,y,0)$ given in the input plane:

$$\begin{aligned}&\underline{\underline{\hat{m}}}_{\perp}^{(F)}(z)G_{m,n}^{(SH)}(x,y,0)\\&=c_{m,n}\exp(-\tfrac{i}{2}\varphi_{m,n})w^{-1}\exp[\tfrac{i}{2}\rho^{-1}(x^2+y^2)]G_{m,n}^{(SH)}(x/w,y/w,0).\end{aligned}\tag{2.141}$$

We then finally get the SHG beam field with its three parameters ρ, w and $\varphi_{m,n}$, all dependent implicitly on z:

$$\begin{aligned}&G_{m,n}^{(SH)}(x,y,z)=c_{m,n}\exp(-\tfrac{i}{2}\varphi_{m,n})w^{-1}\\&\times\exp[\tfrac{i}{2}\rho^{-1}(x^2+y^2)]H_m(x/w)H_n(y/w)\exp[-\tfrac{1}{2}(x^2+y^2)/w^2]\end{aligned}.\tag{2.142}$$

The SHG functions $G_{m,n}^{SH}(x,y,z)$ are eigensolutions of the Hamiltonian $\underline{\underline{\hat{\mathrm{H}}}}$ (2.129) with the eigenvalue m+n+1:

$$i\partial_{\varphi/2}G_{m,n}^{(SH)}(x,y,z)=\underline{\underline{\hat{\mathrm{H}}}}G_{m,n}^{(SH)}(x,y,z)=(m+n+1)G_{m,n}^{(SH)}(x,y,z),$$

$$G_{m,n}^{(SH)}(x,y,z)=(m!n!)^{-1/2}(\hat{a}_x^{+})^m(\hat{a}_y^{+})^nG_{0,0}^{(SH)}(x,y,z),\tag{2.143}$$

and with their lowering $\hat{a}_x^{-}$ and rising $\hat{a}_x^{+}$ operators:

$$\hat{a}_x^{-}(z)=2^{-1/2}[x+v^2\partial_x],$$

$$\hat{a}_x^{+}(z)=2^{-1/2}[x-\bar{v}^2\partial_x],\tag{2.144}$$

still obeying their relations (2.123)-(2.125) given before in the beam waist plane $z=0$ [23]. Outside the beam waist plane these operators are dependent on the propagation distance z. The functions $G_{m,n}^{(SH)}(x,y,z)$ form a complete set of solutions of the Schrödinger equation (2.143) equivalent to the paraxial wave equation (2.29) in free space.

Finally, the definition (2.137) of the complex radius of the beam $v(z)$ yields a more compact form of the SHG beam field:

$$G_{m,n}^{(SH)}(x,y,z)=c_{m,n}H_m(x/w)H_n(y/w)(\bar{v}/v)^{m+n}G(x/v,y/v,z),$$

$$G(x/v, y/v, z) = c_{0,0}^{-1} G_{0,0}^{(SH)}(x, y, z) = v^{-2} \exp[-\tfrac{1}{2}(x^2 + y^2)v^{-2}], \qquad (2.145)$$

where $G(x/v, y/v, z)$; $G(0,0,0) = 1$, is the well-known two-dimensional fundamental Gaussian beam defined for arbitrary value of z. In this way the Equation (2.145) defines the SHG beam at any transverse plane of the first-order optical system. The SHG beam-field-function is scaled in the transverse coordinates x and y and possesses the additional on-axis phase factor $(\overline{v}/v)^{m+n}$. Note that the scaling parameters w and v are dependent on z and both resolve into the (real) beam half-width at the beam waist for $z = 0$ (equal one in the convention assumed in this chapter). The scaling parameters are different for the fundamental Gaussian beam and the Hermite polynomials. Meanwhile these coordinates in the Gaussian function $G(x/v, y/v, z)$ are scaled by the complex beam half-width v, they are scaled by the real beam width w in the Hermite functions $H_m(x/w)$ and $H_n(y/w)$.

The ladder rising operators $\hat{a}_x^+$ and $\hat{a}_y^+$ have been defined in the Cartesian coordinates x and y. Per analogy, however, a new complete set of solutions of the paraxial equation can be also obtained with the aid of the ladder rising operators $\hat{a}_\pm^+$ defined in the circular polarization basis [23]:

$$G_{p,l}^{(SL)}(x, y, z) = (n_+! n_-!)^{-1/2} (\hat{a}_+^+)^{n_+} (\hat{a}_-^+)^{n_-} G_{0,0}^{(SH)}(x, y, z),$$
$$\hat{a}_\pm^+ = 2^{-1/2} (\hat{a}_x^+ \pm i\hat{a}_y^+), \qquad (2.146)$$

where $p = \min(n_+, n_-)$ and $l = n_+ - n_-$. The functions $G_{p,l}^{(SL)}(x, y, z)$ represent the SLG beams and these beams will be described in the next section.

2.8 Laguerre-Gaussian beams

The SHG beams form a complete, orthogonal, infinite-dimensional base for any scalar paraxial beam field, with its transverse distribution represented by a square integrated function. That is, any light beam of linear polarization and finite power can be described as a superposition of the (scalar) SHG beams. The characteristic feature of the SHG beams is their rectangular symmetry in any plane transverse to the propagation direction. Now we present another infinite-dimensional, complete and orthogonal family of beams of circular rather than rectangular symmetry in the transverse planes – a family of the standard Laguerre-Gaussian (SLG) beams [39-40].

Let us introduce the cylindrical coordinates $r_\perp$ and ψ; $x = r_\perp \cos\psi$, $y = r_\perp \sin\psi$, and rewrite the paraxial wave equation in these coordinates:

$$[2i\partial_z + r_\perp^2 \partial_{r_\perp}^2 + \partial_\psi^2] E(x,y,z) = 0 . \tag{2.147}$$

Then it can be shown by inspection that the SLG beams of the order N=2p+l [3,6]:

$$\begin{aligned} &G_{p,l}^{(SL)}(r_\perp, \psi, z) \\ &= (-1)^p c_{p,l} (\overline{v}/v)^{2p+l} (r_\perp / w)^l L_p^l (r_\perp^2 / w^2) \exp(-il\psi) G(x/v, y/v, z) , \end{aligned} \tag{2.148}$$

obey Equation (2.147), where L_p^l is the generalized Laguerre polynomial,

$$p! L_p^l(x) = [x^{-l} \exp(+x)][(d/dx)x]^p [x^l \exp(-x)] . \tag{2.149}$$

By introduction of the normalisation factor [40],

$$c_{p,l} = \pi^{-1/2} [p!/(p+l)!]^{1/2} , \tag{2.150}$$

the SLG function can be normed in its intensity to one:

$$\iint dr_\perp \, r_\perp d\psi \left| G_{p,l}^{(SL)}(r_\perp, \psi, z) \right|^2 = 1 . \tag{2.151}$$

Note that we use interchangeably the Cartesian or cylindrical coordinates as arguments of the beam functions what, for example, may be seen in the expression $G_{p,l}^{(SL)}(r_\perp, \psi, z) \equiv G_{p,l}^{(SL)}(x,y,z)$. The definition (2.148) is given here for positive values of l and p. For negative values of l $G_{p,l}^{(SL)}(x,y,z) = G_{p,-l}^{(SL)}(x,-y,z)$.

There is no need to derive the definition of the SLG beam along the lines shown already for the SHG beams. As both families of these beams form complete sets of solutions of the paraxial wave equation, any SLG beam can be expressed by a linear combination of the SHG beams and vice versa. To compound the SLG beam in this way let us start with the SHG beam, whose principal axes make an angle $\pi/4$ with x and y axes of the Cartesian coordinate frame (x,y,z). Such the "diagonal" SHG beam can be decomposed into the set of "non-diagonal", that is in not rotated in the (x,y) frame, SHG beams of the same order N=n+m according to the rule [40]:

$$G_{m,n}^{(SH)}(2^{-1/2}(x+y),2^{-1/2}(x-y),z)=\sum_{k=0}^{m+n}b(m,n,k)\,G_{N-k,k}^{(SH)}(x,y,z)\,,$$

$$b(m,n,k)$$
$$=(2^{m+n}m!n!)^{-1/2}[(m+n-k)!/k!]^{1/2}(d^k/dt^k)\left[(1-t)^m(1+t)^n\right]|_{t=0}\,. \quad (2.152)$$

Note that the expansion coefficients $b(m,n,k)$ are real and therefore all of them are in phase in the "diagonal" expansion (2.152).

It can be shown that the SLG beam of the order N=2p+l also decomposes into the set of SHG beams of the same order N=m+n in a similar way [40]:

$$G_{p,l}^{(SL)}(x,y,z)=\sum_{k=0}^{N}i^k\,b(m,n,k)\,G_{N-k,k}^{(SH)}(x,y,z)\,, \quad (2.153)$$

with exactly the same coefficients $b(m,n,k)$ augmented by the factor i^k, where m=p, n=l+p for m < n and m=l+p, n=p for m ≥ n. That corresponds to an additional $\pi/2$ relative phase difference between successive expansion coefficients. For example, the diagonal SHG beam of m=0 and n=2 and the SLG beam of p=0, l=2, both of the order N=m+n=2p+l=2, can be represented by the following decompositions in terms of the non-diagonal SHG beams of the same order:

$$G_{0,2}^{(SH)}(2^{-1/2}(x+y),2^{-1/2}(x-y),z)$$
$$=2^{-1}G_{2,0}^{(SH)}(x,y,z)+2^{-1/2}G_{1,1}^{(SH)}(x,y,z)+2^{-1}G_{0,2}^{(SH)}(x,y,z)\,,$$

$$G_{0,2}^{(SL)}(x,y,z)$$
$$=2^{-1}G_{2,0}^{(SH)}(x,y,z)+i2^{-1/2}G_{1,1}^{(SH)}(x,y,z)-2^{-1}G_{0,2}^{(SH)}(x,y,z)\,. \quad (2.154)$$

The "diagonal" decompositions (2.154) are visualised in beam intensity in Fig. 2.1 and Fig. 2.2 (see also figures in [40,41]).

The decomposition (2.154) is not only a pure theoretical result. Any HG beam can be transformed into a corresponding LG beam, and any LG beam can be transformed into a corresponding HG beam, by passing them through an astigmatic beam-mode converter, composed of a specific set of cylindrical lenses [40]. Direct comparison of the two expansions (2.152) and (2.153), for the diagonal SHG beams and the SLG beams, respectively, indicates that

such conversion should change phase in the coefficients $b(m,n,k)$ of these decompositions. It has been shown that this operation can be accomplished by manipulation of the Gouy on-axis phase of the beam [40].

Figure 2.1. Intensity distribution of the components in the decomposition (2.154) of the diagonal SHG beam $G_{0,2}^{(SH)}$ (left) into the non-diagonal SHG beams $G_{2,0}^{(SH)}$, $G_{1,1}^{(SH)}$ and $G_{0,2}^{(SH)}$ of the same order (right). All components of the decomposition are in phase.

Figure 2.2. Intensity distribution of the components in the decomposition (2.154) of the SLG beam $G_{02}^{(SL)}$ (left) into the non-diagonal SHG beams $G_{2,0}^{(SH)}$, $G_{1,1}^{(SH)}$ and $G_{0,2}^{(SH)}$ of the same order (right). The second and the third components of the decomposition differ in phase by $\pi/2$ and π, respectively, with respect to the decomposition components in Fig. 2.1.

There is a distinct asymmetry in arguments of the standard HG beams (2.145) and the standard LG beams (2.148) – the arguments of their Hermite and Laguerre polynomials are scaled by the real beam radius $w(z)$, meanwhile the argument of the fundamental Gaussian function (2.145) is

scaled by the complex beam radius $v(z)$. However, there are also two other parallel families of three-dimensional paraxial beams, with all their arguments scaled by the complex beam parameter $v(z)$ only. They have been named as the complex-valued or "elegant" HG beams and LG beams [6]. Their definitions (up to the normalisation factors) will be given in Section 4, Chapter 7.

The elegant HG and LG beams also form two separate, complete and infinite-dimensional bases for any solution of the paraxial wave equation of finite power. Contrary to the SHG and SLG beams, these sets of the elegant (EHG or ELG) beams are biorthogonal rather than orthogonal [6]. Still, the diagonal relation (2.153) remains valid for the elegant EHG and ELG beams with the same expansion coefficients as for the standard SHG and SLG beams [41]:

$$G_{p,l}^{(EL)}(x,y,z) = \sum_{k=0}^{N} i^k b(m,n,k) G_{N-k,k}^{(EH)}(x,y,z) . \tag{2.155}$$

They play a special role in beam interaction with a planar dielectric interface, or, in general, with any planar dielectric multilayer. Their definitions will be given and their interaction with the interface will be analysed in the last chapter of this book.

2.9 Spinors of beam polarization

The formalism, outlined in previous sections, treats the beam field amplitudes as scalar quantities, independent of beam polarization. Transformations of the beam polarization, assumed to be approximately uniform (constant) at any beam cross-section, will be briefly discussed below.

The amplitude distribution of the beam field has been analysed by use of the beam field expansions in the Hilbert space of square-integrable functions, spanned by the complete and orthogonal (or bi-orthogonal) sets of HG or LG beam fields. Similarly, beam polarization can be analysed in a two-dimensional vector space spanned by one particular pair of orthogonal polarization states. These states are usually taken as of the linear, TM and TE, or the circular, right-handed (CR) and left-handed (CL), polarization

states. Our choice here is the TM polarization state with the base vector $\underline{e}_x$, directed along the x-axis, and TE polarization state with the base vector $\underline{e}_y$, directed along the y-axis:

$$\underline{e}_x = \begin{bmatrix} 1 \\ 0 \end{bmatrix}, \qquad \underline{e}_y = \begin{bmatrix} 0 \\ 1 \end{bmatrix}. \tag{2.156}$$

An arbitrary state of the beam polarization will be expressed by the complementary and equivalent - for coherent beams - entities: Jones spinors, Stokes vectors and polarization matrices. The analysis will be restricted only to paraxial beams of their polarization states uniform in any transverse plane of the optical system.

Recall that the vector beam field $\underline{E}_\perp = E\underline{e}\exp(i\underline{k}_\perp \underline{r}_\perp)$ has been defined in Section 3 as the product of the scalar complex amplitude E and the polarization vector $\underline{e} = [e_x, e_y]^T$, known as the Jones vector. For beams of arbitrary polarization this vector has been defined in Section 3 in terms of the polarization parameter $\chi = E_x / E_y$. An inner product of two such vectors $\underline{e}_1$ and $\underline{e}_2$ is defined by:

$$(\underline{e}_1, \underline{e}_2) \equiv \underline{e}_1^+ \underline{e}_2 . \tag{2.157}$$

Thus two Jones vectors

$$\underline{e} = \begin{bmatrix} e_x \\ e_y \end{bmatrix} = \begin{bmatrix} \chi^{+1/2} \\ \chi^{-1/2} \end{bmatrix},$$

$$\underline{\dot{e}} = \begin{bmatrix} \dot{e}_x \\ \dot{e}_y \end{bmatrix} = \begin{bmatrix} +\overline{\chi}^{-1/2} \\ -\overline{\chi}^{+1/2} \end{bmatrix}, \tag{2.158}$$

are mutually orthogonal:

$$(\underline{e}, \underline{\dot{e}}) = \underline{e}^+ \underline{\dot{e}}_2 = 0 \tag{2.159}$$

and possess a common norm $|\underline{e}|$:

$$|\underline{e}|^2 = \underline{e}^+ \underline{e} = \underline{\dot{e}}^+ \underline{\dot{e}} = |\chi|^{+2} + |\chi|^{-2}, \tag{2.160}$$

where the overbar "-" stands for complex conjugate.

The Jones vectors $\underline{e}$ and $\underline{\dot{e}}$ span a two-dimensional vector space of beam polarization states. For two abitrary polarization vectors $\underline{u}$ and $\underline{v}$:

$$\underline{u} = u_x e_x \underline{e}_x + u_y e_y \underline{e}_y ,$$

$$\underline{v} = v_x e_x \underline{e}_x + v_y e_y \underline{e}_y , \tag{2.161}$$

of arbitrary polarization parameters $\chi u_x / u_y$ and $\chi v_x / v_y$, respectively, their inner product $(\underline{u}, \underline{v}) = \underline{u}^+ \underline{v}$ reads:

$$(\underline{u}, \underline{v}) = \overline{u}_x v_x \,|\chi| + \overline{u}_y v_y \,|\chi|^{-1} . \tag{2.162}$$

For the polarization base composed of the linear or diagonal polarization states of beams, that is for the linear TM ($\chi = \pm\infty$, $e_y = 0$) and TE ($\chi = 0$), linear diagonal ($\chi = \pm 1$, $e_x = 0$) or circular diagonal ($\chi = \mp i$) states, the magnitude of the polarization parameter equals one ($|\chi| = 1$). In the space spanned by one these pairs, the inner product (2.162) of the polarization vectors simplifies to the form independent of χ:

$$(\underline{u}, \underline{v}) = \overline{u}_x v_x + \overline{u}_y v_y . \tag{2.163}$$

Therefore, the TM/TE or diagonal polarization states (linear and circular) should be regarded as special types of beam polarization. The role of these states in the beam polarization representation is similar to the role of the HG beams and LH beams in the beam-field-amplitude representations. Further the analysis in this chapter will be continued in the TM/TE polarization basis.

In optics most of the lossless elements of first-order systems act on a Jones vector $\underline{e}$ according to the linear, unimodular and Jones transformation $\underline{\underline{L}}$:

$$\begin{bmatrix} e'_x \\ e'_y \end{bmatrix} = \underline{\underline{L}} \begin{bmatrix} e_x \\ e_y \end{bmatrix} = \begin{bmatrix} L_{xx} & L_{xy} \\ L_{yx} & L_{yy} \end{bmatrix} \begin{bmatrix} e_x \\ e_y \end{bmatrix}, \tag{2.164}$$

where $\det \underline{\underline{L}} = 1$. For rotations, being the special case of these transformations, the complex Jones matrix $\underline{\underline{L}}$ is unitary in addition to be unimodular. Two-component entities that transform linearly according to unimodular transformations are regarded as two-component spinors. Therefore the vectors $\underline{e}$ are polarization or Jones spinors. In a more general

case, when the polarization transformations are not necessarily unimodular, the vectors $\underline{e}$ are regarded plainly as Jones vectors. Note that the matrix $\underline{\underline{L}}$, representing optical transformations in the two-dimensional space of beam polarization states, possesses the same dimension and the same unimodular property as the ray-transfer matrix $\underline{\underline{m}}$, acting, however, in the different infinite-dimensional phase-space of transverse-field-amplitude distribution of the beams.

With the definitions of the polarization spinors given above all constructs necessary for the description of beam polarization can be conveniently introduced. For completely coherent beams - only such beams are considered here - the polarization spinors define a two-by-two polarization matrix $\underline{\underline{C}}$ [42]:

$$\underline{\underline{C}} = \underline{\underline{C}}^{+} = \underline{e}\,\underline{e}^{+}, \tag{2.165}$$

$$\underline{\underline{C}} = \begin{bmatrix} C_{xx} & C_{xy} \\ C_{yx} & C_{yy} \end{bmatrix} = \begin{bmatrix} e_x \overline{e}_x & e_x \overline{e}_y \\ e_y \overline{e}_x & e_y \overline{e}_y \end{bmatrix}. \tag{2.166}$$

Note that, for any spectral constituent of a partially coherent beam, the counterpart of $\underline{\underline{C}}$ is known as a coherency matrix [8].

The polarization matrix is Hermitian and as such can be expressed as a linear combination of the four basic two-by-two matrices σ_μ, μ=1,2,3,4:

$$\underline{\underline{C}} = \sum_{\mu=1}^{4} \Sigma_\mu \sigma_\mu = \begin{bmatrix} \Sigma_3 + \Sigma_4 & \Sigma_1 - i\Sigma_2 \\ \Sigma_1 + i\Sigma_2 & -\Sigma_3 + \Sigma_4 \end{bmatrix}, \tag{2.167}$$

with the coefficients Σ_μ of this expansion known as the Stokes parameters. The first three matrices σ_k, k=1,2,3, are the well-known Pauli matrices [43], the fourth one is the unit matrix:

$$\underline{\underline{\sigma}}_1 = \begin{bmatrix} 0 & 1 \\ 1 & 0 \end{bmatrix}, \qquad \underline{\underline{\sigma}}_2 = \begin{bmatrix} 0 & -i \\ i & 0 \end{bmatrix},$$

$$\underline{\underline{\sigma}}_3 = \begin{bmatrix} 1 & 0 \\ 0 & -1 \end{bmatrix}, \qquad \underline{\underline{\sigma}}_4 = \begin{bmatrix} 1 & 0 \\ 0 & 1 \end{bmatrix}. \tag{2.168}$$

All of them are Hermitian $\underline{\underline{\sigma}}_\mu^+ = \underline{\underline{\sigma}}_\mu$ and unitary $\underline{\underline{\sigma}}_\mu^+ \underline{\underline{\sigma}}_\mu = \underline{\underline{1}}$. The three Pauli matrices are traceless $tr\underline{\underline{\sigma}}_k = 0$ and obey the anticommutation and commutation relations:

$$\{\underline{\underline{\sigma}}_i, \underline{\underline{\sigma}}_j\} = \underline{\underline{\sigma}}_i \underline{\underline{\sigma}}_j + \underline{\underline{\sigma}}_j \underline{\underline{\sigma}}_i = 2\delta_{ij} \underline{\underline{1}}, \tag{2.169}$$

$$[\underline{\underline{\sigma}}_i, \underline{\underline{\sigma}}_j] = \underline{\underline{\sigma}}_i \underline{\underline{\sigma}}_j - \underline{\underline{\sigma}}_j \underline{\underline{\sigma}}_i = 2i\varepsilon_{ijk} \underline{\underline{\sigma}}_k, \tag{2.170}$$

where i,j,k=1,2,3 and ε_{ijk} is the Levi-Civita skew tensor, $\varepsilon_{ijk} = -\varepsilon_{jik} = -\varepsilon_{ikj}$, $\varepsilon_{123} = 1$.

The Stokes parameters form the Stokes four-vector

$$\underline{\underline{\Sigma}} = \left[\Sigma_1, \quad \Sigma_2, \quad \Sigma_3, \quad \Sigma_4\right]^T. \tag{2.171}$$

With a metric

$$\underline{\underline{g}} = \begin{bmatrix} -1 & 0 & 0 & 0 \\ 0 & -1 & 0 & 0 \\ 0 & 0 & -1 & 0 \\ 0 & 0 & 0 & 1 \end{bmatrix} \tag{2.172}$$

a scalar product of two Stokes vectors $\underline{\underline{\Sigma}}^{(a)}$ and $\underline{\underline{\Sigma}}^{(b)}$ is given by:

$$\begin{aligned} (\underline{\underline{\Sigma}}^{(a)}, \underline{\underline{\Sigma}}^{(b)}) &= (\underline{\underline{g}} \underline{\underline{\Sigma}}^{(a)})^T \underline{\underline{\Sigma}}^{(b)} \\ &= -\Sigma_1^{(a)}\Sigma_1^{(b)} - \Sigma_2^{(a)}\Sigma_2^{(b)} - \Sigma_3^{(a)}\Sigma_3^{(b)} + \Sigma_4^{(a)}\Sigma_4^{(b)}. \end{aligned} \tag{2.173}$$

The norm of the Stokes vector squared

$$\Sigma^2 \equiv |\underline{\underline{\Sigma}}|^2 = (\underline{\underline{g}} \underline{\underline{\Sigma}})^T \underline{\underline{\Sigma}} = -\Sigma_1^2 - \Sigma_2^2 - \Sigma_3^2 + \Sigma_4^2, \tag{2.174}$$

is called a Stokes scalar.

From the expansion (2.167) the components Σ_μ are determined by elements of the polarization matrix $\underline{\underline{C}}$:

$$\Sigma_1 = \tfrac{1}{2}(C_{xy} + C_{yx}) = \tfrac{1}{2}(e_x \overline{e}_y + e_y \overline{e}_x),$$

$$\Sigma_2 = \tfrac{i}{2}(C_{xy} - C_{yx}) = \tfrac{i}{2}(e_x \overline{e}_y - e_y \overline{e}_x),$$

$$\Sigma_3 = \tfrac{1}{2}(C_{xx} - C_{yy}) = \tfrac{1}{2}(e_x\bar{e}_x - e_y\bar{e}_y),$$

$$\Sigma_4 = \tfrac{1}{2}(C_{xx} + C_{yy}) = \tfrac{1}{2}(e_x\bar{e}_x + e_y\bar{e}_y), \tag{2.175}$$

with the fourth Stokes parameter Σ_4 being always positive ($\Sigma_4 > 0$). Note that the matrix $\underline{\underline{C}}$ can be directly expressed by Stokes parameters and depends explicitly on the magnitude $(\chi\bar{\chi})^{+1/2}$ and phase $(\chi/\bar{\chi})^{+1/2}$ of the polarization parameter χ:

$$\underline{\underline{C}} = \begin{bmatrix} \Sigma_3 + \Sigma_4 & \Sigma_1 - i\Sigma_2 \\ \Sigma_1 + i\Sigma_2 & -\Sigma_3 + \Sigma_4 \end{bmatrix} = \begin{bmatrix} (\chi\bar{\chi})^{+1/2} & (\chi/\bar{\chi})^{+1/2} \\ (\chi/\bar{\chi})^{-1/2} & (\chi\bar{\chi})^{-1/2} \end{bmatrix}. \tag{2.176}$$

The Stokes scalar is equal to the determinant of the polarization matrix which, for completely coherent beams, is zero,

$$\Sigma^2 = C_{xx}C_{yy} - C_{xy}C_{yx} = \det\underline{\underline{C}} = 0. \tag{2.177}$$

Therefore, for coherent beams, the condition $\Sigma^2 = 0$ remains valid in any transverse plane of all optical systems, which leave coherency of optical beams invariant.

The definition of the polarization matrix given above differs to some extent from its conventional definition (2.178). The magnitude of the beam complex amplitude $|E_xE_y|$ is extracted from this definition. This choice seems to be natural as the beam polarization depends on the polarization parameter χ, that is $\underline{\underline{C}} \equiv \underline{\underline{C}}(\chi)$, rather than on the complex amplitude of the beam. However, for singular cases of polarization, where the beam amplitude extraction does not make sense, that is for the linear TM ($\chi = \pm\infty$) and TE ($\chi^{-1} = \pm\infty$) polarization, the polarization matrix is conventionally defined as:

$$|E_xE_y|\,\underline{\underline{C}}(\chi) = \begin{bmatrix} E_x\bar{E}_x & E_x\bar{E}_y \\ E_y\bar{E}_x & E_y\bar{E}_y \end{bmatrix} \tag{2.178}$$

and reads:

$$\underline{\underline{C}}(\pm\infty) \propto \begin{bmatrix} \pm 1 & 0 \\ 0 & 0 \end{bmatrix},$$

$$\underline{\underline{C}}(\pm 0) \propto \begin{bmatrix} 0 & 0 \\ 0 & \pm 1 \end{bmatrix}, \tag{2.179}$$

where ± 0 means $\pm 1/\infty$. For other, non-singular cases, both versions (2.176) and (2.178) of the definitions of $\underline{\underline{C}}$ yield the same results up to the unrelevant factor. For example, for the diagonal linear ($\chi = \pm 1$) and the diagonal circular ($\chi = \mp i$) polarization, one gets:

$$\underline{\underline{C}}(\pm 1) \propto \begin{bmatrix} 1 & \pm 1 \\ \pm 1 & 1 \end{bmatrix},$$

$$\underline{\underline{C}}(\mp i) \propto \begin{bmatrix} 1 & \mp i \\ \pm i & 1 \end{bmatrix}. \tag{2.180}$$

Jones vectors are useful in analysis of completely coherent beams. Their introduction is not, however, sufficient to deal with partially coherent beams. To see the above sequence of definitions in more complete perspective, let us mention only that, for beams of arbitrary coherency, the polarization matrix should be time-averaged [8],

$$<\underline{\underline{C}}>=\begin{bmatrix} <C_{xx}> & <C_{xy}> \\ <C_{yx}> & <C_{yy}> \end{bmatrix}, \tag{2.181}$$

where $< >$ represents averaging. Such a matrix is commonly known as the coherency matrix. The same time-averaging pertains also to the Stokes vector

$$<\underline{\Sigma}>=\left[<\Sigma_1>, \quad <\Sigma_2>, \quad <\Sigma_3>, \quad <\Sigma_4>\right]^T, \tag{2.182}$$

now with $<\Sigma>^2 = \det <\underline{\underline{C}}>$, in general, different from zero. The degree of beam coherence is then defined by:

$$P = (<\Sigma_1>^2 + <\Sigma_2>^2 + <\Sigma_3>^2)^{1/2} / <\Sigma_4>. \tag{2.183}$$

For completely coherent beams $P = 1$, for completely incoherent beams the coherency matrix is diagonal and unimodular, that yields $P = 0$, cf. Eq. (2.174). For other, intermediate cases of partially coherent beams $0 < P < 1$. Further, only completely coherent beams ($P = 1$) will be considered, with

singular polarization matrices of their determinant nil ($\det \underline{\underline{C}} = 0$) and Stokes vectors orthogonal to themselves ($\Sigma^2 = 0$).

2.10 Lorentz transformations

Let us now look into the transformation of beam polarization, preserving coherency of a paraxial beam propagating down the optical system. Such transformations imply that the Stokes scalar Σ'^2 in the output plane equals its counterpart Σ^2 in the input plane of the optical system:

$$\Sigma'_4{}^2 - \Sigma'_1{}^2 - \Sigma'_2{}^2 - \Sigma'_3{}^2 = \Sigma_4{}^2 - \Sigma_1{}^2 - \Sigma_2{}^2 - \Sigma_3{}^2 . \tag{2.184}$$

As the Stokes scalar is expressed by components of the polarization matrix $\underline{\underline{C}}$, the above equality reads

$$\Sigma'^2 = \det \underline{\underline{C}}' = \det \underline{\underline{C}} = \Sigma^2 . \tag{2.185}$$

At this point recall that the the polarization matrix $\underline{\underline{C}} = \underline{e}\,\underline{e}^+$ is composed of the product of the polarization spinor and its Hermitian transpose. Therefore, any complex trasformation $\underline{\underline{L}}$ of the polarization spinor $\underline{e}$ induces the transformation of the polarization matrix $\underline{\underline{C}}$:

$$\underline{e}' = \underline{\underline{L}}\,\underline{e} ,$$

$$\underline{\underline{C}}' = \underline{\underline{L}}\,\underline{\underline{C}}\,\underline{\underline{L}}^+ , \tag{2.186}$$

which, under condition that the matrix $\underline{\underline{L}}$ is unimodular, $\det \underline{\underline{L}} = 1$, satisfies the invariance condition (2.184) for coherent beams, as well as for partially coherent beams in a more general case. Note that the transformation $\underline{\underline{L}}$ leaves a value of the fourth component Σ_4 of the Stokes vector positive ($\Sigma_4 > 0$ and $\Sigma'_4 > 0$) and that the transformations $\underline{\underline{L}}$ and $-\underline{\underline{L}}$ induce the same transformation of the polarization matrix $\underline{\underline{C}}$.

There is a direct correspondence between the Stokes four-vector $\underline{\Sigma}$ (2.171), the Stokes scalar Σ^2 (2.174) and its invariance condition $\Sigma'^2 = \Sigma^2$ (2.184), valid under the optical transformations on the one hand, and the space-time vector $\underline{X}$, $\underline{X}^T = [\underline{r}, ct]^T$, its space-time interval $c^2t^2 - \underline{r}^2$ and its invariance condition

$$c^2t'^2-x'^2-y'^2-z'^2=c^2t^2-x^2-y^2-z^2, \tag{2.187}$$

on the other hand [24]. The condition (2.187) is valid under the action of homogeneous Lorentz transformations in the Minkowski space, well known from the special theory of relativity [43]. In the language of spinors, the polarization matrix $\underline{\underline{C}}$ corresponds to a Hermitian second-rank space-time spinor

$$\underline{\underline{C}}_{(\underline{X})}=\begin{bmatrix} z+ct & x-iy \\ x+iy & -z+ct \end{bmatrix}, \tag{2.188}$$

with its matrix elements determined by the components of the space-time vector

$$\underline{X}=[x,\quad y,\quad z,\quad ct]^T. \tag{2.189}$$

The vector $\underline{X}$ corresponds to the Stokes vector $\underline{\Sigma}$ (cf. (2.167) and (2.171)).

For any two-by-two unimodular matrix transformation $\underline{\underline{L}}$ of a space-time spinor $\underline{x}$, the matrix $\underline{\underline{C}}_{(X)}$ is transformed according to the law identical to that of Equation (2.186) specific to the polarization transformations,

$$\underline{x}'=\underline{\underline{L}}\,\underline{x},$$

$$\underline{\underline{C}}'_{(X')}=\underline{\underline{L}}\,\underline{\underline{C}}_{(X)}\,\underline{\underline{L}}^{+}. \tag{2.190}$$

Therefore, optical transformations of beam polarization, represented by the matrix $\underline{\underline{L}}$ in the space of Jones spinors, are equivalent to the transformations operating, without coordinate inversions, in the space-time vectors in the Minkowski space. In both cases the matrices $\underline{\underline{L}}$ are two-dimensional representations of the homogeneous Lorentz transformations. The condition $\det\underline{\underline{L}}=1$ implies that the corresponding Lorentz transformations belong to the six-parameter group of the restricted (proper and orthochronous) Lorentz transformations [43]. Therefore, the group of optical transformations of beam polarization corresponds to the six-parameter group of the restricted Lorentz transformations [25-26]. The correspondence is two-valued, that is for every Lorentz (or optical) transformation there are two corresponding matrix transformation $+\underline{\underline{L}}$ and $-\underline{\underline{L}}$.

Optical transformations of beam field amplitudes introduced in previous sections are also represented by the unimodular two-by-two, this time *abcd*, ray-transfer matrices $\underline{\underline{m}}$. Therefore they also correspond, like the transformations of beam polarization, to the same group of Lorentz transformations. Both types of transformations, those of beam amplitude and these of beam polarization, are defined in planes transverse to the beam propagation direction, under the assumption that the beam axis coincides with the axis of the first-order system. In order to look closer into the family of these transformations let us relate them to the three Pauli matrices σ_i, i=1,2,3.

The Pauli matrices form three generators $\underline{\underline{J}}_i$ of the rotation transformations

$$\underline{\underline{J}}_i = \tfrac{1}{2}\underline{\underline{\sigma}}_i , \tag{2.191}$$

together with three other generators $\underline{\underline{K}}_i$ shifted in phase by $\pi/2$ with respect to $\underline{\underline{J}}_i$,

$$\underline{\underline{K}}_i = \tfrac{i}{2}\underline{\underline{\sigma}}_i . \tag{2.192}$$

Their commutation relations

$$[\underline{\underline{J}}_i, \underline{\underline{J}}_j] = +i\varepsilon_{ijk}\underline{\underline{J}}_k , \tag{2.193}$$

$$[\underline{\underline{J}}_i, \underline{\underline{K}}_j] = +i\varepsilon_{ijk}\underline{\underline{K}}_k , \tag{2.194}$$

$$[\underline{\underline{K}}_i, \underline{\underline{K}}_j] = -i\varepsilon_{ijk}\underline{\underline{J}}_k , \tag{2.195}$$

i=1,2,3, constitute the most general closed set of commutation relations of the restricted Lorentz group [43]. Thus, the six traceless matrices $\underline{\underline{J}}_i$ and $\underline{\underline{K}}_i$ generate, through the exponential representation:

$$\underline{\underline{L}} = \underline{\underline{L}}^{(R)} + \underline{\underline{L}}^{(B)} = \exp\left[-i\sum_{j=1}^{3}(\varphi_j \underline{\underline{J}}_j + \gamma_j \underline{\underline{K}}_j)\right], \tag{2.196}$$

the six-parameter group of Lorentz transformations, represented by the complex, symplectic or unimodular two-by-two matrices $\underline{\underline{L}}$. They consist of

the pure rotations $\underline{\underline{L}}^{(R)}$ and the boosts $\underline{\underline{L}}^{(B)}$, acting in the two-dimensional space of Jones spinors. The boosts are the pure Lorentz transformations between two reference frames moving with different velocities [43]. The pure rotations are generated by Hermitian matrices $\underline{\underline{J}}_j$ represented by the unitary matrices $\underline{\underline{L}}^{(R)}$. Their set of the commutation relations (2.193) is also closed. Thus, the rotations form a three-parameter subgroup of the group of the restricted Lorentz transformations [25]. As, for the unit vector $\underline{n}$ in the direction of the rotation axis, the Pauli matrices obey the identity:

$$(\underline{\underline{\sigma}}_1 n_x + \underline{\underline{\sigma}}_2 n_y + \underline{\underline{\sigma}}_3 n_z)^2 = \underline{\underline{1}}, \tag{2.197}$$

the rotation matrices can be separately written in a more explicit form [44]:

$$\underline{\underline{L}}^{(R)}(\varphi_j) = \exp(-i\varphi_j \underline{\underline{J}}_j) = \underline{\underline{1}}\cos(\varphi_j/2) - i\underline{\underline{\sigma}}_j \sin(\varphi_j/2). \tag{2.198}$$

Let us now show some examples of beam polarization transformations [25-26].

The rotation of the beam polarization state are now represented by the matrix $\underline{\underline{L}}^{(R)}$:

$$\begin{bmatrix} e'_x \\ e'_y \end{bmatrix} = \underline{\underline{L}}^{(R)} \begin{bmatrix} e_x \\ e_y \end{bmatrix} = \begin{bmatrix} e_x \cos(\varphi/2) - e_y \sin(\varphi/2) \\ e_x \sin(\varphi/2) + e_y \cos(\varphi/2) \end{bmatrix},$$

$$\underline{\underline{L}}^{(R)} \equiv \underline{\underline{L}}^{(R)}(\varphi) = \exp(-i\varphi \underline{\underline{J}}_2) = \begin{bmatrix} \cos(\varphi/2) & -\sin(\varphi/2) \\ \sin(\varphi/2) & \cos(\varphi/2) \end{bmatrix}, \tag{2.199}$$

which rotates the polarization spinor components by $\varphi/2$. This transformation describes the action of the optical rotator on the beam polarization state.

Similarly, the transformation $\underline{\underline{L}}^{(P)}$ induced by the generator $\underline{\underline{J}}_3$, leads to the creation of a relative phase shift μ between two orthogonal components e_x and e_y of the polarization spinor:

$$\begin{bmatrix} e'_x \\ e'_y \end{bmatrix} = \underline{\underline{L}}^{(P)} \begin{bmatrix} e_x \\ e_y \end{bmatrix} = \begin{bmatrix} e_x \exp(-i\mu/2) \\ e_y \exp(+i\mu/2) \end{bmatrix},$$

$$\underline{\underline{L}}^{(P)} \equiv \underline{\underline{L}}^{(P)}(\mu) = \exp(-i\sigma \underline{\underline{J}}_3) = \begin{bmatrix} \exp(-i\mu/2) & 0 \\ 0 & \exp(+i\mu/2) \end{bmatrix}. \qquad (2.200)$$

This transformation describes the action of the optical phase shifter on the beam polarization state.

Similar examples can be also given using the generators of the Lorentz transformations of the other type - the boosts. For instance, the generator $\underline{\underline{K}}_3$ induces the transformation $\underline{\underline{L}}^{(M)}$, which increases the magnitude of the x-component of the polarization spinor by $w^2 = \exp\xi$ with respect to the y-component and describes the action of the optical compensator on the beam polarization state:

$$\begin{bmatrix} e'_x \\ e'_y \end{bmatrix} = \underline{\underline{L}}^{(M)} \begin{bmatrix} e_x \\ e_y \end{bmatrix} = \begin{bmatrix} e_x w^{+1} \\ e_y w^{-1} \end{bmatrix},$$

$$\underline{\underline{L}}^{(M)} \equiv \underline{\underline{L}}^{(M)}(w) = \exp(-i\xi \underline{\underline{K}}_3) = \begin{bmatrix} w^{+1} & 0 \\ 0 & w^{-1} \end{bmatrix}. \qquad (2.201)$$

For $w >> 1$ ($w << 1$) the compensator acts as the projection operator, which eliminates the y component (x component) of beam polarization.

The matrix representation (2.199)-(2.201) of the beam polarization transformations $\underline{\underline{L}}^{(R)}$, $\underline{\underline{L}}^{(P)}$ and $\underline{\underline{L}}^{(M)}$ is exactly of the same form as the matrix representation (2.70)-(2.72) of the beam-field-amplitude transformations $\underline{\underline{m}}^{(R)}$, $\underline{\underline{m}}^{(P)}$ and $\underline{\underline{m}}^{(M)}$. Both representations may be regarded as optical analogies of the homogeneous Lorentz transformations. However, they are defined in different spaces – in the beam polarization space of Jones spinors and in the phase space of ray-transfer data, respectively. Certainly, in spite of their formal equivalence, they have quite different physical meaning.

2.11 Comments and conclusions

Polarization properties of coherent beams in first-order optical separable systems can be described by two-component Jones spinors or two-by-two polarization matrices, interrelated by four Stokes parameters of the beam. Evolution of beam polarization along the optical system is then given with

the aid of two-by-two Jones matrices, or operators corresponding to them, acting on Jones spinors, polarization matrices and Stokes parameters.

Similarly, spatial structure of field amplitudes of the paraxial beams in first-order optical systems can be expressed by their expansion in terms of the Hermite-Gaussian or Laguerre-Gaussian beams. Evolution of beam field structure is then described by tracing optical rays with the help of the symplectic ray-transfer matrix or, alternatively, by the integral canonical transformations, involving the impulse response of the optical system. The impulse response function provides a link between these two modes of viewing the beam-field-amplitude evolution in optical systems.

On the other hand, in the special theory of relativity, one deals with the space-time four-component vectors, linear combinations of the two-by-two Pauli matrices and two-component spinors, of the form identical, respectively, to the Stokes vectors, polarization matrices and Jones spinors, used in the treatment of beam polarization. Although these entities are of different origin, transformations of all of them belong to the same group of the homogeneous, restricted Lorentz transformations. Moreover, the ray-transfer symplectic matrices, yielding evolution of beam amplitude distribution in the optical system, are also the representations of the same Lorentz group. Therefore, evolution of field amplitudes and polarization of optical beams in first-order systems can be described in self-contained and unified manner in the language of Lorentz transformations.

In spite of its usefulness and formal clarity, the framework of first-order optics outlined in this chapter is not sufficiently general to cover all possible configurations of optical systems. For example, it pertains only to centred optical systems, where the optical axis of the overall optical system coincides with optical axes of its individual elements. In general, however, axes of individual optical elements may be displaced or tilted with respect to the nominal axis of the overall system. Treatment of dispersive optical elements, such as prism and gratings, should also account for effects equivalent to the shifts in position and direction of optical axes of the system or of the beam. Moreover, considering temporal variations of optical signals complicates the analysis even further. The formalism that accounts for such phenomena needs extension of the presented approach into the range of three-by-three or even four-by-four ray-transfer matrices, inhomogeneous canonical transforms and,

perhaps, inhomogeneous Lorentz transformations. These direct extensions of the homogeneous version of first-order optics remain, however, outside the scope of this chapter. Examples of such treatment of the inhomogeneous problems of first-order optics can be found, for instance, in publications [45-48].

The inhomogeneous contributions to centred first-order optical systems are usually small. Therefore, they can be directly treated as well as additional corrections to predictions obtained within the framework pertinent to the homogeneous first-order systems. These corrections are then understood as geometrical modifications of three-dimensional beam field structure, augmented by additional modifications of beam polarization and on-axis amplitude in its magnitude and phase [49-50]. Similar rearrangements of beam spatial structure can be also observed in nonlinear optics, during beam propagation in nonlinear media [51-53], including beam interactions with nonlinear interfaces [53-55]. They can be also regarded as inhomogeneous contributions, nonlinear this time, to homogeneous centred first-order optics.

Effects of this inhomogeneous type exist, among others, in cases of beam interactions with layered optical structures and beam propagation in, linear and/or nonlinear, inhomogeneous media. They are known as nonspecular (NSP) effects of beam reflection and transmission [49-50] and have their analogy in nonlinear propagation described by aberationless effects of beam propagation [51-52]. The effects of NSP reflection and transmission have been measured in sophisticated experimental setups [56-66] and simulated by advanced numerical methods [67-72]. Some numerical procedures directly mimic dynamics of beam field linear and nonlinear rearrangements by monotonic iteration of the analytical solution obtained [67-68]. Some other procedures have been also used in evaluation of final effects of the beam field rearrangements by use of beam-mode-expansion techniques [68-69], by direct integration of Maxwell equations [69-70], by evaluation of a beam centre of gravity [73-74] or by other methods specific to the problem considered [75-76]. It appeared that, in the beam-mode-expansion analyses, beam modes of the “elegant” type, especially the elegant HG and LG beam modes [6], appear preferable in treatment of such inhomogeneous problems [70,72].

In the inhomogeneous problems like, for example, these of the beam interactions with dielectric interfaces, field structure of the elegant HG and LG modes is strictly correlated with their polarization states. Spin-orbit interaction or exchange between spin and orbital parts of total angular momentum of beams takes place in such cases and is governed by conservation laws of optical angular momentum [70] and [76-78]. That results in field-amplitude distribution-sensitive rearrangements of beam polarization on the one hand and in polarization-sensitive rearrangements of beam-field-amplitude distribution on the other hand [70,72]. The beam field rearrangements exist in parallel to other, already well-known phenomena, like the longitudinal and transverse displacements of beams [49,72]. The first-order transverse displacements have been also recently rederived on the grounds of approximate methods of geometrical optics and related to the Berry geometrical phase [76-77]. All of that confirms that, in opposition to the homogeneous first-order optics, the beam-field amplitude-polarization separation does not occur within the inhomogeneous first-order optics.

The beam amplitude-polarization interactions are discussed separately in the last chapter of this book, in the context of the cross-polarization coupling of opposite beam components at the interface. Other effects of beam interactions with dielectric interfaces may be regarded exactly as the inhomogeneous corrections introduced into the standard, three-dimensional and homogeneous, framework of the homogeneous first-order optics. Some of these phenomena are discussed in detail in next chapters of this book, with implicit understanding that the results obtained can be interpreted as additional corrections to the formal framework of the centred first-order optics presented in this chapter.

Appendix 1: Note on the scaling

Let us now return back to the unscaled spatial (x, y) and spectral (k_x, k_y) coordinates transverse to the beam propagation direction (along the z-axis of the beam) and show how the scaling convention (2.25)-(2.26) works in the case of the fundamental Gaussian beam at its waist plane z=0. For simplicity of notation we limit the discussion below to only one transverse dimension

and write a one-dimensional Fourier transform pair of a beam field in the convention determined by the scaling transformations (2.25)-(2.26):

$$\Psi(x/w_w) = \int \widetilde{\Psi}(k_x w_w) \exp(+ik_x x) d(k_x w_w/2\pi),$$

$$\widetilde{\Psi}(k_x w_w) = \int \Psi(x/w_w) \exp(-ik_x x) d(x/w_w). \qquad \text{(A.2.1)}$$

The integration is performed from $-\infty$ to $+\infty$ with w_w being the scaling parameter of the transverse coordinates x and k_x. Note that x/w_w and $k_x w_w/2\pi$ are the scaled (dimensionless) spatial coordinate and spatial frequency of the beam field Ψ, respectively. Then the Fourier transform pair of the fundamental Gaussian beam G reads:

$$G(x/w_w) = \exp[-\tfrac{1}{2}(x/w_w)^2],$$

$$\widetilde{G}(k_x w_w) = (2\pi)^{1/2} \exp[-\tfrac{1}{2}(k_x w_w)^2]. \qquad \text{(A.2.2)}$$

It is stipulated in Eq. (A.2.2) that the beam has a unit amplitude of the beam at a centre ($x = 0$) of its waist plane.

Similarly, for the fundamental Gaussian beam g taken as the beam normalised in intensity:

$$\int |\, g(x/w_w)\,|^2 \, d(x/w_w) = 1,$$

$$\int |\, \widetilde{g}(k_x w_w)\,|^2 \, d(k_x w_w/2\pi) = 1, \qquad \text{(A.2.3)}$$

its Fourier transform pair reads:

$$g(x/w_w) = \pi^{-1/4} \exp[-\tfrac{1}{2}(x/w_w)^2],$$

$$\widetilde{g}(k_x w_w) = 2^{1/2} \pi^{1/4} \exp[-\tfrac{1}{2}(k_x w_w)^2]. \qquad \text{(A.2.4)}$$

Note that $\int \exp(-x^2) dx = \sqrt{\pi}$. The parameter w_w is equal to the half-width at 1/e power-maximum of the fundamental Gaussian beam (A.2.2) or (A.2.4) of the beam transverse cross-section at the beam waist and known as the radius or half-width of the beam. It also equals to the root-mean-square (rms) spatial

half-width of the beam and its inverse w_w^{-1} equals the rms spectral half-width of the Gaussian beam [7], what entails:

$$\int (x/w_w)^2 g(x/w_w)\, d(x/w_w) \Big/ \int g(x/w_w)\, d(x/w_w) = 1,$$

$$\int (k_x w_w)^2 \tilde{g}(k_x w_w)\, d(k_x w_w) \Big/ \int \tilde{g}(k_x w_w)\, d(k_x w_w) = 1. \qquad \text{(A.2.5)}$$

Note that $\int \exp(-\frac{1}{2}x^2)dx = \sqrt{2\pi}$ and $\int x^2 \exp(-\frac{1}{2}x^2)dx = \sqrt{2\pi}$. The beam half-width w_w, together with the wave number k, determines the diffraction length $z_D = kw_w^2$ of the Gaussian beam, being the scaling parameter of the z-coordinate along the beam axis (cf. the derivation of the beam propagation given in Section 7). Certainly, the same relations (A.2.5) hold for the functions $G(x/w_w)$ and $\tilde{G}(k_x w_w)$ defined by (A.2.2).

There are also other definitions of the mean beam widths based on beam power. The spatial σ_x and spectral σ_{k_x} power-rms half-widths [7]

$$(\sigma_x/w_w)^2 = \int (x/w_w)^2 \,|\, g(x/w_w)\,|^2\, d(x/w_w) \Big/ \int |\, g(x/w_w)\,|^2\, d(x/w_w) = 1/2,$$

$$(\sigma_{k_x} w_w)^2 = \int (k_x w_w)^2 \,|\, \tilde{g}(k_x w_w)\,|^2\, d(k_x w_w) \Big/ \int |\, \tilde{g}(k_x w_w)\,|^2\, d(k_x w_w) = 1/2, \qquad \text{(A.2.6)}$$

are expressed by w_w:

$$\sigma_x = w_w 2^{-1/2},$$

$$\sigma_{k_x} = w_w^{-1} 2^{-1/2}. \qquad \text{(A.2.7)}$$

and yield the well-known width-bandwidth reciprocity relations for the fundamental Gaussian beam [7]:

$$\sigma_x \sigma_{k_x} = 1/2. \qquad \text{(A.2.8)}$$

Note that $\int \exp(-x^2)dx = \sqrt{\pi}$ and $\int x^2 \exp(-x^2)dx = \frac{1}{2}\sqrt{\pi}$. The fundamental Gaussian beam (A.2.2), together with the definition (A.2.1), reads in terms of σ_x and σ_{k_x}:

$$G(x/w_w) = \exp[-\tfrac{1}{4}(x/\sigma_x)^2],$$

$$\widetilde{G}(k_x w_w) = (2\pi)^{1/2} \exp[-\tfrac{1}{4}(k_x/\sigma_{k_x})^2]. \qquad \text{(A.2.9)}$$

Note that quite frequently the equivalent, slightly different definition of the beam half-width $\breve{w}_w = w_w 2^{1/2}$ is used (see [49], [50] and [53]). In such a case the fundamental Gaussian beam (A.2.2), together with the definition (A.2.1), reads:

$$G(x/\breve{w}_w) = \exp[-(x/\breve{w}_w)^2],$$

$$\widetilde{G}(k_x \breve{w}_w) = (2\pi)^{1/2} \exp[-\tfrac{1}{4}(k_x \breve{w}_w)^2], \qquad \text{(A.2.10)}$$

with the diffraction length $z_D = \frac{1}{2} k \breve{w}_w^2 = k w_w^2$. The parameter $\breve{w}_w$ is equal to the half-width at $1/e^2$ power-maximum of the fundamental Gaussian beam. Note that in (A.2.9) and (A.2.10) the Fourier transform pair (A.2.1), still normalised by the parameter w_w, are used.

Appendix 2: Note on the notation

Next chapters of this book treat some aspects of beam-interface interactions as published previously by the author in separate articles. Certain elements of the notation used in those chapters will be taken differently than these taken in this chapter, in order to make them more suitable to the specific issues discussed in these chapters and to fit them closely to the notation taken previously in the respective author's publications. The reader may find below some comments concerning these differences in the notation.

Through all chapters of this book, the scale parameter w_w of beams will be specified according to the definitions (A.2.2) of the Gaussian beam. It will be assumed as the scaling parameter not only for the fundamental Gaussian but also for any higher-order Hermite-Gaussian or Laguerre-Gaussian beam. In some figures of Chapters 3, 4, and 5, however, magnitudes of the normalised spatial frequency will be given for $k\breve{w}_w = k w_w 2^{1/2}$, instead of $k w_w$ (cf. Eqs. (A.2.2) and (A.2.9)), in order to relate them to the numerical data published on the same topic previously. Each such case will be explicitly indicated in the text.

Note that in all figures in this book, the common convention is assumed to view the longitudinal and transverse shifts as normalised to the beam widths and the focal shifts as normalised to the diffraction lengths. Dimensionless coordinates (x,y,z) and (k_x,k_y,k_z), scaled according to the scale prescription (2.25)-(2.26), are used in Chapter 2 and in the treatment of nonlinear problems in Chapter 4. In other cases the unscaled coordinates are used.

In all linear problems treated in the next chapters of this book the on-axis amplitude of the Gaussian beam will be normalised to one at the centre of its waist, according to the definition (A.2.2). Only in the nonlinear problems (at the end of Chapter 3 and in Chapter 4) this unit amplitude will be multiplied, as it should be, by a square root of the beam total intensity.

In Chapter 2 the spectral $\widetilde{\chi}$ (2.33) and direct χ (2.40) polarization parameters of beams are considered, in general, to be nonuniform in transverse cross-sections of the beam and as such, they are in general unequal $\widetilde{\chi} \neq \chi$. In other chapters the polarization parameters will be stipulated as uniform, that is constant in any transverse cross-section of beams, what implies $\widetilde{\chi} = \chi$ in these planes. That justifies in this case their common notation $\chi \equiv \widetilde{\chi}$, and also $e_x \equiv \widetilde{e}_x$ and $e_y \equiv \widetilde{e}_y$. Therefore, from Chapter 3 to Chapter 7, the symbol $\widetilde{\chi}$ will be reserved for the definition of the polarization parameter defined in the coordinate frame (X,Y,Z) tied to the interface plane and the symbol χ still will be defined in the coordinate frame (x,y,z) tied to the beam.

The uniform notation is used through the book for vectors, matrices and (differential and integral) operators: vectors are indicated by symbols underlined once, matrices are indicated by symbols underlined twice, and the operators are indicated by symbols with an upper hat.

Finally, the orientation of the beam (x,y,z) and interface reference frames (X,Y,Z) with respect to the interface will be taken in Chapters 3-5 different from that in Chapters 6-7, as it will be indicated in Figures 6.1 and 7.1 assigned separately to these chapters. These changes result from different frame orientations used in parallel in literature in this field and correspond to author's previous publications, which the subsequent chapters of this book will follow.

References

[1] R. K. Luneburg, *Mathematical theory of optics* (University of California Press, Berkeley, 1964).

[2] D. Marcuse, *Light transmission optics* (Van Nonstrand, New York, 1972).

[3] J. A. Arnauld, *Beam and fiber optics* (Academic Press, New York, 1976).

[4] A. Yariv and P. Yeh, *Optical waves in crystals* (Wiley, New York, 1984).

[5] H. A. Haus, *Waves and fields in optoelectronics* (Prentice-Hall, Englewood Cliffs, NJ, 1984).

[6] A. E. Siegman, *Lasers* (University Science Books, Mill Valley, CA, 1986).

[7] B. E. A. Saleh, M. C. Teich, *Fundamentals of photonics* (Wiley, New York, 1991).

[8] M. Born and E. Wolf, *Principles of optics*, seventh edition (Cambridge University Press, Cambridge, 1999).

[9] J. Petykiewicz, *Wave optics* (Kluver Academic Publishers, 1992).

[10] Y. R. Shen, *The principles of nonlinear optics* (Wiley, New York, 1984).

[11] H. H. Gibbs, *Optical bistability, controlling light by light* (Academic, Florida, 1985)

[12] G. P. Agraval, *Nonlinear fiber optics*, second edition (Academic Press, San Diego, 1995)

[13] H. Kogelnik and T. Li, „Laser beams and resonators", Proc. IEEE **54**, 1312-1328 (1966).

[14] S. A. Collins, Jr., „Lens-system diffraction integral written in terms of matrix optics", J. Opt. Soc. Am. **60**, 1168-1176 (1970).

[15] G. A. Deschamps, „Ray techniques in electromagnetics", Proc. IEEE **60**, 1022-1035 (1972).

[16] M. Moshinsky and C. Quesne, „Linear canonical transformations and their unitary representations", J. Math. Phys. **12**, 1772-1783 (1971).

[17] H. J. Butterweck, „General theory of linear, coherent optical data-processing systems", J. Opt. Soc. Am. **67**, 60-70 (1977).

[18] D. Stoler, „Operator methods in physical optics”, J. Opt. Soc. Am **71**, 334-341 (1981).

[19] H. Bacry, M. Cadilhac, „Metaplectic group and Fourier optics”, Phys. Rev. A **23**, 2533-2536 (1981).

[20] M. Nazarathy and J. Shamir, „First-order optics – a canonical operator representation: lossless systems”, J. Opt. Soc. Am. **72**, 356-364 (1982).

[21] M. Nazarathy and J. Shamir, „First-order optics – operator representation for systems with loss or gain”, J. Opt. Soc. Am. **72**, 1398-1408 (1982).

[22] N. Mukunda, R. Simon, E. C. G. Sudarshan, „Paraxial Maxwell Beams: transformation by general linear optical systems”, J. Opt. Soc. Am. A **2**, 1291-1296 (1985).

[23] G. Nienhuis and L. Allen, „Paraxial wave optics and harmonic oscillators”, Phys. Rev. A **48**, 656-665 (1993).

[24] T. Opatrný and J. Peřina, „Non-image-forming polarization optical devices and Lorentz transformations – an analogy”, Phys. Lett. A **181**, 199-202 (1993).

[25] D. Han, Y. S. Kim, M. E. Noz, „Jones-matrix formalism as a representation of the Lorentz group”, J. Opt. Soc. Am. A **14**, 2290-2298 (1997).

[26] D. Han, Y. S. Kim, M. E. Noz, „Stokes parameters as a Minkowskian four-vector”, Phys. Rev. E **56**, 6065-6076 (1997).

[27] R. Simon, N. Mukunda, „Iwasawa decomposition in first-order optics: universal treatment of shape-invariant propagation for coherent and partially coherent beams”, J. Opt. Soc. Am. A **15**, 2146-2155 (1998).

[28] R. Simon, K. B. Wolf, „Structure of the set of paraxial optical systems”, J. Opt. Soc. Am. A **73**, 342-355 (2000).

[29] M. Lax, W. H. Louisell and W. B. McKnight, „From Maxwell to paraxial optics”, Phys. Rev. A **11**, 1365-1370 (1975).

[30] L. Felsen, N. Marcuvitz, *Radiation and scaterring of waves* (Prentice-Hall, Englewood Cliffs, 1973).

[31] S. Przeździecki and R. A. Hurd, „A note on scalar Hertz potentials for gyrotropic media”, Appl. Phys. **20** 313-317 (1979).

[32] W. Nasalski, „Amplitude-polarization representation of three-dimensional beams at a dielectric interface", J. Opt. A: Pure Appl, Opt. **5**, 128-136 (2003).

[33] K. Iwasawa, „On representations of Lie algebras", Jpn. J. Math. **19**, 513 (1948).

[34] R. Pratesi and L. Ronchi, „Generalized Gaussian beams in free space", J. Opt. Soc. Am. **67**, 1274-1276 (1977).

[35] F. Gori, G. Guattari, C. Padovani, „Bessel-Gauss beams", Opt. Commun., **64**, 491-495 (1987).

[36] V. Bagini, F. Frezza, M. Santarsiero, G. Schettini, G. Schirripa Spagnolo, „Generalized Bessel-Gauss beams", J. Mod. Optics **43**, 1155-1166 (1996).

[37] E. G. Abramochkin, N. Losevsky, V. Volostnikov, „Generation of spiral-type laser beams", Opt. Commun. **141**, 59-64 (1997).

[38] E. G. Abramochkin and V. G. Volostnikov, „Generalized Gaussian beams", J. Opt. A: Pure Appl. Opt. **6**, S157-S161 (2004).

[39] L. Allen, M. W. Beijerrsbergen, R. J. C. Spreeuw, and J. P. Woerdman, „Orbital angular momentum of light and the transformation of Laguerre-Gaussian laser modes", Phys. Rev. A **45**, 8185-8189 (1992).

[40] M. W. Beijerrsbergen, L. Allen, H. E. L. O. van der Veen and J. P. Woerdman, „Astigmatic laser mode converters and transfer of orbital angular momentum", Opt. Commun. **96**, 123-132 (1993).

[41] Y. Pagani and W. Nasalski, „Diagonal relations between elegant Hermite-Gaussian and Laguerre-Gaussian beam fields", Opto-Electon. Rev. **13**, 51-60 (2005).

[42] W. Nasalski, „Three-dimensional beam scattering at multilayers: formulation of the problem", J. Tech. Phys., **45**, 121-139 (2004).

[43] A. O. Barut, *Electrodynamics and classical theory of fields and particles*, (Macmillan, New York, 1964).

[44] J. J. Sakurai, *Modern quantum mechanics*, revised edition; S. F. Tuan, editor (Addison-Wesley, Reading, Massachusetts, 1994).

[45] M. Nazarathy, A. Hardy, J. Shamir, „Misaligned first-order optics: canonical operator theory", J. Opt. Soc. Am. A **3**, 1360-1369 (1986).

[46] E. Martinez, „Matrix formulation for pulse compressors", IEEE J. Quantum. Electron., **24**, 2530-2536 (1988).

[47] A. G. Kostenbauder, „Ray-pulse matrices: a rational treatment for dispersive optical systems", IEEE J. Quantum. Electron., **26**, 1148-1157 (1990).

[48] M. V. Vasnetsov, V. A. Pas'ko and M. S. Soskin, „Analysis of orbital angular momentum of a misaligned optical beam", New J. Phys. **7**, 46-1-17 (2005).

[49] W. Nasalski, "Longitudinal and transverse effects of nonspecular reflection", J. Opt. Soc. Am. A, **13**, 172-181 (1996).

[50] W. Nasalski, "Three-dimensional beam reflection at dielectric interfaces", Opt. Commun. **197**, 217-233 (2001).

[51] W. Nasalski, "Complex ray tracing of nonlinear propagation", Opt. Commun. **119**, 218-226 (1995).

[52] W. Nasalski, "Aberrationless effects of nonlinear propagation", J. Opt. Soc. Am. B **13**, 1736-1747 (1996).

[53] W. Nasalski, "Nonspecular bistability at a delocalized nonlinear interface", J. Modern Optics **44**, 1355-1372 (1997).

[54] W. Nasalski, "Modelling of beam reflection at a nonlinear-linear interface", J. Opt. A: Pure Appl. Opt. **2**, 433-441 (2000).

[55] W. Nasalski, „Beam switching at planar photonic structures", Opto-Electron. Rev. **9**, 280-286 (2001).

[56] L. Dutriaux, A. Le Floch, and F. Bretenaker, „Goos-Hänchen effect in the dynamics of laser eigenstates", J. Opt. Soc. Am. B **9**, 2283-2289 (1992).

[57] E. Pfleghaar, A. Marseille, and A. Weis, „Quantitative investigation of the effect of resonant absorbers on the Goos- Hänchen shift", Phys. Rev. Lett. **70**, 2281- 2284 (1993).

[58] L. Lévesque and B. E. Paton, „Light switching in a glass-AG-polymer structure using attenuated total reflection (ATR)", Can, J. Phys. **72**, 651-657 (1994).

[59] B. M. Jost, A-A R Al-Rashed, and B. E. A. Saleh, „Observation of the Goos-Hänchen effect in a phase-conjugate mirror", Phys. Rev. Lett. **81** 2233-2235 (1998).

[60] A. Haibel, G. Nimtz, and A. A. Stahlhofen, Frustrated total reflection: The double-prism revisited, Phys. Rev. E **63**, 047601-1-3 (2001).

[61] A. Köházi-Kis, „Cross-polarization effects of light beams at interfaces of isotropic media", Opt. Commun. **253**, 28-37 (2005).

[62] R. Dasgupta, P. K. Gupta, „ Experimental observation of spin-independent transverse shift of the centre of gravity of a reflected Laguerre-Gaussian light beam", Opt. Commun. **257**, 91-96 (2006).

[63] D. Müller, D. Tharanga, A. A. Stahlhofen and G. Nimtz, „Nonspecular shift of microwaves in partial reflection", Europhys. Lett., **73**, 526-532 (2006).

[64] V. Delaubert, N. Treps, C. C. Harb, P. K. Lam, and H.-A. Bachor, „Quantum measurements of spatial conjugate variables: displacement and tilt of a Gaussian beam", Opt. Lett. **31**, 1537-1539 (2006).

[65] H. Okuda and H. Sasada, „Huge transverse deformation in nonspecular reflection of a light beam possessing orbital angular momentum near critical incidence", Opt. Express **14**, 8393-8402 (2006).

[66] X. Yin, L. Hesselink, H. Chin, and D. A. B. Miller, „Temporal and spectral nonspecularities in reflection at surface plasmon resonance", Appl. Phys. Lett. **89**, 041102-1-3 (2006).

[67] W. Nasalski, "Nonspecular reflection by an electro-optically driven nonlinear interface", Proc. The 1989 URSI International Symposium on EM Theory, 219-221 (1989).

[68] W. Nasalski, "Nonspecular bistability versus diffraction at nonlinear hybrid interfaces", Optics Commun. **77**, 443-450 (1990).

[69] N. I. Petrov, „Reflection and transmission of strongly focused light beams at a dielectric interface", J. Mod. Opt. **52**, 1545-1556 (2005).

[70] W. Nasalski, "Polarization versus spatial characteristics of optical beams at a planar isotropic interface", Phys. Rev. E **74**, 056613-1-16 (2006).

[71] F. I. Baida, D. Van Labeke, J-M Vigoureux, "Numerical study of the displacement of a three-dimensional Gaussian beam transmitted at total internal reflection, Near field applications", J. Opt. Soc. Am. A **17**, 858-866 (2000).

[72] W. Nasalski and Y. Pagani, “Excitation and cancellation of higher-order beam modes at isotropic interfaces”, J. Opt. A: Pure Appl. Opt. **8**, 21-29 (2006).

[73] V. G. Fedoseyev, “Conservation laws and transverse motion of energy on reflection and transmission of electromagnetic waves” J. Phys. A: Math. Gen. **21**, 2045-2059 (1988).

[74] M. A. Porras, “Nonspecular reflection of general light beams at a dielectric interface”, Optics Commun. **135**, 369-377 (1997).

[75] J. Broe and O. Keller, „Quantum-well enhancement of the Goos-Hänchen shift for p-polarized beams in a two-prism configuration”, J. Opt. Soc. Am. A **19**, 1212-1222 (2002).

[76] M. Onoda, S. Murakami, and N. Nagaosa, „Hall effect of light”, Phys. Rev. Lett. **93**, 083901-1-4 (2004).

[77] K. Y. Bliokh, „Geometrical optics of beams with vortices: Berry Phase and orbital angular momentum Hall effect”, Phys. Rev. Lett. **97**, 043901-1-4 (2006).

CHAPTER 3

Beam reflection at dielectric interfaces

Polarization, amplitude and phase aspects of the three-dimensional beam reflection at dielectric interfaces are analysed in this chapter within a framework of the aberrationless approach. Expressions for all geometrical effects of nonspecular reflection are derived. Roles of the paraxial approximation, the cross-dimensional coupling and the nonparaxial cross-polarization coupling in the beam description are indicated and discussed. Its is shown that the substantial first-order transverse beam modifications exist for both - linear and circular - beam polarization states. Modifications of beam amplitude at a nonlinear interface of Kerr type are shown through numerical simulations of beam reflection. Characteristic features of the single beam bistable switch at such a nonlinear interface are discussed and numerical examples of the reflected beam reshaping are presented.

3.1 Introduction

In this chapter several aspects of three-dimensional (3D) beam reflection at a planar boundary between two dielectric media [1-5] are discussed. The problem is not new and many contributions, mainly devoted to the two-dimensional (2D) beam reflection and transmission in the case of total internal reflection (TIR), have been published since the first reports on this problem [6]. It is impossible to cite all of them; a certain list of references can be found in Refs. [1,2]. Recently, surface plasmon excitation at the dielectric-metal interface was analysed to interpret images of the photon scanning

tunnelling microscope [7]. Beam reflection at plane boundaries between anisotropic [8] or nonlinear [9] media has been discussed. Reports on the 2D pulse reflection/transmission [10-12] indicate the possibility of multidimensional analysis of such transient problems as well.

This chapter contains discussion on characteristics of the 3D-beam reflection within the framework of the aberrationles analysis [2]. The main points of this approach not commonly recognised yet are described in detail. Distinctions between the total field and its paraxial part forming the beamlike field structure in a vicinity of the interface are indicated. Qualitative differences between the 2D reflection and the 3D reflection, displayed in polarization characteristics of the transverse deformations of the reflected beam, are addressed. Results of Ref. [2] remain valid, however, some extensions of this approach, like the cross-dimensional coupling or the reflection at nonlinear interfaces, are also presented.

The paraxial approximation, applied to the exact solution to the problem, leads to a decomposition of a rigorous solution to the 3D problem into a product of two 2D solutions, given in two mutually orthogonal planes: the incidence plane and the plane transverse to the incidence and interface planes. This decomposition results in the straightforward interpretation of the reflected beam field distribution and provides deep insight into the process of beam or pulse shaping in linear [1-8,10-13] and nonlinear [9,14-21] media. In what follows, the optical beam geometrical modifications observed during its reflection at the interface are described by a few beam parameters introduced previously for 2D beams as effects of nonspecular (nsp) reflection [13]. They modify the beam spectrum within a frame of first-order optics and are interpreted in the space domain as beam shape modifications. Sometimes, they are called the beam shifts. Effects of the similar sort occur also in the 3D configurations. All of them, together with changes in the beam amplitude and polarization [2], are inherently originated in finite cross-sections of beams.

The geometrical nsp effects common to the 2D and 3D beam reflection exist in the incidence plane. The other geometrical nsp effects are specific only to the 3D beam reflection and can be observed in planes transverse to the of the states of their polarization, they are characterised by their spatial shape in planes transverse to their beam axes. In the following we limit our incidence plane. What qualitatively distinguishes the 3D beam reflection

from the 2D beam reflection is that these effects are essentially dependent on relative - between the TE and TM polarization - characteristics of the beams, as defined in the beam-interface configuration.

Each section of this chapter is devoted mainly to one aspect of the reflection problem. Basics of the exact electromagnetic formulation of the problem are presented in Section 2. The beam-like paraxial contribution to the exact field is described in Section 3. Extension of the analysis onto the cross-dimensional contribution to the beam field is analysed in Section 4. The nonparaxial part of the reflected field is defined in Section 5. Main features of nsp longitudinal and transverse beam geometrical deformations are shown in Sections 6 and 7, respectively. Nonlinear interfaces and the beam amplitude modifications are discussed in Sections 8 and 9. Section 10 contains conclusions and final comments. In Appendix, definitions of the geometrical effects of nsp reflection are derived and commented.

3.2 Exact analysis

Consider two isotropic, lossless dielectric semi-infinite linear media separated by a plane boundary $X = 0$. The Y-axis is chosen perpendicular to the incidence plane (X,Z), the incident (reflected) beam axis is placed in the incidence plane and is directed at polar angles $\vartheta_{01}^{(i)}$ ($\vartheta_{01}^{(r)}$) with respect to the normal $\underline{e}_X$ (along X-axis) to the interface plane (Y,Z). The incidence and reflection angles are assumed to be equal at the linear interface, that is $\vartheta_{01}^{(i)} = \vartheta_{01}^{(r)} = \vartheta_{01}$, where $0 < \vartheta_{01} < \pi/2$. In general, however, $\vartheta_{01}^{(i)} \neq \vartheta_{01}^{(r)}$ in inhomogeneous or nonlinear media, as discussed in Sections 8 and 9. Moreover, the incidence far from the Brewster angle and close to the critical angle of reflection is assumed.

The right-handed systems of the interface (X,Y,Z) coordinates, as well as the incident (x_1,x_2,x_3), g-o reflected (x_1,x_2,x_3), i.e. predicted by geometrical optics (g-o), and the actual reflected (x_{r1},x_{r2},x_{r3}) beam coordinate frames are sketched in Fig. 3.1. Note common notation for the incident and g-o reflected beams and that $Y = x_2$ for both these beams. Besides the orientation of the coordinate frames of the beams and in spite of the states of their polarization, they are characterised by their spatial shape in planes transverse to their beam axes. In the following we limit our conside-

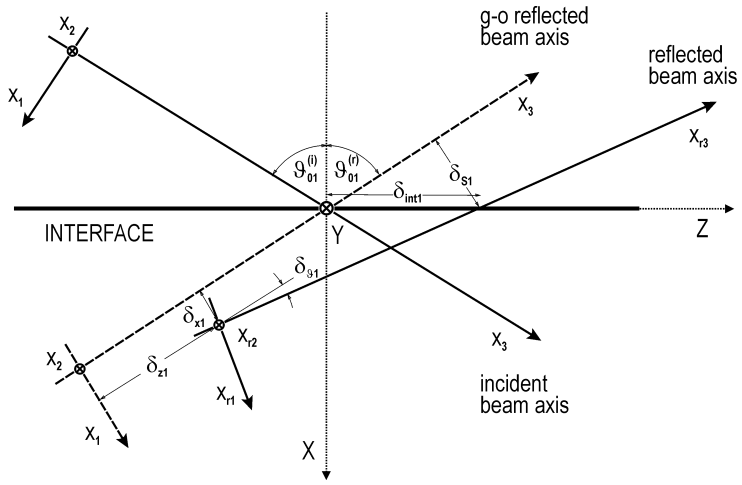

Figure 3.1. The dielectric interface with the beam and interface coordinate frames projected on the incidence plane; the orientation of the beam frames concomitant with internal reflection for the incidence angle $\vartheta_{01}^{(i)}$ larger than the Brewster angle. The lateral (Goos-Hänchen) δ_{x1}, the focal δ_{z1} and the angular $\delta_{\vartheta 1}$ longitudinal nonspecular shifts modify the geometry of the g-o reflected beam and contribute to the net beam shifts δ_{S1} and $\delta_{\mathrm{int}\,1}$ at the interface.

rations only to two parameters in the description of the beam shape deformations - the radii w_1 and w_2 of waist cross-sections of the incident beam in the principal incidence and transverse planes, respectively. They determine completely, together with location of the beam waist planes, a shape of any fundamental Gaussian beam of the elliptical cross-section. Moreover, they are also decisive in the description of beam shape deformations for higher-order Gaussian beams, for example Hermite-Gaussian or Laguerre-Gaussian beams, at least in their second-order-approximated evaluation within a frame of the paraxial limit. Within this convention the radii $\mu_1 w_1$ and $\mu_2 w_2$ of the reflected beam are described by the beam width modification factors μ_1 and μ_2 in the two orthogonal principal planes of the beam, respectively.

The incident (a=i) and reflected (a=r) time-harmonic ($\propto \exp(-i\omega t)$) beam fields are represented by two-element vectors $\underline{E}^{(a)}$, composed of independent electric field components parallel to the interface, i.e., $\underline{E}^{(a)} = (\mp E_Z^{(a)}, E_Y^{(a)})^T = (E_{\|}^{(a)} \cos\vartheta_{01}, E_{\perp}^{(a)})^T$, where "T" means transpose and "$\|$" and "$\perp$" denote TM and TE field polarizations, respectively. Henceforth, the upper and lower signs are assigned to the incident and reflected beams, respectively. Note also that, for arbitrary plane-wave component of the incident beam, the definition of the TM field components $E_{\|}^{(a)} = \mp E_Z^{(a)} / \cos\vartheta_{01}$ depend on the incidence azimuthal angle $\vartheta_{02}^{(i)}$ [2] and complies with the common definition of the TM field component only in the principal incidence plane defined by $\vartheta_{02}^{(i)} = 0$.

The beam fields above the interface are expressed by the superposition of plane waves:

$$\begin{aligned} &\underline{E}^{(a)}(X,Y,Z) = (2\pi)^{-2} \\ &\times \int\int \underline{\widetilde{E}}^{(a)}(\alpha,\gamma) \exp\left[ik\left(\pm\alpha X + \gamma Y + \beta Z\right)\right] k^2 d\alpha\, d\gamma\,, \end{aligned} \tag{3.1}$$

where tilde "~" indicates spectral field quantities. Each plane wave is defined in the local incidence plane with its azimuth incidence angle $\vartheta_{02}^{(i)}$; $\tan\vartheta_{02}^{(i)} = \gamma/\beta = const.$, and the local frame formed by the triplet: $\underline{e}_p^{(a)} = k^{-1}\underline{e}_s^{(a)} \times \underline{k}^{(a)}$, $\underline{e}_s^{(a)} = k^{-1}\underline{k}^{(a)} \times \underline{e}_X$ and $k^{-1}\underline{k}^{(a)}$, with direction cosines $\pm\alpha,\gamma,\beta$; $\beta^2 = 1 - \alpha^2 - \gamma^2$, a wave number k and a wave vectors $\underline{k}^{(a)} = k(\pm\alpha,\gamma,\beta)$ of the beam fields. The (p) and (s) spectral components: $\underline{e}_p^{(a)} \underline{\widetilde{E}}_p^{(a)}$ and $\underline{e}_p^{(a)} \underline{\widetilde{E}}_s^{(a)}$ are parallel and perpendicular to the local incidence plane $\gamma/\beta = const.$, respectively. The plane wave polarization ratios $\widetilde{\chi}_{r(p,s)} = \widetilde{E}_p^{(r)} / \widetilde{E}_s^{(r)}$ and $\widetilde{\chi}_{i(p,s)} = \widetilde{E}_p^{(i)} / \widetilde{E}_s^{(i)}$ of the reflected and incident beams, respectively, are interrelated by the ratio $r = r_p / r_s$ of the reflection coefficients $r_p = \widetilde{E}_p^{(r)} / \widetilde{E}_p^{(i)}$ and $r_s = \widetilde{E}_s^{(r)} / \widetilde{E}_s^{(i)}$. The (p) and (s) reflection coefficients r_p and r_s represent all characteristics of the, in general, stratified or inhomogeneous dielectric medium placed in the half-space ($X > 0$) below the interface. In Appendix, Eqs. (A.3.1) specify these coefficients for the case of plane wave reflection at a single planar interface.

Similar definitions hold for the beam spectral amplitudes $\underline{\widetilde{E}}^{(a)}$, given in the principal incidence plane $\gamma = 0$ by projection onto this plane the beam spectral components determined previously at the local incidence plane. The spectral amplitudes $\underline{\widetilde{E}}^{(a)} \equiv \underline{\widetilde{E}}^{(a)}(\alpha,\gamma)$ are composed of the Jones vectors $\underline{\widetilde{s}}^{(a)} \equiv \underline{\widetilde{s}}^{(a)}(\alpha,\gamma)$, belonging to the orthonormal basis of beam polarization states, and the spectral beam field envelopes $\underline{\widetilde{E}}^{(a)} \equiv \underline{\widetilde{E}}^{(a)}(\alpha,\gamma)$, both specified by the polarization parameter $\widetilde{\chi}_a$:

$$\underline{\widetilde{E}}^{(a)}(\alpha,\gamma) = (\underline{s}^{(a)}\widetilde{E}_a)(\alpha,\gamma),$$

$$\underline{\widetilde{s}}^{(a)} = (1+|\widetilde{\chi}_a|^2)^{-1/2}[\widetilde{\chi}_a, \quad 1]^T,$$

$$\widetilde{E}_a = (1+|\widetilde{\chi}_a|^2)^{1/2}\widetilde{E}_Y^{(a)},$$

$$\widetilde{\chi}_a = \mp \widetilde{E}_Z^{(a)} / \widetilde{E}_Y^{(a)}. \tag{3.2}$$

Note that, in the paraxial approximation, $\widetilde{\chi}_a$ is expressed by the ratio χ_a of the TM and TE beam components:

$$\widetilde{\chi}_a \cong (\widetilde{E}_{\|}^{(a)} / \widetilde{E}_{\perp}^{(a)})\cos\vartheta_{01} = \chi_a \cos\vartheta_{01}. \tag{3.3}$$

That also yields the spectral reflection matrix $\underline{\underline{r}} \equiv \underline{\underline{r}}(\alpha,\gamma)$, relating the spectral beam constituents in the interface coordinate frames (X,Y,Z) and (α,γ,β) (cf. Eq. (61) of Ref. [5]):

$$\underline{\widetilde{E}}^{(r)}(\alpha,\gamma) = \underline{\underline{r}}\,\underline{\widetilde{E}}^{(i)}(\alpha,\gamma),$$

$$\underline{\underline{\mathfrak{R}}} = (\gamma^2+\beta^2)^{-1}\begin{bmatrix} \beta^2 r_p - \gamma^2 r_s & -\gamma\beta\,(r_p + r_s) \\ \gamma\beta\,(r_s + r_p) & \beta^2 r_s - \gamma^2 r_p \end{bmatrix}, \tag{3.4}$$

A detailed derivation of this reflection matrix can be found in the last chapter of this book.

Subsequently, application of the definitions (3.2)-(3.3) in Eqs. (3.4) makes $\underline{\underline{\mathfrak{R}}}$ equivalent to the diagonal matrix $\underline{\underline{r}} \equiv \underline{\underline{r}}(\alpha,\gamma)$ with the following non-zero

TM ($r_{\parallel} \equiv r_{11}$) and TE ($r_{\perp} \equiv r_{22}$) components [2]:

$$(\underline{\widetilde{s}}^{(r)}\widetilde{E}_r)(\alpha,\gamma) = \underline{\underline{r}}(\underline{\widetilde{s}}^{(i)}\widetilde{E}_i)(\alpha,\gamma),$$

$$r_{\parallel} = \Re_{ZZ} + \Re_{ZY}\widetilde{\chi}_i^{-1} = r_p(\gamma^2+\beta^2)^{-1}\left[\beta(\beta-\gamma\widetilde{\chi}_i^{-1}) - \gamma(\gamma+\beta\widetilde{\chi}_i^{-1})r^{-1}\right],$$

$$r_{\perp} = \Re_{YZ}\widetilde{\chi}_i + \Re_{YY} = r_s(\gamma^2+\beta^2)^{-1}\left[\beta(\beta+\gamma\widetilde{\chi}_i^{+1}) - \gamma(\gamma-\beta\widetilde{\chi}_i^{+1})r^{+1}\right]. \quad (3.5)$$

Note that, contrary to the form of $\underline{\underline{\Re}}$, the matrix $\underline{\underline{r}}$ is diagonal ($r_{12} = 0 = r_{21}$). Its elements depend through $\widetilde{\chi}_i$ on the incident beam polarization and through r on the polarization characteristics if the interface. Since the divergence of the electric field equals zero, Eqs. (3.2) and (3.3) provide further interrelations between the polarization parameters $\chi_{i(p,s)}$, $\widetilde{\chi}_i$ and $\chi_{i(p,s)}$, $\widetilde{\chi}_i$ of the incident and reflected fields, respectively:

$$\widetilde{\chi}_{(p,s)r} = r_p r_s^{-1}\widetilde{\chi}_{i(p,s)},$$

$$\widetilde{\chi}_r = r_{\parallel} r_{\perp}^{-1}\widetilde{\chi}_i,$$

$$\widetilde{\chi}_a = (\pm\gamma + \widetilde{\chi}_{(p,s)a}\beta\alpha)(\beta \mp \widetilde{\chi}_{(p,s)a}\gamma\alpha)^{-1}, \quad (3.6)$$

The entities $\underline{\widetilde{s}}^{(a)}$ and $\widetilde{\chi}_a$ in Eqs. (3.2), (3.3) and (3.6) depend on α and γ and determine, in general, local characteristics of beam polarization. However if, in the global description of the beam, $\widetilde{\chi}_a$ is replaced by the approximation $\widetilde{\chi}_a \cong \widetilde{\chi}_{a(p,s)}\cos\vartheta_{01}$ evaluated at $\gamma = 0$, then the last one of Eqs. (3.6) becomes redundant in further considerations. Note also that Eq. (18) in Ref. [2] corresponds to the definition of $-\widetilde{\chi}_i$ applied in (3.6).

The reflection matrix $\underline{\underline{r}}$ is defined in the coordinate system (X,Y,Z) tied to the interface plane. However, sometimes it is convenient to know the reflection matrix $\underline{\underline{r}}_B \equiv \underline{\underline{r}}_B(\alpha_1,\alpha_2)$ that relates the transverse beam field components $\underline{\widetilde{E}}^{(a)}$ in the beam frames (x_1,x_2,x_3) and $(\alpha_1,\alpha_2,\alpha_3)$:

$$\begin{aligned}\underline{\widetilde{E}}^{(r)}(\alpha_1,\alpha_2) &= (\underline{\widetilde{s}}^{(r)}\widetilde{E}_r)(\alpha_1,\alpha_2)\\ &= \underline{\underline{r}}_B\underline{\widetilde{E}}^{(i)}(\alpha_1,\alpha_2) = \underline{\underline{r}}_B(\underline{\widetilde{s}}^{(i)}\widetilde{E}_i)(\alpha_1,\alpha_2).\end{aligned} \quad (3.7)$$

Henceforth, the beam quantities are distinguished from those related to the interface frame just by arguments related to these beam frames. Moreover, in the new beam frames, $\widetilde{\chi}_a$ is replaced by χ_a in the definitions (3.2) of $\underline{\widetilde{s}}^{(a)}$ and $\underline{\widetilde{E}}^{(a)} = (\widetilde{E}_1^{(a)}, \widetilde{E}_2^{(a)})^T$.

To obtain the beam field representation in the incident and reflected beam frames, the rotation of the (X,Y,Z) and (α,γ,β) frames by angles $\pm(\pi/2 - \vartheta_{01})$ around the Y and γ axes, respectively, is applied. In these coordinate frames the spectral representation of the transverse parts $\underline{\widetilde{E}}^{(a)}$ of the beam fields $\underline{\widetilde{E}}_B^{(a)} = (\widetilde{E}_1^{(a)}, \widetilde{E}_2^{(a)}, \widetilde{E}_3^{(a)})^T$ is given by:

$$\begin{aligned} &\underline{E}^{(a)}(x_1,x_2,x_3) = (2\pi)^{-2} \\ &\times \int\int (\underline{\widetilde{s}}^{(a)} \widetilde{E}_a)(\alpha_1,\alpha_2) \exp\left[ik(\pm\alpha_1 x_1 + \alpha_2 x_2 + \alpha_3 x_3)\right] k^2 d\alpha_1 d\alpha_2 , \end{aligned} \tag{3.8}$$

and that yields the reflection matrix $\underline{\underline{r}}_B$:

$$\underline{\underline{r}}_B = \begin{bmatrix} \alpha_3/\alpha & (\gamma/\alpha)\sin\vartheta_{01} \\ 0 & 1 \end{bmatrix} \begin{bmatrix} r_\parallel & 0 \\ 0 & r_\perp \end{bmatrix} \begin{bmatrix} \alpha/\alpha_3 & (\gamma/\alpha_3)\sin\vartheta_{01} \\ 0 & 1 \end{bmatrix}. \tag{3.9}$$

Up to this point, no approximation in Eqs. (3.1)-(3.9) is used. The beam field spectral representation (3.8) fulfils a full set of Maxwell's equations in homogeneous linear media and the continuity conditions of the tangential electromagnetic field components at the interface. That implies that the beam field possesses also the nonzero longitudinal component:

$$\widetilde{E}_3^{(a)} = -(\pm\alpha_1 \widetilde{E}_1^{(a)} + \alpha_2 \widetilde{E}_2^{(a)})\alpha_3^{-1}, \tag{3.10}$$

and the beam reflection matrix $\underline{\underline{r}}_B$ differs from $\underline{\underline{r}}$ by the nonparaxial part $\underline{\underline{r}}_B - \underline{\underline{r}} = \Delta\gamma\, \underline{\underline{r}}$,

$$\Delta\underline{\underline{r}} = (r_\parallel + r_\perp)\alpha^{-1} \sin\vartheta_{01} \begin{bmatrix} 0 & 1 \\ 0 & 0 \end{bmatrix}, \tag{3.11}$$

that couples the TM component $\widetilde{E}_1^{(r)}$ of the reflected beam to the TE component $\widetilde{E}_2^{(i)}$ of the incident beam. Note also that analogical TM-TE coupling appears for the H-field formulation of the beam reflection.

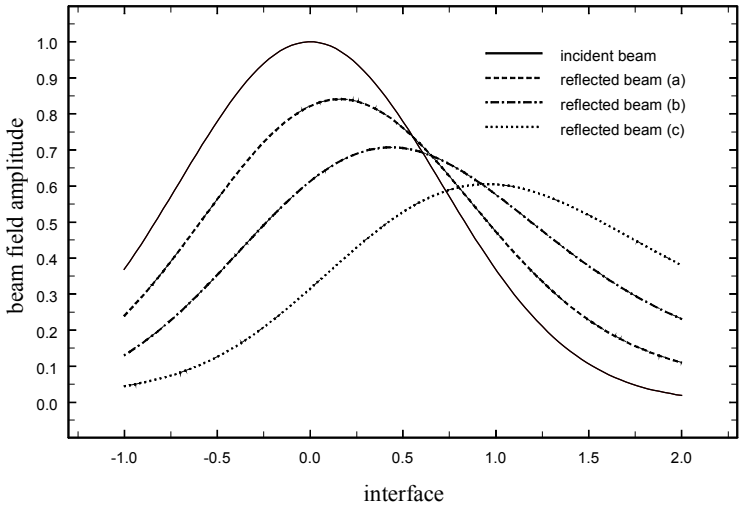

Figure 3.2. Normalised magnitudes of the incident and reflected beam amplitude distributions at the interface for the critical TE incidence and decreasing dielectric interface contrast: $\vartheta_c = 45^o$ (a), $\vartheta_c = 80^o$ (b), $\vartheta_c = 87^o$ (c). Variations of the net shift $\delta_{\text{int}1}$ and the beam amplitude modification $|r_\perp / r_s|$ evaluated at $\vartheta = \vartheta_c$ are clearly visible. The distance along the interface is scaled by the projection of the beam half-width; the beam axis crosses the interface at the point (0.0).

The incident and reflected field amplitude distributions at the cross-section of the incidence and interface planes is depicted in Fig. 3.2 for different values of the dielectric contrast n measured by the angle of critical reflection $\vartheta_c = \arcsin(n^{-1})$ and for $\vartheta_{01} = \vartheta_c$. The procedure of the field incidence plane to the diffraction length z_{D1}, the transverse x_j-coordinates are normalised to the numerical evaluation described in [9] is applied (see the next chapter). The incident beam has a fundamental Gaussian shape and is focused at the interface, the x_3-coordinate is normalised in the incident beam radii $w_{wj} = (2z_{Dj}k^{-1})^{1/2}$ at the waist. It is assumed, as in the most numerical

examples in this chapter, that the normalised wave number $(2kz_{D1})^{1/2}$ equals 50, where w_{wj}, j=1,2, mean waist half-widths at $1/e^2$-maxima of the beam intensity in the incidence and transverse principal planes of the incident beam. Note that, in the numerical examples shown in this chapter, the definition (A.2.9) from Chapter 2 of the Gaussian beam is assumed, that means that $E \propto \exp[-(x_1^2/\breve{w}_{w1}^2 + x_2^2/\breve{w}_{w2}^2)]$ at the beam waist and w_{wj} in fact equals $\breve{w}_{wj}$, according to the convention taken in numerical examples in [2, 9,17].

The net displacement $\delta_{\text{int}\,1}$ of the field amplitude maximum from the g-o beam position is clearly vivid. It increases as the dielectric contrast decreases and approaches values of the order of w_{w1}, as the incidence angle approaches the grazing angle $\vartheta_{01}^{(i)} \cong 90^o$. How this displacement is related to the beam geometrical deformations will be explained in the next section.

3.3 Paraxial approximation

In the paraxial approximation $\alpha_3 \cong 1 - 2^{-1}\alpha_1^2 - 2^{-1}\alpha_2^2$ and the longitudinal field components $\widetilde{E}_3^{(a)}$ are neglected, i.e. $\underline{\widetilde{E}}_B^{(a)} \cong (\widetilde{E}_1^{(a)}, \widetilde{E}_2^{(a)}, 0)^T$. Moreover, the 3D beam field spectral envelopes $\widetilde{E}_a(\alpha_1, \alpha_2, x_3)$ are factored out into the product of two appropriately normalised 2D beam envelopes $\widetilde{E}_{a1}(\alpha_1, x_3) \propto \widetilde{E}_a(\alpha_1, 0, x_3)$ and $\widetilde{E}_{a2}(\alpha_2, x_3) \propto \widetilde{E}_a(0, \alpha_2, x_3)$, defined in the planes $\alpha_2 = 0$ and $\alpha_1 = 0$ in the spectral domain, respectively:

$$\underline{\widetilde{E}}^{(a)}(\alpha_1, \alpha_2, x_3) = \underline{\widetilde{s}}^{(a)} \exp(ikx_3)\widetilde{E}_{a1}(\alpha_1, x_3)\widetilde{E}_{a2}(\alpha_2, x_3),$$

$$\begin{aligned} &E_{aj}(x_j, x_3) \\ &= (2\pi)^{-1} \exp(-ikx_3) \int \widetilde{E}_{aj}((\pm 1)^j \alpha_j, x_3) \exp\left[ik(\alpha_j x_j + \alpha_{3j} x_3)\right] k\, d\alpha_j \\ &\cong (2\pi)^{-1} \int \widetilde{E}_{aj}((\pm 1)^j \alpha_j, x_3) \exp\left[ik(\alpha_j x_j - 2^{-1}\alpha_j^2 x_3)\right] k\, d\alpha_j, \end{aligned}$$

$$\underline{\widetilde{s}}^{(r)} \widetilde{E}_{r1}(\alpha_1, x_3)\widetilde{E}_{r2}(\alpha_2, x_3) = \underline{\underline{r}}\, \underline{\widetilde{s}}^{(i)} \widetilde{E}_{i1}(\alpha_1, x_3)\widetilde{E}_{i2}(\alpha_2, x_3). \qquad (3.12)$$

Within the paraxial regions of the beam axes $\alpha_{3j} \cong 1 - 2^{-1}\alpha_j^2$ and the field representations (3.8) and (3.12) remain equivalent. Hereinafter the spectral

envelopes $\widetilde{E}_a$ and $\widetilde{E}_{aj}$, j=1,2, are assumed to be dependent not only on α_j but also on x_3, to account approximately for possible inhomogeneouities or nonlinearities of the medium [9].

The nonparaxial component $\gamma\Delta r$ disappears in the paraxial approximation. The reflection matrix retains only diagonal elements, i.e. $\underline{\underline{r}}_B \cong \underline{\underline{r}}$ and, in the parabolic approximation, is factored out into the product of the g-o (or zero-order) reflection matrix $\underline{\underline{r}}_g \equiv \underline{\underline{r}}_0$ equal to $\underline{\underline{\widetilde{r}}}(0,0)$ and the matrix of the nsp contribution $\underline{\underline{r}}_\Delta$:

$$\underline{\underline{r}} \cong \underline{\underline{r}}_0 \underline{\underline{r}}_\Delta = \begin{bmatrix} r_{0\|} & 0 \\ 0 & r_{0\perp} \end{bmatrix} \begin{bmatrix} \exp(\delta r_\|) & 0 \\ 0 & \exp(\delta r_\perp) \end{bmatrix},$$

$$\delta r = -ik\left[L_1\alpha_1 + L_2\alpha_2 - 2^{-1}(F_1\alpha_1^2 + F_2\alpha_2^2)\right],$$

$$L_j \cong \delta_{xj} + iz_{Dj}\mu_j^2\delta_{\vartheta j},$$

$$F_j \cong \delta_{zj} + iz_{Dj}\mu_j^2\delta_{wj}, \tag{3.13}$$

j=1,2. In Eqs. (3.13) $\underline{\underline{r}}_\Delta$ is expressed by the complex shifts L_j and F_j of the reflected beam [13] and z_{Dj} denote diffraction lengths of the incident beam in the incidence plane (j=1) and transverse plane (j=2).

For brevity of notation, the suffixes "||" and "⊥" will be henceforth omitted in expressions valid for both polarization's. The matrix $\underline{\underline{r}}_0$ and the shifts L_j and F_j are defined by the TM ($r = r_{0\|}$) and TE ($r = r_{0\perp}$) reflection coefficients and their first two (logarithmic) derivatives, i.e. by: $r_{bj} \equiv \partial_{\alpha_j} \ln r_b$ and $r_{bij} \equiv \partial_{\alpha_i\alpha_j} \ln r_b$, b=||,⊥, evaluated at the beam spectrum centre $\alpha_1 = 0 = \alpha_2$ (cf. also definitions of these expressions given in Appendix). The real and imaginary parts of the complex shifts are commonly expressed by the lateral δ_{xj}, angular $\delta_{\vartheta j}$, focal δ_{zj} and waist radius squared $\delta_{wj} = 1 - \mu_j^{-2}$ shifts, the last one determined by the beam waist size modification factor μ_j. All these effects describe the reflected beam deformations with respect to the g-o predictions determined by the approximation $r_b \cong r_{0b} \equiv r_{gb}$.

The definitions of $\delta_{\vartheta j}$ and μ_j in (3.13) are approximate; in the plane wave representations (3.8) and (3.12) their values are given by [2]:

$$tg\delta_{\vartheta j} = \mathrm{Im}(L_j / z_{Dj}) / [1 + \mathrm{Im}(F_j / z_{Dj})],$$

$$\mu_j^4 = [\mathrm{Im}(L_j / z_{Dj})]^2 + [1 + \mathrm{Im}(F_j / z_{Dj})]^2 . \tag{3.14}$$

The lateral, angular and focal shifts contribute to the net shifts $\delta_{\mathrm{int}\,1}$ down the interface, being the projection of the composite shifts δ_{S1} of the beam axis on the interface (cf. Fig. 3.1):

$$\delta_{\mathrm{int}\,j} = \delta_{Sj} \cos^{-1} \vartheta_{0j} = [\delta_{xj} + (x_3 - \delta_{zj}) \tan \delta_{\vartheta j}] \cos^{-1} \vartheta_{0j} . \tag{3.15}$$

Exactly this shift is shown, in the plane of incidence (j=1), by the beam amplitude peak displacements in Fig. 3.2.

It will be further assumed that the polarization parameters $\chi_a \equiv \chi_a(\alpha_1, \alpha_2)$ loose their local character in favour of the global beam polarization ratios χ_a evaluated at $\alpha_1 = 0 = \alpha_2$. New Jones vectors $\underline{s}^{(a)}$ and new beam envelopes E_a are then expressed in terms of these parameters but still the local character of the beam polarization can be retained in this formalism, if necessary.

The final expressions for polarization, amplitude and shape of the reflected beam $\underline{E}^{(r)} = \underline{s}^{(r)} E_r$ are given, in the reflected beam coordinates, in terms of the first-order L_j and the second-order F_j complex modifications of the g-o reflected beam $\underline{E}^{(g)} = \underline{s}^{(g)} E_g$:

$$\underline{E}^{(g)}(x_1, x_2, x_3) = \underline{\underline{r}}_0 \underline{s}^{(i)} \exp(ikx_3) E_{g1}(x_1, x_3) E_{g2}(x_2, x_3),$$

$$\begin{aligned} &\underline{E}^{(r)}(x_1, x_2, x_3) \\ &= \underline{\underline{r}}_0 \underline{s}^{(i)} \exp(ikx_3) E_{g1}(x_1 - L_1, x_3 - F_1) E_{g2}(x_2 - L_2, x_3 - F_2), \end{aligned} \tag{3.16}$$

where $E_{g1}(x_1, x_3) = E_{i1}(-x_1, x_3)$ and $E_{g2}(x_2, x_3) = E_{i2}(x_2, x_3)$ are the 2D envelopes of the g-o reflected beam, and $\underline{s}^{(g)} E_g = \underline{\underline{r}}_0 \underline{s}^{(i)} E_i$. The signs of the arguments of E_{g1} account for possible incident beam asymmetry in the transverse to x_3-axis planes. In spite of the common amplitude and Jones

vector, the 3D beam envelope E_r is expressed directly, in the paraxial approximation, by the product of two 2D g-o beam envelopes E_{gj} modified by the complex shifts L_j and F_j.

Relations between the beam field representations (3.8) and (3.12), as well as their counterparts (3.19) given in the next section, reflect major features of the beam field description in the paraxial region. They are: the parabolic approximation to the beam spectrum and spatial shape changes in beam amplitude and phase, the transversality of the beam polarization and the decomposition of the 3D beam field into the product of the two 2D factors. The reference frame, in which this decomposition is accomplished, specifies r_p and r_s used in Eqs. (3.4)-(3.5) as the Fresnel reflection coefficients. Note that r_p and r_s are the p and s are coefficients of plane wave reflection at the interface as well as at any planar reflecting and/or transmitting structure.

It should be also stressed that within the paraxial approximation the definitions given in Sections 2-3 are approximately independent of the incident beam shape. They are valid for arbitrary beam shapes, provided that the accuracy of the expansions (3.13) and (A.3.3)-(A.3.4) in Appendix are justified by numerical simulations. Therefore, the results can be applied to more general cases of beams than that of the fundamental Gaussian shape. Moreover, in the next step of this analysis, the incident beam shape can be accounted for by integration of the beam field representations (3.8) and (3.16) (cf. Section 6 and the next chapter).

For a beam with arbitrary shape, i.e. when the field factorisation (3.12) does not directly apply, the presented analysis ought to be applied independently to each component of the pertinent beam field expansion. Upon reflection, the components of such expansion suffer from the nsp deformations determined by the complex shifts L_j and F_j. The reflection, for example, of the Laguerre-Gaussian beams, represented by expansions in terms of Hermite-Gaussian beams in two transverse dimensions, can be analysed in this manner (see, for example, Eqs. (A.3.26) in Appendix).

The analysis is mainly devoted to the beam reflection although it yields also the transmission matrix $\underline{t}$ and the transmitted or total beam field $\underline{E}^{(t)}$ at the interface, e.g. $t_\perp = 1 + r_\perp$ and $E_\perp^{(t)} = E_\perp^{(i)} + E_\perp^{(r)}$ for the TE polarization.

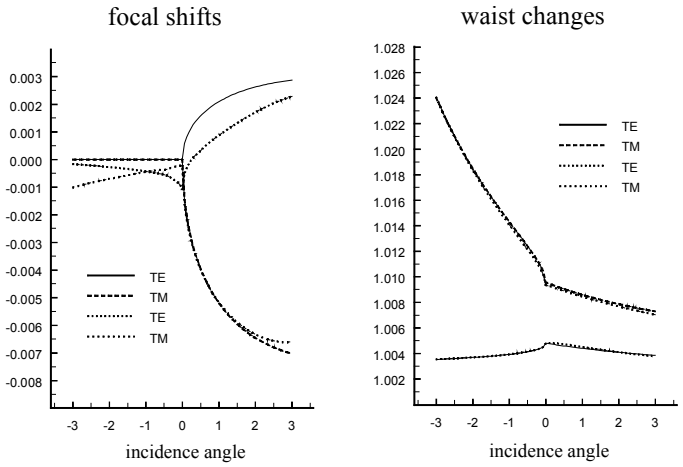

Figure 3.3. Variation of the second-order transverse nps effects for the TE and TM components of the reflected beam: the focal shifts δ_{z2} and the beam waist radius relative modifications μ_2 versus incidence angle changes $\vartheta_{01}^{(i)} - \vartheta_c$ (in degrees) around the critical incidence $\vartheta_{01}^{(i)} = \vartheta_c = 45^o$ for the linear polarization $\chi_i = 1$ of the incident beam. Dotted curves show the nsp effects modified by the cross-dimensional coupling; $kw_1 = kw_2 = 50$. The shifts δ_{z2} are scaled by the diffraction lenght z_{D2} of the incident beam.

Moreover, for the homogeneous medium filled the semi-infinite space below the interface, deformations of the transmitted beam field in the partial transmission case can be also derived. It can be accoplished step by step along the lines of Sections 2 and 3, provided that in the quantities r, α and β for the reflected beam $\underline{E}^{(r)}$ are replaced by their counterparts t, $-\alpha^{(t)}$ and $\beta^{(t)}$ for the transmitted beam $\underline{E}^{(t)}$ (see Chapter 7 for more details). For the stratified medium the backward field constituents can be also evaluated in the similar manner (see Chapter 6 for more details). Other extensions of the formalism will be also sketched in the next sections.

3.4 Paraxial cross-dimensional coupling

The strict beam field decomposition (3.16) into the two 2D beam envelopes leaves next terms in the reflection coefficient expansion (3.13) outside the formalism described above. However, the first cross-dimensional second-order term $(r_{12}+r_{21})\alpha_1\alpha_2$ can be included in the reflection coefficient expansion without changing solution structure. To this end, the second-order complex shifts F_j should be modified by the complex, in general, angle ε, defined by the second-order derivatives of r (cf. Eq. (A.3.9)):

$$\breve{F}_1 = F_1\cos^2\varepsilon + F_2\sin^2\varepsilon - ik^{-1}r_{12}\sin 2\varepsilon\,,$$

$$\breve{F}_2 = F_2\cos^2\varepsilon + F_1\sin^2\varepsilon + ik^{-1}r_{21}\sin 2\varepsilon\,, \tag{3.17}$$

where

$$\tan 2\varepsilon = (r_{12}+r_{21})/(r_{11}-r_{22})\,. \tag{3.18}$$

The cross-dimensional coefficient $r_{12}+r_{21}$ induces rotation of the transverse coordinates in the spatial and spectral domains through the angle ε and that leads to the formal redefinition (3.17) of the second-order complex shifts in the new principal planes $\alpha_1 = 0 = x_1$ and $\alpha_2 = 0 = x_2$.

However, ε appears, in general, a complex quantity, different for TE and TM polarization. Therefore, the direct geometrical interpretation of beam deformations seems to be blurred in these planes. This difficulty proves to be only a formal one, at least in the range of paraxial approximation near the reflected beam axis. The plane wave (3.8) and the paraxial (3.12) representations are equivalent in this range. Therefore, in the primary principal planes $\alpha_1 = 0 = x_1$ and $\alpha_2 = 0 = x_2$ the reflected beam can be then reexpressed by analogy to Eqs. (3.16):

$$\begin{aligned}&\underline{E}^{(r)}(x_1, x_2, x_3)\\ &= \underline{\underline{r}}_0\underline{s}^{(i)}\exp(ikx_3)E_{g1}(x_1 - L_1, x_3 - \breve{F}_1)E_{g2}(x_2 - L_2, x_3 - \breve{F}_2)\,.\end{aligned} \tag{3.19}$$

The beam field retains its factored form in the paraxial approximation. In spite of theintroduced extension, the first-order complex shifts L_j, as well as the real shifts δ_{xj} and $\delta_{\vartheta j}$, continue being unchanged even for $\varepsilon \neq 0$. In other

words, the second-order terms in the expansion of $\ln r$ (A.3.4) result only in the second-order effects (3.17) of beam deformations. Moreover, the expansion coefficient $r_{12}+r_{21}$ is proportional to χ_i (χ_i^{-1}), the cross-dimensional beam deformation effects disappear altogether for the pure TE (TM) incident beam polarization.

The cross-dimensional modifications of the longitudinal shifts are usually negligibly small because the transverse effects are commonly approximately one order of magnitude smaller than their longitudinal counterparts. The second order transverse nsp effects δ_{z2} and μ_2 and their modifications by the cross-dimensional coupling are shown in Fig. 3.3. They still are not substantial although they may become larger close to the grazing incidence. Note that in all figures in this book the common convention is assumed to view the longitudinal and transverse shifts as normalised to the beam widths and the focal shifts as normalised to the diffraction lengths.

3.5 Nonparaxial cross-polarization coupling

The effect of cross-polarization at the interface stems from the presence of the non-zero off-diagonal elements in the reflection matrix (3.4). They are proportional - through γ - to the transverse component k_y of the wave vector $\underline{k}$. Thus, these elements are responsible for excitation of higher-order modes at the interface, as will be shown in detail in Chapter 7. However, the cross-polarization effect arises also from the nonparaxial nature of the beam fields, being solutions of the full set of Maxwell equations. This aspect of the cross-polarization coupling is discussed in this section.

The field representations (3.16) and (3.19) were evaluated within the paraxial approximation and that permits the beam description in terms of effects of nsp reflection. The nonparaxial TE-TM part $\gamma\Delta\underline{\underline{r}}$ (3.11) of the reflection matrix $\underline{\underline{r}}_B$ indicates deviations of the total reflected field distribution and polarization from its presumed beamlike structure. Still, however, this part of the reflected beam can be evaluated per analogy to the evaluation of the paraxial part of the beam given in Section 3. The evaluation of the representations (3.16) and (3.19) yields:

$$\Delta E_{\|}^{(r)}(x_1,x_2,x_3)=(2\pi)^{-2}$$
$$\times\int\int\alpha_2(\Delta r_{12}\tilde{s}_2^{(i)}\tilde{E}_2^{(i)})(-\alpha_1,\alpha_2)\exp[ik(\alpha_1x_1+\alpha_2x_2+\alpha_3x_3)]k^2d\alpha_1d\alpha_2\,,$$

$$\Delta E_{\|}^{(r)}(x_1,x_2,x_3)=-ik^{-1}\Delta r_0 s_2^{(i)}\exp(ikx_3)$$
$$\times E_{g1}(x_1-\Delta L_1,x_3-\Delta\breve{F}_1)\,(\partial E_{g2}/\partial x_2)(x_2-\Delta L_2,x_3-\Delta\breve{F}_2)\,, \tag{3.20}$$

with ΔL_j and $\Delta\breve{F}_j$ obtained by substitution of r by Δr_{12} from [11] in the expressions for, L_j and $\breve{F}_j$ and for

$$\Delta r_0=(r_s+r_p)\tan\vartheta_{01}\,. \tag{3.21}$$

For the fundamental Gaussian incidence with transverse envelope E_{g2} Eq. (3.21) yields the first-order Hermite-Gaussian in the transverse planes x_3=constant:

$$(\partial E_{g2}/\partial x_2)\,(x_2-\Delta L_2,x_3-\Delta\breve{F}_2)$$
$$=-(x_2-\Delta L_2)v_2^{-2}(x_3)E_{g2}(x_2-\Delta L_2,x_3-\Delta\breve{F}_2)\,,$$

$$v_2^2(x_3)=k^{-1}(z_{D2}+i(x_3-\Delta\breve{F}_2))\,, \tag{3.22}$$

where v_2 means the complex transverse half-width of the beam. The nonparaxial contribution (3.20) to the reflected beam field has pure linear TM polarization shifted in its phase by $\pi/2$ with respect to the paraxial beam and its amplitude is proportional to the sum of the p and s reflection coefficients.

The nonparaxial coupling is rather a weak contribution to the beam field, at least not too close to the grazing incidence. In normalised units (cf. Ref. [9] and the next chapter) its amplitude is of the order of the normalised wave number $kw_{w2}=(kz_{D2})^{1/2}$ less than the amplitude of the paraxial part of the field. On the other hand, it is inherent to the finite beam cross-section; for wide beams, that is in the plane wave limit, $(kz_{D2})^{1/2}$ becomes large and the coupling vanishes. The nonparaxial TE-TM coupling appears one more effect of nsp reflection, related this time to the beam polarization and its amplitudedistribution in the transverse cross-section of the beam (see also Chapter 7). The TE-TM coupling effect becomes stronger near the grazing incidence. Its nature suggests possible excitation of surface waves by finite-

width beams at, or instance, metallic interfaces. Note in this context that surface plasmon excitation at the dielectric-metal interface by a narrow 3D Gaussian beam of the TE polarization was recently discussed and numerically confirmed in [7].

3.6 Longitudinal nonspecular effects

The analysis presented seems attractive because it is simple and straightforward. However, numerical evaluation of beam fields that bases directly on the expansions (A.3.3)-(A.3.4) and (A.3.9) of $\ln r$ may be inaccurate, especially in the most interesting cases, such as proximity of the critical incidence, i.e. for $\vartheta_{01} \cong \vartheta_c$, where ϑ_c is the angle of critical reflection. Besides the divergence of the reflection matrix expansion (3.13) at the branch point at $\vartheta_{01} \cong \vartheta_c$, this expansion accounts for the reflection coefficient behaviour only from one side of the spectrum singularities, meanwhile the (wide) beam spectrum is also substantially modified by other side of these singularities, usually with different behaviour characteristics.

To obtain accurate numerical results, more refined numerical techniques should be applied. In numerical calculations applied in this chapter the two-point expansion around the branch point of $\ln r$ is used in evaluation of the beam fields, instead of the one-point expansions of $\ln r$ (A.3.3)-(A.3.4) and (A.3.9). Moreover, the shape of the incident beam should be accounted for by exact integration of subsequent terms in the reflected beam expansion (see Section 4 of the next chapter for details of this approach). Such evaluation of the beam field reveals that, for instance, the longitudinal shifts δ_{x1} and δ_{z1} do not disappear, in general, for $\vartheta_{01} < \vartheta_c$, as well as magnitudes of $\delta_{\vartheta 1}$ and δ_{w1} are even larger for $\vartheta_{01} > \vartheta_c$, contrary to what may appear from straight-forward application of Eqs. (3.13) and (3.14), or (3.17) and (3.19). Moreover, the beam reflection complex coefficient r also appears different from r_g by a factor r/r_g [9,17].

The longitudinal complex shifts L_{b1} and F_{b1}, and beam deformations δ_{x1}, $\delta_{\vartheta 1}$, δ_{z1} and μ_1 depend on r_s and r_p and their derivatives through Eqs. (A.3.3), in a manner known from the 2D beam reflection. The shifts of the TM polarization are larger than those of the TE polarization. All of them

increase as the dielectric contrast $n = \sin^{-1}\vartheta_c$ at the interface decreases (cf. Fig. 3.2). In Figs. 3.4 and 3.5 the first-order and second-order geometrical effects are shown versus variation of the incidence angle around the critical angle (in degrees). The plots are given for $kw_{w1} =$ 50, 100, the parameter regarded as the measure of the propagating beam diffraction. Evidently, magnitudes of the nsp effects and positions of their extremal values depend on the beam diffraction. Their magnitudes are larger and their extreme positions are placed further apart from the critical incidence for smaller values of kw_{w1}.

3.7 Transverse nonspecular effects

For the TE and TM polarization the longitudinal beam shifts depend only separately on the Fresnel coefficients r_s and r_p. On the other hand, the transverse effects depend, through the simple algebraic expressions (A.3.7) and (A.3.8), on the beam (χ_i) and the relative polarization parameters r_p/r_s of the reflecting structure. The first-order complex shifts L_{b2} are proportional to the polarization ratio χ_i (χ_i^{-1}) for the pure TE (TM) polarization and thus the first-order beam deformations δ_{x2} and $\delta_{\vartheta 2}$ disappear for the pure TE (TM) beam polarization, for which $\chi_i = 0$ ($\chi_i^{-1} = 0$) holds. However it is a very exceptional case of the beam polarization. Moreover, the (non-zero) transverse deformations δ_{x2}, $\delta_{\vartheta 2}$, δ_{z2} and δ_{w2} are not inherently related to the elliptic polarization ($\mathrm{Im}(\chi_i) \neq 0$) of the beam. They exist also for the mixture of TE and TM beam field components of the incident beam, with the linear polarization direction inclined with respect to the incidence plane, i.e. for $\mathrm{Im}(\chi_i) = 0$ and $\chi_i \neq 0 \neq \chi_i^{-1}$ [2].

The asymmetry of $\underline{\underline{r}}$ with respect to the transverse direction cosines $\gamma = \alpha_2$ in Eqs. (3.5) implies that the first derivatives $\partial\underline{\underline{r}}/\partial\gamma$ are nonzero quantities at the reflected beam axis and leads, in general, to nonzero values of the transverse first-order nsp effects δ_{x2} and $\delta_{\vartheta 2}$ (cf. Eqs. (A.3.7)). Moreover, the second-order transverse effects of nsp reflection exist even for pure TE and TM polarizations - the second-order complex shits F_{b2}, δ_{z2} and δ_{w2} still possess finite nonzero values in these cases (cf. Eqs. (A.3.8)).

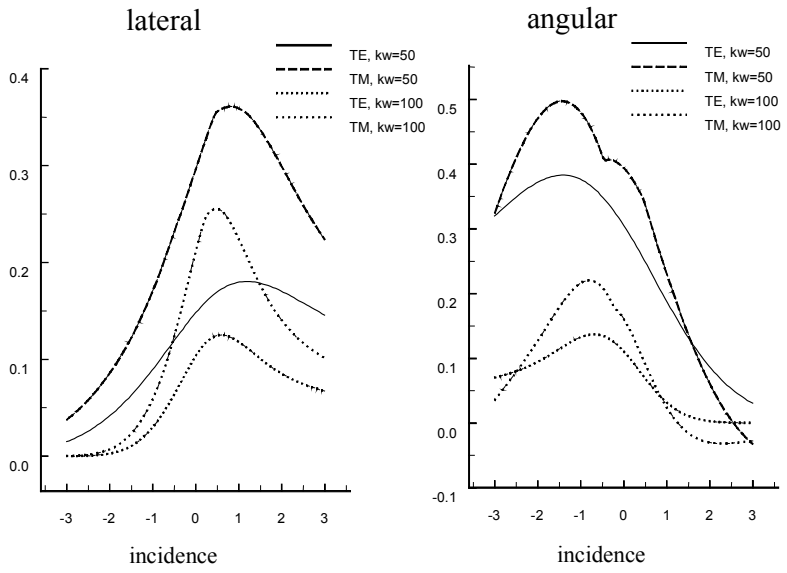

Figure 3.4. First-order longitudinal nsp effects: the lateral shift δ_{x1} and the angular $\delta_{\vartheta 1}$ shift (in degrees), versus incidence angle changes $\vartheta_{01}^{(i)} - \vartheta_c$ around the critical incidence $\vartheta_{01}^{(i)} = \vartheta_c = 45^o$. Cases of the different incident beam polarization (TE and TM) and width ($kw \equiv kw_{w1}$) of the incident beam are shown. The lateral shift is normalised to the incident beam half-width.

Any evaluation of the transverse effects should properly account from the be-ginning for this asymmetric feature of $\underline{\underline{r}}$, being a consequence of the vectorial nature of the problem. For example, for equal contributions of the TM and TE field components, i.e. for $|\chi_i| = 1$, both first-order transverse shifts attain nonzero values. Equations (A.3.7) imply that, in the TIR state $|r_p / r_s| = 1$ and for the incidence angle ϑ_{01} larger that the critical angle ϑ_c, the first-order transverse shifts of the TE beam field are for the (diagonal) linear polarization of the incident beam ($\chi_i = \pm 1$):

$$\delta_{\perp x2}^{(\pm 1)} = \mp k^{-1} \operatorname{Im}(r_p / r_s) ctg\, \vartheta_{01},$$

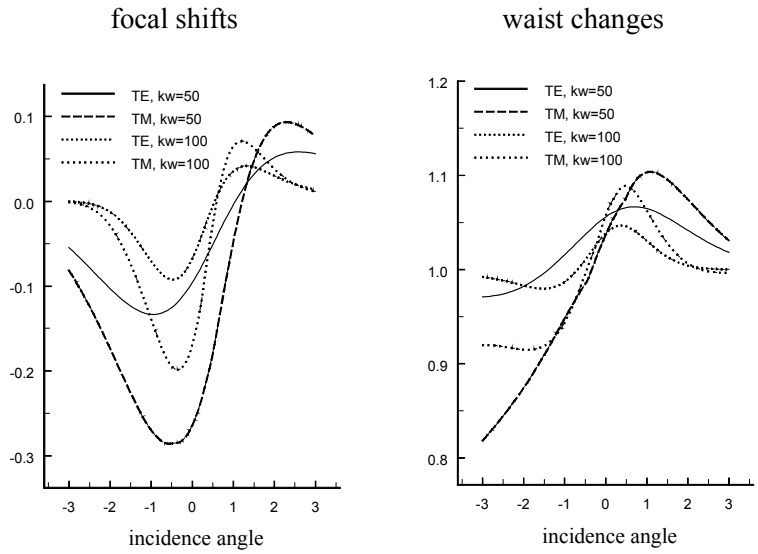

Figure 3.5. Second-order longitudinal nsp effects for the TE and TM components of the reflected beam: the focal shift δ_{z1} and the beam waist radius relative modification μ_1, versus incidence angle changes $\vartheta_{01}^{(i)} - \vartheta_c$ (in degrees) around the critical incidence $\vartheta_{01}^{(i)} = \vartheta_c = 45^o$. Cases of the different beam polarization (TE and TM) and widths ($kw \equiv kw_{w1}$) of the incident beam are shown. The focal shift is scaled to the diffraction length of the incident beam.

$$\delta_{\perp\vartheta 2}^{(\pm 1)} = \pm k^{-1} z_{D2}^{-1} (1 + \mathrm{Re}(r_p / r_s)) ctg\, \vartheta_{01}, \tag{3.23}$$

and for the (diagonal) circular polarization ($\chi_i = \pm i$):

$$\delta_{\perp x2}^{(\pm i)} = \mp k^{-1} (1 + \mathrm{Re}(r_p / r_s)) ctg\, \vartheta_{01},$$

$$\delta_{\perp\vartheta 2}^{(\pm i)} = \mp k^{-1} z_{D2}^{-1}\, \mathrm{Im}(r_p / r_s) ctg\, \vartheta_{01}, \tag{3.24}$$

all of them being evaluated at the beam axis, that is for $\alpha_1 = 0 = \alpha_2$. The TM transverse shifts $\delta_{\parallel x2} = +\delta_{\perp x2} / \cos^2 \vartheta_{01}$ and $\delta_{\parallel\vartheta 2} = -\delta_{\perp\vartheta 2} / \cos^2 \vartheta_{01}$ are larger than the transverse TE shifts by a factor $\cos^{-2} \vartheta_{01}$ for both types of

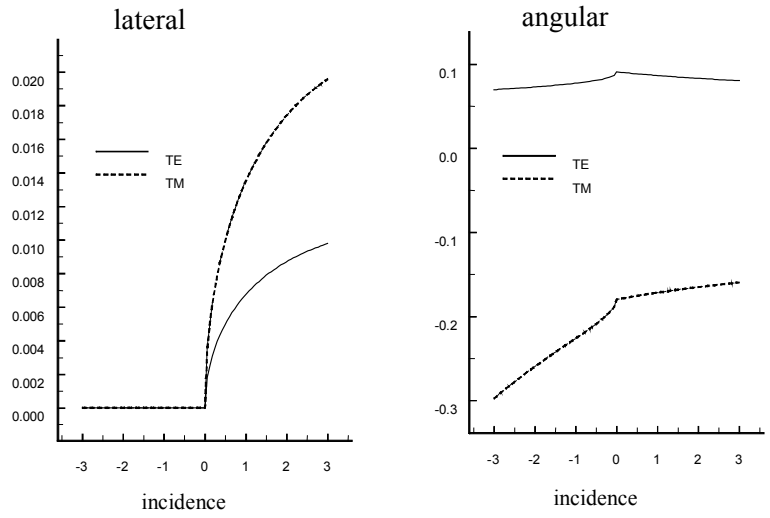

Figure 3.6. First-order transverse nsp effects for the TE and TM components of the reflected beam: the lateral shift δ_{x2} and the angular $\delta_{\vartheta 2}$ shift (in degrees), versus incidence angle changes $\vartheta_{01}^{(i)} - \vartheta_c$ around the critical incidence $\vartheta_{01}^{(i)} = \vartheta_c = 45^o$. The case of the diagonal linear polarization $\chi_i = 1$ of the incident beam; $kw_1 = kw_2 = 50$. The lateral shift is scaled to the incident beam half-width.

beam polarization. Note that, meanwhile all first-order transverse effects depend on the incidence angle, only the angular shifts become larger for narrow beams, i.e. for small values of kz_{D2}. Moreover, in the contrary tothe lateral shifts, the angular shifts are of opposite signs in the TE and TM field components.

As it is seen from Eqs. (3.23), for each lateral (angular) shift for the circular polarization $\delta_{\perp x2}^{(\pm i)}$ ($\delta_{\perp \vartheta 2}^{(\pm i)}$) there exists angular (lateral) shift $\delta_{\perp \vartheta 2}^{(\pm 1)}$ ($\delta_{\perp x2}^{(\pm 1)}$) of the linear polarization, with magnitudes interrelated by the beam diffraction length z_{D2} or, in the dimensionless units [9], by the normalised wave number $(kz_{D2})^{1/2}$:

$$\delta_{\perp \vartheta 2}^{(\pm 1)} = -z_{D2}^{-1} \delta_{\perp x2}^{(\pm i)},$$

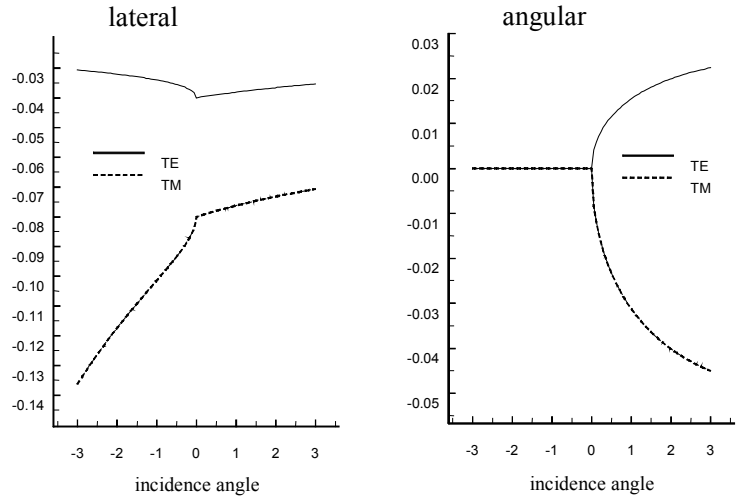

Figure 3.7. First-order transverse nsp effects for the TE and TM components of the reflected beam: the lateral shift δ_{x2} and the angular $\delta_{\vartheta 2}$ shift (in degrees), versus incidence angle changes $\vartheta_{01}^{(i)} - \vartheta_c$ around the critical incidence $\vartheta_{01}^{(i)} = \vartheta_c = 45^o$ for the diagonal circular polarization $\chi_i = i$ of the incident beam; $kw_1 = kw_2 = 50$. The lateral shift is normalised to the incident beam half-width.

$$\delta_{\perp x2}^{(\pm 1)} = +z_{D2}^{+1}\delta_{\perp \vartheta 2}^{(\pm i)}. \tag{3.25}$$

Therefore, the first-order transverse shifts exist simultaneously for both - circular and linear – diagonal polarizations. Their magnitudes are interrelated by the diffraction length of the beam; the lateral shifts prevail for the circular polarization, meanwhile the angular shifts are more vivid for the linear can be polarization and for narrow ($(kz_{D2})^{1/2} < 100$) beams. Similar considerations can be given for the second-order transverse shifts, on the grounds of Eqs. (3.13) and (A.3.8).

The first-order transverse nsp effects are depicted in Fig. 3.6 for the diagonal linear polarization and in Fig. 3.7 for the diagonal circular polarization. Note large values of the lateral shifts for the circular polarization and of the angular shifts for the linear polarization - they are approximately

only five times less that their longitudinal counterparts. In [1] extensive independent numerical simulations were presented for the 3D beam reflection and transmission at the dielectric interface. The numerical method was based on equations equivalent to the exact analysis of Section 2 and the results obtained there seem to comply with predictions of [2] and results of this section.

3.8 Nonlinear interfaces

In Eqs. (3.12) the dependence of the beam spectral envelopes $\hat{E}_a$ on the propagation coordinate x_3 was introduced in order to extend the formalism into the cases of inhomogeneous and/or nonlinear media. Let by n^2 and $\Delta n_a^2 = n_a^2 - n_L^2$ denote the refractive index squared of the inhomogeneous medium and its deviation from some background value n_L^2, respectively. Then, in the paraxial approximation and for the linear polarization, the beam propagation is governed by the parabolic approximation to the Helmhotz equation for the slowly varying beam envelopes $V_a = E_a \exp(-ik_L z_a)$:

$$\left\{2ik_L\partial_{x_3} + \partial_{x_1}^2 + \partial_{x_2}^2 + k_L^2\,\Delta n_a^2 / n_L^2\right\}V_a(x_1, x_2, x_3) = 0\,, \tag{3.26}$$

where k_L is a background value of the wave number k for the beam field and $\Delta n_a^2 \equiv \Delta n_a^2(x_3)$.

In the homogeneous medium $\Delta n_a^2 = 0$, $k_L = k$, and Eq. (3.26) reduces to the Fock equation. Otherwise, the analysis of Sections 2 and 3 still remains valid provided that the solution is sought in a self-similar form specific to the Fock equation, e.g. in a form of Gaussian beams. This approach is widely used in nonlinear optics, where the medium inhomogenuities are induced by beam fields of high intensity [14-20]. The beam amplitude changes the reflection due to the nonlinear effects of self-focusing and cross-focusing and lead to the positive feedback between these changes and the incident beam power. It is the nonlinear medium where the nsp changes of the beam amplitude are vivid the most.

The 3D beam of the TE polarization reflected at the boundary between the nonlinear Kerr type medium and a linear medium was analysed in [9] and this case will be discussed in the next chapter. Cylindrical symmetry for the

incident beam approaching the interface from the nonlinear medium was assumed, i.e. $z_{D1} = z_{D2} = z_D$. Averaging integration of the Lagrangian density specific to Eq. (3.26) in planes parallel to the interface at $X = 0$ was performed. The cross-focusing terms $2n_2 n_L |V_a|^2$ in Δn_a^2, where n_2 and n_L stand for the nonlinear and linear indices of refraction, were incorporated in the self-focusing terms by the cross-focusing factors $g_a \equiv g_a(X)$:

$$\Delta n_i^2 = n_2 n_L \left(|V_i|^2 + 2|V_r|^2 \right) \cong n_2 n_L g_i \, |V_i|^2 ,$$

$$\Delta n_r^2 = n_2 n_L \left(|V_r|^2 + 2|V_i|^2 \right) \cong n_2 n_L g_r \, |V_r|^2 ,$$

$$g_a = 1 + 2 \iint |V_i|^2 |V_r|^2 \, dYdZ \Big/ \iint |V_a|^4 \, dYdZ . \tag{3.27}$$

That leads to two standard nonlinear Schrödinger equations (NLSE's) (3.26), given separately for the incident (a=i) and reflected (a=r) beams, with the nonlinear self-focusing terms modified by the factors g_a dependent on X. The incoherent interaction between the beams was assumed to secure comparison of the results obtained with the reported plane wave predictions [16], although the coherent interaction can be also treated in the similar manner.

The beams are modelled as fundamental Gaussians with parameters (waist centre position, propagation direction and the waist radius) dependent on the propagation distance x_3. In this way, the solution to the reflection problem at the nonlinear-linear interface is obtained in a form typical of the reflection at the linear interface. However, nonlinear changes Δn_a of the refractive index are transferred to the appropriate changes of beam parameters [9,15]. These changes, known as aberrationless effects of nonlinear propagation, can be derived and interpreted in the same form of the complex shifts (3.13). They are induced by nonlinear propagation this time. Let us denote them as $L_j^{(ab)}$ and $F_j^{(ab)}$. At the focusing ($n_2 > 0$) nonlinear-linear interface the effects of nonlinear propagation and nsp reflection may contribute constructively to the total complex shifts $L_j^{(nl)} = L_j + L_j^{(ab)}$ and $F_j^{(nl)} = F_j + F_j^{(ab)}$ and enhance the process of the reflected beam reshaping [9].

For the incidence from a linear side of the linear-nonlinear interface only one, transmitted beam exists in the nonlinear medium. The cross-focusing terms in the NLSE (3.26) disappear, $g_a = 1$, but the nonlinear enhancement of the nsp effects still can be achieved. Nonlocal approximation [18] (with an infinite radius of the nonlocality of n_2) to such a case was discussed in [17] in the context of a defocusing ($n_2 < 0$) linear-nonlinear interface.

The presence of the nsp effects is not restricted to interface configurations based on TIR - any angularly dispersive interface, like that of the phase-conjugate reflection [19], will do as well. The beam shifts have also been observed in soliton dragging configurations [20-21]. Two cross-polarised beams enter the nonlinear medium, mutually interact and experience shifts in their axes positions and directions. The asymmetry produced by the interface makes these shifts essentially different from those produced by the beam collision in the unbouded nonlinear medium.

3.9 Beam amplitude nonspecular modifications

The method of treatment of the nonlinear interface is similar to that of the linear interface, but the results are not [9]. Let us restrict this discussion to the beams of the TE polarization and to the plane of incidence ($Y = 0$). Let simplify also the notation by: $\vartheta_i \equiv \vartheta_{01}^{(i)}$ and $\vartheta_r \equiv \vartheta_{01}^{(r)}$ or $\vartheta_g \equiv \vartheta_{01}^{(g)}$, where the suffix replacement a=r by a=g indicates the g-o approximation in the first step of the numerical iteration of the solution (cf. [17] and the next chapter). The nonlinearly scaled propagation distances z_a, the beam wave numbers k_a, the critical angle ϑ_c and the g-o reflection angle ϑ_g, a=i, g, depend on the normalised beam powers p_a (normalised to one at the self-trapping power level), where, for instance, close to the beam waists [9]:

$$z_a^2 \cong (1 - p_a)^2 x_3^2,$$

$$k_a \cong k_L + p_a 2^{-1} z_D^{-1}. \tag{3.28}$$

On the grounds of the law of reflection:

$$\vartheta_g = \arcsin(k_g^{-1} k_i \sin\vartheta_i),$$

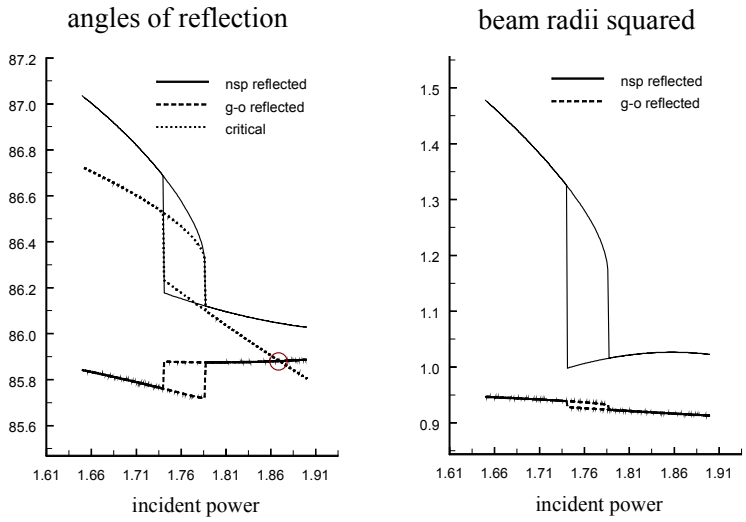

Figure 3.8. Angles of reflection $\vartheta_{01}^{(g)}$ and $\vartheta_{01}^{(r)}$ (in degrees) (a) and relative waist radii squared $\mu_1^{(g)}$ and $\mu_1^{(r)}$ (b) of the g-o reflected and the actual reflected beams, respectively, versus the normalised power p_i of the beam incident of TE polarization at the focusing nonlinear-linear interface. Changes of the angle of critical reflection ϑ_c are also shown by the dotted curve; the small circle indicates the point of the critical incidence $\vartheta_{01}^{(g)} = \vartheta_c$; $\vartheta_{01}^{(i)} = 86.4^o$; $kw_1 = kw_2 = 50$. The waist radii are scaled by the incident beam half-width.

$$\vartheta_c = \arcsin(k_g^{-1} k_i n^{-1}), \tag{3.29}$$

the g-o reflection angle ϑ_g differs from the incident angle ϑ_i and, for the focusing nonlinear medium, $\vartheta_g < \vartheta_i$ in the partial reflection range to r. With the higher-order terms included in the expansion of $\ln r$ (3.13) the actual reflection angle ϑ_r is modified by the angular shift δ_ϑ, i.e. $\vartheta_r = \vartheta_g + \delta_\vartheta$. This modification appears so large that the sign of the inequality between ϑ_r and ϑ_i may become even the opposite of that one between ϑ_g and ϑ_i. That indicates distinct differences between the finite-

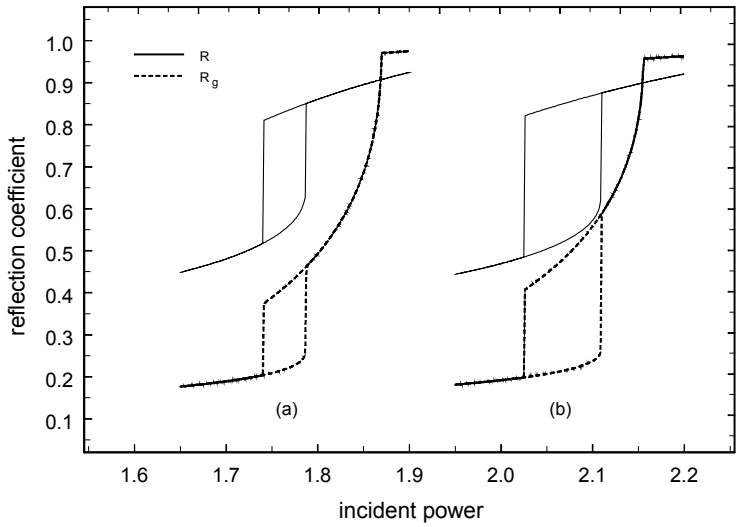

Figure 3.9. Magnitudes R and R_g of the reflection coefficients r and r_g of the nonspecularly reflected and the g-o reflected beams, respectively, versus the normalised power p_i of the beam of TE polarization incident at the focusing nonlinear-linear interface; $kw_1 = kw_2 = 50$. The ratio r/r_g of these coefficients yields the nsp modification of the beam amplitude. In the case (a): $x_3 = 0.13$, q=2.0, the effects of the nonlinear self-focusing prevail over the effects of the angular detuning more than in the case (b): $x_3 = 0.10$ and q=2.1.

width beam reflection [9] and the plane wave reflection [16]. It is pertinent to note here that ϑ_i depends on the type of the incident beam excitation in the nonlinear medium and may, in general, also vary with changes of the beam power.

Plots in Fig. 3.8 confirm these predictions, where the angular and beam radius variations are shown versus variations of the incident normalised beam power p_i. The beam and the reflecting structure parameters are taken such to achieve a bistable reflection, for instance the angle of the low-power critical incidence amounts here 88.2 degrees (cf. [9] and the next chapter). Although, in the power range below the point of critical incidence, the g-o reflection

angle ϑ_g is less than the critical angle ϑ_c, the actual reflection angle ϑ_r is much larger and stays close to ϑ_c within a whole range of the bistable reflection. In this way, ϑ_g is less than the incidence angle ϑ_i and increases at the higher switching threshold (switch-on), meanwhile ϑ_r is larger than ϑ_i and, together with ϑ_c, decreases much at the same time. These angular changes reverse their signs at the lower switching threshold (switch-off), as expected.

Plots of the normalised beam radii squared

$$2^{-1} z_D^{-1} k w_1^2(z_g) = \mu_1^2(z_g)(1 + (z_g - \delta_{z1})^2 z_D^{-2}) \cong z_g \rho_1(z_g) \tag{3.30}$$

indicate substantial impact of this focussing effect on the reflected beam radius w_1, the phase front curvature ρ_1, the critical and reflection angles, and thus on the beam switch [9]. In effect, the average beam spatial spectrum is moved towards the range of TIR. In turn, this induces the increase in magnitude of the reflection coefficient from r_g to a new value of r. Moreover, the positive feedback between r and the nonlinear angular shift δ_ϑ is so strong that the bistable switch can be achieved for some sets of the beam and nonlinear medium parameters [9].

Figure 3.9 depicts this situation for the two cases of the angular detuning $q = (\pi/2 - \vartheta_i)/(\pi/2 - \vartheta_c)$ and the cumulative effect of nonlinear focusing, measured by the positions x_3 of the incident beam waist with respect to the interface. The last parameter indicates the strength of the nonlinear focusing. Large magnitudes of the beam amplitude nsp modification r/r_g are clearly vivid. Distant positions of the switching thresholds from the critical incidence indicate that the narrow beam switching at the nonlinear-linear interface may become qualitatively different from predictions based on the plane wave considerations.

10 Comments and conclusions

The analysis presented treats the 3D beam reflection on the grounds of the exact electromagnetic solution to the problem. The paraxial approximation extracts from this rigorous solution the beamlike part of the total field and yields the description of the reflection within the frame of first-order optics.

In this context, the effects of nsp reflection are parameters, which provide clear qualitative interpretation and precise quantitative evaluation of characteristic features of the beam reflection. The remaining nonparaxial part of the exact solution can be also recognised as the first-order modes - here, for the Gaussian incidence, the first-order Hermite-Gaussian beams excited by the cross-polarization nonparaxial coupling at the reflecting structure.

It is demonstrated that the transverse beam deformations are determined by the relative - between the TE and TM polarization - characteristics of the incident beam. The formalism reveals, in the first place, direct relation between the first-order transverse nsp beam angular deformations for the diagonal linear and circular beam polarization. It is shown that the transverse lateral shifts of the beam of circular polarization are replicas of the transverse shifts for the linear polarization and that these effects are interrelated by the diffraction length of the beams. Several other characteristic features of the longitudinal and transverse effects of nsp reflection are also discussed.

In relation to the previous report on this approach [2] some extensions are outlined. It is shown that the next term in the expansion of the reflection coefficient - the cross-dimensional coupling term - can be directly included in the formalism. This term influences only quantitatively the second-order, mainly transverse, effects of nsp reflection. It is also shown that the method, augmented by the numerical iteration of the nonlinear feedback in the final solution [9], works also well in cases of nonlinear interfaces. The bistable switch of the single finite-cross-section beam at the NLI of small dielectric contrast is confirmed, with characteristics distinct from those of the plane-wave reflection.

Some important aspects or extensions of the approach still need further investigation. It is now well known that the beam polarization changes with propagation and, even for beams initially uniformly polarised, becomes nonuniform across the beam cross-section [22,23]. The process depends on the coherence and vector nature of the beam field, and appears enhanced by the anisotropy locally self-induced in nonlinear media [24]. It seems that analogical behaviour of the coherent field at dielectric interfaces may be investigated by the beam polarization spectral parameters determined by Eqs. (3.3) and (3.6). Impact of the nondiffractive features of beams [25,26], the photon angular momentum [27,28], the azimuthal and radial polarization of

higher-order beam modes [29,30] and the beam rotation [31,32] on the reflection process deserves further specifications as well.

It is pertinent to note that the 3D character of the beam reflection was imposed in this work by the finite transverse cross-section of the incident beam. That results in the coupling of the TE and TM components of the beam field at the interface and in the nonzero cross-coefficients of the reflection matrix (3.4). However, the third dimension of the reflection problem may be introduced instead by anisotropy or periodicity of the media separated by the interface [33,36]. In both cases the finite cross-section of the incident beam leads in addition to the longitudinal and transverse nsp distortions of the beam in the zeroth-order (anisotropic interfaces) or arbitrary-order (periodic interfaces) reflection.

Finally, it should be also noted that the 3D beam reflection is closely related to the (3+1)D wave packet reflection. The paraxial factorisation of the 3D beam field into the product of 2D solutions can be directly extended by adding one more dimension in the presented analysis. In the 2D case the spatio-temporal analogy is complete and straightforward - the spatial beam nsp deformations are just translated into their temporal counterparts, that is besides the pulse delay, also in the pulse velocity, temporal waist location and pulse duration changes [36]. In the multidimensional 4D case the described above the field factorisation into the 2D field factors should be made first, with the cross-dimensional, and this time also the spatio-temporal, coupling coming into play as well. Still, the approach presented in this chapter may serve as the convenient tool in treatment of various aspects of optical beam or pulse shaping, superluminal propagation and photonic tunnelling [37-41].

Appendix: Geometrical effects of nonspecular reflection

Let us start from the definitions of the p and s Fresnel coefficients r_p and r_s of plane wave reflection at the interface:

$$r_p = \left(Z^{(i)} - \eta Z^{(t)}\right) \Big/ \left(Z^{(i)} + \eta Z^{(t)}\right),$$

$$r_s = \left(Y^{(i)} - \eta Y^{(t)}\right) \Big/ \left(Y^{(i)} + \eta Y^{(t)}\right), \qquad \text{(A.3.1)}$$

and the p and s Fresnel coefficients t_p and t_s of plane wave transmission:

$$t_p = 2Z^{(t)} \Big/ \left(Z^{(i)} + \eta Z^{(t)} \right),$$

$$t_s = 2Y^{(i)} \Big/ \left(Y^{(i)} + \eta Y^{(t)} \right), \qquad \text{(A.3.2)}$$

where $\eta = n^{(i)} k_Z^{(t)} \big/ n^{(t)} k_Z^{(i)}$ or $\eta = \cos\vartheta^{(t)} \big/ \cos\vartheta^{(i)}$. The interface is understood as the flat boundary between two homogeneous, isotropic and linear media. The coefficients (A.3.1)-(A.3.2) are assumed in their general form, where $Z^{(b)} = \sqrt{\mu^{(b)} \big/ \varepsilon^{(b)}}$ and $Y^{(b)} = 1 \big/ Z^{(b)}$ are the characteristic impedance and admittance of the the "upper" (b=i or b=r) and "lower" (b=t) media, respectively. The permittivity $\varepsilon^{(b)}$ and permeability $\mu^{(b)}$, together with the refractive index $n^{(b)} = \sqrt{\varepsilon^{(b)} \mu^{(b)}}$, are considered uniform (constant) in both media. The beam phase in the definitions (A.3.1)-(A.3.2) is taken such that the reflection coefficients r_p and r_s equal one at the critical incidence of total internal reflection.

Note that the Fresnel coefficients (A.3.1)-(A.3.2) are defined in the local incidence plane $x-z$ of the plane wave and thus they do not depend on the azimuthal orientation of this plane; that is they do not depend on α_2. For 3D-beam reflection and transmission at the interface, however, all plane waves contributing into the beam field should be described in one plane - the principal plane-of-incidence of the beam. Therefore, to account the third dimension of the problem, the Fresnel coefficients need generalisation of their standard form (A.3.1)-(A.3.2). That was accomplished in this chapter by the replacement of the Fresnel coefficients (A.3.1) by the reflection matrix (3.4), or, adequately, by the generalised Fresnel coefficients of reflection (3.5). Per analogy, the same can be done for beam transmission, as will be explicitly shown in Chapters 5-7.

Therefore, in this appendix, the definitions of the first-order and the second-order beam shifts will be derived from these generalised coefficients along the lines reported in Ref. [2]. We will restrict the analysis only to beam reflection at the interface. The case of beam transmission can be treated in the same manner. The same concerns the beam reflection and transmission at any planar multilayer, provided that the Fresnel coefficients (A.3.1)-(A.3.2) of plane wave reflection and refraction are replaced by their respective counterparts specified to the multilayer.

Let us decompose the p and s Fresnel reflection coefficients r_p and r_s into their magnitudes and phases $r_c = \rho_c \exp(i\upsilon_c)$, $c = s, p$ and denote their ratio by $r = (\rho_p / \rho_s)\exp[i(\upsilon_p - \upsilon_p)]$. They represent the coefficients of plane wave reflection at the interface or at any planar multilayered structure and are evaluated at the reflected beam axis or at the beam spectrum centre at $\alpha_1 = 0 = \alpha_2$. The form of the representation (3.13) of the reflection coefficients r_b:

$$r_{\|} \cong r_{0p} \exp\{-ik[L_{\|1}\alpha_1 + L_{\|2}\alpha_2 - 2^{-1}(F_{\|1}\alpha_1^2 + F_{\|2}\alpha_2^2)]\},$$

$$r_{\perp} \cong r_{0s} \exp\{-ik[L_{\perp 1}\alpha_1 + L_{\perp 2}\alpha_2 - 2^{-1}(F_{\perp 1}\alpha_1^2 + F_{\perp 2}\alpha_2^2)]\}, \qquad \text{(A.3.3)}$$

b=|| for TM polarization and b=⊥ for TE polarization, has been postulated as equivalent to the four-term expansion of these coefficients, separately for the TM and TE components of the incident beam:

$$r_{\|} = \exp\{\ln r_{\|}\} \cong r_{0p} \exp\{r_{\|1}\alpha_1 + r_{\|2}\alpha_2 + 2^{-1}(r_{\|11}\alpha_1^2 + r_{\|22}\alpha_2^2)\},$$

$$r_{\perp} = \exp\{\ln r_{\perp}\} \cong r_{0s} \exp\{r_{\perp 1}\alpha_1 + r_{\perp 2}\alpha_2 + 2^{-1}(r_{\perp 11}\alpha_1^2 + r_{\perp 22}\alpha_2^2)\}, \quad \text{(A.3.4)}$$

where all derivatives are evaluated at $\alpha_1 = 0 = \alpha_2$ and the notation is used: $k\alpha_1 = k_1$, $k\alpha_2 = k_2$, $r_{bj} \equiv \partial_{\alpha_j} \ln r_b = k\partial_{k_j} \ln r_b$, $r_{bij} \equiv \partial_{\alpha_i \alpha_j} \ln r_b = k^2 \partial_{k_i k_j} \ln r_b$, with b=||,⊥. The subscripts $i, j = 1$ and $i, j = 2$ indi-cate the longitudinal effects (along the x_1-axis) and the transverse effects (along the x_2-axis), respectively. Note that in the next chapters the notation $x_1 \equiv x$, $x_2 \equiv y$, $x_3 \equiv z$ and $k_1 \equiv k_x$, $k_2 \equiv k_y$, $k_3 \equiv k_z$ is also alternatively used.

Comparison of the two equations in (A.3.3) with the two equations in (A.3.4) yields the first-order longitudinal complex shifts L_{b1},

$$L_{\|1} = +ik^{-1} r_{p1} = -k^{-1}(\upsilon'_{p1} - i\rho''_{p11}/\rho_c),$$

$$L_{\perp 1} = +ik^{-1} r_{s1} = -k^{-1}(\upsilon'_{s1} - i\rho''_{s11}/\rho_{sc}), \qquad \text{(A.3.5)}$$

the second-order longitudinal complex shifts F_{b1},

$$F_{\|1} = -ik^{-1} r_{p11} = +k^{-1}\left[\upsilon''_{p11} - i(\rho''_{p11}/\rho_p - (\rho'_{p1}/\rho_p)^2)\right],$$

$$F_{\perp 1} = -ik^{-1} r_{s11} = +k^{-1}\left[v''_{s11} - i(\rho''_{s11}/\rho_s - (\rho'_{s1}/\rho_s)^2)\right], \tag{A.3.6}$$

the first-order transverse complex shifts L_{b2},

$$L_{\|2} = +ik^{-1} r_{\|2} = -ik^{-1}(1+r^{-1})\,\tilde{\chi}_i^{-1}(\sin\vartheta_{01})^{-1},$$

$$L_{\perp 2} = +ik^{-1} r_{\perp 2} = +ik^{-1}(1+r^{+1})\,\tilde{\chi}_i^{+1}(\sin\vartheta_{01})^{-1}, \tag{A.3.7}$$

and the second-order transverse complex shifts F_{b2},

$$F_{\|2} = -ik^{-1} r_{\|22} = +ik^{-1}\left[2(1+r^{-1}) + (1+r^{-1})^2\,\tilde{\chi}_i^{-2}\right](\sin\vartheta_{01})^{-2},$$

$$F_{\perp 2} = -ik^{-1} r_{\perp 22} = +ik^{-1}\left[2(1+r^{+1}) + (1+r^{+1})^2\,\tilde{\chi}_i^{+2}\right](\sin\vartheta_{01})^{-2}. \tag{A.3.8}$$

In the equations above the primes indicate derivatives with respect to α_1 or α_2 evaluated at the reflected beam axis. Thus $\rho'_{sj} \equiv \partial_{\alpha_1}\rho_s$, $\rho''_{sij} \equiv \partial_{\alpha_i}\partial_{\alpha_j}\rho_s$ at $\alpha_1 = 0 = \alpha_2$, and so on.

In more accurate calculations, by applying the rotation through the angle ε_b (3.18) around the Y-axis to the second-order terms in the fifth-order expansion of r:

$$r_{b11}\alpha_1^2 + r_{b22}\alpha_2^2 + (r_{b12} + r_{b21})\alpha_1\alpha_2 = ik(\breve{F}_{b1}\alpha_1^2 + \breve{F}_{b2}\alpha_2^2), \tag{A.3.9}$$

one obtains new, more accurate definitions $\breve{F}_{bj}$ (3.17) of the second-order complex shifts. Note that signs in the expressions of effects of nsp deformations depend on the vector and angular change senses of the coordinate frame chosen in the calculations. The coordinate orientations depend also on ϑ_{01}; cf. Fig. 3.1 in this chapter and Fig. 4.45b of Ref. [42] with e.g. Fig. 4.45a of Ref. [42] or Fig. 6 of Ref. [5].

Basic characteristics of the beam shifts derived above have been analysed in this chapter. All of them are rotted in the form of definitions (A.3.5)-(A.3.8). Let us only mention about general features of the first-order shifts (A.3.5) and (A.3.7). The longitudinal first-order beam shifts (A.3.5), contrary to the transverse beam shifts (A.3.7), do not depend on the state of the incident beam polarization. For the linear, TM or TE, polarization ($\chi_i^{-1} = 0$ or $\chi_i = 0$) of the incident beam, the transverse shifts disappear. For the

circular, right-handed or left-handed, polarization ($\chi_i = \mp i$) of the incident beam, the transverse shifts are of finite magnitudes and opposite directions for the opposite circular polarization states $\chi_i = \mp i$ of the incident beam.

With the complex nsp shifts known, one can describe the reflected beam field as the field $\underline{E}^{(g)}(x_1, x_2, x_3)$ obtained from the g-o estimation (3.16)

$$\underline{E}^{(g)}(x_1, x_2, x_3) = \underline{\underline{r}}_0 \underline{s}^{(i)} \exp(ikx_3) E_{g1}(x_1, x_3) E_{g2}(x_2, x_3),$$

$$\underline{s}^{(i)} = (1 + |\chi_i|^2)^{-1/2} [\chi_i, \quad 1]^T, \tag{A.3.10}$$

and next, nonspecularly modified by the complex shifts independently for the TM and TE beam components (3.16):

$$E_{\|}^{(r)}(x_1, x_2, x_3) = r_{\|0}\, \chi_i (1 + |\chi_i|^2)^{-1/2} \exp(ikx_3)$$
$$\times E_{g1}(x_1 - L_{\|1}, x_3 - F_{\|1}) E_{g2}(x_2 - L_{\|2}, x_3 - F_{\|2}),$$

$$E_{\perp}^{(r)}(x_1, x_2, x_3) = r_{\perp 0}\, (1 + |\chi_i|^2)^{-1/2} \exp(ikx_3)$$
$$\times E_{g1}(x_1 - L_{\perp 1}, x_3 - F_{\perp 1}) E_{g2}(x_2 - L_{\perp 2}, x_3 - F_{\perp 2}). \tag{A.3.11}$$

In Eq. (A.3.10) $\underline{s}^{(i)}$ is the Jones vector of the incident beam polarization (cf. Eqs. (3.2)) written in the coordinate frame (x_1, x_2, x_3) of the g-o reflected beam and $\underline{\underline{r}}_0$ is the g-o reflection matrix $\underline{\underline{r}}_g$ evaluated for the plane wave incidence along the incident beam axis.

Let us now return to the spectral representation of the reflected beam field (3.12), given here in the incidence (x_1, x_3) and transverse (x_2, x_3) principal planes, respectively, for both, TM (b=||) and TE (b=⊥), field components:

$$E_{br1}(x_1, x_3) = (2\pi)^{-1} r_{0b}^{-1}$$
$$\times \int r_b \widetilde{E}_{bi1}(-\alpha_1, x_3) \exp\left[ik(\alpha_1 x_1 - 2^{-1}\alpha_1^2 x_3)\right] k\, d\alpha_1,$$

$$E_{br2}(x_2, x_3) = (2\pi)^{-1} r_{0b}^{-1}$$
$$\times \int r_b \widetilde{E}_{bi2}(+\alpha_2, x_3) \exp\left[ik(\alpha_2 x_2 - 2^{-1}\alpha_2^2 x_3)\right] k\, d\alpha_2. \tag{A.3.12}$$

Note that the paraxial beams, like the HG or LG beams of arbitrary order, show, at least approximately, Gaussian damping of their field amplitudes in

planes transverse to their propagation direction. It was indicated by Deschamps [43] that such beam fields can be obtained from exact solutions of the Helmhotz equation through their displacements by the imaginary shifts along the beam axis. Their magnitudes are equal to the diffraction lengths of the beams. In the case considered here these shifts are equal to iz_{D1} in the main incidence plane and iz_{D2} in the main transverse plane, respectively.

Therefore, the spectral amplitudes of the reflected beam in Eqs. (A.3.11) are proportional to the exponential terms expressed by z_{D1} and z_{D2}:

$$\widetilde{E}_{bi1} = \widetilde{e}_{bi1} \exp(-2^{-1} k\alpha_1^2 z_{D1}) ,$$

$$\widetilde{E}_{bi2} = \widetilde{e}_{bi2} \exp(-2^{-1} k\alpha_2^2 z_{D2}) , \qquad \text{(A.3.13)}$$

After taking into account Eqs. (A.3.3)-(A.3.4) and (A.3.13), the beam field representations (A.3.12) can now be put into the following form:

$$E_{br1}(x_1, x_3) = (2\pi)^{-1}$$
$$\times \int \widetilde{e}_{bi1}(-\alpha_1, x_3) \exp\{ik[\alpha_1(x_1 - L_{b1}) - 2^{-1}\alpha_1^2 (x_3 - F_{b1} - iz_{D1})]\} k d\alpha_1 ,$$

$$E_{br2}(x_2, x_3) = (2\pi)^{-1}$$
$$\int \widetilde{e}_{bi2}(+\alpha_2, x_3) \exp\{ik[\alpha_2(x_2 - L_{b2}) - 2^{-1}\alpha_2^2 (x_3 - F_{b2} - iz_{D2})]\} k d\alpha_2 . \qquad \text{(A.3.14)}$$

It has been proved in Refs. [44] and [45] that the Gaussian beams (A.3.14), displaced by the complex shifts (A.3.5)-(A.3.8), can be interpreted also in terms of real shifts. These real shifts are the lateral δ_{bxj} and longitudinal δ_{bzj} shifts of the beam coordinate frame centre, augmented by this frame rotation through the angles equal to angular shifts $\delta_{b\vartheta j}$. Real displacements and rotations are given here separately for the TM (b=||) and TE (b=⊥) components of the reflected beam, and also separately in the principal incidence (j=1) and transverse (j=2) planes (cf. Refs. [2], [44] and [45]):

$$x_{brj} = (x_j - \delta_{bxj}) \cos\delta_{b\vartheta j} - (x_3 - \delta_{bzj}) \sin\delta_{b\vartheta j} ,$$

$$x_{3brj} = (x_j - \delta_{bxj})\sin\delta_{b\vartheta j} + (x_3 - \delta_{bzj})\cos\delta_{b\vartheta j}. \quad \text{(A.3.15)}$$

They should be accompanied by the same rotation of the coordinate frame in the spectral domain [2]:

$$\alpha_{brj} = \alpha_j \cos\delta_{b\vartheta j} - \alpha_3 \sin\delta_{b\vartheta j},$$

$$\alpha_{3brj} = \alpha_j \sin\delta_{b\vartheta j} + \alpha_3 \cos\delta_{b\vartheta j}. \quad \text{(A.3.16)}$$

Besides the beam frame shifts and rotations, the reflected beams suffer also from changes of the beam waist radii, expressed by the factors μ_{bj} and in addition, by changes of their on-axis complex amplitude, as described in Refs. [2], [44] and [45].

By applying the transformations (A.3.13)-(A.3.14) to the beam field representation (A.3.10), its beam field factors, defined in the incidence and transverse planes, respectively, take the form equivalent to the expressions (A.3.14):

$$E_{br1}(x_1, x_3) = (2\pi)^{-1}$$
$$\times \int \tilde{e}_{bi1}(-\alpha_1, x_3)\exp\{ik[\alpha_{br1}(x_{br1} - \delta_{xb1}) - 2^{-1}\alpha_{br1}^2(x_{3br1} - i\mu_1^2 z_{D1})]\}kd\alpha_1,$$
$$E_{br2}(x_2, x_3) = (2\pi)^{-1}$$
$$\times \int \tilde{e}_{bi2}(+\alpha_2, x_3)\exp\{ik[\alpha_{br2}(x_{br2} - \delta_{xb2}) - 2^{-1}\alpha_{br2}^2(x_{3br2} - i\mu_2^2 z_{D2})]\}kd\alpha_2. \quad \text{(A.3.17)}$$

Direct comparison of the beam field representations (A.3.14) and (A.3.17) yields the definitions of the real geometrical effects of nsp reflection [2]. One obtais, for the TM (b=||) and TE (b=⊥) polarization of the reflected beam, in the incidence (j=1) and transverse (j=2) planes, the longitudinal and transverse lateral first-order shifts δ_{bx1} and δ_{bx2},

$$\delta_{bxj} = \mathrm{Re}(L_{bj}), \quad \text{(A.3.18)}$$

the longitudinal and transverse second-order focal shifts δ_{bz1} and δ_{bz2},

$$\delta_{bzj} = \mathrm{Re}(F_{bj}), \quad \text{(A.3.19)}$$

the longitudinal and transverse first-order angular shifts $\delta_{b\vartheta 1}$ and $\delta_{b\vartheta 2}$,

$$\delta_{b\vartheta j} \cong (z_{D_j}\mu_j^2)^{-1}\,\mathrm{Im}(L_{bj})\,, \tag{A.3.20}$$

and the longitudinal and transverse waist radius squared second-order modifications δ_{bw1} and δ_{bw2},

$$\delta_{bwj} \cong (z_{D_j}\mu_j^2)^{-1}\,\mathrm{Im}(F_{bj})\,, \tag{A.3.21}$$

The waist modification factors μ_j are given by:

$$\mu_{bj}^{-2} = 1 - \delta_{bwj}\,. \tag{A.3.22}$$

These real shifts are directly expressed by real and imaginary parts of the complex shifts (3.13) or (A.3.5)-(A.3.8). The definitions (A.3.20)-(A.3.21) are approximate. More accurate definitions of δ_{ϑ_j} and δ_{w_j} may be given with the help of Eqs. (3.14). On the other hand, as usually $\mu_j \cong 1$, the definitions (A.3.20)-(A.3.21) can be further approximated by:

$$\delta_{b\vartheta j} \cong z_{Dj}^{-1}\,\mathrm{Im}(L_{bj})\,, \tag{A.3.23}$$

$$\delta_{bwj} \cong z_{Dj}^{-1}\,\mathrm{Im}(F_{bj})\,. \tag{A.3.24}$$

The definitions of the beam nsp shifts have been given for beams of arbitrary incidence angle, polarization and amplitude spatial distribution, provided that the transverse amplitudes of them can be factorised in the two transverse coordinates x_1 and x_2, according to Eq. (A.3.10). These definitions are valid, for example, for the three-dimensional Hermite-Gaussian (HG) paraxial beams of arbitrary order $m+n$, defined as a product of the two-dimensional HG beams in these coordinates x_1, x_3 and x_2, x_3, and of the orders m and n, respectively. They are valid for both cases of the internal and external reflection. Per analogy, their derivation can be also directly repeated for beam transmission.

For a beam which does not obey the factorisation condition (A.3.10) one has first to decompose it into series of the beam fields, which obey this condition and belong to the set of functions complete in the space of beam functions of finite power (cf. footnote 1 in Opt. Commun. **197**, 217 (2001)). Such functions are still the HG beam fields. They comply with with the mirror symmetry condition (A.3.10), with respect to planes $x_1 - x_3$ and

$x_2 - x_3$ (cf. Fig. 3.1). For incidence, for example, of the standard higher-order Laguerre-Gaussian (LG) beams $G_{p,l}^{SL}$, this decomposition, given in terms of the standard HG beams $G_{l,k}^{SH}$ of the same order $N = m + n = 2p + l$, leads to the following expressions for the incident beam (see Ref. [46] and Section 8 of Chapter 2):

$$\begin{aligned} &\underline{E}^{(i)}(x_1, x_2, x_3) = \underline{s}^{(i)} \exp(ikx_3) G_{p,l}^{SL}(x_1, x_2, x_3) \\ &= \underline{s}^{(i)} \exp(ikx_3) \sum_{k=0}^{N} i^k b(n, m, k)\, G_{N-k}^{SH}(x_1, x_3) G_k^{SH}(x_2, x_3)\,, \end{aligned} \tag{A.3.25}$$

with the coefficients explicitly given from the diagonal relations between LG and HG beams [46]. Then, in each term of this expansion, the complex nsp shits can be applied separately for the TM and TE component of the reflected beam:

$$\begin{aligned} &E_{\|}^{(r)}(x_1, x_2, x_3) = r_{\|0}\, \chi_i (1 + |\chi_i|^2)^{-1/2} \exp(ikx_3) \\ &\times \sum_{k=0}^{N} i^k b(n, m, k)\, G_{N-k}^{SH}(x_1 - L_{\|1}, x_3 - F_{\|1}) G_k^{SH}(x_2 - L_{\|2}, x_3 - F_{\|2})\,, \\ &E_{\perp}^{(r)}(x_1, x_2, x_3) = r_{\perp 0}\, (1 + |\chi_i|^2)^{-1/2} \exp(ikx_3) \\ &\times \sum_{k=0}^{N} i^k b(n, m, k)\, G_{N-k}^{SH}(x_1 - L_{\perp 1}, x_3 - F_{\perp 1}) G_k^{SH}(x_2 - L_{\perp 2}, x_3 - F_{\perp 2})\,. \end{aligned} \tag{A.3.26}$$

In this way, for any incident paraxial beam of arbitrary shape, polarization and incidence angle, the beam reflected at the interface or, in general, at any multilayered dieletric structure, can be rigorously described up to the second-order approximation. The beam is considered as the replica of the incident beam with its amplitude, polarization and spatial position of its waist being modified by the Fresnel reflection coefficients and the nsp effects defined above.

The same procedure can be applied in description of beams transmitted at any planar multilayered dielectric structure, including this composed of weakly nonlinear or inhomogeneous stratified media. In the next chapter, the

problem of beam reflection at a plane boundary of a weekly nonlinear medium of Kerr type will be analysed in detail in the manner following the analysis given above.

Main content of this chapter has been published in Optics Communications ***197****, 217-233 (2001).*

References

[1] F. I. Baida, D. Van Labeke, J-M Vigoureux, Numerical study of the displacement of a three-dimensional Gaussian beam transmitted at total internal reflection, Near field applications, J. Opt. Soc. Am. A **17**, 858-866 (2000).

[2] W. Nasalski, "Longitudinal and transverse effects of nonspecular reflection", J. Opt. Soc. Am. A **13**, 172-181 (1996).

[3] J-J. Greffet and C. Baylard, "Nonspecular astigmatic reflection of a 3D Gaussian beam on an interface", Opt. Commun. **93**, 271-276 (1992).

[4] R. G. Turner, "Shifts of coherent light beams on reflection at planar interfaces between isotropic media", Aust. J. Phys. **33**, 319-335 (1980).

[5] J. P. Hugonin, R. Petit, "Étude généralie des déplacements a la réflection totale", J. Optics (Paris) **8**, 73-87 (1977).

[6] J. Picht, "Beitrag zur Theorie der total reflection", Ann. Phys. Leipzig **5**, 433-496 (1929).

[7] F. I. Baida, D. Van Labeke, J-M Vigoureux, "Theoretical study of near-field surface plasmon excitation, propagation and diffraction", Opt. Commun. **171**, 317-331 (1999).

[8] N. Bonomo and R. A. Depine, "Nonspecular reflection of ordinary and extraordinary beams in uniaxial media", J. Opt. Soc. Am A **14**, 3402-3409 (1997).

[9] W. Nasalski, "Modelling of beam reflection at a nonlinear-linear interface", J. Opt. A: Pure Appl. Opt. **2**, 433-441 (2000).

[10] F. Schreier, M. Schmitz, and O. Bryngdahl, "Pulse delay at diffractive structures under resonance conditions", Optics Lett. **23**, 1337-1339 (1998).

[11] A. Stahlhofen, "Photonic tunelling time in frustrated total internal reflection", Phys. Rev. A **62**, 012112-1-7 (2000).

[12] D. Chauvat, O. Emile, F. Bretenaker, and A. Le Floch, "Direct measuremet of the Wigner delay associated with the Goos-Hänchen effect", Phys. Rev. Lett. **84**, 71-74 (2000).

[13] T. Tamir, "Nonspecular phenomena in beam fields reflected by multilayered media", J. Opt. Soc. Am. A **3**, 558-565 (1986).

[14] M. Karlsson, D. Anderson, A. Höök and M. Lisak, "A variational approach to optical soliton collisions", Phys. Scr. **50**, 265-270 (1994).

[15] W. Nasalski, "Complex ray tracing of nonlinear propagation", Opt. Commun. **119**, 218-226 (1995).

[16] D. Daisy and B. Fisher, "Optical bistability in a nonlinear-linear local interface", Optics Lett. **17**, 847-849 (1992).

[17] W. Nasalski, "Nonspecular bistability at a delocalized nonlinear interface", J. Modern Optics, **44**, 1355-1372 (1997).

[18] D. J. Mitchell and A. W. Snyder, "Soliton dynamics in a nonlocal medium", J. Opt. Soc. Am. B **16**, 236-239 (1999).

[19] B. M. Jost, A-A. R. Al-Rashed, and B. E. A. Saleh, "Observation of the Goos-Hänchen effect in a phase-conjugate mirror", Phys. Rev. Lett. **81**, 2233-2235 (1998).

[20] R. McLeod, K. Wagner, and S. Blair, "(3+1) – dimensional optical soliton dragging logic", Phys. Rev. A **52**, 3254-3278 (1995).

[21] M. Zitelli, E. Fazio, and M. Bertolotti, "All-optical NOR gate based on the interaction between cosine-shaped input beams of orthogonal polarization", J. Opt. Soc. Am. B **16**, 214-218 (1999).

[22] G. P. Agrawal and E. Wolf, "Propagation-induced polarization changes in partially coherent optical beams", J. Opt. Soc. Am. A **17**, 2019-2023 (2000).

[23] F. Gori, M. Santarsiero, G. Piquero, R. Borghi, A. Mondello and R. Simon, "Partially polarized Gaussian Schell-model beams", J. Opt. A: Pure and Appl. Opt. **3**, 1-9 (2001).

[24] R. Volle, V. Boucher, K. D. Dorkenoo, R. Chevalier, X. Nguyen Phu, "Local polarization state observation and third-order nonlinear susceptibility measurements by self-induced polarization state changes method", Opt. Commun. **182**, 443-451 (2000).

[25] F. Gori, G. Guattari, and C. Padovani, "Bessel-Gauss beams", Opt. Commun. **64**, 491-495 (1987).

[26] M. Santarsiero, "Propagation of generalized Bessel-Gauss beams through ABCD optical systems", Opt. Commun. **132**, 1-7 (1996).

[27] J. Courtial, D. A. Robertson, K. Dholakia, L. Allen, and M. J. Padgett, "Rotational frequency shift of a light beam", Phys. Rev. Lett. **89**, 4828-4830 (1998).

[28] L. Allen, J. Courtial and M. J. Padgett, "Matrix formulation for the propagation of light beams with orbital and spin angular momenta", Phys. Rev. E **60**, 7497-7503 (1999).

[29] A. A. Tovar and G. H. Clark, "Concentric-circle-grating, surface-emitting laser beam propagation in complex optical systems", J. Opt. Soc. Am. A **14**, 3333-3340 (1997).

[30] P. L. Greene and D. G. Hall, "Properties and diffraction of vector Bessel-Gauss beams", J. Opt. Soc. Am. A **15**, 3020-3027 (1998).

[31] J. Serna, P. M. Mejias, R. Martinez-Herrero, "Rotation of partially coherent beams propagating through free space", Opt. Quant. Electr. **24**, S873-S880 (1992).

[32] E. Abramochkin, N. Losevsky, V. Volostnikov, "Generation of spiral-type laser beams", Opt. Commun. **141**, 59-64 (1997).

[33] T. P. Sosnowski, "Polarization mode filters for integrated optics", Opt. Commun. **4**, 408-412 (1972).

[34] M. G. Moharam and T. K. Gaylord, "Three-dimensional vector coupled-wave analysis of planar-grating diffraction", J. Opt. Soc. Am. **73**, 1105-1112 (1983).

[35] P. C. Logofătu, S. A. Coulombe, B. K. Minhas, and J. R. McNeil, "Identity of the cross-reflection coefficients for symmetric surface-relief gratings", J. Opt. Soc. Am. A **16**, 1108-1114 (1999).

[36] N. E. Bonomo, R. A. Depine, "Aberrationless approach for diffraction of pulses at linear interfaces", Opt. Commun. **190**, 19-27 (2001).

[37] Ph. Balcou and L. Dutriaux, "Dual optical tunneling times in frustrated total internal reflection", Phys. Rev. Lett. **78**, 851-854 (1997).

[38] R. Güther and B. H. Kleemann, "Shift and shape of grating diffractive beams", J. Modern Optics **45**, 1375-1393 (1998).

[39] F. Schreier, O. Bryngdahl, “Femtosecond pulse shaping with a stratified diffractive structure”, Opt. Commun. **185**, 227-231 (2001).

[40] R. Y. Chiao and A. M. Steinberg, “Tunneling times and superluminality”, Progress in Optics **37**, 347-405 (1997).

[41] G. Nimtz and W. Heitmann, “Superluminal photonic tunneling and quantum electronics”, Progr. Quant. Electron **21**, 81-108 (1997).

[42] E. Hecht, *Optics*, third ed., Addison-Wesley, Reading, 1998.

[43] G. A. Deschamps, “Gaussian beam as a bundle of complex rays”, Electron. Lett. **7**, 684-685 (1971).

[44] W. Nasalski, "Modified reflectance and geometrical deformations of Gaussian beams at a dielectric interface", J. Opt. Soc. Am. A **6**, 1447-1454 (1989).

[45] W. Nasalski, "Ray analysis of Gaussian beam nonspecular scattering", Opt. Commun. **92**, 307-314 (1992).

[46] L. Allen, M. W. Beijerrsbergen, R. J. C. Spreeuw, and J. P. Woerdman, „Orbital angular momentum of light and the transformation of Laguerre-Gaussian laser modes”, Phys. Rev. A **45**, 8185-8189 (1992).

CHAPTER 4

Beam reflection at a nonlinear-linear interfaces

An analytic model of beam reflection at a nonlinear-linear interface is presented. An incident field approaches a nonlinear side of the interface at an angle close to a critical angle of total internal reflection. A nonlinearity of the plain Kerr focusing type is considered. A beam field at the interface is described by changes of the beam parameters during propagation and reflection, that is, by aberrationless effects of nonlinear propagation and longtudinal nonspecular effects of reflection. Numerical iterations of the analytical solution indicate that, for certain sets of incident beam and interface parameters, a bistable switch of the reflected beam can be obtained. Characteristic features of this switch appear different from those of a plane wave reflection.

4.1 Introduction

Plane wave reflection of light at the interface between two dielectrics, at least one of which is nonlinear, has been intensively investigated for more than two decades [1-10]. The main interest in the light-beam reflection at the interface stems from its potential application in all-optical switching and com-puting. In contrast to electro-optic devices in which the external feedback is necessary for bistable operation, the switching devices based on nonlinear in-terfaces relay on an intrinsic nonlinear feedback mechanism. Since nonlinear interfaces are not resonant structures, they offer the

possibility of ultrafast switching and can operate with light of a broad spectrum.

The beam or pulse reflection at linear interfaces has also recently attracted great attention [11-16] and potential applications in optical switching, optical imaging and beam or pulse shaping were indicated [17-19]. However, the fundamental question of a possible bistable beam and/or pulse switch at the linear-nonlinear interface has still not received conclusive explanation [8-9]. Recently, however, a problem of plane wave reflection at a nonlinear-linear dielectric interface was discussed [20]. It was indicated that this type of structure exhibits strong nonlinear behaviour due to cross-phase modulation (XPM) between the incident and reflected waves. Optical bistability was shown by numerical iterations of the analytic solution derived.

A motivation of the work is to extend the plane wave analysis to a finite-width-beam reflection at the nonlinear-linear interface and to find suitable description of a beam field near interfaces of this type. The case of narrow beam incident upon a nonlinear-linear interface at an angle close to the critical angle of total internal reflection (TIR) is considered. Formulation of the problem is based on the analytic techniques previously developed by the author in treatment of the nonlinear propagation and nonspecular (nsp) reflection phenomena [21-23]. This leads to a solution which, although to some extent approximate, is of analytic form and enables direct interpretation of the results obtained. Numerical iterations of this solution aim mainly at the possibility of achieving a bistable switch of the reflected beam.

The content of this chapter is organised as follows. In Section 2 the reflection problem is formulated. The reduced variational technique, well known from analyses of a single beam nonlinear propagation [24-25] and optical soliton collisions [26-28], is adapted to the beam reflection at the nonlinear interface. The incident and reflected beam envelopes are modelled by envelopes of the Gaussian shape, with beam parameters defined by aberrationless effects of nonlinear propagation [21]. In Section 3 the spectral representation of the beam field at the interface, that also yields the integral equation for the beam reflection coefficient, is derived. Section 4 is devoted to the solution of this equation with increasing level of accuracy, i.e., from the geometric optics (g-o) approximation to the exact beam field evaluation at the interface [22-23]. The reflected beam deformations are described by the

lon-gitudinal effects of nsp reflection [11-12] and the nonlinear feedback between beam powers is simulated by the numerical monotonic iteration of the solution [23]. The transverse effects of nsp reflection will be neglected as small in relation to the longitudinal effects. In Section 5 results of numerical simulations are discussed. The optical bistable switch in all the beam parameters is obtained and it is shown that the origin of this phenomenon is different from that of the plane wave reflection. In Appendix the parabolic approximation to the nonlinear Schrödinger equation (NLSE) for a single beam is discussed and definitions of the aberrationless effects of nonlinear propagation are given.

Note that all equations in this chapter are written in scaled coordinates, as described in Appendix and by Eqs. (2.24)-(2.29) in Chapter 2. Therefore, the relations given here do not depend on magnitudes of the field wave number and radius of a beam transverse cross-section.

4.2 Formulation of the problem

The problem of interest involves the reflection of a narrow beam of light at the boundary between the nonlinear and linear media. The nonlinear medium is of a Kerr focusing type, i.e., with the linear dependence of its refractive index $n = n_L + \frac{1}{2} n_2 |E|^2$ on the total field intensity $|E|^2$, where $n_2>0$. The low-power refractive index n_L and the nonlinear index of refraction n_2 are given in relation to the index of refraction of the linear medium. It is assumed that $n_L>1$ and that dielectric contrast of the interface is small, i.e. $n_L \cong 1$. In numerical simulations the case of incidence close to the critical angle of total internal reflection (TIR) is analysed.

The basic geometry of the problem is shown in Fig. 4.4.1, in which coordinate frames of the nonlinear-linear interface (X,Y,Z), the incident beam $E_i(x_i,y_i,z_i)$, the g-o reflected beam $E_g(x_g,y_g,z_g)$ and the actual reflected beam $E_r(x_r,y_r,z_r)$ are sketched in the incidence plane $Y=y_i=y_r=y_g=0$. The transverse electric (TE) case is considered with the electric field perpendicular to the incidence plane. All the beams, their parameters and frames are denoted by subscripts ‘i’, ‘r’ and ‘g’, respectively. The g-o reflected beam E_g serves as the reference beam in analysis of the actual reflected beam field distribution

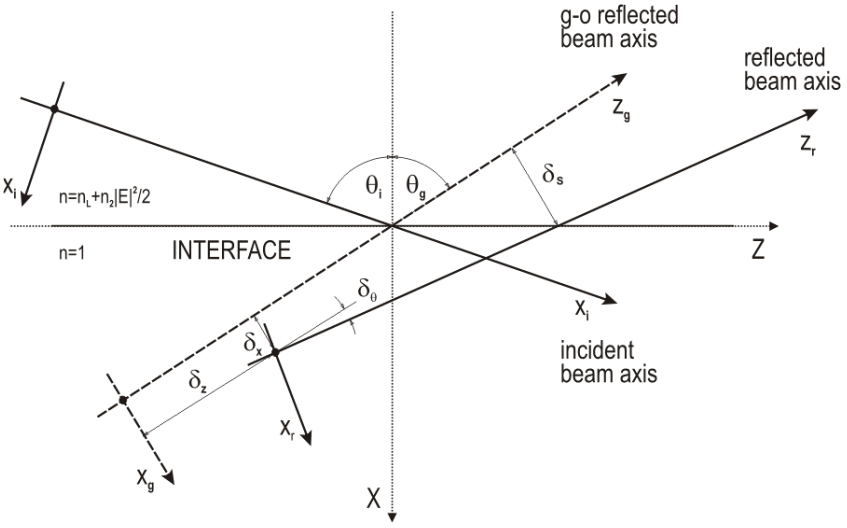

Figure 4.1. Schematic of the beam-coordinate system at the nonlinear-linear interface.

E_r, that is E_r is interpreted as the beam E_g deformed during the nsp reflection.

The four effects of these deformations: the lateral or Goos-Hänchen (G-H) shift δ_x, the focal shift δ_z and the composite shift δ_s of the g-o beam waist position, and the angular shift δ_θ of the g-o beam axis direction, are indicated in Fig. 4.1. Note that, in general, the angles of reflection θ_g and $\theta_r=\theta_g+\delta_\theta$ are different from the incidence angle θ_i.

The total field E near the interface is decomposed into a sum of the incident E_i and reflected E_r beam fields and expressed by their slowly varying beam envelopes U_i and U_r:

$$\begin{aligned} &E(X,Y,Z)=E_i(x_i,y_i,z_i)+E_r(x_r,y_r,z_r) \\ &=U_i(x_i,y_i,z_i)\exp(ik_L z_D z_i)+U_r(x_r,y_r,z_r)\exp(ik_L z_D z_r), \end{aligned} \tag{4.1}$$

where k_L is the linear (low-power) wave number of both beams and the beam field is written in the scaled coordinate system (see Appendix for the definitions of the scaling). The evolution of the beam envelopes is governed by two NLSEs. Far from the interface, the incident and reflected beams

propagate independently according to the standard uncoupled NLSEs with the self-phase-modulation (SPM) terms equal $|U_i|^2 U_i$ and $|U_r|^2 U_r$, respectively – see Appendix for details of analysis in this case. Near the interface, these equations are coupled through the incoherent XPM interaction and the uncoupled NLSEs are augmented by the XPM terms $|U_r|^2 U_i$ and $|U_i|^2 U_r$ for the incident and reflected beam, respectively.

The beam reflection is determined by the reflection coefficient r to be found. Therefore, in normalised units (see Appendix) the NLSEs are written as:

$$\left\{i\partial_{z_i} + \tfrac{1}{2}\left(\partial^2_{x_i} + \partial^2_{y_i}\right) + \left|U_i\right|^2 + 2\left|U_r\right|^2\right\}U_i(x_i, y_i, z_i) = 0,$$

$$\left\{i\partial_{z_r} + \tfrac{1}{2}\left(\partial^2_{x_r} + \partial^2_{y_r}\right) + \left|U_r\right|^2 + 2\left|U_i\right|^2\right\}U_r(x_r, y_r, z_r) = 0. \qquad (4.2)$$

With the appropriate Lagrangian density L:

$$L(U_i, \overline{U}_i, U_r, \overline{U}_r) = L_{NLS}(U_i, \overline{U}_i) + L_{NLS}(U_r, \overline{U}_r) - 2\left|U_i\right|^2\left|U_r\right|^2,$$

$$L_{NLS}(U, \overline{U}) = \tfrac{1}{2}\left(iU^2\partial_z\left(\overline{U}/U\right) + \left|\partial_x U\right|^2 + \left|\partial_y U\right|^2 - \left|U\right|^4\right), \qquad (4.3)$$

the system of equations (4.2) can be recast as a variational problem and derived from standard Euler-Lagrange equations [24].

The purpose of this work is to derive an analytic solution to this problem, suitable for numerical simulations and for the description of basic characteristics of the beam reflection. It is well known that the set of the NLSEs (4.2) is not analytically tractable. Therefore, like in the reduced variational analysis, some averaging procedure should be applied first to reduce the number of independent spatial coordinates and to convert the system of partial differential equations (4.2) into a simpler system of ordinary differential equations (ODEs). A key point in this approach is to determine the form of the beam envelopes U_a, a=i,r, adequate for the problem analysed.

To this end, let us introduce the new Lagrangian density <L> averaged in planes parallel to the interface (X=const):

$$< L >= \int\int L(U_i, \overline{U}_i, U_r, \overline{U}_r) dZdY, \qquad (4.4)$$

and observe that exactly the same reduced Lagrangian <L> is attributed to the system of the standard NLSEs with their (SPM) terms $|U_a|^2U_a$ appropriately modified by the averaged XPM factors γ_a:

$$\left\{ i\partial_{z_a} + (1/2)\left(\partial^2_{x_{ai}} + \partial^2_{y_a}\right) + \gamma_a |U_a|^2 \right\} U_a(x_a, y_a, z_a) = 0,$$

$$\gamma_a \equiv \gamma_a(X) = 1 + 2 \iint |U_i|^2 |U_r|^2 \, dYdZ \Big/ \iint |U_a|^4 \, dYdZ, \tag{4.5}$$

a=i,r, Therefore, the systems (4.2) and (4.5) are equivalent on the level of the reduced variational equations, as both systems lead to the same Euler-Lagrange equations based on the same reduced Lagrangian density (4.4). The system (4.5), however, has solutions in the form of beam envelopes Ψ_a specific to the standard uncoupled NSLEs, i.e. to the system (4.5) with the substitution γ_a=1. In this case, the reduced Lagrangians of these NLSEs

$$< L^{(a)}_{NLS} >= \iint L_{NLS}(\Psi_a, \overline{\Psi}_a) dx_a dy_a \tag{4.6}$$

provide the variational solutions Ψ_a with the beam power density averaged in space and time:

$$p_a = (1/2) \iint |\Psi_a|^2 \, dx_a dy_a, \tag{4.7}$$

and this quantity will be used below as the solution parameter.

The averaged perturbation γ_a to these solutions modifies, through the XPM factors γ_a, the parameters of the (single) beam envelopes Ψ_a; meanwhile the beam amplitudes should remain unchanged. This leads to the following form of the beam fields:

$$E_a(x_a, y_a, z_a) = U_a(x_a, y_a, z_a) \exp(ik_L z_D z_a),$$

$$U_a(x_a, y_a, z_a) = B_a \gamma_a^{-1/2} \Psi_a(x_a, y_a, z_a; \breve{p}_a), \tag{4.8}$$

with the new beam power parameters

$$\breve{p}_a = \gamma_a p_a \tag{4.9}$$

defined as the beam power densities p_a modified by the factors γ_a. Equations (4.8)-(4.9) state that, in the mutual beam interaction, the averaged incoherent

XPM coupling modifies only the shapes, not the amplitudes, of the beam envelopes U_a. Note that in Eq. (4.8) the parameter $\breve{p}_a$ is explicitly indicated in the notation of the beam envelopes Ψ_a.

The reduced variational analysis of a single NLSE is well known [24-25]. Its solution:

$$\Psi_a(x_a, y_a, z_a; \breve{p}_a) = \Phi_a(x_a, y_a, \breve{z}_a; \breve{p}_a, \mu_{wa}) \exp(i\sigma_a + i\Delta k_a z_D z_a),$$

$$\Phi_a(x_a, y_a, \breve{z}_a; \breve{p}_a, \mu_{wa}) = (2\breve{p}_a)^{1/2} \mu_a v_a^{-2} \exp\left(-\tfrac{1}{2}(x_a^2 + y_a^2) v_a^{-2}\right) \qquad (4.10)$$

is exactly governed by the parabolic approximation to the NSLE (see Appendix and Refs. [21,32]). Apart from the last, nonlinear phase-correction factor in Eq. (4.10), Ψ_a is given by the fundamental Gaussian envelopes Φ_a known from the beam linear propagation, but with new definitions of the propagation distance $\breve{z}_a$ and new beam wave numbers $k_a = k_L + \Delta k_a$. Note that the wave numbers k_a determine also the angle of reflection θ_r through the Snell law:

$$k_r \sin\theta_r = k_i \sin\theta_i . \qquad (4.11)$$

In Eq. (4.10) the parameter μ_{wa} stands for the beam waist radius μ_a at the new waist position $\breve{z}_a = 0$. The relations between the beam complex width v_a, the beam (real) radius w_a, the beam phase-front curvature ρ_a and the distance $\breve{z}_a$ remain exactly the same as in the case of linear propagation:

$$v_a^{-2} = w_a^{-2} - i\rho_a^{-1}, \qquad (4.12)$$

$$\breve{z}_a = \mu_a^2 w_a^2 \rho_a^{-1} . \qquad (4.13)$$

All the beam parameters, including the waist radius μ_a, are defined in a new scaled space $(x_a, \breve{z}_a)$. They depend on the propagation distance $\breve{z}_a$ and on the distance X between the observation point and the interface. Due to the self-similar shape of the beam envelopes they were previously introduced as the aberrationless effects of nonlinear propagation [21]. It is pertinent to observe that these definitions are valid for arbitrary beam power densities p_a, including those much above the self-trapping level $p_a = 1$. They are even valid

at beam collapse points. This makes it possible to apply them in numerical simulations carried out in this work.

Changes of the waist radius and on-axis phase of the beam propagation in the bulk nonlinear Kerr medium, for the propagation range up to one diffraction length $z_a=z_D$, including also a collapse point ($\mu_a=0$), are shown in Fig. 4.2. Plots are given for three representative power levels: $p_a=0$ (linear propagation), $p_a=2$ (nonlinear propagation with a moderate beam power) and $p_a=8$ (nonlinear propagation with a high beam power). The last power level is really high, however, values of p_a in Fig. 4.2 correspond to the effective parameters $\breve{p}_a$ that modify only the envelope shapes of the solution (4.8)-(4.10); the beam amplitudes are proportional to a much smaller quantity $\breve{p}_a/\gamma_a$.

Moreover, the propagation ranges z_a considered here are short enough to obey limitations characteristic to a thin nonlinear refractor [29]. Therefore, the self-similar Gaussian shape of the reduced variational solution (4.8)-(4.10) still remains accurate in numerical simulations presented here. In spite of this, the changes of the beam parameters, even within these short propagation ranges, will appear large enough to influence substantially the beam reflection. The waist radius changes modify the beam on-axis phase, the slope of which equals the nonlinear increment Δk_a of the beam wave numbers (cf. Eqs. (A.4.13)-(A.4.18) in Appendix).

The definitions of the beam envelopes (4.8)-(4.10) entail also, through the beam amplitudes $B_a(2p_a)^{1/2}$, the definition of the reflection coefficient r:

$$r=(B_r/B_i)(p_r/p_i)^{1/2}. \tag{4.14}$$

The coefficient r describes the beam reflection but, unlike the plane wave analysis, depends decisively on the beam representation. Moreover, the incidence θ_i and reflection θ_r angles are in general not equal and the ratio of the beam power densities

$$p_r/p_i=|r|^2\cos\theta_i/\cos\theta_r \tag{4.15}$$

differs from the beam reflectance $|r|^2$, as can be directly derived from the reduced variational equations. Therefore, in the nonlinear medium, a normal

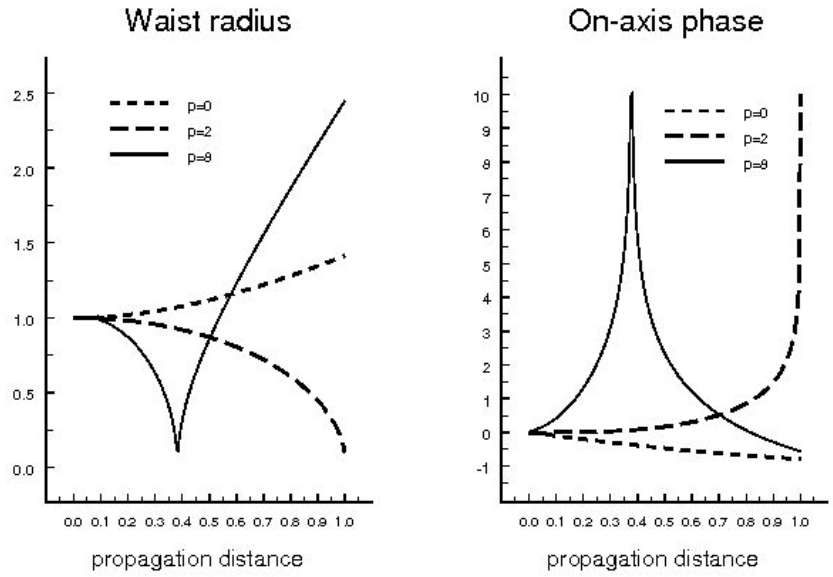

Figure 4.2. Waist radius μ_a and on-axis phase $\Delta\varphi_a$ versus propagation distance z_a for different effective power parameters p_a. The propagation distance is scaled by the diffraction length.

to the interface component of the total field power flux remains constant during the beam reflection, in contrast to its tangential component. This is consistent with the beam penetration of the linear medium at the TIR incidence and results in the G-H shift of the reflected beam. Outside the beam interaction region, the tangential component of the power flux remains also conserved in the TIR case, what leads to other nsp deformations of the waist radius, waist position, propagation direction and complex amplitude of the reflected beam.

Certainly, the fundamental Gaussian beam envelope ansatz (4.8)-(4.10) does not describe all possible phenomena resulting from the nonlinear propagation of the beam, such as, for example, the beam splitting or beam

shadowing [28]. Such phenomena, however, do not seem representative in the description of basic properties of the beam reflection. Within this limitations the beam representation defined above is quite general and allows all the beam parameters: central position, width, spatial chirp, amplitude, phase and spatial frequency, to vary down the propagation direction z_a and with the distance X from the interface. Their dependence on z_a is explicitly given in Appendix, their relation to X can be obtained by substitution of the ansatz (4.8)-(4.10) in the system (4.5) of NSLEs.

In this chapter, the beam reflection problem will be solved, that is, the reflection coefficient r and the beam-field distribution at the interface will be found. The solution to the full propagation-reflection-propagation problem, that is, to the sequence of the incident beam propagation from some input plane to the interface, the beam reflection at the interface and the reflected beam propagation to some output plane, is also possible to obtain within the presented formalism. However, it is outside the scope of this chapter. Note only that to solve this general problem, the beam reflection coefficient r should be known first. Inclusion of all possible propagation phenomena in the presented solution implies a relation, through the beam power parameters p_a, between the incidence angle θ_i at the interface and the incidence angle θ_{i0} at some input plane $z_i=z_{i0}$. Here θ_i is included in the final solution as a certain constant quantity, but it can be treated as an independent parameter in a more general case as well, to account fully for the nonlinear beam propagation between the input/output planes and the interface.

In order to find r, it is sufficient to know only the beam fields and their first derivatives at the interface. Moreover, for $\theta_i \cong \theta_r$, the XPM factors are given by

$$\gamma_a(X) \cong 1 + 2|r|^{\pm 2} \exp(-2X^2 \sin^2\theta_a / w_a^2), \tag{4.16}$$

for a=i, r, respectively, the beam interaction depth decays exponentially with the distance X from the interface and the first derivatives of γ_a with respect to X are nil for X=0. Therefore the reflection coefficient r depends only on $\gamma_a \equiv \gamma_a(0) = 1 + 2|r|^{\pm 2}$ evaluated at the interface (X=0). Thus, at the interface, all the beam parameters are explicitly specified by the effective power

parameter $\breve{p}_a$ (4.8) with the XPM factors γ_a and the only parameter in the field representation (4.7)-(4.10) to be found is just the reflection coefficient r.

4.3 Derivation of the reflection coefficient

Let us concentrate on the field distribution in the incidence plane Y=0 and express the incident and reflected beam fields in terms of their spectral representations in this plane:

$$E_a(x_a,0,z_a) = B_a p_a^{1/2}\pi^{-1/2}\mu_a v_a^{-1} \times \exp(i\sigma_a + ik_a z_D z_a)\int \exp\left(-(1/2)s^2 v_a^2 + isx_a\right)ds\,. \tag{4.17}$$

From the field continuity relations at the interface X=0 and the dispersion relations

$$c_a = k_a z_D \big/ \mu_a^2 \kappa_a - \tfrac{1}{2}s^2\,, \tag{4.18}$$

each spectral component of the incident and reflected beams related by the spectral reflection coefficient r, and the spectral representation of the reflected beam can be restated as

$$E_r(x_r,0,z_r) = B_r p_r^{1/2} r^{-1}\pi^{-1/2}\mu_r v_r^{-1} \times \int r(-s)\exp\left(-\tfrac{1}{2}s^2(\mu_r^2 - i\Delta\breve{z}_r) + isx_r + ic_r(\breve{z}_r + \Delta\breve{z}_r\right)ds\,. \tag{4.19}$$

The shifts $\Delta\breve{z}_a$ of the beam waist positions down the nonlinear propagation directions are defined by Eqs. (A.4.9) in Appendix.

By definition, r differs from the standard Fresnel reflection coefficient r_F. The Fresnel reflection coefficient relates the incident and reflected plane waves with the same amplitudes

$$\widetilde{E} \propto \exp\left(isx_i + ic_i(\breve{z}_i + \Delta\breve{z}_i)\right) + r_F(-s)\exp\left(isx_r + ic_r(\breve{z}_r + \Delta\breve{z}_r)\right) \tag{4.20}$$

meanwhile the beam reflection coefficient r relates the plane waves with different amplitudes determined by the spectral representations (4.17). That leads to the explicit expression for r:

$$r(s) = r_F\left(\mu_i\nu_r\right)\left(\mu_r\nu_i\right)^{-1}\exp\left(i\sigma_i - i\sigma_r\right)\exp(is^2F_{ab}/2)\,, \tag{4.21}$$

$$F_{ab} = \Delta\breve{z}_i - \Delta\breve{z}_r + i\left(\mu_i^2 - \mu_r^2\right) \tag{4.22}$$

with its amplitude and phase nonlinearly modified by all the parameters of the incident and reflected beams. Note that Fresnel reflection coefficient r_F also differs from its linear counterpart owing to the nonlinear modifications of the beam wave numbers Δk_a.

4.4 Evaluation of the beam field at the interface

Evaluation of the integral (4.19) describes the reflected field distribution at the interface and yields values of the reflection coefficient r. Note that, because the incident beam distribution is known, the solution of the reflected field (4.19) at the interface yields not only the distribution of the total beam field above the interface but the transmitted beam field distribution below the interface as well. In the following section, subsequent approaches to evaluation of the integral (4.19) with increasing accuracy will be outlined.

4.4.1 G-o approximation to the reflected field

In the g-o approximation, the spectral reflection coefficient $r(s)$ is replaced by its value at the centre of the beam spectrum:

$$r_g = r(0). \tag{4.23}$$

That value of r is used in evaluation of all the reflected beam parameters. This will be indicated by replacing of the subscript r by g in all field expressions. Among other parameters, the XPM factors γ_a and the beam wave numbers $k_a = k_L + \Delta k_a$ are found from Eqs. (4.16) and (A.4.18), respectively. The direction angle $\theta_g = \arcsin(k_g^{-1} k_i \sin\theta_i)$ of the reflected beam axis was specified by the Snell law (4.11). Therefore, the expression of the g-o reflected beam

$$E_r(x_r, 0, z_r) = \mathrm{r_g}\, p_i^{1/2} \mathrm{p_g}^{-1/2} \Phi_g\left(x_g, 0, \breve{z}_g; \breve{p}_g, \mu_{wg}\right) \exp\left(i\sigma_g + ik_g z_D z_g\right) \tag{4.24}$$

can be derived without any integration of the representation (4.19).

The g-o beam serves as the reference frame in interpretation of the deformations of the actual reflected beam [11-12]. The g-o reflection coefficient r_g follows, in spite of its modifications given by Eq. (4.21),

characteristic features of the Fresnel coefficient r_F. It depends, instead of the actual reflection angle θ_r, on the g-o reflection angle θ_g. Amplitude and phase of the g-o beam represent, loosely speaking, predictions of the plane wave analysis adapted to the description of the beam reflection.

4.4.2 Parabolic approximation to the reflected field

The accuracy of the reflected beam evaluation can be much improved by using the parabolic approximation of the spectral reflection coefficient $r(s)$ evaluated at the centre of the beam spectrum $s = 0$:

$$\ln r(s) \cong \ln(r_g) - isL + (i/2)s^2 F\,. \tag{4.25}$$

Note that, because the transverse modifications of r (in a plane $Z = 0$) are much smaller than its longitudinal modifications (in the incidence plane $Y = 0$), only the latter ones will be accounted for in this analysis. The two longitudinal complex beam shifts:

$$L = ir^{-1}\,\partial r/\partial s\,|_{s=0}\,, \tag{4.26}$$

$$F = -ir^{-2}\left(r\,\partial^2 r/\partial s^2 - (\partial r/\partial s)^2\right)|_{s=0} \tag{4.27}$$

are immediately incorporated in the paraxial description of the reflected beam (4.19) and describe the beam field distribution quite accurately far from the singularities of the beam spectrum:

$$E_r(x_r,0,z_r) = \mathrm{r_g}\,p_i^{1/2}\mathrm{p_g^{-1/2}} \times \Phi_g\left(x_g - L,0,\breve{z}_g - F;\breve{p}_g;\mu_{wg}\right)\exp\left(i\sigma_g + ik_g z_D z_g\right). \tag{4.28}$$

The field is evaluated only in the principal incidence plane, that is for $y_g = 0$, and the transverse modifications of the beam, being small in relation to the modifications in the incidence plane, are neglected what yields also $y_r = 0$.

The complex shifts L and F give rise to the deformation of the g-o reflected beam [11-12]. Note that the aberrationless effects, defined in Appendix, that is the waist radius modifications, the waist displacements and the self-shortening of the propagation distance, contribute to the beam deformation during reflection through the shift F_{ab} defined in Eq. (4.22). Due

to this let us coin F_{ab} as the aberrationless complex focal shift of the beam reflection.

4.4.3 Effects of nonspecular reflection

The reflected beam parameters, for example the actual angle θ_r of the beam propagation, are still unknown because the beam shifts L and F are defined as complex quantities. Therefore, the next step of this analysis provides direct interpretation of the complex shifts in terms of the g-o beam modifications given as real quantities. According to the well known definitions of the longitudinal effects of the nsp reflection [11-12]:

$$\delta_x = \mathrm{Re}(L),$$

$$\delta_z = \mathrm{Re}(F),$$

$$\delta_\theta \cong \mathrm{Im}(L)\big/\left(z_D \mu_{ns}^2\right),$$

$$\mu_{ns}^2 \cong 1 + \mathrm{Im}(F), \tag{4.29}$$

here given in their normalised version (see Appendix), the g-o reflected beam is modified by the transverse δ_x and focal δ_z shifts of its waist centre, its waist radius expansion or reduction by the factor μ_{ns}, and rotation of its scaled axis $\breve{z}_g$ by an angular shift δ_θ:

$$x_r/\mu_{ns} = (x_g - \delta_x)\cos\delta_\theta - (z_D/w_w)(\breve{z}_g - \delta_z)\sin\delta_\theta,$$

$$\breve{z}_r/\mu_{ns}^2 = (w_w/z_D)(x_g - \delta_x)\sin\delta_\theta + (\breve{z}_g - \delta_z)\cos\delta_\theta. \tag{4.30}$$

Therefore, the actual reflected beam axis direction is given by the (actual) reflection angle:

$$\theta_r = \theta_g + \delta_\theta \tag{4.31}$$

and the total composite beam shift δ_S of the beam axis is given by δ_x, δ_z, δ_θ (cf. Ref. [22] and [23]):

$$\delta_s = \delta_x + (z_g - \delta_z)(z_D/w_w)\tan\delta_\theta. \tag{4.32}$$

Note that values of δ_x, δ_z, δ_θ are usually large enough to make the composite shift δ_S substantially different from the G-H shift δ_x. A factor z_D/w_w appears in Eqs. (4.30) and (4.32) due to different normalisation scales, w_w and z_D, in the transverse and longitudinal beam axes directions. Eqs. (4.30) correspond to Eqs. (A.3.12) in Chapter 3 written in the unnormalised spatial coordinates $x_g, z_g)$ in the linear medium.

It can be proved [12] that the geometrical beam deformations defined above should be augmented by the modification of the reflected coefficient r_g:

$$r = r_g \mu_{ns}^{-1/2} \exp(ik_r \delta_z), \tag{4.33}$$

in order to obtain the reflected beam distribution:

$$\begin{aligned} &E_r(x_r, 0, z_r) = \mathrm{r}\, p_i^{1/2} \mathrm{p}_\mathrm{r}^{-1/2} \\ &\times \Phi_r(x_r, 0, \breve{z}_r; \breve{p}_r, \mu_{wr}\mu_{ns}) \exp(i\sigma_r + ik_r z_D z_r) \end{aligned} \tag{4.34}$$

equivalent to that given by the complex longitudinal shifts L and F by Eq. (4.28).

4.4.4 Exact evaluation of the reflected field

The beam representations (4.28) and (4.34) seem very appealing due to the straightforward interpretation of the solution derived. However, great care must be taken in using this representations in cases where the beam spectrum possesses some singularity in the vicinity of the g-o reflection angle θ_g. Exactly such a case is considered in this chapter. The spectral coefficient r exhibits a branch point singularity at the critical incidence $\theta_g \cong \theta_c$:

$$\theta_c = \arcsin\left[k_L / (k_r n_L)\right] \tag{4.35}$$

and the incident beam excites a lateral wave guided by the interface. The interaction between the lateral wave and the beam field is the main source of the reflected beam deformations. That results, however, in divergence of the expansion (4.25) of r near its branch point singularity. Therefore, in numerical simulations presented here, a different, exact this time, analysis is used [22].

The expansion (4.25) is replaced by the double and infinite Taylor expansion of r at angles $\theta_{\pm} \equiv \theta_c \pm \varepsilon'$ placed on both sides of θ_c:

$$r(s) = \sum_{m=0}^{\infty} (m!)^{-1} \left(d^m r / du^m\right)(u_{\pm})(u - u_{\pm})^m \,, \tag{4.36}$$

where the new variable with the same branch point singularity as in $\widetilde{r}$ is used:

$$u \equiv u(\theta_g, \theta_{\pm}) = \left(k \sin(\theta_c - \theta_{\pm}) - k \sin(\theta_g - \theta_{\pm})\right)^{1/2}, \tag{4.37}$$

$u_{\pm} \equiv u(\theta_{\pm}, \theta_{\pm})$. In opposition to the representation (4.25), the expansion (4.36) provides an exact representation of the spectral reflection coefficient r. Moreover, after substitution (4.36) into the beam representation (4.19), the integral can be evaluated exactly, term by term [22], by using the definition of the parabolic cylinder functions [30, 31]:

$$D_{-1-m/2}(i\beta) = \Gamma(m/2+1)\exp(\beta^2/4) \int_0^{\infty} \exp(-i\beta v - v^2/2) v^{m/2} dv \,. \tag{4.38}$$

Finally, the reflected field distribution can be given in terms of appropriate modification of the g-o reflected field E_g:

$$\begin{aligned} &E_r(x_r, 0, z_r) = \\ &\left[1 + \sum_{m=0}^{\infty} \left(c_m^{(+)} D_{-1-m/2}(i\beta) + c_m^{(-)} D_{-1-m/2}(-i\beta)\right)\right] E_g(x_g, 0, z_g) \,, \end{aligned} \tag{4.39}$$

with the expansion coefficients $c_m^{(\pm)}$ and the arguments β dependent on the spatial coordinates (x_g, z_g) [22]. Note that the complex shifts (4.26)-(4.27) and the effects of nsp reflection (4.29)-(4.32) are only implicit in the exact field representation (4.39).

The field representation (4.39) yields the exact solution to the reflection problem for the assumed form of the beam envelopes (4.8)-(4.10). Four terms in the expansion (4.39) appear sufficient to evaluate the field near the branch point singularity with a high accuracy [22]. The representation (4.39) yields also the complex shifts L and F, as well as all the nsp effects δ_x, δ_z, δ_θ, μ_{ns} and r/r_g, evaluated exactly this time. However, the approximate (up to the second-order) representations (4.28) and (4.34) still remain valid. Details of

this analysis, specified to the linear case, can be found in Ref. [22]. In the nonlinear case the linear analysis has to be augmented by monotonic iteration of the nonlinear feedback between the reflection coefficient r and the ratio of the beam power densities p_r/p_i, what was explicitly given in Eqs. (4.8), (4.14)-(4.16). A description of such an iteration, specified to the case of the electro-optic or nonlocal linear-nonlinear interfaces, can be found in Ref. [23].

The incident and reflected field amplitude distribution at the nonlinear interface is shown in Fig. 4.3 for the incidence at the critical angle of TIR and the small dielectric contrast n_L=1.0005. The reflected beam is assumed to be narrow, i.e. the ratio between the longitudinal and transverse scales z_D and w_w is small: $z_D/w_w = 50$. The reflected beam is represented alternatively by the g-o reflected beam according to Eq. (4.24), the g-o beam modified by nsp effects according to Eq. (4.34), and the actual nonspecularly reflected beam described by the exact representation (4.39). Evidently, the g-o approximation overestimates the beam amplitude in this case and does not provide adequate description of the reflected beam. On the other hand, the parabolic approximation to the reflection coefficient (4.25) and the "nsp" representation (4.34) appear quite accurate.

There are a few reasons for the apparent difference between the amplitudes of the g-o reflected beam and the actual reflected beam at the interface. For a wide spectrum of the narrow incident beam - here of the order of $(z_D/w_w)^{-1} = 0.02$ - a substantial part of the reflected beam spectrum is placed in the partial reflection range, i.e., below the critical angle of TIR (4.35). That should lower the effective amplitude of the reflected beam. The opposite effect - the spectral shift of the beam spectrum towards larger angles of reflection, i.e., into the TIR range - results from relative changes of the critical angle θ_c and the angle θ_g of g-o reflection with the incident beam power.

These two effects approximately compensate each other in the case shown in Fig. 4.3. However, the other effect pertinent here is the nsp focal shift δ_z of the waist plane along the g-o beam axis. This effect finally reduces the reflected beam amplitude as shown in Fig. 4.3. In general, all these three

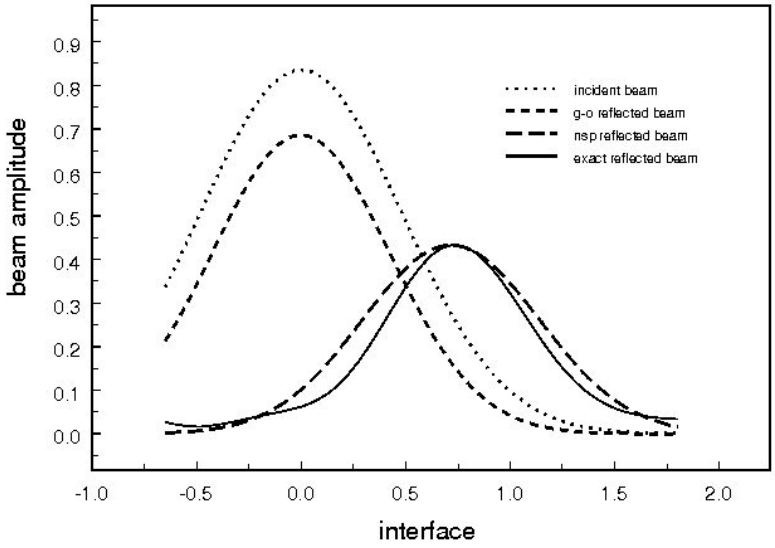

Figure 4.3. Amplitudes of the incident, g-o reflected, nonspecularly reflected and exactly reflected beam field distributions at the nonlinear focusing interface. Amplitudes are given with respect to the maximum value of the amplitude of the incident beam; the distance along the interface is scaled by the incident beam half-width.

effects may contribute substantially to the net change of the reflected field amplitude at the interface.

4.5 Bistability of nonspecular reflection

The effects of nsp reflection: the G-H shift δ_x, the composite shift δ_S, the waist modification μ_{ns}, and the focal shift δ_z, are depicted in Fig. 4.4 for consecutive increasing and decreasing of the incident beam power parameter p_i. All these effects are large, much larger than their counterparts in the beam reflection at a linear interface [22], and noticeably modify the reflected beam according to the beam representation (34). For example, the lateral composite shift is of the order of the beam -waist radius w_w, the waist modification factor varies from 1.4 to 0.8 and the angular shift δ_θ approaches even 1.5

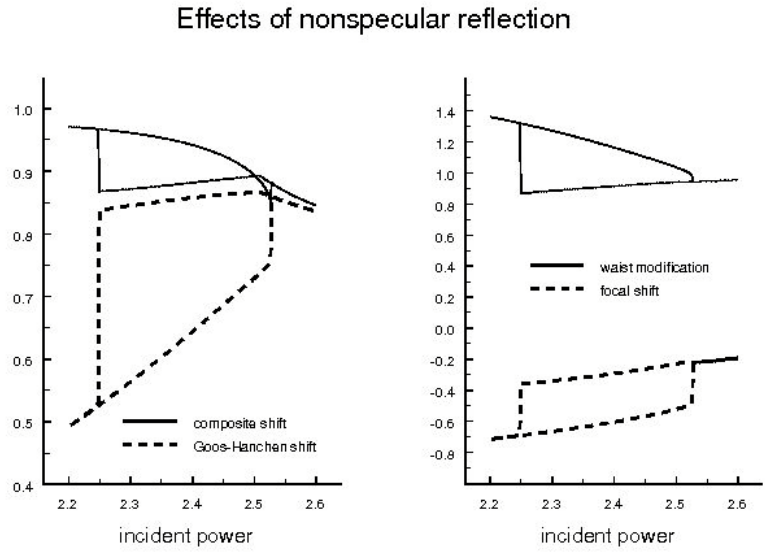

Figure 4.4. Nsp effects of reflection: the composite shift δ_S, the Goos-Hanchen (G-H) δ_x shift, the waist modification squared μ_{ns}^2 and the focal shift δ_z versus the incident power parameter p_i. The shifts δ_S and δ_x are scaled by the beam half-width, the focal shift is scaled the diffraction length of the incident beam.

degrees. Note also large difference between the G-H shift δ_x and the composite shift δ_S (32) at low power levels, that is in the partial reflection state of the interface. Due to large values of the focal and angular shifts, the lateral composite shift is substantial in both cases of beam reflection: partial transmission and TIR. However, the most interesting feature of the nsp effects is their apparent bistable change, as indicated in Fig. 4.4 by their clear hysteresis loops. A similar effect is expected in the reflected beam amplitude and, consequently, in the reflection coefficient as well.

Magnitudes of the reflection coefficients of the g-o beam r_g and the actual (nonspecularly reflected) beam r are shown in Fig. 4.5 in relation to the increasing and decreasing incident power parameter p_i. The two cases: (a)

$q = 1.9$, $z_i = 0.13$ and (b) $q = 2.2$, $z_i = 0.10$ are distinguished by the different angular detuning q and the (normalised by z_D) propagation distance z_i between the incident beam waist and the interface. The angular detuning $q = (\pi/2 - \theta_i)/(\pi/2 - \theta_{cL})$ is introduced as a measure of the difference between the incidence angle θ_i and the low-power critical angle θ_{cL}. Large differences between r and r_g, represented by the nsp modification of the beam complex amplitude r/r_g, indicate that the behaviour of the beam reflection clearly deviates from the plane wave predictions. Bistability loops are obtained in both reflection coefficients: r and r_g. Their range and switching contrast (height) increase with the increase of angular detuning, at the expense of the increase of the incident beam power. Note that basic characteristics of r_g follow closely those of the Fresnel coefficient r_F.

Some pecularities in the bistability loops, not encountered in, for example, bistable switching of the electro-optic or nonlocal interfaces [23], can be observed. The shape of the g-o reflection coefficient r_g appears irregular in case (b) and the bistability loop of the beam reflection coefficient r is shifted towards higher values than those of r_g in case (a). Moreover, it is clearly seen in case (a) that the switching thresholds are displaced from the branch point singularity of r_g towards lower power values. It seems that these pecularities are caused by the displacement of the beam spectrum into the TIR range, as given by changes of the angles θ_g and θ_r of reflection with respect to the critical angle θ_c. This conjecture is confirmed by Fig. 4.6, where changes of the critical θ_c angle, angle of g-o reflection θ_g and the actual reflection angle $\theta_r = \theta_g + \delta_\theta$ are drawn versus the incident beam power. The actual angle θ_r of reflection appears larger than its g-o counterpart θ_g and remains close to θ_c in the whole bistability range. Both switching thresholds (switch-up and switch-down) coincide with the common points of the curves θ_r and θ_c in both cases (a) and (b).

On the contrary, the g-o reflection angle θ_g is smaller than θ_c in the bistability range and crosses the branch point of R_g (crossing point of the curves θ_g and θ_c) outside this range. Moreover, it happens that this branch

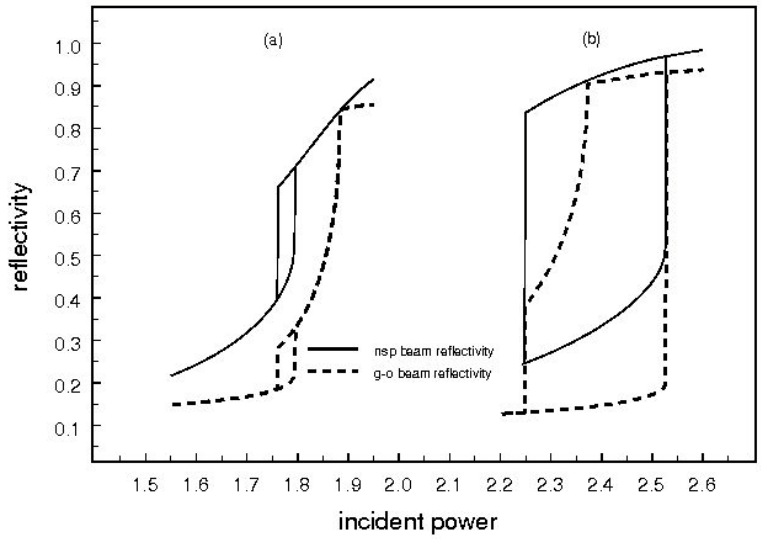

Figure 4.5. Magnitudes of the nsp beam reflection coefficient r and the g-o reflection coefficient r_g vs. the incident power parameter p_i : (a) - $q = 1.9$, $z_i = 0.13$, (b) - $q = 2.2$, $z_i = 0.10$.

Point singularity does not even coincide with the higher threshold of the beam switching. This is precisely the case of Fig. 4.6 (a). Note that the difference $\theta_r - \theta_g$ is just the nsp angular shift δ_θ of the g-o beam. Therefore this nsp shift displaces the spectrum of reflected beam into its higher values and determines the beam switch.

The examples discussed above indicate that the role of the nsp effects is decisive in the bistable beam reflection. Large nsp distortions of the reflected beam spectrum and shape modify the wave numbers of both beams according to Eq. (A.4.18) and the reflection angle according to the Snell law (4.11). This, in turn, modifies the beam reflection coefficient and the beam amplitude to such the extent that the bistable switch can be achieved for some values of the angular detuning. Evidently, characteristic features of this switch appear different from those predicted by the plane wave analysis.

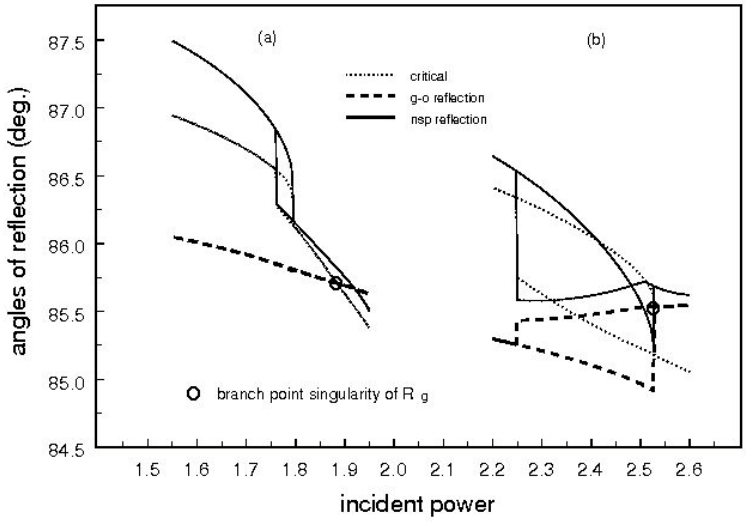

Figure 4.6. Critical angle θ_c, g-o reflection angle θ_g and nsp reflection angle θ_r (in degrees) vs. the incident power parameter p_i: (a) - $q = 1.9$, $z_i = 0.13$, (b) - $q = 2.2$, $z_i = 0.10$.

4.6 Comments and conclusions

The beam reflection at the nonlinear-linear interface is analysed for incidence near the critical angle of TIR. The solution obtained is derived in terms of aberrationless effects of nonlinear propagation and nsp effects of reflection. Results of the analysis indicate that the nonlinear-linear interface may exhibit bistable switching behaviour of the beam reflection/transmission, for some particular sets of beam and interface parameters. All nsp effects of reflection show similar bistable behaviour with the large contrast of switching.

The nature of the bistable switch of reflection at the nonlinear-linear interface appears different from that predicted by the plane-wave analysis. For example, the shift of the bistability loop from a branch point singularity of TIR can be observed for certain sets of the beam and interface parameters. Contrary to the plane wave predictions, where the switching is exclusively

related to the singularity of the Fresnel reflection coefficient at the critical angle of TIR, the switching of narrow beams is also determined by large nsp deformations of the reflected beam. In addition, these effects of nsp reflection are substantially enhanced by self-focusing and by mutual interaction of the incident and reflected beams.

The presented treatment of the beam reflection problem bases on the iterated exact evaluation of the beam field at the interface. However, the incident and reflected beam envelopes can be also modelled on the grounds of the reduced variational formulation of the auxiliary nonlinear propagation problem. The accuracy of this approximation is of the same order as that encountered in the variational analysis of coupled solitons dynamics. Therefore, the solution indicates rather qualitative characteristics of reflection, useful in the author's opinion, however, in possible further numerical and experimental studies of this problem. This work is, to the best of the author's knowledge and together with his other recent communication [32], the first report on the bistable switch of the finite-width beam at the nonlinear-linear interface. The analysis presented confirms, contrary to common opinions on this problem, that bistable switching of the nonlinear interface could, at least in principle, be obtained by a single beam incidence.

The analysis is not restricted only to beams and to nonlinear media with the plain refractive Kerr-type nonlinearity. Finite-width pulse and/or beam reflection/transmission at interfaces between nonlinear media of other types of nonlinearity may be treated in a similar manner. In the context of possible direct applications it must be stressed that the parameters of the beam-interface system necessary to obtain the bistable switch are rather demanding –first of all, the beam power should be very high. However, this analysis concerning the refractive nonlinearity of the local Kerr type may serve as the first step in modelling interfaces consisting of other nonlinear media, like these of nonlocal saturated nonlinearities [9, 33-34], semiconductors operating near the exciton-polariton resonance [35] or electro-optic structures guiding surface plasmon resonance modes [36]. In these cases it is expected that significant improvement of the switching conditions may be obtained.

Appendix: Aberrationless effects of nolinear propagation

Let us consider a single fundamental Gaussian beam of TE polarization ($E \equiv E_y$) propagating in a nonlinear Kerr medium with the refractive index $n = n_L + \frac{1}{2} n_2 |E|^2$, where n_L and n_2 are the linear (low-power) and nonlinear (high-power) indices of refraction, respectively. In the parabolic approximation, that is up to second-order terms in transverse coordinates x and y, the propagation of the Gaussian beam in this nonlinear medium can be described in a way reminiscent of the well-known formulae describing the Gaussian beam propagation in a linear medium. Within this approach the beam remains Gaussian in each transverse cross-section. However, the longitudinal coordinate (propagation distance) along the beam axis, as well as the beam parameters, like the beam radius or phase-front curvature, should be appropriately rescaled or normalised. The rescaling depends on the power of the beam and on the (propagation) distance of the cross-section plane from an actual beam waist plane. The method, known as the scaled complex ray tracing (SCRT) [21], allows to trace the nonlinear propagation of beams with the help of well-known results of tracing the linear propagation of beams.

Define the envelope or SVA $\Psi(x, y, z)$ of the beam by extraction of the plane wave phase factor $\exp(ik_L z_D z)$ from the beam field $E(x, y, z)$:

$$E(x, y, z) = \Psi(x, y, z) \exp(ik_L z_D z). \tag{A.4.1}$$

In Eq. (A.4.1) k_L and z_D are the low-power (linear) wave number and diffraction length of the beam field, respectively. It is postulated that $z_D = k_L w_w^2$, where w_w stands for a low-power radius (half-width) of a beam transverse cross-section at its waist. The beam propagates in direction of the z-axis and its field distribution $E(x, y, z_0)$ is assumed to be known in the input plane at $z = z_0$.

The high-power (nonlinear) longitudinal coordinate $\breve{z}$ and the low-power (linear) longitudinal coordinate z are assumed to be in general different from each other besides the input plane $z = z_0$, where $\breve{z} = \breve{z}_0 = z_0 = z$. It is stipulated that the transverse coordinates x and y of the beam are scaled to w_w, the longitudinal coordinates z and $\breve{z}$ are scaled to z_D, and the field

amplitude $E(x,y,z)$, together with its SVA $\Psi(x,y,z)$, are normalised or scaled to $\left[(1/2)(k_L w_w)^2 (n_2/n_L)\right]^{-1/2}$:

$$x/w_w,\ y/w_w \to x,\ y,$$

$$z/z_D,\ \breve{z}/z_D \to z,\breve{z},$$

$$\tfrac{1}{2}(k_L w_w)^2 (n_2/n_L)|\Psi(x,y,z)|^2 \to |\Psi(x,y,z)|^2 = |E(x,y,z)|^2. \qquad \text{(A.4.2)}$$

For more details of the beam scaling procedure see also the discussion in Section 1 of Chapter 2.

Evolution of the SVA $\Psi(x,y,z)$ of the beam is then governed by the standard normalised NLSE:

$$\left\{i\partial_z + \tfrac{1}{2}(\partial_x^2 + \partial_y^2) + \left|\Psi(x,y,z)\right|^2\right\}\Psi(x,y,z) = 0. \qquad \text{(A.4.3)}$$

A solution of (A.4.4) is postulated here in the form of fundamental Gaussian beam [21]:

$$\Psi(x,y,z) = A(\varsigma)\exp\left[-\tfrac{1}{2}(x^2+y^2)/v^2(\varsigma)\right],$$

$$A(\varsigma) = a(\varsigma)\exp[i\varphi(\varsigma)] = A_0\exp[i\Delta\varphi(\varsigma)]\mu(\varsigma)v^{-2}(\varsigma), \qquad \text{(A.4.4)}$$

known from the case of its linear propagation, in which case $z = \varsigma$, $\mu = 1$ and $\Delta\varphi = 0$. Contrary to the linear case, however, the spatial chirp parameter ς is not equal to the propagation distance $\breve{z}$, but is equal to $\breve{z}$ scaled by the factor $\mu^2(\varsigma)$ that is also dependent on ς:

$$\varsigma = \breve{z}\mu^{-2}(\varsigma). \qquad \text{(A.4.5)}$$

The real $a(\varsigma)$, $\varphi(\varsigma)$, $\mu(\varsigma)$ and complex $v(\varsigma)$ beam parameters are to be found by solution to the NLSE (A.4.3).

The beam complex amplitude A is related, through the factor $A_0 = \sqrt{2p}$, to the power parameter p, which stands, up to the admittance factor, the averaged (in space and time) power density of the beam:

$$p = \tfrac{1}{2}\iint\left|\Psi(x,y,z)\right|^2 dxdy. \qquad \text{(A.4.6)}$$

The power parameter p is normalised in the way that makes it equal to one at the self-trapping power level, where beam intensity $|E(x,y,z)|^2$ does not change from one transverse plane to another one. It is stipulated that $\varsigma = \varsigma_0 = z_0$, $\Delta\varphi = \Delta\varphi_0 = 0$ and $\mu = \mu_0 = 1$ in the input plane $\breve{z} = \breve{z}_0 = z_0$ and that the beam waist plane is placed at $\breve{z} = 0$. The ansatz (A.4.4) becomes an exact solution to the NLSE (A.4.3) in the low-power limit $p \cong 0$, where $\breve{z} = z$, $\mu = 1$ and $\Delta\varphi = 0$ for all values of z. In the high-power limit, that is for finite values of p, the Gaussian beam, in the form (A.4.4) known from linear propagation, is nonlinearly modified by the nonlinear SPM effect. This means that the beam Gaussian shape propagating in the nonlinear medium depends on $\breve{z}$ (or ς) instead of z and is nonlinearly modified through the quantities μ and $\Delta\varphi$. Definitions of these quantities follow directly from the solution to the NLSE (A.4.3) in its parabolic approximation and this will be outlined by Eqs. (A.4.19)-(A.4.27) below. Let us describe the solution obtained by this method first [32].

The nonlinear modifications of the beam can be described by two factors: the self-shortening factor $\kappa(\varsigma)$ of the linear propagation distance z and the nonlinear on-axis phase modification $\Delta\varphi(\varsigma)$, both expressed, besides the power parameter p, by the spatial chirp parameter ς [21]:

The self-shortening factor

$$\kappa(\varsigma) = \pm(1 - p + \varsigma^2)(1 + \varsigma^2)^{-1} \tag{A.4.7}$$

scales the distance z to its nonlinear counterpart $\breve{z}$,

$$\breve{z} = \kappa(\varsigma) z - \Delta z, \tag{A.4.8}$$

and displaces, by the nonlinear focal shift Δz, the beam waist from its position at the low-power waist plane $z = 0$ to its new position at the high-power waist plane $\breve{z} = 0$:

$$\Delta z = z_0 \kappa(\varsigma)\left(1 \mp \kappa^{-1}(\varsigma_0)\right). \tag{A.4.9}$$

The signs $\mp$ in Eqs. (A.4.7) and (A.4.9) are chosen such that the condition $\mu^2(\varsigma_0) = 1$ is fulfilled in the input plane $z = z_0 = \varsigma = \varsigma_0$. Now the beam complex $\nu(\varsigma)$ and real $w(\varsigma)$ radii (half-widths) of the beam and the beam phase front curvature ρ:

$$v^{-2}(\varsigma)=\mu^{-2}(\varsigma)\left(1+i\varsigma\right)^{-1}=w^{-2}(\varsigma)-i\rho^{-1}(\varsigma)\,, \tag{A.4.10}$$

are given in a form known from linear propagation of the Gaussian beam, with the parameter μ expressed by the self-shortening factor (A.4.7):

$$\mu^2(\varsigma)=\kappa(\varsigma)/\kappa(\varsigma_0)\,. \tag{A.4.11}$$

Therefore, the parameter μ represents the beam waist radius $w(0)$ at the new waist position $\varsigma=0$ and the relation between w^2, ρ and ς is:

$$w^2(\varsigma)=\mu^2(\varsigma)\left(1+\varsigma^2\right)=\rho(\varsigma)\varsigma\,, \tag{A.4.12}$$

Eq. (A.4.12) follows the relation $w^2=\rho z$ known from the linear propagation of the Gaussian beam. However, the new propagation distance $\breve{z}=\mu^2\varsigma$ (A.4.5) equals the chirp parameter ς scaled by μ^{-2}, meanwhile both these quantities equal each other in the linear case, where $z=\varsigma$ and $\mu=1$. Note also that the normalised power parameter $p=\frac{1}{2}a_0^2w_0^2$ is expressed by the real amplitude $a=a_0$ and the real beam radius $w=w_0$ known in the input plane [21].

Besides the nonlinear effect of self-shortening decribed by the factor $\kappa(\varsigma)$, SPM of the beam induces also the nonlinear increment $\Delta\varphi(\varsigma)$ of the beam on-axis phase $\varphi(\varsigma)$ [21],

$$\varphi(\varsigma)=\varphi_L(\varsigma)+\Delta\varphi(\varsigma)\,,$$

$$\Delta\varphi(\varsigma)=\delta\varphi(\varsigma)-\delta\varphi(\varsigma_0)\,, \tag{A.4.13}$$

$$\delta\varphi(\varsigma)=(1-\tfrac{3}{2}p)(1-p)^{-1/2}\varphi_L(\varsigma(1-p)^{-1/2})-\varphi_L(\varsigma)\,,$$

$$\varphi_L(\varsigma)=-\arctan(\varsigma)\,, \tag{A.4.14}$$

where these phase quantities are assumed to be known in the input plane $\varsigma=\varsigma_0$, that is $\varphi(\varsigma_0)=\varphi_L(\varsigma_0)$. Note that in the low-power limit the phase term $\varphi(\varsigma)$ resolves into the low-power on-axis phase $\varphi_L(z)$ of the beam, that is $\varphi(\varsigma)=\varphi_L(z)$ for $p=0$.

The nonlinear phase increment $\Delta\varphi(\varsigma)$ depends on ς and changes during the beam nonlinear propagation. Therefore it modifies also the wave number

$k \equiv k(\varsigma)$ of the beam field. As the derivatives of $\Delta\varphi(\varsigma)$ and $\varphi(\varsigma)$ are known from (A.4.13)-(A.4.14) [21], [32]:

$$(d/dz)\varphi(\varsigma) = -(1-\tfrac{3}{2}p)w^{-2}(\varsigma),$$

$$(d/dz)\Delta\varphi(\varsigma) = \tfrac{1}{2}pw^{-2}(\varsigma)(1+3\varsigma^2)(1+\varsigma^2)^{-1}, \qquad \text{(A.4.15)}$$

then, to evaluate k explicitly, it is sufficient to approximate the on-axis beam phase $\varphi(\varsigma)$ by the first two terms in its Taylor expansion. At some transverse interface defined here, say, at $\varsigma = \varsigma'$, this approximation yields:

$$\Delta\varphi(\varsigma) \cong \sigma(\varsigma') + z(d(\Delta\varphi)/dz)(\varsigma'),$$

$$\sigma(\varsigma') = \Delta\varphi(\varsigma') - z'(d(\Delta\varphi)/dz)(\varsigma'), \qquad \text{(A.4.16)}$$

and the reformulation of the exponent terms in the definition (A.4.1) of SVA of the beam:

$$\exp[i\Delta\varphi(\varsigma)]\exp(ik_L z_D z) \cong \exp[i\sigma(\varsigma)]\exp[ik(\varsigma)z_D z], \qquad \text{(A.4.17)}$$

leads to the expression for the (nonlinear) effective wave number of the beam field:

$$k(\varsigma) = k_L\beta(\varsigma) = k_L\left[1+\tfrac{1}{2}p(k_L w_w)^{-2}w^{-2}(\varsigma)(1+3\varsigma^2)(1+\varsigma^2)^{-1}\right]. \qquad \text{(A.4.18)}$$

Therefore, the linear wave number k_L is increased or decreased to its nonlinear value k by the wave number modification factor β. Note that β is not linear in p; both quantities w and ς depend on p as well.

It can be shown by inspection that the ansatz (A.4.4), together with the definitions (A.4.5)-(A.4.18), satisfies the NLSE (A.4.3) in the parabolic approximation of the beam intensity [21]:

$$|E(x,y,z)|^2 \cong \tfrac{1}{2}pw^{-2}(\varsigma)\left[3-(x^2+y^2)w^{-2}(\varsigma)\right] \qquad \text{(A.4.19)}$$

for arbitrary values of beam powers, that is below or above the self-trapping level $p=1$, provided that the propagation distance z is small enough to ensure that the assumed Gaussian beam shape approximation still remains valid. The form of approximation (A.4.19) has not been postulated a priori – it can be rigorously derived, together with other beam parameters, by the SCRT method [21] in parabolic approximation to the NLSE:

$|E(x,y,z)|^2 \cong c(\varsigma) - b(\varsigma)(x^2+y^2)$ [21]. Note that the parabolic form of the nonlinear term in the NLSE (A.4.19) has been obtained first within the reduced variational approach to the problem [24], [25]. It differs substantially from the first order approximation to the ansatz (A.4.4) conventionally assumed in the past, that is from:

$$\left|E(x,y,z)\right|^2 \neq a^2(\varsigma)\,|1-(x^2+y^2)v^{-2}(\varsigma)\,|\,. \tag{A.4.20}$$

The form (A.4.19) of the nonlinear term in the NLSE is a fundamental result of the method. Only then the analysis presented accounts in the self-consistent manner for the nonlinear modifications of the Gaussian beam transverse and longitudinal spatial distribution in its amplitude and phase, within the solution (A.4.4)-(A.4.19) of the parabolic approximation (A.4.19) to the NLSE (A.4.3).

Let us summarise the derivation of the solution obtained above for parabolic approximation of the NLSE:

$$\left\{i\partial_z + \tfrac{1}{2}\left(\partial_x^{\,2} + \partial_y^{\,2}\right) + \tfrac{1}{2}\,pw^{-2}\left(3-\left(x^2+y^2\right)w^{-2}\right)\right\}\Psi(x,y,z) = 0\,, \tag{A.4.21}$$

as given in Refs. [21] and [32]. The (exact) solution to the NLSE (A.4.21) can be found in the form $\Psi = A\exp[-\frac{1}{2}(x^2+y^2)v^{-2}]$ of the SVA of the Gaussian beam (A.4.4) with its complex radius v and its complex amplitude A. Indeed, inserting Ψ in the NLSE (A.4.21) and grouping terms of the zero and second order in x and y, we obtain the nonlinear complex ray and amplitude ordinary differential equations [21], [32]:

$$dv^2/dz = i\left(1 - pv^4w^{-4}\right), \tag{A.4.22}$$

$$dA/dz = -iAv^{-2}\left(1-\tfrac{3}{2}\,pv^2w^{-2}\right), \tag{A.4.23}$$

with the solution postulated in the form:

$$A = A_0\mu\, v^{-2}\exp\left[i(\varphi-\varphi_L\right], \tag{A.4.24}$$

$$v^2 = (w^{-2} - i\rho^{-1})^{-1}\,, \tag{A.4.25}$$

formally equivalent to that of linear propagation but with beam parameters dependent now on ς (A.4.5) instead of z (cf. Eqs. (A.4.4), (A.4.10),

(A.4.13) and (A.4.14)). The SCRT method [21] yields explicitly this relation for all the beam parameters in (A.4.24) and (A.4.25), that is for the real beam radius w (A.4.12) (at arbitrary $\breve{z}$), the beam radius μ (A.4.11) at the beam waist (at $\breve{z}=0$), the beam phase front curvature ρ (A.4.12) and the nonlinear phase-correction $\Delta\varphi=\varphi-\varphi_L$ (A.4.13)-(A.4.14). These parameters are dependent on the spatial chirp parameter ς (A.4.5) interrelated with the nonlinearly modified propagation distance $\breve{z}$ (A.4.8) by the waist radius μ.

The solution implies that the new distance $\breve{z}$ of the Gaussian beam propagation is shortened with respect to its linear couterpart z by the factor κ (A.4.7) and the beam waist position is displaced along the beam axis by Δz (A.4.9). Moreover, as Δz depends of $\breve{z}$, the waist position $\breve{z}=0$ is changing during propagation with respect to its linear counterpart at $z=0$. In addition, the nonlinear correction of the on-axis phase $\Delta\varphi$ (A.4.13)-(A.4.14) yields the additional on-axis phase σ (A.4.16) of the beam and the new nonlinearly modified wave number k (A.4.18) of the beam field. Finally, the beam field representation is given by:

$$\begin{aligned} E(x,y,z) &= \Psi(x,y,z)\exp(ik_L z_D z) \\ &= \sqrt{2p}\,\mu\, v^{-2}\exp\left[-\tfrac{1}{2}(x^2+y^2)v^{-2}\right]\exp(i\sigma+ikz_D z)\,, \end{aligned} \tag{A.4.26}$$

where the beam parameters μ, v, σ and k vary, through the nonlinear chirp parameter ς, with the new propagation distance $\breve{z}$. Details of the above analysis, based on the complex ray tracing of beam propagation in nonlinear media of the Kerr type (SCRT method), can be found in [21] and [32]. In these articles, complete results of numerical simulation of all aberrationless effects of nonlinear propagation, especially in the context of the Z-scan measurements, and derivation of the nonlinear *ABCD* matrix for the Gaussian beam nonlinear propagation, have been presented.

Note that exactly the same ODEs (A.4.22)-(A.4.23) can be derived directly within the reduced variational analysis of the NLSE (A.4.3) [24], [25]. After performing, in any plane (x,y) - transverse to the beam propagation direction, the integration of the Lagrangian density $L_{NLS}(x,y,z;\Psi,\overline{\Psi})$ specific to the NLSE (A.4.3):

$$\breve{L}_{NLS}(z;\Psi,\overline{\Psi}) = \int\int L_{NLS}(x,y,z;\Psi,\overline{\Psi})dxdy\,, \tag{A.4.27}$$

$$L_{NLS}(x,y,z;\Psi,\overline{\Psi}) = (1/2)\left\{\gamma\Psi^2\partial_z\left(\overline{\Psi}/\Psi\right) + \left|\partial_x\Psi\right|^2 + \left|\partial_y\Psi\right|^2 - \left|\Psi\right|^4\right\}, \quad \text{(A.4.28)}$$

the reduced variational principle implies the Euler-Lagrange equations for the beam real parameters $u = w$, $u = \rho$, $u = a$ and $u = \varphi$:

$$(\partial/\partial z)\left(\partial\breve{L}_{NLS}/\partial(\partial\overline{u}/\partial z)\right) - \partial\breve{L}_{NLS}/\partial\overline{u} = 0. \quad \text{(A.4.29)}$$

In this way, the infinite-dimensional variational problem, defined by the Lagrangian density $L_{NLS}(x,y,z;\Psi,\overline{\Psi})$, is projected onto the finite-dimensional problem defined by the averaged (reduced) Lagrangian $\breve{L}_{NLS}(z;\Psi,\overline{\Psi})$. The Euler-Lagrange equations (A.4.29) yield four real ODEs for w, ρ, a and φ equivalent to the two complex ODEs (A.4.22)-(A.4.23) with the solution given in Eqs. (A.4.4)-(A.4.14). Details of the reduced variational analysis can be found in [24] and [25] and their relation with the SCRT method in [21] and [32].

Summing up, it was shown how propagation of the Gaussian beam in the nonlinear medium of the Kerr type could be described within the parabolic approximation (A.4.19) to the NLSE (A.4.3) by the beam parameters (or variables). The beam parameters under consideration are: the beam waist position Δz and radius μ, the beam radius w and the phase front curvature ρ, together with the beam chirp ς, the beam on-axis field magnitude a and phase φ, and the nonlinearly modified wave number k of the beam field. All these parameters are dependent on the propagation distance $\breve{z}$ nonlinearly modified with respect to its counterpart z in the linear case.

The analysis described above remains valid not only for the one-, two- or three-dimensional monochromatic beams but also for (four-dimensional) polychromatic wave packets [21]. Moreover, in the two-dimensional case, with the longitudinal variable (z) and one transverse variable (x), the beam propagation in free space corresponds to the case of nonlinear pulse propagation in fibres, provided that the spatial transverse variable (x) is replaced by time (t) and the diffraction term in the NLSE is replaced by the group-velocity dispersion term. This case has been recently investigated by the method called the collective variable approach [37]. In this case, the collective variables correspond to the beam parameters, evolution of which has been described here and in [21], and the parabolic approximation to the

NLSE (A.4.21) corresponds to the bare approximation applied to the NLSE in the collective variable treatment.

Main content of this chapter has been published in Journal of Optics A: Pure and Applied Optics ***2****, 433-441 (2000).*

References

[1] A. E. Kaplan, “Theory of hysteresis reflection and refraction of light at the boundary of a nonlinear medium”, Zhurnal-Eksperimental'noi-i-Teoreticheskoi-Fiziki. **72**, 1710-1726 (1977).

[2] D. Marcuse, “Reflection of a Gaussian beam from a nonlinear interface”, Appl. Opt. **19** 3130-3139 (1980).

[3] P. W. Smith, W. J. Tomlinson, P. J. Maloney and A. E. Kaplan, “Bistability at an electro-optic interface”, Optics Lett. **2**, 57-59 (1982).

[4] W. J. Tomlinson, J. P. Gordon, P. W. Smith, and A. E. Kaplan, “Reflection of a Gaussian beam at a nonlinear interface”, Appl. Opt. **21**, 2041-2051 (1982).

[5] K. H. Strobl, and R. Cuykendall, “ Single-step switching at a nonlinear interface “, Phys. Rev. A **40** 5143-5146 (1989).

[6] A. B. Aceves, J. V. Moloney and A. C. Newell, “Theory of light-beam propagation at nonlinear interfaces”, Phys. Rev. A **39** 1809-1840 (1989).

[7] D. R. Andersen and J. J. Regan, “Reflection and refraction of a three-dimensional Gaussian beam at a nonlinear interface”, J. Opt. Soc. Am. **6** 1484-1492 (1989).

[8] S. De Nicola S., A. E. Kaplan, S. Martellucci, P. Mormile, G. Pierattini, and J. Quartieri, “Stable hysteretic reflection of light at a nonlinear interface”, Appl. Phys. B **49** 441-444 (1989).

[9] K. Strobl and I. Golub, “All-optical switching of reflectivity and transmissivity by a nonlinear sandwich”, IEEE J. Quantum Electron. **28** 1435-1438 (1992).

[10] M. Azadeh and L. W. Casperson, “Reflection and refraction of light at saturating active boundaries”, J. Mod. Optics **44** 29-40 (1997).

[11] T. Tamir, “Nonspecular phenomena in beam fields reflected by multilayered media”, J. Opt. Soc. Am. A **3**, 558-565 (1986).

[12] W. Nasalski, "Longitudinal and transverse effects of nonspecular reflection", J. Opt. Soc. Am. A, **13**, 172-181 (1996).

[13] M. A. Porras, “Nonspecular reflection of general light beams at a dielectric interface”, Optics Commun. **135**, 369-377 (1997).

[14] N. Bonomo and R. A. Depine, “Nonspecular reflection of ordinary and extraordinary beams in uniaxial media”, J. Opt. Soc. Am A **14**, 3402-3409 (1997).

[15] M. Lehman, “An entropic foundation of the angular change in the reflected beam from a planar interface”, Optik **107,** 73-78 (1997).

[16] J.-J. Greffet, M. Nieto-Vesperinas, “Field theory for generalized bidirectional reflectivity: derivation of Helmholtz's reciprocity principle and Kirchhoff's law”, J. Opt. Soc. Am. A **15** 2735-2744 (1998).

[17] F. I. Baida, D. Van Labeke, J-M Vigoureux, “Theoretical study of near-field surface plasmon excitation, propagation and diffraction”, Opt. Commun. **171**, 317-331 (1999).

[18] F. Schreier, M. Schmitz, and O. Bryngdahl, “Pulse delay at diffractive structures under resonance conditions”, Optics Lett. **23**, 1337-1339 (1998).

[19] R. Güther R. and B. H. Kleemann, “Shift and shape of grating diffracted beams “, J. Modern Optics **45** 1375-1393 (1998).

[20] D. Daisy and B. Fischer B., “Optical bistability in a nonlinear-linear interface with two-wave mixing”, Optics Lett. **17** 847-849 (1992).

[21] W. Nasalski, "Complex ray tracing of nonlinear propagation", Opt. Commun. **119**, 218-226 (1995); ibid **127**, 381 (1996); “Aberrationless effects of nonlinear propagation”, J. Opt. Soc. Am. B **13**, 1736-1747 (1996); “Scale formulation of first-order nonlinear optics”, Opt. Commun. **137**, 107-112 (1997).

[22] W. Nasalski, T. Tamir and L. Lin, “Displacement of the intensity peak in narrow beams reflected at a dielectric interface”, J. Opt. Soc. Am. A **5**, 132-140 (1988).

[23] W. Nasalski, "Nonspecular bistability versus diffraction at nonlinear hybrid interfaces", Optics Commun. **77**, 443-450 (1990); “Nonspecular bistability at a delocalized nonlinear interface”, J. Modern Optics **44**, 1355-1372 (1997).

[24] D. Anderson, “ Variational approach to nonlinear pulse propagation in optical fibers”, Phys. Rev. A **27**, 3135-3145 (1983).

[25] M. Desaix, D. Anderson and M. Lisak, “ Variational approach to collapse of optical pulses”, J. Opt. Soc. Am. B **8**, 2082-2086 (1991).

[26] T. Ueda and W. L. Kath, “Dynamics of coupled solitons in nonlinear optical fibers”, Phys. Rev. A **42**, 563-571 (1990).

[27] C. Paré and M. Florianczyk, “Approximate model of soliton dynamics in all-optical couplers”, Phys. Rev. A **41** 6287-6295 (1990).

[28] M. Karlsson, D. Anderson, A. Höök and M. Lisak, “A variational approach to optical soliton collisions”, Physica Scripta **50**, 265-270 (1994).

[29] P. B. Chapple, J. Staromlyska, J. A. Hermann and T. McKay, “Single-beam Z-scan: Measurement techniques and analysis”, J. Nonlin. Opt. Phys. and Mtrls **6** 251-293 (1997).

[30] L. S. Grandshteyn and L. M. Ryshik , *Tables of Integrals, Series and Products* (New York, Academic, 1980) p.1064

[31] C. C. Chan, T. Tamir, “Beam phenomena at and near critical incidence upon a dielectric interface”, J. Opt. Soc. Am. A **4,** 655-663 (1987).

[32] W. Nasalski W., “Beam switching at a nonlinear-linear interface”, J. Techn. Phys. **41,** 201-218 (2000).

[33] K. H. Strobl, and R. Cuykendall, “Nonlinear interface: “Three dimensional versus saturated model predictions in light of new experimental findings”, Opt. Commun. **70**, 389-392 (1990).

[34] D. J. Mitchell and A. W. Snyder, “Soliton dynamics in a nonlocal medium”, J. Opt. Soc. Am. B **16**, 236-239 (1999).

[35] J. L. Birman, D. N. Pattanayak, and A. Puri, “Prediction of a resonance-enhanced laser-beam displacement at total internal reflections in semiconductors”, Phys. Rev. Lett. **50**, 1664-1667 (1983).

[36] L. Lévesque and B. E. Paton, „Light switching in a glass-AG-polymer structure using attenuated total reflection (ATR)”, Can, J. Phys. **72**, 651-657 (1994).

[37] P. T. Dinda, A. B. Moubissi and K. Nakkeeran, “A collective variable approach for dispersion-managed solitons”, J. Phys. A: Math. Gen. **34**, L103-L110 (2001).

CHAPTER 5

Amplitude-polarization representation of beams at a dielectric interface

Three-dimensional optical beams incident on a dielectric interface undergo deformations upon reflection and refraction. Within first-order optics, and as far as only first-order beam deformations are considered, these deformations may be interpreted as longitudinal and transverse displacements and deflections of beam axes. In general, they are different for TE and TM components of the beam field. The problem of beam reflection and refraction at the interface is reformulated and solved in such a manner that the beams are obtained with new, uniquely defined uniform displacements of their axes in a spatial domain and their spectrum centres in a spectral domain. Additional modifications of the beam polarization state remain generally small and non-uniform throughout the entire beam spectrum. In this context, a special role of diagonal, linear and circular, polarization states in the interface plane is indicated.

5.1 Introduction

The prediction of an optical beam spatial displacement upon reflection from a dielectric interface was first reported by Picht (1929) [1], although the notion of such a displacement has been known even in Newton's time. While a number of papers have been published on this problem in two-dimensional

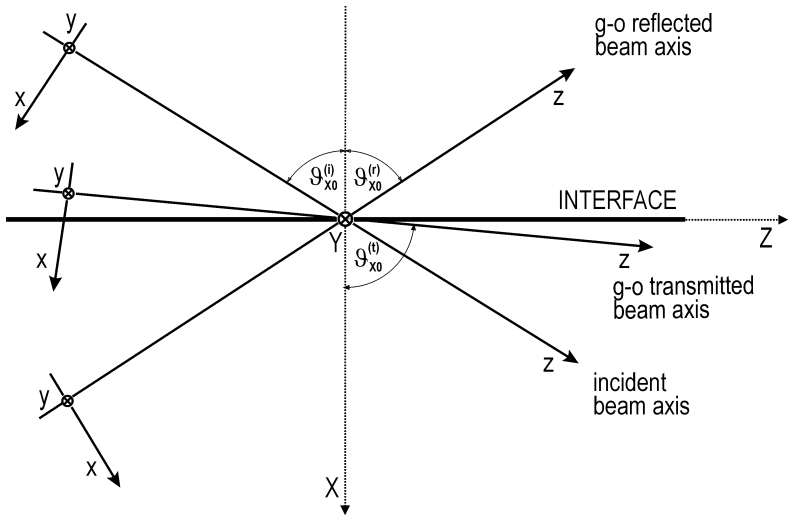

Figure 5.1. The interface reference frame (X, Y, Z) and the reference frames (x, y, z) for the incident, reflected and transmitted beams in the case of internal reflection and partial transmission at a dielectric interface.

(2D) configurations, less attention has been paid to the problem of three-dimensional (3D) beams at the interface [2-7]. This chapter concerns main aspects of 3D beam reflection and transmission at the dielectric interface, especially these exclusively inherent in 3D geometries. Discussions related to 2D problems can be found, for instatnce, in reports referred to in [5].

From differences between characteristics of these two configurations, those pertaining to the beam polarization and their interrelations with the beam amplitude spatial distribution are among the most important. Selection of the two, mutually independent, linear TM and TE polarization states of the beams seem to be proper in analysing 2D configurations, as they distinguish two separate, orthogonal planes, the incidence plane (x, z) and the transverse plane (y, z), respectively, in which the 2D distribution of beam-field amplitudes can be independently defined. Arbitrary elliptic beam polarization should be considered instead in the general 3D case, as it corresponds, in

general, to the 3D beam-field-amplitude distribution in the 3D space (x, y, z). Even for a special case of circular polarization of an incident beam, different approximate methods, based on analysis of internal spin effect [8], stationary-phase method [9] or energy-flux conservation treatment [10-11], have been developed. However, results of one method applied to this problem have appeared at variance with the findings of another method, with complete explanation of these facts apparently still not available [8-12].

The reports [2-7] treat beams, in principle, in a similar rigorous manner, essentially related to the stationary-phase method, although other techniques of the methods of moments [2] or nonlinear self-focusing [7] were also applied. Beams with two mutually perpendicular meridional planes of symmetry are considered. The electric field vectors of the incident, reflected and/or refracted beams are decomposed into orthogonal, linearly or circularly polarised states. The solution is obtained in a form of angular spectral decomposition into plane waves and further interpreted in terms of effects of nonspecular (nsp) reflection and refraction of the first and, as in Refs. [5] and [7], second order.

In general, however, beam modifications upon reflection/transmission are of astigmatic nature; they are different for TM and TE beam field components. The questions hence arise: what actually are the total beam deformations, that is for example spatial shifts of the beam axis or spectral shifts of the beam spectrum, and, certainly, what are actual polarization states of 3D beams reflected and transmitted at the interface? Answers to these are essential not only for beams but also for pulses and wave packets upon reflection or transmission [13].

This chapter presents an attempt to answer these questions. The idea of this novel approach is to replace TM and TE polarization vectors in beam field decomposition by another basis formed directly by the Jones vectors specific to the incident, reflected and transmitted beams. An exact solution to the problem is given, that follows the results obtained previously for the 3D beam reflection [5, 7], and further interpreted in terms of first-order optics [14-15] of 3D beams. This solution obtained in the TM-TE representation can be then reformulated in the interface plane in a form independent of the beam field redistribution between its TM and TE components.

The conventional solution to beam reflection and transmission is presented in Section 2 and the first order beam deformations are discussed in Section 3. That provides all details necessary to introduce the amplitude-polarization representation of 3D beams. Results are given in Section 4 and summarised in Section 5, where quantitative discrepancies between earlier predictions of transverse spatial shifts of beams are also briefly commented on.

5.2 Beam fields at a dielectric interface - an exact solution

The solution presented in this chapter for the problem of 3D beam reflection was devised in Ref. [5] and discussed in Ref. [7], where examples of numerical simulations were also given. That was presented in Chapter 3. In this section those results are summarised to establish the notation, point out their main characteristics and explicitly show that the solution obtained previously for beam reflection [5,7] yields also the entire solution for beam refraction. Both solutions are interrelated through the beam field continuity relations in the interface plane, in which all the derivations of this work will be made.

Let us consider monochromatic optical 3D beam fields near the plane boundary $X = 0$, i.e. the interface between two dielectric homogeneous and isotropic media with different refractive indices n_i and n_t, respectively (cf. Fig. 5.1). The 2D vectors $\underline{E}^{(b)} \equiv \underline{E}^{(b)}(X,Y,Z)$, composed of the incident (b=i), reflected (b=r) or transmitted (b=t) electric field parallel to the interface $\underline{E}^{(b)} = [\pm E_Z^{(b)}, E_Y^{(b)}]$ (see their definitions in Eqs. (5.3)), are expressed in terms of the angular plane-wave (spatial) spectra:

$$\begin{aligned} &\underline{E}^{(b)}(X,Y,Z) \\ &= (2\pi)^{-2} \iint \underline{\widetilde{E}}^{(b)}(k_Z,k_Y) \exp[i(\pm k_X^{(b)} X + k_Y Y + k_Z Z)]\, dk_Z dk_Y \,, \end{aligned} \tag{5.1}$$

with $\exp(-i\omega t)$ time-dependence assumed and suppressed. In Eq. (5.1) the upper (lower) sign in the exponent is attributed to the reflected (incident and refracted) beam. The integration is performed along the wave-vector components k_Z and k_Y parallel to the interface. By the dispersion relation $k_X^{(b)2} + k_Y^2 + k_Z^2 = k^{(b)2}$, the representation (5.1) is equivalent to that used in Ref. [7], with the integration given in the $(k_X^{(b)}, k_Y)$ plane. The representation

(5.1) seems more suitable for treatment of the details of the beam transmission close to the normal incidence, whereas its counterpart in Ref. [7] is more appropriate in analysing the beam deflection and refraction near the grazing incidence. Nevertheless, the reflection and transmission coefficients should take the same form in both cases.

The wave vector components:

$$k_X^{(b)} = k^{(b)} c_X^{(b)},$$

$$k_Y = k s_X s_Y,$$

$$k_Z = k s_X c_Y, \tag{5.2}$$

$c_X^{(t)} = (1 - s_X^2 / s_c^2)^{1/2}$, are further expressed by sines s_X and s_Y and cosines c_X and c_Y of the polar $\vartheta_X \equiv \vartheta_X^{(i)}$ and azimuthal $\vartheta_Y \equiv \vartheta_Y^{(i)}$ incidence angles of the incident beam axis direction, measured in the incidence (X, Z) and interface (Y, Z) planes, respectively. The direction of the incident beam axis is specified in the incidence plane $\vartheta_Y = 0$ by $\vartheta_X = \vartheta_{X0}$ or $s_X = s_{X0}$ and $c_X = c_{X0}$. The upper (incidence or ambient) medium is presumed to be homogeneous and linear, what ensures equality of wave numbers $k^{(r)} = k^{(i)} \equiv k$. Hence $\vartheta_X^{(r)} = \vartheta_X$, $\vartheta_Y^{(r)} = \vartheta_Y$ and $c_X^{(r)} = c_X^{(i)} \equiv c_X$. For the critical incidence of total internal reflection (TIR) $\vartheta_X = \vartheta_c$ and $s_X = s_c = k^{(t)} / k$.

Let us decompose the field vectors $\underline{\widetilde{E}}^{(b)} \equiv \underline{\widetilde{E}}^{(b)}(k_Z, k_Y)$ into orthogonal linearly polarised parts,

$$\underline{\widetilde{E}}^{(i)} = -\widetilde{E}_Z^{(i)} \underline{e}_Z + \widetilde{E}_Y^{(i)} \underline{e}_Y,$$

$$\underline{\widetilde{E}}^{(r)} = +\widetilde{E}_Z^{(r)} \underline{e}_Z + \widetilde{E}_Y^{(r)} \underline{e}_Y,$$

$$\underline{\widetilde{E}}^{(t)} = -\widetilde{E}_Z^{(t)} \underline{e}_Z + \widetilde{E}_Y^{(t)} \underline{e}_Y, \tag{5.3}$$

$\widetilde{E}_Z^{(b)} \equiv \widetilde{E}_Z^{(b)}(k_Z, k_Y)$ and $\widetilde{E}_Y^{(b)} \equiv \widetilde{E}_Y^{(b)}(k_Z, k_Y)$, where $\underline{e}_Z = [1,0]$ and $\underline{e}_Y = [0,1]$ are polarization vectors in the direction of the Z-axis and the X-axis in the interface plane, respectively. Then, through rotation of the local coordinate

frame between the planes $s_Y = \text{constant}$ and $s_Y = 0$ [5], we are able to relate the reflected and incident beam field components by the following matrix of 3D beam reflection [5, 7]:

$$\begin{bmatrix} \widetilde{E}_Z^{(r)} \\ \widetilde{E}_Y^{(r)} \end{bmatrix} = \begin{bmatrix} r_{\parallel} & 0 \\ 0 & r_{\perp} \end{bmatrix} \begin{bmatrix} -\widetilde{E}_Z^{(i)} \\ \widetilde{E}_Y^{(i)} \end{bmatrix}. \tag{5.4}$$

In Eq. (5.4) the TM and TE beam reflection coefficients $r_{\parallel}$ and $r_{\perp}$ are the common (p) and (s) Fresnel coefficients r_p and r_s, augmented by the additional transverse, i.e. proportional to s_Y and/or s_Y^2, components [5,7]:

$$r_{\parallel} = r_p + \Delta r_{\parallel},$$

$$r_{\perp} = r_s + \Delta r_{\perp}, \tag{5.5}$$

$$\Delta r_{\parallel} = -s_Y (r_p + r_s)(s_Y + c_Y / \widetilde{\chi}^{(i)}),$$

$$\Delta r_{\perp} = -s_Y (r_p + r_s)(s_Y - c_Y \widetilde{\chi}^{(i)}). \tag{5.6}$$

The coupling between $\widetilde{E}_Z^{(b)}$ and $\widetilde{E}_Y^{(b)}$ is introduced in Equation (5.6) by the spectral polarization parameters:

$$\widetilde{\chi}^{(i)} = -\widetilde{E}_Z^{(i)} / \widetilde{E}_Y^{(i)},$$

$$\widetilde{\chi}^{(r)} = +\widetilde{E}_Z^{(r)} / \widetilde{E}_Y^{(r)},$$

$$\widetilde{\chi}^{(t)} = -\widetilde{E}_Z^{(t)} / \widetilde{E}_Y^{(t)}, \tag{5.7}$$

defined in the interface plane $X = 0$, contrary to the conventional definition of the complex polarization parameters given in planes $z = 0$ transverse to the beam axes [16]. The detailed derivation of Eqs. (5.4)-(5.7) is given in Chapter 7.

Since the incident beam is considered as given, Eqs. (5.1)-(5.7) determine completely and exactly not only the reflected field but also *the total field* and hence the transmitted beam field at the interface as well. Indeed, the continuity relations of the electric field components $\widetilde{E}_Z^{(b)}$ and $\widetilde{E}_Y^{(b)}$ at the inter-face together with Eqs. (5.1)-(5.7), readily lead to the following transmission matrix:

$$\begin{bmatrix} -\widetilde{E}_Z^{(t)} \\ \widetilde{E}_Y^{(t)} \end{bmatrix} = \begin{bmatrix} t_Z & 0 \\ 0 & t_\perp \end{bmatrix} \begin{bmatrix} -\widetilde{E}_Z^{(i)} \\ \widetilde{E}_Y^{(i)} \end{bmatrix}, \tag{5.8}$$

$$t_Z = 1 - r_\parallel = t_\parallel c_X^{(t)} / c_X^{(i)},$$

$$t_\perp = 1 + r_\perp . \tag{5.9}$$

The transmission coefficients t_Z and $t_\perp$ are evaluated for field components parallel to the interface plane and the coefficient $t_\parallel$ is determined by the field scaling [5,7], as shown below by Equations (5.12) and (5.13).

The reflection and transmission matrices (5.4) and (5.8) are given in the diagonal form. The coupling between field components is introduced into the reflection and transmission coefficients $r_\parallel$, $r_\perp$, t_Z and $t_\perp$ by the polarization parameters $\widetilde{\chi}^{(b)}$. In the incidence plane (here at $Y = 0$) these coefficients resolve into r_p, r_s, $t_{Z0} = 1 - r_p = t_p c_X^{(t)} / c_X^{(i)}$ and $t_s = 1 + r_s$, the field coupling disappears and the reflection/transmission 3D problem can be then treated as a pair of 2D scalar problems for two independent TM and TE polarization states. However, for the incidence oblique to the incidence plane, both problems of plane wave reflection and refraction are inherently of 3D nature. In effect, for beams of finite spatial spectrum upon reflection and transmission, the first-order and the second-order, transverse and longitudinal effects of beam deformations, in general exist even in the incidence plane (cf. the next Section).

The normal mode solutions, that is solutions to the equation

$$\underline{\widetilde{E}}^{(r)} = r_\parallel \underline{\widetilde{E}}^{(i)} = r_\perp \underline{\widetilde{E}}^{(i)}, \tag{5.10}$$

for which the state of polarization of the incident beam is unchanged on reflection, have especially interesting characteristics. They exist at the critical incidence of TIR, i.e. for $r_p = r_s$, and for the beam polarization states $\widetilde{\chi}^{(i)} = \mp i$ circular in the interface plane - not for the circular polarization states $\widetilde{\chi}^{(i)} / c_X^{(i)} = \mp i$, commonly defined in the plane transverse to the beam propagation direction. Per analogy to Eq. (5.10) written for reflection, we can also write for transmission:

$$\underline{\widetilde{E}}^{(t)} = t_{\perp}\underline{\widetilde{E}}^{(i)},$$

$$t_Z\underline{\widetilde{E}}^{(i)} = 0. \tag{5.11}$$

Since the a Z-component of the total field equals zero at the critical incidence, a normal mode solution for transmission still exists but trivially, only in the TE polarization state. We will refer to special features of these polarization states in the next sections of this chapter.

The exact solution to the beam reflection/transmission problem is described by Eqs. (5.1)-(5.9). Some link, however, to notions of paraxial optics would be useful. To this end we scale the beam field vectors:

$$\widetilde{E}_{\parallel}^{(i)} = -\widetilde{E}_Z^{(i)}/c_X^{(i)},$$

$$\widetilde{E}_{\parallel}^{(r)} = +\widetilde{E}_Z^{(r)}/c_X^{(r)},$$

$$\widetilde{E}_{\parallel}^{(t)} = -\widetilde{E}_Z^{(t)}/c_X^{(t)}, \tag{5.12}$$

and polarization parameters:

$$\chi^{(b)} = \widetilde{\chi}^{(b)}/c_X^{(b)}, \tag{5.13}$$

where $\widetilde{E}_{\perp}^{(b)} \equiv \widetilde{E}_Y^{(b)} \equiv \widetilde{E}_y^{(b)}$. The relation between the coefficients t_Z and $t_{\parallel}$ was already given in Eqs. (5.9). Next, let us substitute Eqs. (5.12)-(5.13) to Eqs. (5.4) and (5.8). The scaling (5.12)-(5.13) does not change the reflection coefficients in the scaled reflection matrix equation [5,7]:

$$\begin{bmatrix} \widetilde{E}_{\parallel}^{(r)} \\ \widetilde{E}_{\perp}^{(r)} \end{bmatrix} = \begin{bmatrix} r_{\parallel} & 0 \\ 0 & r_{\perp} \end{bmatrix} \begin{bmatrix} \widetilde{E}_{\parallel}^{(i)} \\ \widetilde{E}_{\perp}^{(i)} \end{bmatrix}, \tag{5.14}$$

whereas, in the scaled transmission matrix equation

$$\begin{bmatrix} \widetilde{E}_{\parallel}^{(t)} \\ \widetilde{E}_{\perp}^{(t)} \end{bmatrix} = \begin{bmatrix} t_{\parallel} & 0 \\ 0 & t_{\perp} \end{bmatrix} \begin{bmatrix} \widetilde{E}_{\parallel}^{(i)} \\ \widetilde{E}_{\perp}^{(i)} \end{bmatrix}, \tag{5.15}$$

the coefficient t_Z is rescaled to $t_{\parallel}$ according to the relations (5.9).

Equations (5.14)-(5.15) still remain exact. The electric field in these equations, as well as in Eqs. (5.4) and (5.8), complies with a complete set of the source-free Maxwell's equations, where the Gauss's law yields the remaining field components $\widetilde{E}_X^{(b)}$. The field continuity relations (5.9), together with the spectral representation (5.1) of the beam fields, make the beam refraction, as given by Eqs. (5.8) or (5.15), consistent with the beam reflection, determined by Eqs. (5.4) or (5.14). In other words, the relations (5.9) are fulfilled simultaneously and exactly by all the spectral components of the beam fields in the interface plane. Note that in our notation $\widetilde{E}_{\|}^{(b)}$ is still only the $\widetilde{E}_Z^{(b)}$ component of a single plane wave scaled by $c_X^{(b)}$ in its local incidence plane (cf. [5]). The TM field component of the total beam is obtained by scaling the Z-component of the total beam by $c_{X0}^{(b)}$, that is by $c_X^{(b)}$ evaluated at the principal incidence plane at the beam axis.

Certainly, in planes (x,y) transverse to the beam axes directions (cf. Fig. 5.1), Eqs. (5.14)-(5.15) also preserve their form in the paraxial approximation, with the transverse field decomposition into TM and TE components $\widetilde{E}_{\|}^{(b)}$ and $\widetilde{E}_{\perp}^{(b)}$, respectively:

$$\underline{\widetilde{E}}_T{}^{(b)} = \widetilde{E}_{\|}^{(b)} \underline{e}_{\|} + \widetilde{E}_{\perp}^{(b)} \underline{e}_{\perp}, \tag{5.16}$$

where $\underline{e}_{\|} = [1,0]$ and $\underline{e}_{\perp} = [0,1]$ are polarization vectors defined in planes $z = const.$ of transverse cross-sections of the beams. Now, in the beam frames (x,y,z), the beam spectral representation takes the form [5,7]:

$$\begin{aligned} &\underline{E}_T^{(b)}(x,y,z) = \exp(ik^{(b)}z) \\ &\times(2\pi)^{-2} \iint \underline{\widetilde{E}}_T^{(b)}(k_x,k_y) \exp[i((k_z^{(b)} - k^{(b)})z + k_y y + k_x x)]\, dk_x dk_y , \end{aligned} \tag{5.17}$$

adequate for both, exact and approximate (paraxial), modes of the analysis. In Eq. (5.17), as well as in Fig. 5.1, x-axes and y-axes point in the directions of the respective TM and TE beam field components for the incidence angles within the range between the Brewster angle and the critical angle. Note different meanings of the scaled ||, ⊥ and transversal TM, TE indicators in the notation assumed in this chapter; ||≡TM and ⊥≡TE only in the paraxial approximation. Still, for simplicity, we shall use these names interchangeably even for exact beam fields.

The factor $\exp(ik^{(b)}z)$ in Eq. (5.17) and its projection $\exp(iks_{X0}Z)$ on the interface plane represent a contribution of a central ray of the beam to an on-axis phase of this beam. These factors will be irrelevant in further analysis, that is, each beam profile will be evaluated in the plane $Z=0$ transverse to the Z-axis. Therefore, the beam fields $\underline{E}^{(b)}$ and the wave vector component $k_Z = ks_X c_Y$ in the representation (5.1)-(5.2) will be hereinafter replaced by $\underline{E}^{(b)}\exp(-iks_{X0}Z)$ and $k_Z = ks_X c_Y - ks_{X0}$, respectively.

The analysis of the 3D beam reflection and transmission problem was recently reported in the interesting contribution [6]. For the beam reflection, those results (Eqs. (13) in [6]) agree with the results given previously by Eqs. (17) in [5] or more recently by Eqs. (3)-(5) in [7] and Eqs. (5.4)-(5.7) in this chapter. For beam transmission, however, Eqs. (12) in [6] differ from Eqs. (5.8)-(5.9), together with (5.5)-(5.7) in this chapter. The method of analysis applied in this work is different from the method presented in Ref. [6].

5.3 First-order optics of beam reflection and refraction

The transformations (5.14) and (5.15) provide a convenient basis for direct interpretation of the beam distortions in terms of the effects of nsp reflection/transmission [5,7]. The reflection $r_\parallel$, $r_\perp$ and transmission $t_\parallel$, $t_\perp$ coefficients depend on the polar $\vartheta_X^{(i)}$ and azimuthal $\vartheta_Y^{(i)}$ incidence angles. An antisymmetric part of this dependence contributes to the first-order effects of nsp reflection/transmission, whereas a symmetric part, besides the geometric optic (g-o) predictions for beams, results in the second-order effects of nsp reflection/transmission. Both types of these effects exist in the incidence plane $Y=0$ (longitudinal effects) and in the transverse plane $Z=0$ (transverse effects) for beams of a finite spatial spectrum [5, 7]. Whereas the longitudinal effects are well known in 2D problems (see e.g. a list of references in [5]), the transverse effects are not. They are inherent only in 3D beams and disappear in 2D geometries.

A complete discussion of the first-order and the second-order effects of the 3D beam nsp reflection was given in Ref. [7], as well as in Chapter 3 of this book. For the purpose of further analysis, we will give below only basic relations of the first-order nsp effects, including also the case of refraction. These effects are derived in this chapter in the interface plane $X=0$ (cf.

[16]), instead of the usual procedures applied in planes $z = 0$ transverse to the beam axis direction [1-5].

The beam distortions upon reflection can be found by approximation of the reflection r_a (a=||, ⊥) and transmission coefficients t_Z and $t_\perp$, around a beam axis direction. Their values r_{a0}, t_{Z0} and $t_{\perp 0}$ are predicted by geometrical optics at the beam axis, that is they resolve into the Fresnel coefficients evaluated for $\vartheta_X^{(i)} = \vartheta_{X0}^{(i)}$ and $\vartheta_Y^{(i)} = 0$. Introduction of the complex displacements $L_{ax}^{(r)} / c_{X0}^{(r)}$, $L_{ax}^{(t)} / c_{X0}^{(t)}$, $L_{aY}^{(r)}$ and $L_{aY}^{(t)}$; a=||, ⊥, along the interface as eigenvalues of the differential equations

$$i(\partial/\partial k_Z)\ln r_a = L_{ax}^{(r)} / c_{X0}^{(r)},$$

$$i(\partial/\partial k_Z)\ln(-t_Z) = L_{\|x}^{(t)} / c_{X0}^{(t)},$$

$$i(\partial/\partial k_Z)\ln t_\perp = L_{\perp x}^{(t)} / c_{X0}^{(t)}, \tag{5.18}$$

specific to the beam longitudinal deformations (in the plane $Y = 0$), and the equations

$$i(\partial/\partial k_Y)\ln r_a = L_{ay}^{(r)},$$

$$i(\partial/\partial k_Y)\ln(-t_Z) = L_{\|y}^{(t)},$$

$$i(\partial/\partial k_Y)\ln t_\perp = L_{\perp y}^{(t)}, \tag{5.19}$$

specific to the beam transverse deformations (in the plane $Z = 0$), yields the first-order approximation of the beam reflection coefficients:

$$r_a \cong r_{a0} \exp\left[-i(k_Z L_{ax}^{(r)} / c_{X0}^{(r)} + k_Y L_{ay}^{(r)})\right],$$

$$t_Z \cong t_{Z0} \exp\left[-i(k_Z L_{\|x}^{(t)} / c_{X0}^{(t)} + k_Y L_{\|y}^{(t)})\right],$$

$$t_\perp \cong t_{\perp 0} \exp\left[-i(k_Z L_{\perp x}^{(t)} / c_{X0}^{(t)} + k_Y L_{\perp y}^{(t)})\right]. \tag{5.20}$$

From the definition all derivatives, and thus the complex shifts, are evaluated at the beam axes. The subscripts (small) x and y in Eqs. (5.18)-(5.20) indicate that the beam shifts are directed along x- and y-axes of the

beams (cf. Fig. 5.1). For beam transmission, the shifts are determined entirely by their counterparts for reflection and the continuity relations (5.9) in the interface plane. The generators of the beam complex displacements in Eqs. (5.18) and (5.19), as well as the coefficients r_a, t_Z and $t_\perp$, depend explicitly on the wave vector components k_Z and k_Y parallel to the interface plane. Hence, besides their evaluation at the beam axes, no further approximation is needed in evaluating these displacements from Eqs. (5.18)-(5.19); cf. also the Appendix in [7] and in Chapter 3.

The definitions (5.18)-(5.20) lead to the interpretation of the beam distortions in terms of the beam axis and spectrum displacements from their g-o predictions. The beams are displaced: by real spatial $\delta_{ax}^{(r)}$, $\delta_{ax}^{(t)}$ and spectral $k\varepsilon_{ax}^{(r)}$, $k\varepsilon_{ax}^{(t)}$ shifts in the phase space (x,k_x), that is by longitudinal shifts in the plane of incidence $y=0$, and by real spatial $\delta_{ay}^{(r)}$, $\delta_{ay}^{(t)}$ and spectral $k\varepsilon_{ay}^{(r)}$, $k\varepsilon_{ay}^{(t)}$ shifts in the phase space (y,k_y), that is by transverse shifts in the plane $x=0$ transverse to the incidence plane. That means, for example, for the TM component of the reflected beam: $(x,k_x)\to(x-\delta_{\|x}^{(r)},k_x-k\varepsilon_{\|x}^{(r)})$ for the longitudinal shifts and, by analogy, $(y,k_y)\to(y-\delta_{\|y}^{(r)},k_y-k\varepsilon_{\|y}^{(r)})$ for the transverse shifts. The shifts are in the position and direction (momentum) coordinate frame (x,y,k_x,k_y).

For fundamental Gaussian beams, i.e. for beams with minimal quality factors [15], and for a propagation distance z normalised to diffraction lengths z_{D_x} and z_{D_y} in planes $y=0$ and $x=0$, respectively, real and imaginary parts of the complex shifts define real, spatial and spectral, shifts of the 3D beams for reflection [5,7] and refraction. They read in the incidence plane $y=0$:

$$L_{ax}^{(r)}=\delta_{ax}^{(r)}+iz_{D_x}\varepsilon_{ax}^{(r)},$$

$$L_{ax}^{(t)}=\delta_{ax}^{(t)}+iz_{D_x}\varepsilon_{ax}^{(t)}, \tag{5.21}$$

and in the transverse plane $x=0$:

$$L_{ay}^{(r)}=\delta_{ay}^{(r)}+iz_{D_y}\varepsilon_{ay}^{(r)},$$

$$L_{ay}^{(t)} = \delta_{ay}^{(t)} + iz_{D_y}\varepsilon_{ay}^{(t)} \ , \tag{5.22}$$

where $\varepsilon_{ax}^{(r)}$, $\varepsilon_{ay}^{(r)}$ and $\varepsilon_{ax}^{(t)}$, $\varepsilon_{ay}^{(t)}$ are referred to as the angular shifts of beam axes and a=||, ⊥.

Explicit expressions for all complex shifts, in the incidence and transverse planes, are given for the beam reflection in the Appendix of Ref. [7] and of Chapter 3. A form of those expressions, by substitution of the reflection coefficients by their counterparts for transmission, is valid for beam transmission as well. These expressions remain valid for beams with arbitrary quality factors in their paraxial approximation. One can also directly observe from Eqs. (5.5)-(5.6) that, in contrast to the first-order transverse TE and TM shifts of the reflected/transmitted beam, the second-order transverse TE and TM shifts and all the longitudinal TE and TM shifts do not depend on the incident beam polarization parameter $\tilde{\chi}^{(i)}$. In the dimensionless version of the phase space, the shifts are normalised [7] to characteristic beam diameters w_{x0} and w_{y0}, e.g. in the phase space (x/w_{x0}, $k_x w_{x0}$) the spatial and spectral shifts take the form $\delta_{ax}^{(t)}/w_{x0}$ and $kw_{x0}\varepsilon_{ax}^{(r)}$, $kw_{x0}\varepsilon_{ax}^{(t)}$, respectively, where $kw_{0x} = z_{Dx}/w_{x0}$. The same applies to the transverse shifts with the subscript x replaced by y. For the 2D Gaussian beam $\exp(-\frac{1}{2}x^2/w_{x0}^2)$ at its waist, the beam half-width w_{0x} means the beam half-width at 1/e-maximum of beam power.

Let us briefly refer to the case of the normal mode solutions (5.10) to the beam reflection of the in-plane-of-interface circular polarization states $\tilde{\chi}^{(i)} = \mp i$. Such modes suffer from spatial and spectral shifts of equal magnitude in both the left-handed and right-handed circular polarization states, in contrast to the linear in-plane-of-interface diagonal polarization states $\tilde{\chi}^{(i)} = \pm 1$, for which these first-order shifts are of opposite signs. Certainly, no such symmetry is observed for the common diagonal, linear $\tilde{\chi}^{(i)}/c_{X0}^{(i)} = \pm 1$ or circular $\tilde{\chi}^{(i)}/c_{X0}^{(i)} = \mp i$, polarization states, defined in transverse planes of the beams.

5.4 Amplitude-polarization decomposition of beam fields

The solution of the reflection/transmission problem presented in Sections 2 and 3 is unique. Its form, however, depends on a polarization basis chosen for the beam field decomposition. The field decompositions (5.3) and (5.16) in a 2D vector (complex) space spanned by base vectors of TM and TE polarization, follow the intuition borrowed from the 2D analysis and in the 3D case is by no means unique. What we actually need in the 3D case, besides geometrical characteristics of the 3D beam like a beam waist position and its axis direction, is to know the (complex) amplitude and polarization of the beam, the latter being described by the (complex) polarization parameters $\widetilde{\chi}^{(b)}$ or $\widetilde{\chi}^{(b)}/c_{X0}^{(b)}$.

It seems suitable to describe the incident (b=i), reflected (b=r) and transmitted (b=t) beams in vector spaces spanned by two base orthonornal vectors, in which one of them is directly the Jones polarization vector $\underline{s}^{(b)}$ specific to the respective beam [5,7], that is:

$$\underline{\widetilde{E}}^{(b)} = \widetilde{E}^{(b)} \, | \underline{e}^{(b)} | \, \underline{s}^{(b)}, \tag{5.23}$$

$$\underline{s}^{(b)} \equiv \underline{s}^{(b)}(\widetilde{\chi}^{(b)}) = \underline{e}^{(b)} / | \underline{e}^{(b)} |, \tag{5.24}$$

$$\underline{e}^{(b)} \equiv \underline{e}(\widetilde{\chi}^{(b)}) = \begin{bmatrix} (\widetilde{\chi}^{(b)})^{+1/2} \\ (\widetilde{\chi}^{(b)})^{-1/2} \end{bmatrix}, \tag{5.25}$$

where $\underline{e}^{(b)}$ is an unnormalised Jones vector and $\widetilde{E}^{(b)}$ stands for the unnormalised amplitude of the beam:

$$\widetilde{E}^{(b)} = \left(\widetilde{E}_Z^{(b)} \widetilde{E}_Y^{(b)} \right)^{+1/2}. \tag{5.26}$$

The normalisation factor $| \underline{e}^{(b)} | = (| \widetilde{\chi}^{(b)} | + | \widetilde{\chi}^{(b)} |^{-1})^{+1/2}$ does not contain more information about the beam polarization than the vector $\underline{e}^{(b)}$. Thus, in what follows we use, instead of Eq. (5.23), the more suitable beam representation

$$\underline{\widetilde{E}}^{(b)} = \widetilde{E}^{(b)} \underline{e}^{(b)} = \left(\widetilde{E}_Z^{(b)} \widetilde{E}_Y^{(b)} \right)^{+1/2} \begin{bmatrix} (\widetilde{\chi}^{(b)})^{+1/2} \\ (\widetilde{\chi}^{(b)})^{-1/2} \end{bmatrix}, \tag{5.27}$$

with unnormalised polarization vector $\underline{e}^{(b)}$ defined in the interface plane. In the presented formalism the beam field is determined exactly but its factorisation into the amplitude and polarization factors depends on our choice. Note that the reflection and transmission matrices [7] are also dependent on this factorisation. Here, from all possible beam field representations, the representation (5.27) implies the following diagonal and unimodular form of two matrices of beam reflection and transmission:

$$\begin{bmatrix} (\widetilde{\chi}^{(r)})^{+1/2} \\ (\widetilde{\chi}^{(r)})^{-1/2} \end{bmatrix} = \begin{bmatrix} r^{+1/2} & 0 \\ 0 & r^{-1/2} \end{bmatrix} \begin{bmatrix} (\widetilde{\chi}^{(i)})^{+1/2} \\ (\widetilde{\chi}^{(i)})^{-1/2} \end{bmatrix}, \tag{5.28}$$

$$\begin{bmatrix} (\widetilde{\chi}^{(t)})^{+1/2} \\ (\widetilde{\chi}^{(t)})^{-1/2} \end{bmatrix} = \begin{bmatrix} t^{+1/2} & 0 \\ 0 & t^{-1/2} \end{bmatrix} \begin{bmatrix} (\widetilde{\chi}^{(i)})^{+1/2} \\ (\widetilde{\chi}^{(i)})^{-1/2} \end{bmatrix}, \tag{5.29}$$

respectively, where $r = r_{\parallel}/r_{\perp}$, $t = t_Z/t_{\perp}$ and, in addition, the matrix of reflection becomes unitary for TIR. The same matrices are given, by substituting $\widetilde{\chi}^{(b)}$ by $\widetilde{\chi}^{(b)}/c_{X0}^{(i)}$ and t_Z by $t_{\parallel}$ in Eqs. (5.30)-(5.31), for the conventional definitions of the beam polarization (5.13) and the definition of the beam complex amplitude $\widetilde{E}^{(b)} = (\widetilde{E}_{\parallel}^{(b)} \widetilde{E}_{\perp}^{(b)})^{1/2}$, adequate to this case. The matrices in Eqs. (5.28)-(5.29) seem particularly suitable for description of the reflection/transmission problem in terms of the scattering matrix of the interface.

The relations (5.25)-(5.29) reduce the beam reflection/transmission problem to the following scalar relations for beam amplitude and polarization parameters of the beams:

$$\widetilde{E}^{(r)} = \left(r_{\parallel} r_{\perp}\right)^{1/2} \widetilde{E}^{(i)},$$

$$\widetilde{E}^{(t)} = \left(t_Z t_{\perp}\right)^{1/2} \widetilde{E}^{(i)}, \tag{5.30}$$

$$\widetilde{\chi}^{(r)} = (r_{\parallel}/r_{\perp})\widetilde{\chi}^{(i)},$$

$$\widetilde{\chi}^{(t)} = (t_Z/t_{\perp})\widetilde{\chi}^{(i)}. \tag{5.31}$$

The beam amplitude modifications (5.30) are now determined by a geometrical mean of the TM and TE reflection/transmission coefficients, while the

beam polarization changes are specified by the quotient of these coefficients. This changes the common meaning of the effects of nsp reflection and transmission of the 3D beams. They are now directly specified by the beam field factorisation (5.25)-(5.27), instead of the conventional beam field decomposition (5.16). The derivation of definitions of these effects, as given in the next section, is a main result of this chapter.

5.5 New definitions of the nonspecular effects

The first-order effects of *the beam complex amplitude modifications*, that is the shifts of the beam axis and the spectrum centre upon reflection (b=r) and transmission (b=t), are now given by new complex shifts $L_c^{(b)}$, c=x,y, expressed by the sum of the conventional TM and TE complex shifts (5.21) and (5.22):

$$L_c^{(b)} = \tfrac{1}{2}(L_{\|c}^{(b)} + L_{\perp c}^{(b)}) = \delta_c^{(b)} + iz_{D_c}\varepsilon_c^{(b)}. \tag{5.32}$$

The shifts (5.32) modify the beam complex amplitudes $\widetilde{E}^{(b)}$ with respect to their g-o values $\widetilde{E}_0^{(b)}$:

$$\widetilde{E}^{(b)} \cong \widetilde{E}_0^{(b)} \exp\left[-i(k_Z L_x^{(b)}/c_{X0}^{(b)} + k_Y L_y^{(b)})\right], \tag{5.33}$$

$$\widetilde{E}_0^{(r)} = \left(r_{p0} r_{s0}\right)^{1/2} \widetilde{E}^{(i)}$$

$$\widetilde{E}_0^{(t)} = \left(t_{Z0} t_{s0}\right)^{1/2} \widetilde{E}^{(i)}. \tag{5.34}$$

Therefore, in the phase space (x, y, k_x, k_y), the beam axis upon reflection or transmission is displaced by the spatial shifts $\delta_c^{(b)}$ and the spectrum centre of the beam is shifted by the spectral shifts $k\varepsilon_c^{(b)}$. We obtain analogous expressions for the first-order effects of *the beam polarization modifications*:

$$\widetilde{\chi}^{(b)} \cong \widetilde{\chi}_0^{(b)} \exp\left[-2i(k_Z K_x^{(b)}/c_{X0}^{(b)} + k_Y K_y^{(b)})\right], \tag{5.35}$$

$$K_c^{(b)} = \tfrac{1}{2}(L_{\|c}^{(b)} - L_{\perp c}^{(b)}) = \kappa_c^{(b)} + iz_{D_x}\sigma_c^{(b)}, \tag{5.36}$$

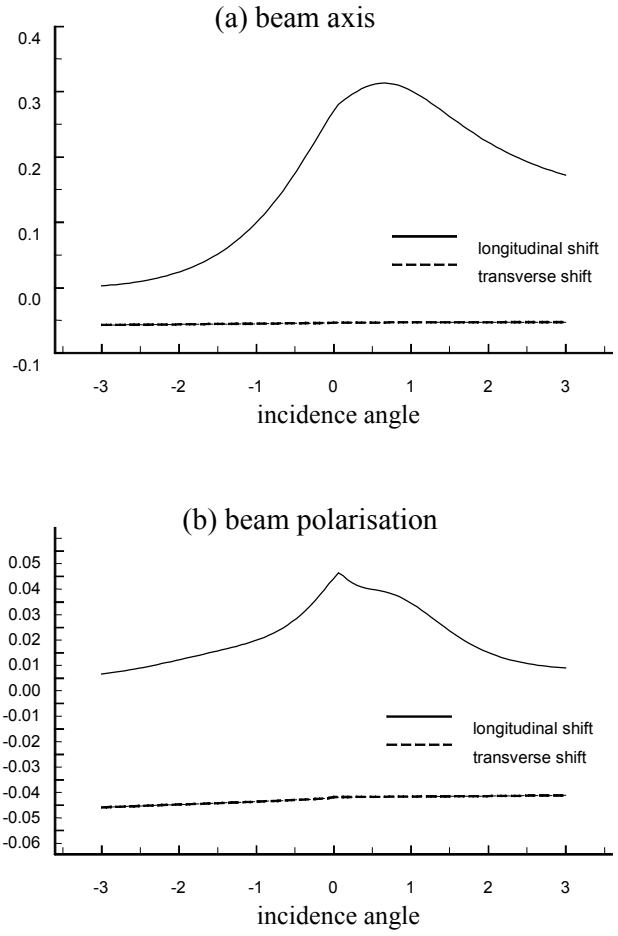

Figure 5.2. First-order longitudinal $L_x^{(r)}$ and transverse $L_y^{(r)}$ spatial shifts of the beam axis (a) and the longitudinal $K_x^{(r)}$ and transverse $K_y^{(r)}$ spatial shifts of the beam polarization (b) for reflection versus incidence angles $\vartheta_{X0} - \vartheta_c$ around the critical angle $\vartheta_c = 75^o$. The case of circular polarization of the incident beam $\chi^{(i)} = \tilde{\chi}^{(i)} / c_{X0}^{(i)} = i$, $\tilde{\chi}_0^{(r)} = (r_{p0} / r_{s0}) \tilde{\chi}^{(i)}$ and the normalised wave number $kw_0 2^{-1/2} = 80$. The shifts are normalised to the beam half-width.

$$\widetilde{\chi}_0^{(t)} = (t_{Z0}/t_{s0})\,\widetilde{\chi}^{(i)}, \tag{5.37}$$

with the new polarization complex shifts $K_c^{(b)}$, expressed by the difference between the conventional TM and TE complex shifts (5.21)-(5.22). Both the spatial $\kappa_c^{(b)}$ and spectral $k\sigma_c^{(b)}$ shifts contribute to the final polarization states and make them, in general, non- uniform through the beam spectrum. Note that both, the complex amplitudes and the complex polarization parameters of the reflected and transmitted beams, were evaluated in Eqs. (5.32)-(5.37) through the reflection and transmission coefficients evaluated at the beam axes, as indicated by the subscript "0" in Eqs. (5.34) and (5.37).

The definitions (5.18)-(5.19) of the effects of nsp reflection and transmission imply that magnitudes of these effects are independent of the shape and phase profile of beams. Note however that the approximations (5.20) remain accurate for paraxial beams, provided that the beams with profiles separable in x and y are considered and that the beam incidence is far from any discontinuity of the reflection/transmission coefficients [7]. Otherwise the beam field expansion should be used instead (see footnote 1 in [7] and the Appendix in Chapter 3) or, in the singular case of reflection at the critical incidence, the rigorous integration procedure that still yields convergent results should be applied (see [17] or Chapter 4). Moreover, the definitions (5.18)-(5.19) are only valid for non-vanishing values of the reflection/transmission coefficients. In the opposite case, like this of the beam of the TM polarization state impinging onto the interface at the Brewster angle, the beams attain profiles of higher-order modes and the analysis outlined in Section 5 of Ref. [7] or Chapter 3 becomes more appropriate.

An example of spatial shifts of the reflected beam axis position and the beam polarization state is given in Fig. 5.2, for the case of at and around the critical incidence of the fundamental Gaussian beam. A method of analytical and numerical evaluation of the shifted beam field from its integral representations (5.1) or (5.17), as described in Ref. [17] or Chapter 4, is used. That yields *finite* shifts of the reflected beam, even close to the critical angle of incidence. The beam shifts for the (conventional) circular polarization ($\chi^{(i)} = \widetilde{\chi}^{(i)}/c_{X0}^{(i)} = i$) of the incident fundamental Gaussian beam of cylindrical symmetry, incidence, the polarization effects are about one by order of

magnitude smaller than the amplitude effects and the transverse effects are about one order of magnitude less than longitudinal effects. All these effects are nonzero and finite both below and above the critical angle of incidence.

A polarization state of the beam can be also described, instead of the complex polarization parameter $\chi^{(b)} = \widetilde{\chi}^{(b)} / c_{X0}^{(i)}$, by the inclination $\varphi^{(b)}$ and elipticity $\theta^{(b)}$ angles of the polarization ellipse with the ellipticity $e^{(b)} = \tan\theta^{(b)}$ [16]:

$$\tan 2\varphi^{(b)} = 2\,\mathrm{Re}[\chi^{(b)}] \Big/ (\left|\chi^{(b)}\right|^2 - 1)\,, \tag{5.38}$$

$$\sin 2\theta^{(b)} = 2\,\mathrm{Im}[\chi^{(b)}] \Big/ (\left|\chi^{(b)}\right|^2 + 1)\,. \tag{5.39}$$

Modifications of the beam polarization are then expressed by changes of these angles with respect to their g-o predictions defined by Eq. (5.37), that is by real and imaginary parts of the complex polarization shifts $K_c^{(b)}$ or by the real shifts $\kappa_c^{(b)}$ and $k\sigma_c^{(b)}$; c=x, y, b=r, t. Both angles of a beam polarization ellipse projected onto the incidence plane are shown in Fig. 5.3 for the (conventional) circular $\chi^{(i)} = i$ and diagonal-linear $\chi^{(i)} = 1$ polarization states of the incident beam.

For moderate values of the incidence angle, the modifications of a beam polarization state are not substantial. Influence of transverse shifts on the beam polarization state is even much smaller and it seems that besides, perhaps, in some extreme cases, they can be considered as negligible. Note also that, for incidence angles less than the critical angle, the real parts of the polarization parameters are always zero. The azimuth angle of beam polarization equals $\pi/4$ and a phase shift difference between the TE and TM field components equals $\pi/2$ for the circular polarization of the incident beam. Only at the critical incidence the reflected beams remain exactly in the diagonal-circular or linear - polarization states.

It is gratifying to refer once more to the polarization states of the incident beam that are diagonal in the interface plane $X = 0$. In Eqs. (5.5)-(5.6) the first-order terms in k_Y are of opposite signs for TM and TE components of the incident beam field. Therefore, from the definitions (5.19), (5.32) and

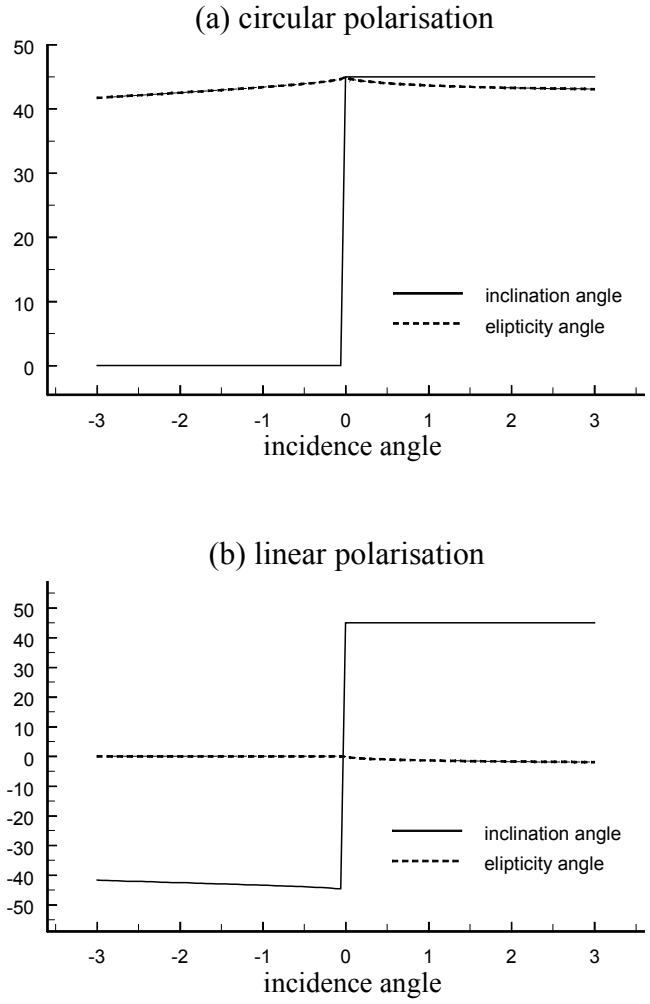

Figure 5.3. Inclination $\varphi^{(r)}$ and ellipticity $\theta^{(r)}$ angles (in degrees) of the reflected beam elliptic polarization state for the circular $\chi^{(i)} = \tilde{\chi}^{(i)} / c_{X0}^{(i)} = i$ (a) and the diagonal-linear $\chi^{(i)} = \tilde{\chi}^{(i)} / c_{X0}^{(i)} = 1$ (b) polarization states of the incident beam, versus incidence angles $\vartheta_{X0} - \vartheta_c$ around the critical angle $\vartheta_c = 75^o$; other beam and interface parameters are the same as in Fig. 5.2.

(5.36), it is evident that while the first-order transverse shifts $\delta_y^{(r)}$ and $k\varepsilon_y^{(r)}$ *of the beam axis and the beam spectrum* disappear for the incident diagonal-linear polarization states $\tilde{\chi}^{(i)} = \pm 1$, meanwhile the first-order transverse shifts $\kappa_y^{(r)}$ and $k\sigma_y^{(r)}$ *of the beam polarization* disappear for the incident diagonal-circular polarization states $\tilde{\chi}^{(i)} = \mp i$. Therefore, there are only transverse changes *of the beam polarization* in the linear diagonal polarization states $\tilde{\chi}^{(i)} = \pm 1$ of the incident beams, as well as there are only transverse shifts *of the beam axis and the beam spectrum* in the circular diagonal polarization states.

Note that the above statements are valid for the definitions of beam amplitude and beam polarization specified by the beam field factorisation (5.27), with the polarization vector defined in the interface plane. Within these definitions, the deformations of amplitudes of the reflected and transmitted beams can be measured for the incident beams of diagonal-circular polarization $\tilde{\chi}^{(i)} = \mp i$ independently of the beam polarization deformations, which are nil in these cases. Similarly, the deformations of polarization of the reflected and transmitted beams can be measured for the incident beams of diagonal-linear polarization $\tilde{\chi}^{(i)} = \pm 1$ independently of the beam shape deformations, which are nil in these cases.

The diagonal, circular, $\tilde{\chi}^{(i)} = \mp i$ and linear, $\tilde{\chi}^{(i)} = \pm 1$, polarization states defined in the interface plane seem to be fundamental polarization states for the reflection/transmission problem of 3D beams at the interface. In analysing this problem, these diagonal polarization states are more suitable than the linear TM, $\tilde{\chi}^{(i)} = \pm\infty$ and TE, $(\tilde{\chi}^{(i)})^{-1} = \pm\infty$ polarization states. Certainly, they are also more suitable than the TM, $\chi^{(i)} = \pm\infty$ and TE, $(\chi^{(i)})^{-1} = \pm\infty$ linear polarization states, conventionally defined in planes transverse to the beam propagation direction and commonly employed in the cases of 2D beams.

5.6 Comments and conclusions

Let us comment on a single but important case of TIR of circularly polarised beam at critical incidence. This case has been extensively investigated in the past. Different expressions for the transverse shifts of a beam

have been derived by several authors [8-12], using essentially two approaches: the first approach based on the energy-flux conservation arguments, the second one based on the stationary-phase or phase-shift arguments. Different results presented have been the subjects of many discussions and even a source of persistent controversies (see, for example, [3,11,18,19] and references herein). It seems nothing appears entirely definitive within the problems of this sort. As one of the authors: 'Despite the considerable volume of theoretical work on transverse shifts, and the considerations of this paper, the situation remains confused and the experimental background remains meagre' [18].

Observe that, for the case of the conventional circular polarization state $\chi^{(i)} = \tilde{\chi}^{(i)} / c_{X0}^{(i)} = \mp i$ and at the critical incidence, Eqs. (5.19) and (5.22) of this section yield the following spatial displacements for TM and TE beam field components (cf. also Eq. (A.3a) in Ref. [7] or Eqs. (A.3.4) in Chapter 3):

$$\delta_{\|y}^{(r)} = \pm 2k^{-1} / c_{X0} s_{X0}\,, \tag{5.40}$$

$$\delta_{\perp y}^{(r)} = \pm 2k^{-1} c_{X0} / s_{X0}\,. \tag{5.41}$$

It appears that the expressions suggested by Ricard [10] and Imbert [11] by the energy-flux conservation considerations agree with Eq. (5.40), whereas the formulae obtained by Schilling [9] by the stationary-phase analysis agrees with Eq. (5.41). The result given by Schilling seems consistent with our outcome since, at the interface, for the critical incidence of TIR and for wide beams, the Z-component of the total electric field essentially equals zero.

It is not the purpose of these considerations to dwell on the problem of differences between these two methods. This issue has been addressed e.g. in [18, 19]. It should be noted, however, that the energy-flux conservation method was devised, as many other methods, under a number of simplifications and approximations that may substantially deform a modelled physical picture of the reflection/transmission problem. In contrast to the above, the method presented here is exact, complete and self-contained. Besides the full set of Maxwell's equations and continuity relations at the interface, the method is determined only by the definition (5.27) of the beam

amplitude and polarization. The description of beams in terms of first-order shifts is also uniquely defined by generators of the spatial beam displacements (5.18) and (5.19). The method does not need to resort to the paraxial approximation and hence allows non-zero longitudinal beam field components as well. Therefore it is also suitable in treatments of very narrow/short (of the order of wavelength or/and period) beams, pulses and wave packets.

Moreover, results presented in this chapter yield *only one* transverse displacement $\delta_y^{(r)}$ of the beam axis, independent of the TM-TE field redistribution. For the conventional circular polarization, that is for $\chi^{(i)} = \mp i$, of the beam incident at TIR, the transverse shift has a form of the average of displacements of TM and TE field components:

$$\delta_y^{(r)} = \pm k^{-1}(1/c_{X0} + c_{X0})/s_{X0} . \tag{5.42}$$

At the same time, the beam polarization suffers from the additional real spatial modification $\kappa_y^{(r)}$, expressed by the difference of these displacements:

$$\kappa_y^{(r)} = \pm k^{-1}(1/c_{X0} - c_{X0})/s_{X0} . \tag{5.43}$$

Eq. (5.42) determines the shift of the reflected beam axis and Eq. (5.43) determines the additional correction to the ellipticity of the beam polarization, both of them specified with respect to the predictions of g-o optics. Note that these displacements, as well as all other first-order nsp effects, can be evaluated directly from their definitions (5.18)-(5.19) or from those given in [5,7], without any approximation, simultaneously for reflection and transmission.

It is also interesting to observe that all versions of the transverse shifts of the beam axis, as presented in (5.40)-(5.42) for the beam of conventional circular polarization $\chi^{(i)} = \mp i$ incident at the critical angle of TIR, are exactly equal to each other for the circular polarization $\widetilde{\chi}^{(i)} = \mp i$. However, they are defined here in the interface plane. For this type of incidence and incident beam (circular) polarization

$$\delta_{\|y}^{(r)} = \delta_{\perp y}^{(r)} = \delta_y^{(r)} = \pm 2k^{-1}/s_{X0} \tag{5.44}$$

and all different approaches mentioned above yield *exactly the same result*. Evidently, defining the beam polarization at the interface plane instead of the transverse plane of the beam, greatly simplifies the analysis of the problem and shows some more physics hidden behind just only formal definitions. We shall return to this observation in the last chapter of this book.

The above mentioned features of the presented solution distinguish this treatment from other, approximate approaches applied to such problems in the past (cf. [20] for refraction). It should be also emphasised here that the nonzero magnitudes of the transverse shifts in reflection and transmission, result directly from the *asymmetry* of the reflection (5.5) and transmission (5.9) coefficients with respect to their azimuthal variation (5.6) of the beam incidence [5,7]. It seems that this fact has been finally appreciated in the recent, still very approximate however, analysis of 3D beams at periodic structures (cf. [21] for reflection).

It is worthwhile to observe as well that an attempt to consider only a beam field magnitude, *instead of its magnitude and phase* or its Poynting vector, would make a quite fair range of the calculated *first-order transverse shifts simply equal zero*. In this case, the first-order shifts calculated for the critical incidence ($|r_p|=|r_s|$) and arbitrary polarization or for the elliptic polarization ($\mathrm{Re}(\tilde{\chi}^{(i)})=0$) and arbitrary incidence disappear. That follows directly from the explicit form of the first-order transverse (proportional to s_Y) terms in Eqs. (5.6), accounted for in the evaluation of the reflected beam field magnitude. For example, Eqs. (5.41)-(5.43) would yield in this case $\delta_{\|y}^{(r)}=0=\delta_{\perp y}^{(r)}$ and $\delta_{y}^{(r)}=0=\kappa_{y}^{(r)}$, respectively. In real physical situations most of *these shifts are not zero* and the considerations based only on the field magnitude are of limited use.

Several aspects of the solution presented were not discussed, mainly because of lack of space. The simplicity of the problem of the 3D beam interaction with the dielectric planar structures seems to be rather apparent. Relations to foundations of first-order optics [14,15,22,23] and analogies with elements of special relativity and quantum mechanics [23-25] can be found. Exactness and completeness of the solution presented may appear helpful in searching these relations.

Several aspects of the solution presented have not been discussed in this chapter. Relations to foundations of first-order optics [14,15,22,23] and analogies with elements of special relativity and quantum mechanics [23-25] can be found. To be more definite, the transformations (5.28)-(5.37), of the beam amplitude and polarization, are enumerated below in relation to the two-by-two spinor representation of the six-parameter Lorentz group described, for example, in [24].

The transformations (5.28) and (5.29) are the two-by-two unimodular matrix transformations of the (unnormalised) Jones polarization vectors (5.25). In general, for arbitrary complex values of the matrix elements r and t, these transformations are the 2D representations of the six-parameter Lorentz group. If r and t are real, partial transmission occurs and the transformations (5.28) and (5.29) become, in the terminology used in [24], the attenuator or squeeze transformations. For r being a complex quantity of unit amplitude, that is in the TIR case, the transformation (5.28) is analogous to the phase-shift transformation [24]. Furthermore, the transformations (5.28) and (5.29) are equivalent to the bilinear transformations also mentioned in [24], in the same manner as they are equivalent to the scalar transformations (5.31) and (5.37) of the polarization parameters $\tilde{\chi}^{(b)}$ introduced here. All these transformations yield the first-order shifts (5.36) for the *polarization states* (5.35) of the reflected/transmitted beams.

The remaining elements of the beam representation given in Section 4, that is the beam complex amplitudes (5.27), are referred to in [24] as the overall multiplication factors of the beam transformation matrices. These factors, or simply the beam complex amplitudes, are transformed according to Eqs. (5.30) and (5.34). That yields the first-order shifts (5.32) for the *complex amplitudes* (5.33) of the reflected/transmitted beams. Note that the same relations between the beam amplitude-polarization transformations (5.28)-(5.37) and the Lorentz group can be also obtained for the beam polarization (5.13) conventionally defined in planes transverse to beam axes. Still, there are other benefits of the presented formalism left to be indicated.

A similar list of transformations of *beam profile parameters*, like a beam width and its phase-front curvature [15] and *on-axis complex amplitude parameters*, like beam on-axis intensity and on-axis Gouy phase, can be spelled further in the context of the second-order beam shifts [5,7]. In analy-

sis of these second-order shifts, the lens-magnifier-rotation Iwasawa decomposition [14] of a ray-transfer matrix specified to the dielectric interface may appear particularly suitable.

Let us finally conclude that we have presented the new amplitude-polarization frame suitable for analysis of the 3D beam reflection and transmission. The solution to the reflection and transmission problem is given for beams at a dielectric interface, although the formalism can be extended to accommodate the cases of wavepackets [25], beams at dielectric stratified [23] and/or nonlinear [17] planar structures. Similar beams of other problems, like reflection/transmission of vortex, Laguerre-Gaussian or Bessel beams or, in general, beams with non-meridional symmetry [26], are also possible.

Explicit expressions for the first-order beam deformations are given in a form valid for the total beam field, not separately for the beam TM and TE field components. The amplitude effects, that is the beam axis and spectrum centre displacements, appear substantial and, in paraxial approximation, uniform in the beam spatial and spectral cross-sections. On the contrary, the polarization effects are much smaller, although generally non-uniform through the entire beam spectrum. In the latter context, a special role of the beam modes of diagonal polarization in the interface plane was indicated.

Main content of this chapter has been published in Journal of Optics A: Pure and Applied Optics ***5****, 128-136 (2003).*

References

[1] J. Picht, “Beitrag zur Theorie der total Reflection”, Ann. Phys. Leipzig **5**, 433-496 (1929).

[2] J. P. Hugonin and R. Petit, “Étude générale des déplacements à la réflexion totale”, J. Optics (Paris), **8**, 73-87 (1977).

[3] R. G. Turner, “Shifts of coherent light beams on reflection at plane interfaces between isotropic media”, Aust. J. Phys. **33**, 319-335 (1980).

[4] J.-J. Greffet and C. Baylard, “Nonspecular astigmatic reflection of a 3D gaussian beam on an interface”, Opt. Commun. **93**, 271-276 (1992).

[5] W. Nasalski, "Longitudinal and transverse effects of nonspecular reflection", J. Opt. Soc. Am. A, **13**, 172-181 (1996).

[6] F. I. Baida, D. Van Labeke, and J.-M. Vigoureux, “Numerical study of the displacement of a three-dimensional Gaussian beam transmitted at total internal reflection. Near field applications”, J. Opt. Soc. Am. A **17**, 858-866 (2000).

[7] W. Nasalski, “Three-dimensional beam reflection at dielectric interfaces”, Opt. Commun. **197**, 217-233 (2001).

[8] O. Costa de Beauregard, “Translational internal spin effect with photons”, Phys. Rev. **139**, B1443-B1446 (1965).

[9] H. Shilling, “Die Strahlversetzung bei der Reflection linear oder elliptisch polarisierter ebener Wellen an der Trennebene zwischen absorbierenden Medien”, Ann. Phys. Leipzig **16**, 122-134 (1965).

[10] J. Ricard, “Courbes de flux d'énergie de l'onde évanescente et nouvelle explication du déplacement d'un faisceau lumineux dans la réflexion totale,” Nouv. Rev. Opt. **1**, 275-286 (1970).

[11] C. Imbert, “Calculation and experimental proof of the transverse shift induced by total internal reflection of a circularly polarized light beam”, Phys. Rev. D **5**, 787-796 (1972).

[12] O. Costa de Beauregard and C. Imbert, “Quantized longitudinal and transverse shifts associated with total internal reflection”, Phys. Rev. D **7**, 3555-3563 (1972).

[13] E. Pollak and W. H. Miller, " New physical interpretation for time in scattering theory "Phys. Review Lett. **53**, 115-118 (1984).

[14] R. Simon, N. Mukunda, „Iwasawa decomposition in first-order optics: universal treatment of shape-invariant propagation for coherent and partially coherent beams", J. Opt. Soc. Am. A **15**, 2146-2155 (1998).

[15] J. Serna, R. Martinez-Herrero and P. M. Mejias, "Parametric characterization of general partially coherent beams propagating through ABCD optical systems", J. Opt. Am. A **8**, 1094-1098 (1991).

[16] P. Yeh, *Optical waves in layered media*, (Wiley, New York, 1976).

[17] W. Nasalski, "Modelling of beam reflection at a nonlinear-linear interface", J. Opt. A: Pure Appl. Opt. **2**, 433-441 (2000).

[18] M. A. Player, J. Phys. A: Math. Gen., "Angular momentum balance and transverse shifts on reflection of light", **20**, 3667-3678 (1987).

[19] V. G. Fedoseyev, "Conservation laws and transverse motion of energy on reflection and transmission of electromagnetic waves" J. Phys. A: Math. Gen. **21**, 2045-2059 (1988).

[20] V. S. Liberman and B. Ya. Zel'dovich, " Spin-orbit interaction of a photon in an inhomogeneous medium", Phys. Rev. A **46**, 5199-5207 (1992).

[21] R. Güther, B. H. Kleemann, J. Elschner and G. Schmidt, "Determination of longitudinal and transverse shifts of three-dimensional Gaussian beams reflected at a grating near an anomaly", J. Mod. Opt. **49**, 1785-1793 (2002).

[22] K. B. Wolf and G. Krötzsch, "Fractional Fourier transformers through reflection", J. Opt. Soc. Am. A 19, 1191-1196 (2002).

[23] J.-M. Vigoureux and R. Giust, "The use of the hyperbolic plane in studies of multilayers", Opt. Commun. **186**, 231-236 (2000).

[24] Y. S. Kim, "Lorentz group in polarization optics" J. Opt. B: Quantum Semiclass. Opt. **2**, R1-R5 (2000).

[25] G. Nimtz and W. Heitman, "Superluminal photonic tunneling and quantum electronics", Prog. Quant. Electr. **21**, 81-108 (1997).

[26] L. Allen, "Introduction to the atoms and angular momentum of light special issue", J. Opt. B: Quantum Semiclass. Opt. **4**, S1-S5 (2002).

CHAPTER 6

Beams at multilayers - formulation of the problem

A problem of three-dimensional optical beam scattering at a dielectric multilayer is analysed. Scattering and transfer matrices of the layered structure are derived for incidence of beams of arbitrary polarization. Transmission and reflection matrices are given in a diagonal form dependent on polarization of an incident beam. Factorisation of these matrices results in scalar complex transformations separately for beam polarization and for beam amplitudes. While the polarization transformations describe the multilayer action in terms of Lorentz transformations, the amplitude transformations yield spatial beam shaping. The scattering vector problem resolves into two independent scalar transformations.

6.1 Introduction

The problem of scattering of two-dimensional (2D or 1+1 dimensional) beams at a 2D planar, isotropic and lossless structure can be described by a scattering matrix defined in a spectral domain of these beams [1]. Owing to the well-known symmetry of the Maxwell's equations, such a scattering problem can be decomposed into two independent 2D scattering problems for TM and TE polarizations. Each one of these problems possesses a solution in a form of two independent second-order scattering matrices, one for the TM polarization and other for the TE polarization. The form of these scattering

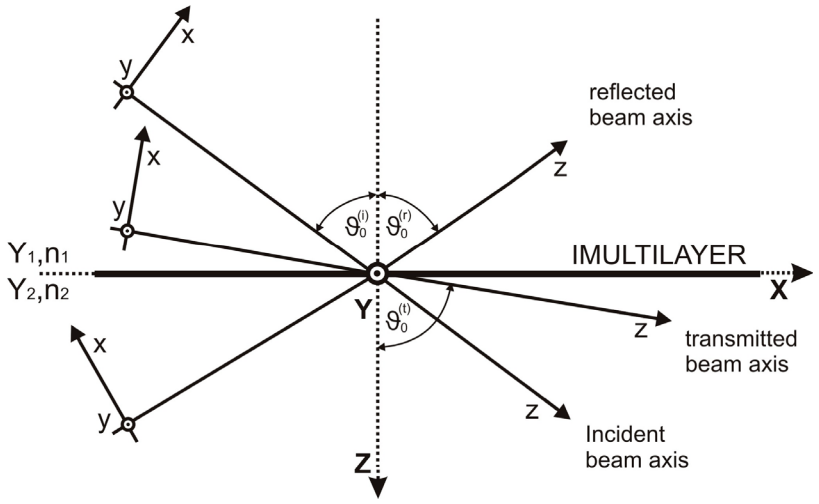

Figure 6.1. Multilayer and beam reference frames for transmission and reflection viewed in the main plane-of-incidence; n_j, Y_j, j=1,2 are refractive indices and characteristic admittances of the superstrate (j=1) and substrate (j=2) media.

matrices is restricted by the principle of reciprocity and the Stokes relations, which hold for any isotropic structure.

However, for three-dimensional (3D or 2+1-dimesional) beams the TM and TE field components are coupled at planar discontinuities of the multilayer. The scattering problem is then understood as the collection of the partial plane-wave scattering-problems, defined first in different (local) incident planes and specified by their separate azimuthal angles-of-incidence. Then the global scattering problem becomes inherently of the vectorial nature [2-4], with a solution in a form of a four-by-four scattering and transfer matrices for the scattering structure.

In this chapter, the scattering and transfer matrices of the optical multilayer, composed of isotropic, homogeneous and dispersionless layers of different medium parameters, are derived for a general case of incidence of a 3D beam of arbitrary polarization. The layered structure may be periodic or aperiodic. The analysis differs from the common approaches to such

problems in several aspects. For all spectral constituents of beam fields, the reflection and transmission coefficients are derived in the one reference frame assigned to the main plane-of-incidence [2], [4]. The reflection and transmission matrices are made diagonal by relating their elements to a polarization parameter of the incident beam. A spectral representation of the beam fields is defined in new polarization frames composed of two mutually orthogonal Jones vectors, where different frames are assigned separately to the incident, transmitted and reflected beams [2]. The Stokes time-reversal relations are given in the most general 3D form. Then the four-by-four scattering and transfer matrices can be readily defined as double-dimensional counterparts of the respective two-by-two matrices, known from the 2D problem for the TM and TE polarizations.

Layered media play an important role in many applications in modern optics. Several features of the multilayer action on a plane wave impinging upon the structure have been recently reported in the formulation equivalent to the case of 2D beams [5-8]. It is the intention of this chapter to provide a convenient framework to discuss such problems in the more general case of 3D beams. To this end the transverse field of beams is factorised into its amplitude and polarization components [2]. The solution resolves into two sets of scalar relations independently for polarization and amplitude of beams. Then, in the spectral (momentum) domain, the transmission and reflection matrices for beam polarization appear to be unimodular and, as such, can be interpreted in terms of transformations of the six-parameter restricted Lorentz group [3]. The solution can be further restated in a spatial (configuration) domain of beams, as it has been shown in Ref. [4]. Then, the remaining amplitude transformations yield description of beam shaping in the course of beam interaction with the multilayered structure.

Our presentation will be somewhat pedantic to make the analysis as clear and self-contained as possible. In Section 2 a formulation of the problem is given and derivation of the transmission and reflection matrices for oblique incidence of a single beam is outlined. Equivalence of these matrices with scalar relations for beam amplitude and polarization parameters is shown in Section 3 in a form already known for the case of a single interface [2]. In Section 4 polarization spinors of two types are defined and used to express a general form of a spectral representation of beam fields. The formalism is

referred to polarization matrices and Stokes vectors in Section 5. The scattering and transfer matrices of the multilayer are derived and their characteristics are briefly discussed in Section 6. In Section 7, the method is applied, as an example, to the problem of scattering at an anti-reflection multilayer. Conclusions close this chapter in Section 8. The author hopes that the presented formulation of the scattering problem provides a proper framework to treat optical 3D beams - of arbitrary shape, polarization and incidence direction - scattered at multilayered optical or photonic structures.

6.2 Transmission and reflection matrices

Consider 3D monochromatic optical (incident, reflected and transmitted) beams with their reference coordinate frames (x,y,z) different, in general, from a coordinate frame (X,Y,Z) of an optical system, which is assumed to be a planar dielectric structure in (X,Y) planes (cf. Fig. 6.1). Beam axes coincide with z-axes of beam frames, a Z-axis of the optical system frame is normal to the planar structure. The coordinates Y and y of all frames coincide as being transverse to the main (principal) incidence plane $Y=0=y$, also referred to as the incidence plane. Note that the Z-axis is assumed normal to the optical structure, meanwhile in Ref. [2] and Ref. [4] the Z-axis indicates the grazing incidence along a surface of the structure. The present choice reflects the main interest of this analysis in beam transmission through the planar structure rather than generation of waves progressed in planes parallel to this structure.

The structure is two-dimensional and consists of a stack of planar homogeneous layers. A third dimension is introduced to the problem by a 2D spatial distribution of the beam field in the transverse planes (X,Y). The polar and azimuthal rotation angles of the beam frames (x,y,z) with respect to the system frame (X,Y,Z) are denoted by $\vartheta^{(b)}$ and φ, respectively, where b=i means incidence and b=t (or b=r) means transmission (or reflection).

The incident beam is partially transmitted and partially reflected at the multilayer (Fig. 6.1). The action of the multilayer is described by a set of linear relations between amplitudes of these beams for the 2D problem and, in addition, between beam amplitude and beam polarization parameters for the 3D problem analysed here. Only the beam fields outside the structure, in a

superstrate (or ambient; for $n = n_1$ and $Y = Y_1$) and in a substrate (for $n = n_2$ and $Y = Y_2$), are considered. The symbols n_a, Y_a, $Z_a = 1/Y_a$, a=1,2, denote refractive indices, characteristic admittances and characteristic impedances of both media, respectively [1]. In this section, the transmission and reflection of a single beam incidence is discussed, assuming that, say, the Fresnel coefficients for a single plane wave incidence at the multilayer are known. These coefficients can be easily evaluated by a simple composition law [5], from the Fresnel coefficients for a single interface.

The beam has, by definition, narrow angular spectrum concentrated about the beam axis and propagates through an optical system from some input plane at $z = z^{(i)}$ (or at $Z = Z^{(i)}$) to the output planes at $z = z^{(t)}$ (or at $Z = Z^{(t)}$) and $z = z^{(r)}$ (or at $Z = Z^{(r)}$). In the angular spectrum representation

$$\underline{E}^{(b)}(x,y) = (2\pi)^{-2} \iint \underline{\widetilde{E}}^{(b)}(k_x^{(b)}, k_y) \exp[+i(k_x^{(b)} x + k_y y)]\, dk_x^{(b)} dk_y , \quad (6.1)$$

the beam electric field $\underline{E}^{(b)} \equiv \underline{E}^{(b)}(x,y)$ is composed of the superposition of plane waves with vector amplitudes $\underline{\widetilde{E}}^{(b)} \equiv \underline{\widetilde{E}}^{(b)}(k_x^{(b)}, k_y)$, defined here at the input and output planes of the system. A wave number in the substrate (b=t) or superstrate (b=i or b=r) is denoted by $k^{(b)}$, the transverse to the Z-axis components k_X and k_Y of the wave vector $\underline{k}^{(b)}$ remain constant through the structure and are interrelated by the dispersion relation $k_X^2 + k_Y^2 + k_Z^{(b)2} = k^{(b)2}$. Exponential dependence $\exp(-i\omega t)$ on time is assumed and suppressed henceforth.

We consider only transverse (to the propagation direction) spatial $E_x^{(b)}$ and $E_y^{(b)}$ and spectral $\widetilde{E}_x^{(b)}$ and $\widetilde{E}_y^{(b)}$ components of the electric beam fields $\underline{E}^{(b)} = \left[E_x^{(b)}, E_y^{(b)}\right]^T$ and $\underline{\widetilde{E}}^{(b)} = \left[\widetilde{E}_x^{(b)}, \widetilde{E}_y^{(b)}\right]^T$. The superscript "T" denotes the transpose of a column vector. Remaining field components $E_z^{(b)}$ and $\widetilde{E}_y^{(b)}$ are determined by the Gauss law:

$$k_x^{(b)} \widetilde{E}_x^{(b)} + k_y \widetilde{E}_y^{(b)} + k_z^{(b)} \widetilde{E}_z^{(b)} = 0 . \quad (6.2)$$

The propagation direction of the central plane wave ($\vartheta^{(b)} = \vartheta_0^{(b)}$, $\varphi = 0$) is placed in the *main plane-of-incidence*. Other spectral components propagate

either in the main plane-of-incidence for $\vartheta^{(b)} \neq \vartheta_0^{(b)}$ or in the *local planes-of-incidence*, that is in the planes inclined, by the azimuthal angle $\varphi \neq 0$, to the main plane-of-incidence. Still, however, polarization characteristics of all beam spectral components, as well as characteristics of the total beam, will be described in relation to the main plane-of-incidence $\varphi = 0$.

The components $\widetilde{E}_x^{(b)}$ and $\widetilde{E}_y^{(b)}$ are not, in general, independent quantities; they are interrelated through a spatial structure of the beam, medium inhomogeneities and anisotropic properties of the optical system. In the 2D planar isotropic configuration, however, the separate p ($\widetilde{E}_x^{(b)} = \widetilde{E}_p^{(b)}$, $\widetilde{E}_y^{(b)} = 0$) and s ($\widetilde{E}_x^{(b)} = 0$, $\widetilde{E}_y^{(b)} = \widetilde{E}_p^{(b)}$) spectral components of a plane wave propagate independently through the optical system. Their transmission through the multilayered structure is described by the Fresnel or plane wave diagonal transmission matrix $\underline{\underline{t}}_F$:

$$\begin{bmatrix} \widetilde{E}_p^{(t)} \\ \widetilde{E}_s^{(t)} \end{bmatrix} = \underline{\underline{t}}_F \begin{bmatrix} \widetilde{E}_p^{(i)} \\ \widetilde{E}_s^{(i)} \end{bmatrix}, \qquad \underline{\underline{t}}_F = \begin{bmatrix} t_p & 0 \\ 0 & t_s \end{bmatrix}. \tag{6.3}$$

The diagonal matrix elements t_p and t_s of p type and s type, respectively, denote the p and s transmission coefficients of the planar, in general multilayered, structure. We shall call them the Fresnel (geometric-optical (g-o) or plane wave) coefficients even for the structure built from several layers and interfaces.

In the system frame (X, Y, Z), the transfer matrix possesses the diagonal form (6.3) only for the field spectral components $\underline{\widetilde{E}}^{(b)}$ with propagation directions in the main plane-of-incidence. The transfer matrix for other field components is obtained by the azimuthal rotation by φ of the projection $(\widetilde{E}_X^{(b)}, \widetilde{E}_Y^{(b)})^T = (\pm \widetilde{E}_x^{(b)} c_z^{(b)}, \widetilde{E}_y^{(b)})^T$ of the transverse field vectors $\underline{\widetilde{E}}^{(b)}$ onto the interface planes Z=constant of the planar structure:

$$\begin{bmatrix} \widetilde{E}_X^{(b)} \\ \widetilde{E}_Y^{(b)} \end{bmatrix} = \begin{bmatrix} \pm \widetilde{E}_x^{(b)} c_z^{(b)} \\ \widetilde{E}_y^{(b)} \end{bmatrix} = \begin{bmatrix} c_y & s_y \\ -s_y & c_y \end{bmatrix} \begin{bmatrix} \pm \widetilde{E}_p^{(b)} c_z^{(b)} \\ \widetilde{E}_s^{(b)} \end{bmatrix}, \tag{6.4}$$

where $c_y = \cos\varphi$, $s_y = \sin\varphi$, $c_z^{(b)} = \cos\vartheta^{(b)}$ and $s_z^{(b)} = \sin\vartheta^{(b)}$, with the subscripts y and z indicating y-axes and z-axes being rotated in planes (X,Y) and (X,Z) by the rotation angles φ and $\vartheta^{(b)}$, respectively. In the expression $\pm\widetilde{E}_x^{(b)}c_z^{(b)}$ the upper sign (+) is assigned to b=i, t and the lower sign (-) to b=r, respectively; cf. Fig. 6.1. The vectors $(\widetilde{E}_X^{(b)},\widetilde{E}_Y^{(b)})^T$ rotate around the Z axis, through the angle φ, from the local incidence plane $\varphi \neq 0$ to the main incidence plane $\varphi = 0$, and that, in turn, yields for the transverse vectors $\underline{\widetilde{E}}^{(b)}$ [2]:

$$\begin{bmatrix} \widetilde{E}_x^{(b)} \\ \widetilde{E}_y^{(b)} \end{bmatrix} = \underline{\underline{R}}^{(b)} \begin{bmatrix} \widetilde{E}_p^{(b)} \\ \widetilde{E}_s^{(b)} \end{bmatrix},$$

$$\underline{\underline{R}}^{(b)} = \begin{bmatrix} c_y & \pm s_y / c_z^{(b)} \\ \mp s_y c_z^{(b)} & c_y \end{bmatrix}. \tag{6.5}$$

The convention of a positive sign of φ for the clockwise rotation is used. For different superstrate (b=i) and substrate (b=t) media $c_z^{(i)}$ is different from $c_z^{(t)}$. Then, the rotation matrices $\underline{\underline{R}}^{(b)} \equiv \underline{\underline{R}}^{(b)}(\vartheta^{(b)},\varphi)$ differs for the beam incidence (b=i) and transmission (b=t).

By the rotation $\underline{\underline{R}}^{(b)}$ the (Fresnel) transmission matrix $\underline{\underline{t}}_F \equiv \underline{\underline{t}}(\vartheta^{(i)},\varphi)$ yields the generic transmission matrix $\underline{\underline{t}} \equiv \underline{\underline{t}}(\vartheta^{(i)},\varphi) = \underline{\underline{R}}^{(t)}\underline{\underline{t}}_F\underline{\underline{R}}^{(i)-1}$, evaluated in the main incidence plane $Y = 0$:

$$\begin{bmatrix} \widetilde{E}_x^{(t)} \\ \widetilde{E}_y^{(t)} \end{bmatrix} = \begin{bmatrix} t_{xx} & t_{xy} \\ t_{yx} & t_{yy} \end{bmatrix} \begin{bmatrix} \widetilde{E}_x^{(i)} \\ \widetilde{E}_y^{(i)} \end{bmatrix},$$

$$\begin{bmatrix} t_{xx} & t_{xy} \\ t_{yx} & t_{yy} \end{bmatrix} = \begin{bmatrix} c_y^2 t_p + s_y^2 t_s \, c_z^{(i)} / c_z^{(t)} & -s_y c_y (t_p / c_z^{(i)} - t_s / c_z^{(t)}) \\ -s_y c_y (t_p c_z^{(t)} - t_s c_z^{(i)}) & s_y^2 t_p \, c_z^{(t)} / c_z^{(i)} + c_y^2 t_s \end{bmatrix}, \tag{6.6}$$

with nonzero off-diagonal elements for $\varphi \neq 0$. Still, however, even for $\varphi \neq 0$, the matrix $\underline{\underline{t}}$ can also be made diagonal by imposing on its components explicit dependence on the incident beam polarization [2]:

$$\underline{\underline{t}} = \begin{bmatrix} t_{\parallel} & 0 \\ 0 & t_{\perp} \end{bmatrix} = \begin{bmatrix} t_{xx} + t_{xy}\chi^{(i)-1} & 0 \\ 0 & t_{yx}\chi^{(i)} + t_{yy} \end{bmatrix}, \tag{6.7}$$

$$t_{\parallel} = t_p - s_y(t_p - t_s\eta^{-1})c_y(\chi^{(i)}c_z^{(i)})^{-1} - s_y^2(t_p - t_s\eta^{-1}),$$

$$t_{\perp} = t_s - s_y(t_p\eta - t_s)c_y\chi^{(i)}c_z^{(i)} + s_y^2(t_p\eta - t_s), \tag{6.8}$$

$$\chi^{(b)} = \widetilde{E}_x^{(b)} \big/ \widetilde{E}_y^{(b)}, \tag{6.9}$$

where $\eta = c_z^{(t)} \big/ c_z^{(i)}$ and the TM ($t_{\parallel}$) and TE ($t_{\perp}$) transmission coefficients are evaluated in the main incidence plane. They depend, besides the Fresnel coefficients t_p and t_s, on two parameters: a polarization parameter $\chi^{(b)}$, b=i, being the quotient between transverse components of the incident beam, and on a scaling parameter η being the quotient between the transmission $c_z^{(t)}$ and reflection $c_z^{(i)}$ cosines.

The role of the polarization parameter $\chi^{(b)}$ is evident from its definition (6.9); e.g. it resolves into the helicity of the beam for $\chi^{(b)} = \pm i$ and indicates the diagonal linear polarization for $\chi^{(b)} = \pm 1$. The parameter η relates the coefficient $t_{\parallel}$ for the p field components $\widetilde{E}_x^{(b)}$ with the coefficient t_X for the field components $\widetilde{E}_X^{(b)}$ parallel to the planar structure:

$$\widetilde{E}_X^{(t)} = t_X \widetilde{E}_X^{(i)}, \qquad t_X = t_{\parallel}\eta \tag{6.10}$$

and, in fact, precisely yields the relations between these field components which determine the beam transmission and reflection [2].

The expressions for $t_{\parallel}$ and $t_{\perp}$ are exact. Nevertheless, in the right-hand-sides of (6.8), they contain consecutively the zero-order, first-order and second-order terms with respect to the azimuthal angle φ (or its sine s_y). Ap-proximations to these orders at the beam axis can be applied to describe the total beam in a spatial domain in terms of zero-order, first-order and second-order changes of parameters describing a spatial structure of the beam field [4]. The polarization parameter $\chi^{(i)}$ affects $t_{\parallel}$ and $t_{\perp}$ only through the first-order terms in such a manner that these terms become substantial for

highly elliptic beams in the opposite polarization field components, that is in the TM transmitted field component for the TE incident field component, and vice versa [4]. Moreover, these terms are asymmetric with respect to the main plane-of-incidence and as such they induce finite first-order effects of transverse deformations - first-order complex shifts - of the transmitted (and reflec-ted) beam. That happens even for the incident beam being symmetric with respect to the main plane-of-incidence [2], [4].

In the following, $t_{\parallel}$ and $t_{\perp}$ will be understood as polarization-dependent when $s_y \neq 0$ and $\chi^{(i)} \neq 0, \pm\infty$. Otherwise $t_{\parallel} = t_p$ and $t_{\perp} = 0$ for the pure TM (p) polarization ($\chi^{(i)} = \pm\infty$) or $t_{\perp} = t_s$ and $t_{\parallel} = 0$ for the pure TE (s) polarization ($(\chi^{(i)})^{-1} = \pm\infty$). Note also that, in order to determine the field amplitudes $\widetilde{E}_x^{(b)}$ and $\widetilde{E}_y^{(b)}$, besides $\chi^{(b)}$ the second parameter $\kappa^{(b)} = \widetilde{E}_x^{(b)} \widetilde{E}_y^{(b)}$, coined further as the amplitude parameter, should also be introduced. Both parameters $\chi^{(b)}$ and $\kappa^{(b)}$ depend, in general, on the wave vector components $k_x^{(b)}$ and k_y.

Similar considerations hold also for the beam reflection with pertinent replacements of the transmission matrices $\underline{\underline{t}}_F$, $\underline{\underline{t}}$ by the reflection matrices $\underline{\underline{r}}_F$, $\underline{\underline{r}}$, and the transmission coefficients t_p, t_s, $t_{\parallel}$ and $t_{\perp}$ by the reflection coefficients r_p, r_s, $r_{\parallel}$ and $r_{\perp}$, respectively:

$$\begin{bmatrix} \widetilde{E}_p^{(r)} \\ \widetilde{E}_s^{(r)} \end{bmatrix} = \underline{\underline{r}}_F \begin{bmatrix} \widetilde{E}_p^{(i)} \\ \widetilde{E}_s^{(i)} \end{bmatrix}, \qquad \underline{\underline{r}}_F = \begin{bmatrix} r_p & 0 \\ 0 & r_s \end{bmatrix}, \tag{6.11}$$

$$\begin{bmatrix} \widetilde{E}_x^{(r)} \\ \widetilde{E}_y^{(r)} \end{bmatrix} = \underline{\underline{r}} \begin{bmatrix} \widetilde{E}_x^{(i)} \\ \widetilde{E}_y^{(i)} \end{bmatrix}, \qquad \underline{\underline{r}} = \begin{bmatrix} r_{\parallel} & 0 \\ 0 & r_{\perp} \end{bmatrix}. \tag{6.12}$$

The transmitted and reflected wave amplitudes are not independent. They are interrelated by the field continuity relations at interfaces of the planar structure. The transmission and reflection coefficients of the overall system can be built in a standard manner from coefficients specific to separate interfaces of medium discontinuities and the matrices of propagation in the homogeneous dielectric slabs. As the propagation matrices are trivial and obviously known, only the coefficients at interfaces need to be specified.

Then, the action of the whole optical system can be determined by modification of these coefficients and this can be carried out, e.g., by a straightforward composition law [5].

For a single interface, the field continuity relations yield:

$$1-r_p=t_p\eta\,,\qquad 1+r_s=t_s\,,$$

$$1-r_{\parallel}=t_{\parallel}\eta\,,\qquad 1+r_{\perp}=t_{\perp}\,, \tag{6.13}$$

where $r_{\parallel}$ and $r_{\perp}$ are the actual TM and TE reflection coefficients of the spectral component of the beam, specified by $\vartheta^{(i)}$ and φ [2]:

$$r_{\parallel}=r_{xx}+r_{xy}\chi^{(i)^{-1}}=r_p-s_y(r_p+r_s)c_y(\chi^{(i)}c_z^{(i)})^{-1}-s_y^2(r_p+r_s)\,,$$

$$r_{\perp}=r_{yx}\chi^{(i)}+r_{yy}=r_s+s_y(r_p+r_s)c_y\chi^{(i)}c_z^{(i)}-s_y^2(r_p+r_s)\,. \tag{6.14}$$

The signs of the Fresnel coefficients are imposed such that $r_p=1=r_s$ in the case of critical incidence of total internal reflection (TIR), that is for $\vartheta^{(i)}<\vartheta^{(t)}=\pi/2$. The expressions (6.14) of the coefficients $r_{\parallel}$ and $r_{\perp}$ for reflection are of similar characteristics as those (6.8) for transmission. They can be also directly derived by the rotation (6.5) of the matrices (6.11)-(6.12) for beam reflection. That yields $\underline{\underline{r}}\equiv\underline{\underline{r}}(\vartheta^{(i)},\varphi)=\underline{\underline{R}}^{(r)}\underline{\underline{r}}_F\underline{\underline{R}}^{(i)^{-1}}$ evaluated in the main plane-of incidence $Y=0$. In this way the continuity relations (6.13) make the analysis for beam reflection consistent with the analysis for beam transmission, as that certainly should be expected.

To summarise this section, the action of the optical system on the incident beam is generally described in the spectral domain by the diagonal transmission $\underline{\underline{t}}$ and reflection $\underline{\underline{r}}$ matrix transformations. Both matrices are polarization-dependent, that is they are dependent not only on the p and s Fresnel coefficients t_p, t_s, r_p, r_s but also on the polarization parameter $\chi^{(i)}$ of the incident (input) beam. The system action is described by changes in the beam polarization parameters $\chi^{(b)}$ and by changes in the beam amplitude parameters $\kappa^{(b)}$. Both these parameters are scalars. Therefore, it seems that the action of the optical system can be described in pure algebraic scalar manner.

6.3 Amplitude-polarization spectral decomposition

The transverse field vector $\underline{\widetilde{E}}^{(b)}$ contains the information not only on the polarization but also on the amplitude of each spectral component of the beam. The beam polarization depends, by definition, only on the polarization parameter $\chi^{(b)}$. Therefore, we have to decompose the transverse field vector $\underline{\widetilde{E}}^{(b)}$ into its amplitude $\widetilde{E}^{(b)} \equiv \widetilde{E}^{(b)}(k_x^{(b)}, k_y)$, which is expressed by the product $\kappa^{(b)} = \kappa^{(b)}(k_x^{(b)}, k_y)$ of these field components and its (unnormalised) Jones polarization base vector $\underline{e}^{(b)} \equiv \underline{e}^{(b)}(k_x^{(b)}, k_y)$. The Jones vectors depend only on the quotient $\chi^{(b)} \equiv \chi^{(b)}(k_x^{(b)}, k_y)$ between the transverse field components [2]:

$$\underline{\widetilde{E}}^{(b)} = \widetilde{E}^{(b)} \underline{e}^{(b)}, \tag{6.15}$$

$$\widetilde{E}^{(b)} = \left(\widetilde{E}_x^{(b)} \widetilde{E}_y^{(b)}\right)^{1/2} = \kappa^{(b)1/2}, \tag{6.16}$$

$$\underline{e}^{(b)} = \begin{bmatrix} \left(\widetilde{E}_x^{(b)} / \widetilde{E}_y^{(b)}\right)^{+1/2} \\ \left(\widetilde{E}_x^{(b)} / \widetilde{E}_y^{(b)}\right)^{-1/2} \end{bmatrix} = \begin{bmatrix} \left(\chi^{(b)}\right)^{+1/2} \\ \left(\chi^{(b)}\right)^{-1/2} \end{bmatrix}. \tag{6.17}$$

The function $\widetilde{E}^{(b)}(k_x^{(b)}, k_y)$ evidently plays the role of the complex amplitude of each beam spectral component. Its phase is an arithmetic mean of phases of the TM and TE transverse field components:

$$\ln \widetilde{E}^{(b)} = \tfrac{1}{2}\left[\ln \widetilde{E}_x^{(b)} + \ln \widetilde{E}_y^{(b)}\right] = \tfrac{1}{2} \ln \kappa^{(b)}, \tag{6.18}$$

and its magnitude $\left|\widetilde{E}^{(b)}\right|$, multiplied by a norm $N^{(b)}$ of the Jones vector, yields the intensity $I_0^{(b)}$ of the spectral component $\underline{\widetilde{E}}^{(b)}$ of the beam:

$$I_0^{(b)} = \left|\widetilde{E}_x^{(b)}\right|^2 + \left|\widetilde{E}_y^{(b)}\right|^2 = \left|\widetilde{E}^{(b)}\right|^2 \left(N^{(b)}\right)^2,$$

$$\left(N^{(b)}\right)^2 = \left(\underline{e}^{(b)}\right)^{+} \underline{e}^{(b)} = \left|\chi^{(b)}\right| + \left|\chi^{(b)}\right|^{-1}, \tag{6.19}$$

where the dagger "+" stands for the complex conjugate transpose. The extraction of the norm $N^{(b)}$ from the beam amplitude $\widetilde{E}^{(b)}$ is not accidental

and results in invariance of the polarisation vectors $\underline{e}^{(b)}$ under the action of the six-parameter restricted Lorentz group transformations [3]. Note that this feature has been recently assigned to a transfer matrix of systems of first-order optics [5-8].

The factorisation (6.15)-(6.17) of the transverse field vector implies that the transmission and reflection matrices of the optical system should also be factorised:

$$\underline{\widetilde{E}}^{(\mathrm{t})} = \underline{\underline{t}}\,\underline{\widetilde{E}}^{(i)}, \tag{6.20}$$

where $\underline{\underline{t}} = t_A \underline{\underline{t}}_P$,

$$\underline{\widetilde{E}}^{(r)} = \underline{\underline{r}}\,\underline{\widetilde{E}}^{(i)}, \tag{6.21}$$

where $\underline{\underline{r}} = r_A \underline{\underline{r}}_P$, into the complex, in general, scalar transmission coefficients t_A and r_A of beam amplitudes:

$$\widetilde{E}^{(t)} = t_A \widetilde{E}^{(i)} = t_\kappa^{1/2} \widetilde{E}^{(i)}, \tag{6.22}$$

where $t_\kappa = t_\parallel t_\perp$,

$$\widetilde{E}^{(r)} = r_A \widetilde{E}^{(i)} = r_\kappa^{1/2} \widetilde{E}^{(i)}, \tag{6.23}$$

where $r_\kappa = r_\parallel r_\perp$,

and the diagonal transmission $\underline{\underline{t}}_P$ and reflection $\underline{\underline{r}}_P$ matrices of beam polarization:

$$\underline{e}^{(t)} = \underline{\underline{t}}_P \underline{e}^{(i)}, \qquad \underline{\underline{t}}_P = \begin{bmatrix} t_\chi^{+1/2} & 0 \\ 0 & t_\chi^{-1/2} \end{bmatrix}, \tag{6.24}$$

where $t_\lambda = t_\parallel / t_\perp$,

$$\underline{e}^{(r)} = \underline{\underline{r}}_P \underline{e}^{(i)}, \qquad \underline{\underline{r}}_P = \begin{bmatrix} r_\chi^{+1/2} & 0 \\ 0 & r_\chi^{-1/2} \end{bmatrix}, \tag{6.25}$$

where $r_\chi = r_\parallel / r_\perp$.

Note that, due to the appropriate definitions of the transmission and reflection coefficients, the matrices $\underline{\underline{t}}_P$ and $\underline{\underline{r}}_P$ are diagonal and, due to the appropriate definitions of the beam amplitudes, they are also unimodular [2].

The amplitude coefficients t_κ and r_κ are expressed by a product of the TM and TE transmission coefficients $t_\parallel$, $r_\parallel$, $t_\perp$, and $r_\perp$. At the same time the polarization coefficients t_χ and r_χ are expressed by the ratio of the coefficients $t_\parallel$, $r_\parallel$, $t_\perp$, and $r_\perp$. Thus the polarisation and the amplitudes of beams are described by simple scalar transformations of the beam polarization $\chi^{(b)}$ and amplitude $\widetilde{E}^{(b)}$ parameters:

$$\chi^{(t)} = t_\chi \chi^{(i)}, \qquad \chi^{(r)} = r_\chi \chi^{(i)},$$

$$\kappa^{(t)} = t_\kappa \kappa^{(i)}, \qquad \kappa^{(r)} = r_\kappa \kappa^{(i)}, \tag{6.26}$$

and the coupling between the TM and TE field components yields the dependence of the scalar transformation coefficients t_χ, r_χ, t_κ, and r_κ on the polarization parameter $\chi^{(i)}$ of the incident beam.

In Ref. [2] it has been explicitly shown how to translate the scalar transformations (6.26) in the spectral domain into the polarization and shape changes of the total beam in the spatial domain. It appears that different changes are induced by different coefficients dependent on $t_\parallel$ and $t_\perp$. While the polarization coefficients t_χ and r_χ lead to the beam polarization modifications, the amplitude coefficients t_κ and r_κ entail changes in the beam complex amplitude, in the position of the beam waist and in the direction of the beam axis. The analysis has pertained so far to the case of only one incident beam. To account for incidence of two beams, in independent (in general) polarization states, a second type of Jones vector is necessary to introduce. The whole construction of the field representation relies on the symmetry of Maxwell's equations with respect to time reversal, what leads to Stokes relations at the multilayer and, in turn, to its scattering matrix. It is assumed, in the following, that the optical system under consideration is sourceless, lossless and reciprocal.

6.4 Spinor representation of beam polarization

The polarization space for the beam fields is spanned by two independent solutions of Maxwell's equations, known as undotted and dotted spinors [3], or in the optical terminology, as mutually orthogonal Jones vectors. Suppose

that the spinors are to be obtained from the spinors by replacement of the electric and magnetic spectral field components with their counterparts also being solutions of complex conjugates of Maxwell's equations:

$$\underline{\widetilde{E}}, \underline{\widetilde{H}} \qquad \Rightarrow \qquad \underline{\overline{\widetilde{H}}}/Y, \underline{\overline{\widetilde{E}}}Y \tag{6.27}$$

where Y is a (a real) characteristic admittance of a lossless medium and the complex conjugate, indicated by the overbar "‾", implies also the reversal of the beam propagation direction. The replacement (6.27) is equivalent to the exchange of the (undotted by dotted) transverse field components, beam amplitudes and Jones' polarization spinors:

$$\underline{\widetilde{E}}^{(b)} = \begin{bmatrix} \widetilde{E}_x^{(b)} \\ \widetilde{E}_y^{(b)} \end{bmatrix} \qquad \Rightarrow \qquad \underline{\widetilde{\dot{E}}}^{(b)} = \begin{bmatrix} +\overline{\widetilde{E}}_y^{(b)} \\ -\overline{\widetilde{E}}_x^{(b)} \end{bmatrix}, \tag{6.28}$$

$$\widetilde{E}^{(b)} = \left(\kappa^{(b)}\right)^{1/2} \qquad \Rightarrow \qquad \widetilde{\dot{E}}^{(b)} = \left(\overline{\kappa}^{(b)}\right)^{1/2}, \tag{6.29}$$

$$\underline{e}^{(b)} = \begin{bmatrix} \left(\chi^{(b)}\right)^{+1/2} \\ \left(\chi^{(b)}\right)^{-1/2} \end{bmatrix} \qquad \Rightarrow \qquad \underline{\dot{e}}^{(b)} = \begin{bmatrix} \left(\overline{\chi}^{(b)}\right)^{-1/2} \\ \left(\overline{\chi}^{(b)}\right)^{+1/2} \end{bmatrix}, \tag{6.30}$$

in the spectral representation of the new (dotted) field. Note that the time-reversal invariance of Maxwell's equations leads also to another replacement [1]:

$$\underline{\widetilde{E}}, \underline{\widetilde{H}} \qquad \Rightarrow \qquad \underline{\overline{\widetilde{E}}}, -\underline{\overline{\widetilde{H}}} \tag{6.31}$$

that yields just the complex conjugate of the dotted and undotted field quantities defined in Eqs. (6.28)-(6.30), together with the additional propagation direction reversal. In a general case of a lossy structure a conjugate medium is specified by $\overline{n}$ and $\overline{Y}$ in both replacements above.

The spectral amplitudes $\widetilde{E}^{(b)}$ and $\widetilde{\dot{E}}^{(b)}$ are of equal magnitudes and opposite phases. The polarization spinors $\underline{e}^{(b)}$ and $\underline{\dot{e}}^{(b)}$ are mutually orthogonal,

$$\left(\underline{\dot{e}}^{(b)}\right)^{+} \underline{e}^{(b)} = 0, \tag{6.32a}$$

possess the same norm $N^{(b)}$,

$$\left(\dot{\underline{e}}^{(b)}\right)^{+}\dot{\underline{e}}^{(b)} = (N^{(b)})^2 \tag{6.32b}$$

and are mutually interrelated by a metric spinor $\underline{\underline{c}}$ ($c_{11}=0=c_{22}$ and $c_{12}=-1=c_{21}$) [3]:

$$\dot{\underline{e}}^{(b)} = \underline{\underline{c}}^{-1}\overline{\underline{e}}^{(b)}, \qquad \underline{e}^{(b)} = \underline{\underline{c}}\,\overline{\dot{\underline{e}}}^{(b)}. \tag{6.32c}$$

For any dotted beam field the amplitude-polarization decomposition (6.15) can be also directly applied. In general, the beam amplitude and the beam polarization are expressed in the input (b=i) and output (b=t or b=r) planes by a superposition of independent spinor fields of two types $\underline{e}^{(b)}$ and $\dot{e}^{(b)}$, with different amplitudes $\widetilde{E}^{(b)}$ and $\widetilde{\dot{E}}^{(b)}$, respectively. For some preferred, say forward, propagation direction (along the z-axis) the beam field is expressed by:

$$\begin{aligned}
&\underline{E}_{+}^{(b)}(x,y) = (2/Y^{(b)})^{1/2}(2\pi)^{-2}\iint\underline{\widetilde{E}}_{+}^{(b)}(k_x^{(b)},k_y)\,dk_x^{(b)}dk_y,\\
&\underline{\widetilde{E}}_{+}^{(b)}(k_x^{(b)},k_y) = \widetilde{E}^{(b)}(k_x^{(b)},k_y)\,\underline{e}^{(b)}\exp[+i(k_x^{(b)}x+k_y y)]\\
&\qquad\qquad + \widetilde{\dot{E}}^{(b)}(k_x^{(b)},k_y)\,\dot{\underline{e}}^{(b)}\exp[+i(k_x^{(b)}x+k_y y)],
\end{aligned} \tag{6.33}$$

where, in general, the spinors $\underline{e}^{(b)}$ and $\dot{\underline{e}}^{(b)}$ may also depend on $k_x^{(b)}$ and k_y. In the opposite, backward direction, the beam field $\underline{E}_{-}^{(b)}$ is expressed by the complex conjugate of $\underline{E}_{+}^{(b)}$.

The normalisation of the beam amplitudes $E^{(b)}{}_{(new)} = E^{(b)}{}_{(old)}(\frac{1}{2}Y^{(b)})^{+1/2}$, the polarization parameters $\chi^{(b)}{}_{(new)} = \chi^{(b)}{}_{(old)}/c_z^{(b)2}$, $c_z^{(b)} \equiv \cos\vartheta_z^{(b)}$, and the amplitude parameters $\kappa^{(b)}{}_{(new)} = \kappa^{(b)}{}_{(old)}(\frac{1}{2}Y^{(b)})$, is applied in Eqs. (6.33) to make the time-averaged power flow density $\frac{1}{2}\mathrm{Re}[\underline{E}\times\overline{\underline{H}}]_z$ in the direction normal to the (planar) optical structure, independent of the characteristic medium admittances $Y^{(b)} = (\varepsilon^{(b)}/\mu^{(b)})^{1/2}$ and impedances $Z^{(b)} = 1/Y^{(b)}$ of both media [1]. Note that, in our notation, $Y^{(b)} = Y_1$ for b=i,r and $Y^{(b)} = Y_2$ for b=t. The components $\widetilde{E}_x$ and $\widetilde{E}_y$ of the Jones vectors (6.28) are normalised

in (6.33) by the wave admittances $Y_{\parallel}^{(b)} = Y^{(b)}/c_z^{(b)}$ and $Y_{\perp}^{(b)} = Y^{(b)}c_z^{(b)}$, respectively. Thus $\widetilde{E}_{x(new)} = \widetilde{E}_{x(old)}(\frac{1}{2}Y_{\parallel}^{(b)})^{1/2}$ and $\widetilde{E}_{y(new)} = \widetilde{E}_{y(old)}(\frac{1}{2}Y_{\perp}^{(b)})^{1/2}$.

It is already taken into account in Eqs. (6.33) that the vectors $\underline{\mathrm{E}}_{+}^{(b)}$ and $\underline{\mathrm{E}}_{-}^{(b)}$ are complex conjugate of each other. For the undotted part of the beam field, the complex conjugation $\overline{\underline{\mathrm{E}}}_{+}^{(b)} = \underline{\mathrm{E}}_{-}^{(b)}$ replaces the forward waves in $\underline{\mathrm{E}}_{+}^{(b)}$, that is that part of $\underline{\mathrm{E}}_{+}^{(b)}$ with the spectral amplitudes $\widetilde{E}^{(b)}$ propagating in the z-direction, by the backward waves in $\underline{\mathrm{E}}_{-}^{(b)}$, that is by that part of $\underline{\mathrm{E}}_{-}^{(b)}$ with the spectral amplitudes $\overline{\widetilde{E}}^{(b)}$ propagating in the reverse z-direction. The dotted parts of the beam field, with the spectral amplitudes $\overline{\widetilde{E}}^{(b)}$ and $\overline{\dot{\widetilde{E}}}^{(b)}$, propagate in reverse directions with respect to the undotted parts.

In an inhomogeneous medium both types (undotted and dotted) of the field are coupled by the wave impedance of the medium [9]. On the other hand, in a homogeneous isotropic medium these parts of the field are decoupled and the polarization and spatial structure of the propagating beam are mutually independent. The beam propagation does not influence the beam polarization and the state of beam polarization does not change the beam spatial structure during the propagation. Therefore only one type of the polarization spinors is necessary to describe the polarization of the beam propagating inside the layers of such media.

On the other hand, the beam transmission and refraction at dielectric interfaces obviously are polarization-dependent, because the transmission and reflection coefficients are such. However, this dependence has been already accounted for by the definitions of the different reference frames (6.15)-(6.17) and (6.28)-(6.30) of the beam polarization, assigned to the incident, trans-mitted and reflected beams by the scalar equations (6.26) for the beam polar-ization and amplitude parameters. Therefore, for the multilayered structure composed of isotropic and homogeneous dielectric layers, the incidence with one type of (undotted or dotted) polarization vectors does not excite the beams with the second type of polarization. For this reason, in the following, only the undotted spinors (6.17), together with the associated with them amplitudes (6.16) and their transformations (6.20)-(6.25), will be used. Still, however, the beam reference polarization frames can be built only by

use of both types of these spinors. That will be shown in the example given in Section 7.

6.5 Polarization matrices and Stokes vectors

Some reference to the polarization matrices, Stokes vectors, as well as to their transformations, should also be made. Their definitions are well known [10-12]. However, for the amplitude-polarization field decomposition (6.15)-(6.26) they attain a form specific only for the approach presented in this book.

We refer to Hermitian matrices $\underline{\underline{C}}^{(b)} = \underline{e}^{(b)}\underline{e}^{(b)+} = \underline{\underline{C}}^{(b)+}$, defined by their eigenvectors $\underline{e}^{(b)}$ and $\dot{\underline{e}}^{(b)}$ and eigenvalues $N^{(b)2}$ and 0, respectively:

$$\underline{\underline{C}}^{(b)} = \begin{bmatrix} C_{xx}^{(b)} & C_{xy}^{(b)} \\ C_{yx}^{(b)} & C_{yy}^{(b)} \end{bmatrix} = \begin{bmatrix} (\chi^{(b)}\overline{\chi}^{(b)})^{+1/2} & (\chi^{(b)}/\overline{\chi}^{(b)})^{+1/2} \\ (\chi^{(b)}/\overline{\chi}^{(b)})^{-1/2} & (\chi^{(b)}\overline{\chi}^{(b)})^{-1/2} \end{bmatrix},$$

$$\underline{\underline{C}}^{(b)}\underline{e}^{(b)} = N^{(b)2}\underline{e}^{(b)}, \qquad \underline{\underline{C}}^{(b)}\dot{\underline{e}}^{(b)} = 0, \tag{6.34}$$

as to the spectral polarization matrices, rather than to the spectral coherence matrices [10-11], because only completely polarized beams are considered in this book. These matrices are normalised here by $\left|\widetilde{E}^{(b)}\right|^2$, in order to make them dependent only on the polarization parameters $\chi^{(b)}$.

As usual, $\underline{\underline{C}}^{(b)}$ can be written as linear combinations of the Pauli and identity matrices [3]:

$$\underline{\underline{C}}^{(b)} = \sum_{j=1}^{4} \Sigma_j^{(b)} \underline{\underline{\sigma}}_j,$$

$$\underline{\underline{\sigma}}_1 = \begin{bmatrix} 0 & 1 \\ 1 & 0 \end{bmatrix}, \qquad \underline{\underline{\sigma}}_2 = \begin{bmatrix} 0 & -i \\ i & 0 \end{bmatrix},$$

$$\underline{\underline{\sigma}}_3 = \begin{bmatrix} 1 & 0 \\ 0 & -1 \end{bmatrix}, \qquad \underline{\underline{\sigma}}_4 = \begin{bmatrix} 1 & 0 \\ 0 & 1 \end{bmatrix}, \tag{6.35}$$

where $\underline{\underline{\sigma}}_3 = -\underline{\underline{c}}$ for direct correspondence with notions of special relativity [3], a convention different from the usual available in optical textbooks [10-

11] is given. Coefficients $\Sigma_j^{(b)}$ of these expansions yield the Stokes four-component real vectors $\underline{\Sigma}^{(b)}$ for coherent beams:

$$\underline{\Sigma}^{(b)T} = \tfrac{1}{2}\left[\Sigma_{xy}^{(b)} + \Sigma_{yx}^{(b)},\, i(\Sigma_{xy}^{(b)} - \Sigma_{yx}^{(b)}),\, \Sigma_{xx}^{(b)} - \Sigma_{yy}^{(b)},\, \Sigma_{xx}^{(b)} + \mathrm{T}_{yy}^{(b)}\right]. \tag{6.36}$$

The first two components of $\underline{\Sigma}^{(b)}$ depend on the phase $(\chi^{(b)}/\overline{\chi}^{(b)})^{+1/2}$ and the last two components depend on the amplitude $(\chi^{(b)}\overline{\chi}^{(b)})^{+1/2}$ of the polarization parameter $\chi^{(b)}$. The determinant of $\underline{\underline{C}}^{(b)}$ is equal to the Stokes interval $\Delta\Sigma^{(b)}$ squared:

$$\det \underline{\underline{C}}^{(b)} = \Sigma_1^{(b)2} + \Sigma_2^{(b)2} + \Sigma_3^{(b)2} - \Sigma_4^{(b)2} = \Delta\Sigma^{(b)2} = 0 \tag{6.37}$$

and both of them equal zero for completely polarized beams.

Any complex two-by-two matrix $\underline{\underline{A}}$, representing action of the non-image-forming optical element [12] on the beam polarization, transforms the polarization spinors and polarization matrices according to the relations:

$$\underline{e}'^{(b)} = \underline{\underline{A}}\,\underline{e}^{(b)},$$

$$\underline{\underline{C}}'^{(b)} = \underline{\underline{A}}\,\underline{\underline{C}}^{(b)}\,\underline{\underline{A}}^{+}, \tag{6.38}$$

where the matrix $\underline{\underline{A}}$ induces also transformations of the Stokes vectors $\underline{\Sigma}^{(b)}$ corresponding to the polarization matrices $\underline{\underline{C}}^{(b)}$. In the general case of polarized, partially polarized or unpolarized beams, if $\underline{\underline{A}}$ is unimodular, then $\underline{\underline{A}}$ leaves a norm of the Stokes interval $\Delta C^{(b)}$ invariant, per analogy to Lorentz transformations of a Minkowskian space-time four-vector $[x, y, z, ct]^T$.

The transformations $\underline{\underline{A}}$ constitute the group SL(2,C) of the complex unimodular two-by-two transformations and as such, they form a two-dimensional representation (by a two-to-one homomorphism) of the restricted Lorentz group [3], which is usually denoted by SO(3,1). It is well known [12] that the action of the non-image-forming polarization devices on optical field is represented by elements of this Lorentz group. Therefore the

transformations $\underline{\underline{A}}$ represent also the action of multilayers on the polarization of optical beams.

6.6 Scattering and transfer matrices

With the definitions of the polarization reference frames (6.17) the derivation of the scattering matrix of the multilayered structure is straightforward. For the 2D case the time reversibility [1] yields the Stokes relations which specify the complex reflection and transmission TM/TE coefficients for incidence from the substrate. These coefficients are indicated here by primes, contrary to the "unprimed" coefficients for the incidence from the superstrate (cf. Fig. 6.2). For the incidence from the superstrate (substrate) the beam fields are represented by $\underline{E}_{+}^{(b)}$ ($\underline{E}_{-}^{(b)}$) in the field representation (6.33).

For the 2D case the most general Stokes relations can be derived from the time-reversal and power conservation requirements applied to the multilayered structure [1]. Details of this issue are well understood. They can be found e.g. in Ref. [14] and in references therein. Here, let us only state that for the 2D case, the Stokes and power conservation relations read in the region outside the multilayer:

$$r_a' = -\bar{r}_a\, t_a / \bar{t}_a\,, \qquad t_a' = (1 - r_a \bar{r}_a)/\bar{t}_a\,,$$

$$t_a' = t_a\,, \qquad |\, r_a\,|^2 + |\, t_a\,|^2 = 1\,, \tag{6.39}$$

a=||, ⊥, and the "primed' coefficients are completely determined by the "unprimed" coefficients. Note that in the four equations (6.39) only three of them are independent.

Next, let us return to the 3D case of beam scattering. In the language of the amplitude-polarization field decomposition, the above relations yield analogous conditions for the beam amplitude and polarization coefficients:

$$r_\kappa^{'} = \bar{r}_\kappa\, t_\kappa / \bar{t}_\kappa\,, \qquad r_\chi^{'} = \bar{r}_\chi\, t_\chi / \bar{t}_\chi\,,$$

$$t_\kappa^{'} = t_\kappa\,, \qquad t_\chi^{'} = t_\chi\,. \tag{6.40}$$

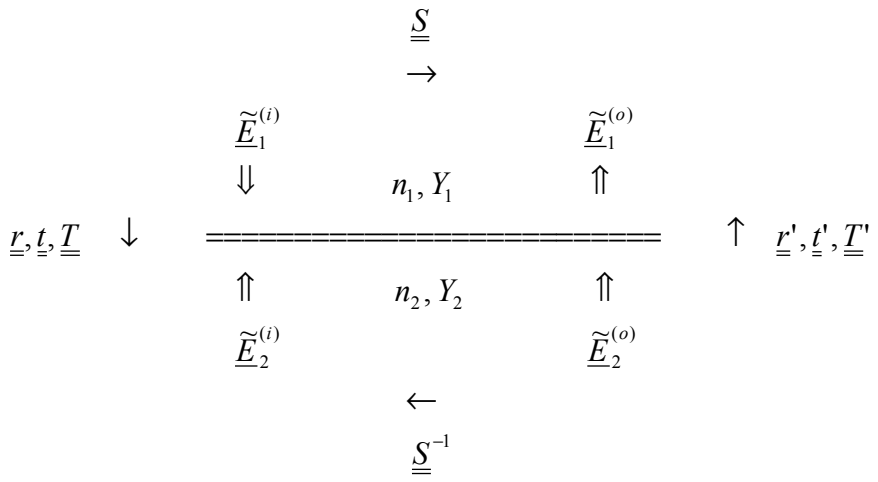

Figure 6.2. Schematic diagram with notation for reflection, transmission, scattering and transfer matrices. Incidence need not be normal.

Moreover, as a result of the diagonal form of the matrices for reflection (6.7) and transmission (6.12), and thanks to the normalisation of the field amplitudes applied in (6.33), the 3D version of the Stokes and power conservation relations (6.39) read:

$$\underline{\underline{r}}' = -\bar{\underline{\underline{r}}}\,\underline{\underline{t}}\,\bar{\underline{\underline{t}}}^{-1}, \qquad \underline{\underline{t}}' = (\underline{\underline{1}} - \underline{\underline{r}}\,\bar{\underline{\underline{r}}})\bar{\underline{\underline{t}}}^{-1},$$

$$\underline{\underline{t}}' = \underline{\underline{t}}, \qquad \underline{\underline{r}}\,\bar{\underline{\underline{r}}} + \underline{\underline{t}}\,\bar{\underline{\underline{t}}} = \underline{\underline{1}}, \tag{6.41}$$

where $\underline{\underline{1}}$ stands for the two-by-two identity matrix. In spite of their two-by-two matrix form, the Stokes relations (6.41) for 3D case are identical to those (6.39) of the 2D case. The third equation in (6.41) directly displays the reciprocity feature of the optical system under consideration. Thanks to the diagonal form of all the reflection and transmission matrices, the last equation in (6.41) (for power conservation) can be derived from the first three equations, similarly to the 2D case. The 'unprimed' and 'primed' scattering matrices are equal for transmission and their matrix elements are of equal magnitudes for reflection. For a symmetric structure $\underline{\underline{r}}' = \underline{\underline{r}}$, that is $\underline{\underline{r}}\,\bar{\underline{\underline{t}}} = -\bar{\underline{\underline{r}}}\,\underline{\underline{t}}$ and a phase of the field for transmission is shifted by $\pm\pi/2$ from a phase for reflection.

The transmission (6.7) and reflection (6.12) matrices are diagonal, with their elements (6.8) and (6.14) known and the Stokes relations (6.41) explicitly given. Therefore the scattering matrix for the 3D problem is also completely determined. Denote the field vectors of the beam field incident from the superstrate by $\underline{\widetilde{E}}_1^{(\mathrm{i})}=\widetilde{E}_1^{(\mathrm{i})}\underline{e}_1^{(\mathrm{i})}$, that one incident from the substrate by $\underline{\widetilde{E}}_2^{(\mathrm{i})}=\widetilde{E}_2^{(\mathrm{i})}\underline{e}_2^{(\mathrm{i})}$ and the outgoing beam fields by $\underline{\widetilde{E}}_1^{(o)}=\widetilde{E}_1^{(o)}\underline{e}_1^{(o)}$ and $\underline{\widetilde{E}}_2^{(o)}=\widetilde{E}_2^{(o)}\underline{e}_2^{(o)}$, respectively (cf. Fig. 6.2). The relation between the outgoing (output) beams and the incident (input) beams is then given by the four-by-four scattering matrix $\underline{\underline{S}}$:

$$\begin{bmatrix} \underline{\widetilde{E}}_1^{(o)} \\ \underline{\widetilde{E}}_2^{(o)} \end{bmatrix} = \underline{\underline{S}} \begin{bmatrix} \underline{\widetilde{E}}_1^{(i)} \\ \underline{\widetilde{E}}_2^{(i)} \end{bmatrix}, \qquad \underline{\underline{S}} = \begin{bmatrix} \underline{\underline{r}} & \underline{\underline{t}}' \\ \underline{\underline{t}} & \underline{\underline{r}}' \end{bmatrix}, \tag{6.42}$$

where the lower bar indicates matrices and vectors in four-dimensional vector space. The matrix $\underline{\underline{S}}$ is symmetric, i.e. $\underline{\underline{t}}'=\underline{\underline{t}}$ and its two-by-two matrix elements $\underline{\underline{r}}$, $\underline{\underline{t}}$, $\underline{\underline{r}}'$ and $\underline{\underline{t}}'$ are given by Eqs. (6.7), (6.8), (6.12), (6.14) and (6.41). The scattering matrix (6.42) for the 3D problem follows directly the relations known from the 2D problems. For the isotropic lossless structure, the scattering matrix satisfies the reciprocity and time reversibility relations:

$$\underline{\underline{S}}=\underline{\underline{S}}^{T}, \qquad \underline{\underline{S}}^{-1}=\overline{\underline{\underline{S}}}. \tag{6.43}$$

Therefore the scattering matrix is unitary; $\underline{\underline{S}}\,\underline{\underline{S}}^{+}=\underline{\underline{1}}$, according to the power conservation requirements. Moreover, in the partial transmission case, i.e. when $\underline{\underline{r}}=\overline{\underline{\underline{r}}}$ and $\underline{\underline{t}}=\overline{\underline{\underline{t}}}$, the matrix $\underline{\underline{S}}$ is unimodular; $\det\underline{\underline{S}}=-1$, and in addition, the fundamental invariance of multilayers [5]:

$$\underline{\widetilde{E}}_1^{(\mathrm{i})2}-\underline{\widetilde{E}}_1^{(\mathrm{o})2}=-(\underline{\widetilde{E}}_2^{(\mathrm{o})2}-\underline{\widetilde{E}}_2^{(\mathrm{i})2}), \tag{6.44}$$

or equivalently $\underline{\underline{T}}^{T}\underline{\underline{\sigma}}_3\underline{\underline{T}}=\underline{\underline{\sigma}}_3$, also holds in this case. A definition of the four-by-four transfer matrix $\underline{\underline{T}}$ is given below. The four-by-four matrix $\underline{\underline{\sigma}}_3$ is obtained from the two-by-two matrix $\underline{\underline{\sigma}}_3$ (6.35) by replacing in the matrix components the unit scalars ± 1 by the two-by-two unit matrices $\pm\underline{\underline{1}}$.

Let us define the "upper" $\underline{\widetilde{E}}_1^T = [\underline{\widetilde{E}}_1^{(i)}, \underline{\widetilde{E}}_1^{(o)}]$ and "lower" $\underline{\widetilde{E}}_2^T = [\underline{\widetilde{E}}_2^{(i)}, \underline{\widetilde{E}}_2^{(o)}]$ field-vectors above and below the multilayer, respectively, (cf. Fig. 6.2) in a four-dimensional vector space with a field norm $\left|\underline{\widetilde{E}}_j\right|^2 = \underline{\widetilde{E}}_j^+ \underline{\underline{\sigma}}_3 \underline{\widetilde{E}}_j$; j=1,2. In this space, the scattering matrix $\underline{\underline{S}}$ and its inverse $\underline{\underline{S}}^{-1}$ are equivalent to the four-by-four matrices $\underline{\underline{T}}$ and $\underline{\underline{T}}'$ of the 3D beam transfer through the multilayer. Action of these matrices reads, for incidence from the top of the structure:

$$\begin{bmatrix} \underline{\widetilde{E}}_2^{(o)} \\ \underline{\widetilde{E}}_2^{(i)} \end{bmatrix} = \underline{\underline{T}} \begin{bmatrix} \underline{\widetilde{E}}_1^{(i)} \\ \underline{\widetilde{E}}_1^{(o)} \end{bmatrix}, \qquad \underline{\underline{T}} = \begin{bmatrix} \underline{\underline{t}}^{-1} & -\underline{\underline{r}}\,\underline{\underline{t}}^{-1} \\ -\underline{\underline{r}}\,\underline{\underline{t}}^{-1} & \underline{\underline{t}}^{-1} \end{bmatrix}, \qquad (6.45a)$$

and for incidence from the bottom of the structure:

$$\begin{bmatrix} \underline{\widetilde{E}}_1^{(o)} \\ \underline{\widetilde{E}}_1^{(i)} \end{bmatrix} = \underline{\underline{T}}' \begin{bmatrix} \underline{\widetilde{E}}_2^{(i)} \\ \underline{\widetilde{E}}_2^{(o)} \end{bmatrix} \qquad \underline{\underline{T}}' = \begin{bmatrix} \underline{\underline{t}}^{-1} & +\underline{\underline{r}}\,\underline{\underline{t}}^{-1} \\ +\underline{\underline{r}}\,\underline{\underline{t}}^{-1} & \underline{\underline{t}}^{-1} \end{bmatrix}. \qquad (6.45b)$$

For the multilayer taken in reverse order the transfer matrix reads $\underline{\underline{T}}' = \underline{\underline{T}}^{-1}$. Both matrices $\underline{\underline{T}}$ and $\underline{\underline{T}}'$ are unimodular; $\det \underline{\underline{T}} = 1 = \det \underline{\underline{T}}'$, with the property $\underline{\underline{T}}^+ \underline{\underline{\sigma}}_3 \underline{\underline{T}} = \underline{\underline{\hat{\sigma}}}_3$. This means that the norm $\left|\underline{\widetilde{E}}_j\right|$ and the field power density are preserved by action of $\underline{\underline{T}}$ on the field-vector $\underline{\widetilde{E}}_1$:

$$|\underline{\widetilde{E}}_2^{(o)}|^2 - |\underline{\widetilde{E}}_2^{(i)}|^2 = -(|\underline{\widetilde{E}}_1^{(o)}|^2 - |\underline{\widetilde{E}}_1^{(i)}|^2). \qquad (6.46)$$

For the symmetric case $\underline{\underline{T}}' = \underline{\underline{T}}$ and the off-diagonal elements of $\underline{\underline{T}}$ and $\underline{\underline{T}}'$ are purely imaginary, that is $\underline{\underline{r}}\,\underline{\underline{t}}^{-1} = -\underline{\underline{r}}\,\underline{\underline{t}}^{-1}$. The matrices $\underline{\underline{T}}$ and $\underline{\underline{T}}'$ are given in Eqs. (6.45) in the most general form, valid for multilayers in which total internal reflection (TIR) or frustrated total internal reflection (FTIR) may occur.

The scattering matrices $\underline{\underline{S}}$ (6.42) and the transfer matrices $\underline{\underline{T}}$ (6.45) are semi-diagonal, i.e. their matrix elements are diagonal. Therefore, all features of the geometrical interpretation of the plane wave or 2D beam propagation in multilayers, that have been described for example in Refs. [5-8] and [12-13], can be directly translated into the 3D beam case. Only for this reason, the

formalism presented should be regarded as a convenient tool for treatment of the propagation and scattering problems of 3D beams of arbitrary polarization at multilayered structures composed, in general, of linear [2], [4] as well as nonlinear [4], [15] interfaces and isotropic layers.

In addition, however, the transmission $\underline{\underline{t}}_p$ (6.24) and reflection $\underline{\underline{r}}_p$ (6.25) polarization matrices, from which the scattering and transfer matrices have been built, are also unimodular; $\det \underline{\underline{r}}_p = 1 = \det \underline{\underline{t}}_p$. Thus, the transformations $\underline{\underline{t}}_p$ and $\underline{\underline{r}}_p$ are also examples of the unimodular two-by-two complex matrix transformations $\underline{\underline{A}}$ (6.36) of the beam polarization spinors $\underline{e}^{(b)}$ (6.17) and polarization matrices $\underline{\underline{C}}^{(b)}$ (6.38). These transformations also correspond to the six-parameter restricted Lorentz transformations of the Stokes vectors $\underline{\Sigma}^{(b)}$ and provide one more explicit connection with the relativistic-like treatment of multilayer optics elements.

6.7 Anti-reflection multilayer

Still, the amplitude-polarization decomposition (6.15)-(6.17) and the definitions of the polarization frames (6.32)-(6.33) have not been explicitly applied yet. To demonstrate the strength of the approach let us consider, as an example, the anti-reflection multilayer.

In this case $|r_\parallel| = |r_\perp| = 0$ and $|t_\parallel| = |t_\perp| = 1$. The transmission coefficients (6.8) are defined by:

$$t_\parallel = \exp(i\phi_{t\parallel}), \qquad t_\perp = \exp(i\phi_{t\perp}), \tag{6.47}$$

and polarization $\chi^{(t)}$ and amplitude $\kappa^{(t)}$ parameters for transmitted beam are related to those of the incident beam $\chi^{(i)}$ and $\kappa^{(i)}$, respectively, by the polarization t_χ and amplitude t_κ coefficients for transmission (6.26):

$$\chi^{(t)} = t_\chi \chi^{(i)}, \qquad t_\chi = \exp(2i\phi_{t-}), \tag{6.48}$$

$$\kappa^{(t)} = t_\kappa \kappa^{(i)}, \qquad t_\kappa = \exp(2i\phi_{t+}), \tag{6.49}$$

where

$$\phi_{t-} = \tfrac{1}{2}(\phi_{t||} - \phi_{t\perp}),$$

$$\phi_{t+} = \tfrac{1}{2}(\phi_{t||} + \phi_{t\perp}) \tag{6.50}$$

are phase increments attributed to the transmitted beam polarization and complex amplitude, respectively.

Using of the unitary (up to a norm) transformation:

$$\underline{\underline{U}}^{(b)} = (N^{(b)})^{-2}\begin{bmatrix} (\bar{\chi}^{(b)})^{+1/2} & (\bar{\chi}^{(b)})^{-1/2} \\ (\chi^{(b)})^{-1/2} & -(\chi^{(b)})^{+1/2} \end{bmatrix},$$

$$(N^{(b)})^2 \underline{\underline{U}}^{(b)+} = \underline{\underline{U}}^{(b)-1}, \tag{6.51}$$

the old polarization reference frame $(\underline{e}_x, \underline{e}_y)$ is replaced by the new polarization reference frames $(\underline{e}^{(b)}, \underline{\dot{e}}^{(b)})$, attributed separately to the incident (b=i) and transmitted (b=t) beams. That yields the base spinors,

$$\underline{e}^{(b)} \to \underline{\underline{U}}^{(b)} \underline{e}^{(b)} = \begin{bmatrix} 1 \\ 0 \end{bmatrix},$$

$$\underline{\dot{e}}^{(b)} \to \underline{\underline{U}}^{(b)} \underline{\dot{e}}^{(b)} = \begin{bmatrix} 0 \\ 1 \end{bmatrix}, \tag{6.52}$$

polarization matrices

$$\underline{\underline{C}}^{(b)} \to \underline{\underline{U}}^{(b)} \underline{\underline{C}}^{(b)} \underline{\underline{U}}^{(b)+} = \begin{bmatrix} 1 & 0 \\ 0 & 0 \end{bmatrix}, \tag{6.53}$$

and Stokes vectors in a form common, this time, for both beams:

$$\underline{\Sigma}^{(b)} \to [0,0,½,½], \tag{6.54}$$

where new notation in new reference frames has been replaced by arrows.

Now, the transmission matrix resolves into a product $t_\kappa^{1/2}\,\underline{\underline{1}}$ of the amplitude coefficient and the identity matrix, that is:

$$\underline{\underline{t}} \to \underline{\underline{U}}^{(t)}\,\underline{\underline{t}}\,\underline{\underline{U}}^{(i)+} = \underline{\underline{1}} \exp(i\phi_{t+}), \tag{6.55}$$

and constitutes anti-diagonal and diagonal elements of the scattering and transfer matrices, respectively:

$$\underline{\underline{S}} \to \begin{bmatrix} 0 & \underline{\underline{1}}\exp(i\phi_{t+}) \\ \underline{\underline{1}}\exp(i\phi_{t+}) & 0 \end{bmatrix}, \tag{6.56}$$

$$\underline{\underline{T}} \to \begin{bmatrix} \underline{\underline{1}}\exp(i\phi_{t+}) & 0 \\ 0 & \underline{\underline{1}}\exp(-i\phi_{t+}) \end{bmatrix}, \tag{6.57}$$

determined by only one parameter φ_{t+}, that is by changes of the complex amplitude of the transmitted beam. Therefore, the anti-reflection multilayer is equivalent to the free-propagation with the phase increment equal to φ_{t+}.

In fact, the matrices (6.55)-(6.57) are dependent on both the scalar coefficients (6.48)-(6.49) for the beam transmission: the polarization coefficient t_χ and the amplitude coefficient t_κ. In the amplitude-polarization field decomposition (6.15), the coefficient t_χ determines the beam Jones vector $\underline{e}^{(t)}$ together with the polarization reference frame $(\underline{e}^{(t)}, \dot{\underline{e}}^{(t)})$ (6.50) and thus the transmitted beam polarization. On the other hand, the coefficient t_κ yields the beam field spectral amplitude $\widetilde{E}^{(t)}$ (6.22), and thus the transmitted beam field $\underline{\widetilde{E}}^{(t)} = \underline{\underline{t}}\,\underline{\widetilde{E}}^{(i)}$ (6.20) in this frame, that is t_κ describes the transmitted beam amplitude, phase and shape changes. In this way, the vector problem of scattering of 3D beams with arbitrary polarization is reduced to two scalar problems: the first for the beam polarization and the second one for the beam complex amplitude or the beam shape.

The diagonal form of the transfer matrix (6.57) clearly demonstrates how the field amplitude-polarization decomposition may simplify the 3D problem of beam scattering. Further, numerical analysis of the problem can be accomplished on the way already presented for the Gaussian incidence at a single dielectric interface: for the beam polarization - in Ref. [2] and for the beam amplitude, phase and shape - in Ref. [4].

6.8 Comments and conclusions

Explicit expressions for the transmission, reflection, scattering and transfer matrices are given for 3D beams of arbitrary polarization, incident upon the

dielectric multilayered structure. Some of these expressions concerning a single interface have been presented by the author in Ref. [2]. They are collected together here for the sake of clarity and attempts to make the whole text more transparent to the reader. The very idea to generalise the scattering matrix for 2D beams into the 3D beam case should not be new. However, as far as it is known to the author, the explicit expressions for this matrix elements presented here are new, at least their diagonal, attractive for further analysis, form. This diagonal form of the matrices derived results from the polarization dependence imposed on the spectral transmission and reflection coefficients of beams. That, in turn, leads to the so direct correspondence between 2D and 3D problems of the beam scattering at multilayers. In short, if the Fresnel transmission t_p, t_s and reflection r_p, r_s coefficients for the multilayered structure in the 2D problem are known, then the solution to the 3D problem can readily be explicitly given.

The expressions presented are valid in the general case, including TIR and FTIR, that is now the most interesting cases of beam scattering with presence of evanescent waves. The approach bases on the replacement of the TM and TE reference frames by the beam polarization frames, separately specified for each beam under consideration, as well as on the amplitude-polarization decomposition of the 3D beam fields. Such a formulation of the beam scattering problem is, to the best of the author's knowledge, also new.

The approach leads, in essence, to simpler, although still rigorous, scattering problem of seeking for the scalar field amplitudes in the spectral decomposition of the beam, with the polarization reference frames determined also by scalar relations. The solution of the 3D beam scattering problem in the spatial domain can be readily obtained by next steps of this analysis and that has been presented and numerically verified in Ref. [4]. Then the difference between the 2D and 3D cases becomes vivid, the most in the presence of transverse changes of the beam polarization, amplitude and spatial structure [2], as it was shown for a single interface some time ago [16].

Transverse effects of beam deformations have been also discussed in the case of anisotropic uniaxial interfaces, e.g., in Refs. [17-19]. A method applied in these analyses followed closely the aberrationless approach devised

previously for 3D beams at an isotropic interface [16]. In a recent paper [19] some comments have been also given pertaining to the rather old issue (cf. Ref. [16]) of non-existence/existence of transverse deformations of beams which possess linear TM or TE polarization. To make this issue clear let us recall that, even in the case of an isotropic planar scattering structure, linear TM or TE polarization of the incident beam and symmetry of this beam field intensity distribution with respect to the main plane-of-incidence, the beam-structure configuration generally remains asymmetric with respect to this incidence plane. That is due to the specified direction of the incident beam-field polarization [16].

As a result of this asymmetry, the transverse deformations of the reflected and/or transmitted beam generally exist, although only in the opposite orthogonal polarization beam component, that is in the TE reflected or transmitted field component for the incident TM polarization or vice versa [16]. They contribute to the overall beam complex amplitude and polarization [2]. Note that, even for the pure TM or TE linear polarization of the 3D incident beam at 2D isotropic planar structures, the other, orthogonal beam field components still are, in general, excited during beam transmission and beam reflection [16].

Certainly, the TM or TE transmitted/reflected field components also exist and may be stronger for the elliptic polarization (including a circular one) of the incident beam, as in this case the incident beam field consists of both the linear TM and TE polarization components of finite magnitudes. The problem becomes even more involved for beams of complex spatial structure, like, for example, the Bessel-Gauss beams of zero order [20] or higher order [21]. In general, the transverse effects - in a form of beam deformations, shifts or orthogonal field component excitations - are always present for 3D beam scattering at isotropic structures [2], [4], [16].

The characteristic feature of the transverse electromagnetic waves or 2D beams propagating in an isotropic layered medium is the possible split of their two, TM and TE, independent normal modes. That is not so for the case of 3D beams. Therefore, the formalism presented in this chapter may appear suitable in solving problems concerning polarization of 3D beams and wave packets at isotropic and anisotropic, periodic and aperiodic, linear and nonlinear multilayers, as encountered, for example, in ellipsometry [22],

near-field microscopy [23], or in microwave [24] and optical [25] tunnelling. A similar treatment can be also applied to scattering problems in acoustics, mechanics and quantum electronics [26-28]. In general, the method seems to be useful in any analysis of 3D beams and wave packets of arbitrary polarization and complex shape, under their interaction with multilayers.

Main content of this chapter has been published in Journal of Technical Physics ***45****, 121-139 (2004).*

References

[1] H. A. Haus, *Waves and Fields in Optoelectronics,* (Prentice-Hall, Englewood Cliffs, 1984).

[2] W. Nasalski, "Amplitude-polarization representation of three-dimensional beams at a dielectric interface", J. Opt. A: Pure Appl. Opt. **5**, 128-136 (2003).

[3] O. Barut, *Electrodynamics and Classical Theory of Fields and Particles*, Macmillan Company, New York, 1964.

[4] W. Nasalski, "Three-dimensional beam reflection at dielectric interfaces", Optics Commun. **197**, 217-233 (2001).

[5] J. M. Vigoureux, R. Giust, "New relations in the most general expressions of the transfer matrix", Optics Commun. **186**, 21-25 (2000).

[6] J. J. Monzon and L. L. Sanchez-Soto, "Fresnel formulas as Lorentz transformations", J. Opt. Soc. Am. A **17**, 1475-1481 (2000).

[7] J. J. Monzon, L. L. Sanchez-Soto, "A simple optical demonstration of geometric phases from multilayer stacts: the Wigner angle as an anholonomy", J. Mod. Opt. **48**, 21-34 (2001).

[8] R. Giust, J. M. Vigoureux, "Hyperbolic representation of light propagation in a multilayer medium", J. Opt. Soc. Am. A **19**, 378-384 (2002).

[9] I. Białynicki-Birula, "Photon wave function", Prog. Optics, **36**, 245-294 (1996).

[10] L. Mandel and E. Wolf, *Optical coherence and quantum optics* (Cambridge University Press, Cambridge, 1995).

[11] J. Perina, *Coherence of light* (Reidel, Dordrecht, 1985).

[12] T. Opatrný and J. Peřina, "Non-image-forming polarization optical devices and Lorentz transformations - an analogy", Phys. Lett. A **181**, 199-202 (1993).

[13] H. H. Arsenault and B. Macukow, "Factorization of the transfer matrix for symmetrical optical systems", J. Opt. Soc. Am **73**, 1350-1359 (1983).

[14] J. J. Monzon, T. Yonte, L. L. Sanchez-Soto, J. F. Cariñena, "Geometrical setting for the classification of multilayers", J. Opt. Soc. Am. A **19**, 985-991 (2002).

[15] W. Nasalski, "Modelling of beam reflection at a nonlinear-linear interface", J. Opt. A: Pure Appl. Opt. **2**, 433-441 (2000).

[16] W. Nasalski, "Longitudinal and transverse effects of nonspecular reflection", J. Opt. Soc. Am. A **13**, 172-181 (1996).

[17] N. Bonomo and R. A. Depine, "Nonspecular reflection of ordinary and extraordinary beams in uniaxial media", J. Opt. Spc. Am. A **14**, 3402-3409 (1997).

[18] N. E. Bonomo and R. A. Depine, "Aberrationless approach for diffraction of pulses at linear interfaces", Optics Commun. **190**, 19-27 (2001).

[19] L. I. Perez, "Nonspecular transverse effects of polarized and unpolarized symmetric beams in isotropic-uniaxial interfaces", J. Opt. Soc. Am A **20**, 741-751 (2003).

[20] F. Gori, G. Guattari and C. Padovani, "Bessel-Gauss beams", Optics Commun. **64**, 491-495 (1987).

[21] V. Bagini, F. Frezza, M. Santarsiero, G. Schettini and G. Schirripa Spagnolo, "Generalized Bessel-Gauss beams", J. Mod. Optics **43**, 1155-1166 (1996).

[22] R. M. A. Azzam and N. M. Bashara, *Ellipsometry and polarized light* (North-Holland, Amsterdam, 1977).

[23] F. I. Baida, D. Van Labeke, J. M. Vigoureux, "Near-field surface plasmon microscopy: A numerical study of plasmon excitation, propagation and edge interaction using a three-dimensional Gaussian beam", Phys. Rev. B **60**, 7812-7815 (1999).

[24] A. Haibel, G. Nimtz, and A. A. Stahlhofen, "Frustrated total reflection: The double-prism revisited", Phys. Rev. E **63**, 047601-1-3 (2001).

[25] Ph. Balcou and L. Dutriaux, "Dual optical tunneling times in frustrated total internal reflection", Phys. Rev. Lett. **78**, 851-854 (1997).

[26] M. Shaarawi, I. M. Besieris, A. M. Attiya and E. El-Diwany, "Acoustic X-wave reflection and transmission at a planar interface: Spectral analysis", J. Acoust. Soc. Am. **107**, 70-86 (2000).

[27] D. J. Griffits and C. A. Steinke, "Waves in locally periodic media", Am. J. Phys. **69**, 137-154 (2001).

[28] D. W. L. Sprung, G. V. Morozow and J. Martorell, "Geometrical approach to scattering in one dimension", J. Phys. A: Math. Gen. **37**, 1861-1880 (2004).

CHAPTER 7

Spatial distribution versus polarization of beam fields at a planar isotropic interface

Three-dimensional monochromatic optical beams of uniform polarization interacting with a planar boundary between two homogeneous, isotropic and lossless media are analyzed. Generalized Fresnel transmission and reflection coefficients for beam spectra are given. Interrelations induced by cross-polarization coupling between the beam profile and phase and beam polarization, or between spin and orbital angular momentum of beams are derived. Beam transmission for normal incidence is discussed in detail. It is shown that elegant Hermite-Gaussian beams of linear polarization and Laguerre-Gaussian beams of circular polarization, all projected on the interface, are normal modes at this interface. Creation and annihilation of these modes at the interface are shown with total angular momentum being conserved on a single photon level. In addition, basic relations concerning effects of nonspecular refraction and reflection are collected.

7.1 Introduction

There are two basic families of three-dimensional (3D) solutions of the paraxial wave equation - Hermite-Gaussian (HG) beams of rectangular symmetry and Laguerre-Gaussian (LG) beams of cylindrical symmetry. Both of them form two separate, complete, orthogonal, infinite-dimensional bases for

any paraxial beam field with its transverse distribution represented by a square integrated function. In particular, any HG beam can be expressed by a linear combination of LG beams and vice versa [1]. There are also two basic two-dimensional (2D) bases for beam polarization - linear, with transverse magnetic (TM) and transverse electric (TE) states, and circular, with right-handed (CR) and left-handed (CL) states. Any linear state of beam polarization can be represented by a linear combination of circular states and vice versa [2].

Transformations of beam spatial structure and beam polarization are usually implemented optically by astigmatic mode converters and birefringent plates, respectively [3]. Equivalence of their action is similar to the same extent as analogies between orbital angular momentum (OAM), associated with helical phase fronts of beams, and spin angular momentum (SAM), associated with circular polarization of beams [4]. This chapter deals with such transformations produced by interaction of 3D beams with planar discontinuity (interface) between two optically transparent semi-infinite media, and with interrelations between OAM and SAM that appear as a result of this process.

Spatial profile of the beam intensity and phase of a 3D paraxial beam is independent of beam polarization during propagation in homogeneous, isotropic and lossless medium. However, when the beam is incident on a planar discontinuity of medium parameters, its spatial structure and polarization become interrelated. These interrelations result from the action of cross-polarization coupling (XPC) that occurs for incidence of beams of finite cross-sections [5]. They cannot be explained only with the help of the standard Fresnel transmission and reflection coefficients, well known for 2D plane wave incidence. Their generalization to the 3D case appears necessary to deal properly with the beam-interface interactions.

Behavior of beams at medium planar interfaces has been under intense studies for many decades [2,6], recently also in the context of several aspects of singular optics [7]. Spatial shifts and deformations of a 3D beam spatial structure have attracted attention as well [8–10]. This issue, however, remains outside the scope of this contribution. The analysis, although being valid for general incidence of arbitrary beams, will be concentrated mainly on the case of normal incidence of the symmetric HG and LG beams. Such a

case can be treated exactly, without the need of invoking the approximate notions of beam shifts and deformations.

The beams will be considered narrow, with a beam radius of the order of one wavelength at a beam waist. Beam polarization and shape coupling will be defined in a spectral or momentum domain, for arbitrary distribution of beam field magnitude, phase and polarization. In a spatial or direct domain, specific cases of the higher-order HG beams of linear TM/TE uniform polarization and LG beams of circular CR/CL uniform polarization will be analyzed in detail. These sets of HG and LG beams will be considered in their biorthogonal versions of complex arguments, known as complex–valued or "elegant" (EHG) and (ELG) beams, respectively [11–13]. Moreover, their commonly known definitions will be further modified by their projection at the interface plane. It appears that such an elegant form of the projected HG and LG transmitted and reflected beam modes is naturally enforced by the interface being illuminated by an arbitrary incident 3D beam. The same process specifies uniquely the coupling between SAM and OAM of circularly polarized ELG beams. These phenomena will be traced here step by step by exact derivation of analytical expressions for the beam field spectral com-ponents.

Characteristic features of OAM of LG beams are well known [14]. Let me only mention that, due to the beam symmetry, an average of their transverse momentum is zero and their (mean) OAM, averaged over the total beam field, is intrinsic with respect to their beam axes [15]. On the other hand, the projected ELG beams introduced in this chapter are defined with respect to a normal to the interface, not with respect to their beam axes. Therefore OAM of the projected ELG beams is extrinsic for oblique incidence of beams and intrinsic for their normal incidence. Mainly the latter, intrinsic case of beam incidence is discussed in this chapter. Note however that, contrary to the averaged OAM of LG beams, densities of their OAM depend on position of the axis about which they are measured. This means that OAM density of a LG beam reveals a quasi-intrinsic character of averaged OAM of this beam [16] and that the "intrinsic" and "extrinsic" cases of the beam incidence are interrelated.

Both the spin and orbital parts of beam total angular momentum (TAM) attract considerable attention recently due to their possible applications as

carriers of information on classical and quantum levels [17–20]. The spin or polarization part can be described in the 2D basis of circular polarization and provides a physical realization of a qubit. The orbital part, usually associated with beam helical wavefronts, has an infinite number of eigenstates and thus may serve as a suitable mean for encoding information in qunits in an N-dimensional space, with N restricted only by a finite aperture of an optical system. Both HG and LG beams may be used in these processes as they are interrelated uniquely by HG-LG mode converters [1,3].

Optical coding of information needs sorting beam modes or single photons on the basis on SAM, OAM and/or TAM. It can be accomplished by interferometric methods capable of measuring angular momentum by rotating devices build from prisms, cylindrical lenses, half-wave plates or other types of phase shifters [21]. It would be interesting to see also application of layered optical structures, composed only of several layers and interfaces, in these processes. This contribution may be regarded as a preliminary step towards such applications. A solution to the problem at hand may appear also useful in analyzing phenomena of transfer of the angular and linear momentum of light beams to a dielectric material [22,23]. Nevertheless, discussion on other, more direct applications, for example within the range of optical visualization or near-field optics, is out of the scope of this work.

In Section 7.2 theoretical analysis of 3D beams in a spectral domain leads to generalization of the standard, p and s, Fresnel coefficients. That summarizes the results derived by the author in the past in another context [5,9,24,25], still given for arbitrary beam profile, phase and polarization. In Section 7.3 decomposition of beam transmission and reflection into parts characteristic to normal and critical incidence of total internal reflection (TIR) will be presented, together with distinct properties of their transmission and reflection partial coefficients. Beam field redistribution between opposite orthogonal polarization TM and TE or CR and CL components will be exactly derived in a spectral domain.

Transmission of the projected elegant higher-order HG and LG beams of uniform polarization, incident at normal incidence upon the interface, will be analyzed in a spatial domain in Section 7.4. Theoretical results will be illumi-nated by numerical simulations. The beam mode conversion through

the XPC effect at the interface will be described in detail. Definitions of beam normal modes at the interface will be given. Coupling between OAM and SAM of beams at the interface will be explained in Section 7.5 in terms of a conser-vation principle of their TAM. It will be shown that the analysis accounts this principle on both - macroscopic and single photon - levels. Conclusions close this chapter in Section 7.6.

7.2 Action of the interface in a spectral domain

Spectral components of 3D beams at the interface are defined in three local reference frames $Ox_p y_s z_k$,each one for the incident (b=i), reflected (b=r) and transmitted (b=t) beams [5]. These three frames are defined for separate spectral (plane wave) components of the beams. The total field of the beams is defined in frames $Oxyz$, one frame for each beam. There is also an interface frame $OXYZ$, for the total field of all three beams at the interface, here placed at the plane $Z = 0$. The z_k -axes indicate propagation directions of the plane waves, the z -axes coincide with the propagation directions of the beams, and the Z –axis is normal to the interface. Geometry of the problem is outlined in Figure 1.

The plane $x_p - z_k$ is the local incidence plane and the planes $x - z$ or $X - Z$ define the beam or main incidence plane [5]. There are also three transverse planes: the local transverse plane $x_p - y_s$ - for one spectral beam field component, the beam transverse plane $x - y$ - for the total beam field, and the interface plane $X - Y$ - transverse to the normal $\underline{e}_Z$ to the interface. For normal incidence the beam transverse plane $x - y$ coincides with the interface plane $X - Y$. For oblique incidence the z -axis makes with the Z -axis an incidence angle $\theta^{(i)}$ of the beam.

In the local reference frames $Ox_p y_s z_k$, one transverse spectral component $\underline{\widetilde{E}}^{(b)}$ of the beam field is given by the scalar multiplication $\underline{e}_{(p,s)} \underline{\widetilde{E}}^{(b)}_{(p,s)}$ of beam polarization $\underline{e}_{(p,s)} = [\underline{e}_p, \underline{e}_s]$ and field amplitude $\underline{\widetilde{E}}^{(b)}_{(p,s)} = [\widetilde{E}^{(b)}_p, \widetilde{E}^{(b)}_s]^T$ vectors; “T” means transpose. The amplitude vector is composed of p and s field components $\widetilde{E}^{(b)}_p$, and $\widetilde{E}^{(b)}_s$ in the local transverse plane $x_p - y_s$. A pair of the unit vectors - $\underline{e}_p$ placed in this plane and $\underline{e}_s$ or-

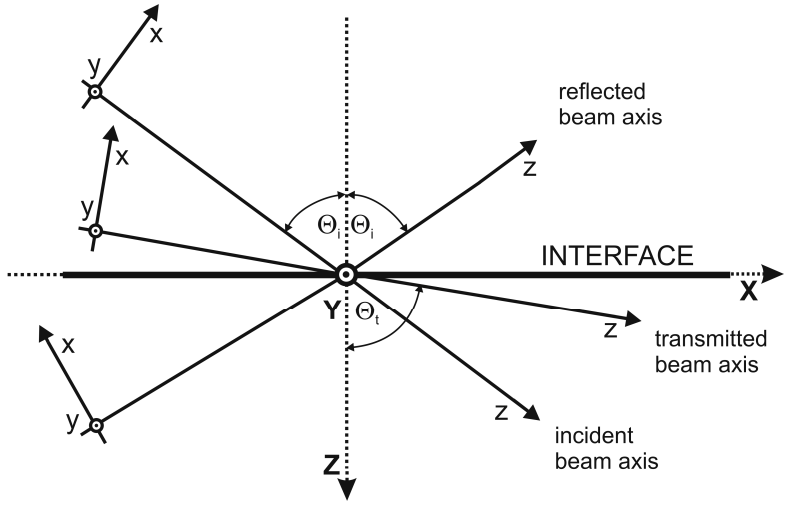

Figure 7.1. Interface $OXYZ$ and beam $Oxyz$ reference frames for transmission and reflection viewed in a beam plane of incidence $X-Z$; local frames $Ox_p y_s z_k$ are given by rotation of the plane $X-Z$ by an azimuthal angle φ around the axis Z. Beam waists are placed in centres of beam frames, incidence of internal reflection is assumed.

thogonal to this plane - spans the local 2D polarization space transverse to the wave vector $\underline{k}^{(b)} = [\underline{k}_\perp, \underline{k}_Z^{(b)}]$ of one spectral field component [5].

The Fresnel transmission and reflection coefficients, generalised to the case of beams with finite cross-sections, have been exactly derived in the beam frames $Oxyz$ [25]. However, the beam-interface interactions are more conveniently described in the interface reference frame $OXYZ$ [24]. In this frame, the transverse $k_\perp$; $k_\perp^2 = k_X^2 + k_Y^2$, and longitudinal $k_Z^{(b)}$; $(k_Z^{(b)})^2 = (k^{(b)})^2 - k_\perp^2$, components of $\underline{k}^{(b)}$ determine, through $k_\perp = k^{(b)} \sin\vartheta^{(b)}$, $k_Z^{(b)} = k^{(b)} \cos\vartheta^{(b)}$, $k_X = k_\perp \cos\varphi$ and $k_Y = k_\perp \sin\varphi$, the polar $\vartheta^{(b)}$ and azimuthal φ incidence angles in the local cylindrical coordinate frame $Ok_\perp \varphi k_Z^{(b)}$.

In the direct reference frame $Or_{\perp}\psi Z$ the polar $\theta^{(b)}$ and azimuthal ψ angles are defined in the same manner. Orientations of both frames $Ok_{\perp}\varphi k_Z^{(b)}$ and $Or_{\perp}\psi Z$ are taken also the same, with the same incidence polar angles $\vartheta_0^{(i)} = \theta_0^{(i)}$ in the same main incidence plane $\varphi = 0 = \psi$. In this plane the local plane $x_p - z_k$ coincides with the beam incidence plane $x - z$. For brevity, the dependence of field vectors $\underline{\widetilde{E}}^{(b)}$ and $\underline{\widetilde{E}}_{(p,s)}^{(b)}$ on k_X, k_Y and Z are taken through this chapter as implicit.

7.2.1 Beam transmission

For each spectral transverse components $\underline{\widetilde{E}}^{(b)}$ of the incident (b=i) and transmitted (b=t) beam fields,

$$\underline{\widetilde{E}}^{(b)} = \widetilde{E}_p^{(b)} \underline{e}_p + \widetilde{E}_s^{(b)} \underline{e}_s , \tag{7.1}$$

$$\underline{\widetilde{E}}_{(p,s)}^{(t)} = \underline{\underline{t}}_{(p,s)} \underline{\widetilde{E}}_{(p,s)}^{(i)} , \tag{7.2}$$

the field vector amplitudes $\underline{\widetilde{E}}_{(p,s)}^{(b)}$ are composed of the transverse field components $\widetilde{E}_p^{(b)}$ and $\widetilde{E}_s^{(b)}$. The elements of the diagonal transmission matrix $\underline{\underline{t}}_{(p,s)}$ are the well-known Fresnel coefficients $t_p \equiv t_p(\vartheta^{(i)})$ and $t_s \equiv t_s(\vartheta^{(i)})$ that already account for the Snell law. The total field of the beam is composed of continuum of plane waves defined in different local incidence planes $x_p - z_k$. However, all spectral components of the beam field need to be presented in one reference frame, usually taken as the beam frame $Oxyz$ [26]. Here the interface frame $OXYZ$ is chosen instead. In this frame the definitions (7.1) and (7.2) should read

$$\underline{\widetilde{E}}^{(b)} = \widetilde{E}_X^{(b)} \underline{e}_X + \widetilde{E}_Y^{(b)} \underline{e}_Y , \tag{7.3}$$

$$\underline{\widetilde{E}}_{(X,Y)}^{(t)} = \underline{\underline{t}}_{(X,Y)} \underline{\widetilde{E}}_{(X,Y)}^{(i)} , \tag{7.4}$$

with new polarization $\underline{e}_{(X,Y)} = [\underline{e}_X, \underline{e}_Y]$ and amplitude $\underline{\widetilde{E}}_{(X,Y)} = [\widetilde{E}_X^{(b)}, \widetilde{E}_Y^{(b)}]^T$ vectors, and transmission matrix $\underline{\underline{t}}_{(X,Y)}$.

Further analysis aims to find field amplitudes and transmission coefficients for each spectral field component in the frame $OXYZ$ by conversion of the expressions (7.1) and (7.2), given in any local incidence plane $\varphi \neq 0$ to their counterparts (7.3) and (7.4) in the global incidence plane $\varphi = 0$. It can be accomplished by two 3D rotations: $\underline{\underline{R}}_Y$ about the Y-axis by $\vartheta^{(b)}$ and $\underline{\underline{R}}_Z$ about the Z-axis by φ or by projection of $\underline{\widetilde{E}}^{(b)}_{(p,s)}$ on the plane $X-Z$ [5, 24]. However, after taking into account the divergence equation $\widetilde{E}^{(b)}_Z k^{(b)}_Z = -\underline{\widetilde{E}}^{(b)}_{(X,Y)} \circ \underline{k}_\perp$, only the 2D rotation matrices,

$$\underline{\underline{R}}_Y(\vartheta^{(b)}) = (k^{(b)})^{-1}\begin{bmatrix} k^{(b)}_Z & 0 \\ 0 & k^{(b)} \end{bmatrix} = \begin{bmatrix} \cos\vartheta^{(b)} & 0 \\ 0 & 1 \end{bmatrix}, \tag{7.5}$$

$$\underline{\underline{R}}_Z(\varphi) = k^{-1}_\perp \begin{bmatrix} k_X & -k_Y \\ k_Y & k_X \end{bmatrix} = \begin{bmatrix} \cos\varphi & -\sin\varphi \\ \sin\varphi & \cos\varphi \end{bmatrix}, \tag{7.6}$$

may be used instead in evaluation of the field components and transmission matrix elements,

$$\underline{\widetilde{E}}^{(b)}_{(X,Y)} = \underline{\underline{R}}_Z(\varphi)\underline{\underline{R}}_Y(\vartheta^{(b)})\underline{\widetilde{E}}^{(b)}_{(p,s)}, \tag{7.7}$$

$$\underline{\underline{t}}_{(X,Y)} = \underline{\underline{R}}_Z(\varphi)\underline{\underline{R}}_Y(\vartheta^{(t)})\underline{\underline{t}}_{(p,s)}\underline{\underline{R}}^{-1}_Y(\vartheta^{(i)})\underline{\underline{R}}^{-1}_Z(\varphi). \tag{7.8}$$

That yields

$$\begin{bmatrix} \widetilde{E}^{(b)}_X \\ \widetilde{E}^{(b)}_Y \end{bmatrix} = (k^{(b)}k_\perp)^{-1}\begin{bmatrix} k_X k^{(b)}_Z & -k_Y k^{(b)} \\ k_Y k^{(b)}_Z & k_X k^{(b)} \end{bmatrix}\begin{bmatrix} \widetilde{E}^{(b)}_p \\ \widetilde{E}^{(b)}_s \end{bmatrix}, \tag{7.9}$$

$$\underline{\underline{t}}_{(X,Y)} = k^{-2}_\perp \begin{bmatrix} \eta t_p k^2_X + t_s k^2_Y & (\eta t_p - t_s)k_X k_Y \\ (\eta t_p - t_s)k_X k_Y & \eta t_p k^2_Y + t_s k^2_X \end{bmatrix}, \tag{7.10}$$

where $\eta = \cos\vartheta^{(t)}/\cos\vartheta^{(i)}$. Still, by introduction of the linear polarization parameter in the spectral domain of the incident beam

$$\widetilde{\chi}^{(b)}_{(X,Y)} = \widetilde{E}^{(b)}_X / \widetilde{E}^{(b)}_Y, \tag{7.11}$$

b=i, the transmission matrix $\underline{\underline{t}}_{(X,Y)}$ can be rewritten in the diagonal form [24]:

$$\underline{\underline{t}}_{(X,Y)} = \begin{bmatrix} \eta t_{TM} & 0 \\ 0 & t_{TE} \end{bmatrix} = \begin{bmatrix} \eta t_p + \Delta_{TM} & 0 \\ 0 & t_s + \Delta_{TE} \end{bmatrix}, \tag{7.12}$$

$$\Delta_a \equiv \Delta_a(\vartheta^{(i)}, \varphi) = (\eta t_p - t_s) k_\perp^{-2} k_Y [(\widetilde{\chi}^{(i)}_{(X,Y)})^{\mp 1} k_X \mp k_Y)], \tag{7.13}$$

where $a = TM$ ($a = TE$) for the upper (lower) signs in (7.13). In the following, the parameter $\widetilde{\chi}^{(i)}_{(X,Y)}$ will be assumed as independent of k_X and k_Y. It remains common for all points of the interface plane. That means that the incident beam is considered in an arbitrary uniform polarization state.

The coefficients $t_{TM} \equiv t_{TM}(\vartheta^{(i)}, \varphi; \widetilde{\chi}^{(i)}_{(X,Y)})$ and $t_{TE} \equiv t_{TE}(\vartheta^{(i)}, \varphi; \widetilde{\chi}^{(i)}_{(X,Y)})$ of transmission should be understood as the Fresnel coefficients ηt_p and t_s modified, due to the 3D character of the beams, by the modification terms Δ_{TM} and Δ_{TE}, respectively. They are caused by the XPC effect, are proportional to the difference $\eta t_p - t$ of these coefficients and consist of the first-order and second order ingredients with respect to k_Y. They disappear at the beam incidence plane, i.e. for $k_Y = 0$. For pure TM and TE incident polarization $(\widetilde{\chi}^{(i)}_{(X,Y)})^{-1} = 0$ and $\widetilde{\chi}^{(i)}_{(X,Y)} = 0$, respectively, and then ηt_p and t_s are modified only by the second-order terms $\mp(\eta t_p - t_s) k_Y^2 k_\perp^{-2}$ [24].

7.2.2 Beam reflection

Similar considerations to those given in Section 7.2 can be repeated for the reflected beam (cf. Figure 7.1). The transverse field spectral components

$$\underline{E}^{(r)} = E_p^{(r)} \underline{e}_p + E_s^{(r)} \underline{e}_s \tag{7.14}$$

are defined in the local frame $Ox_p y_s z_k$ by the field amplitude $\underline{\widetilde{E}}^{(r)}_{(p,s)} = [\widetilde{E}_p^{(r)}, \widetilde{E}_s^{(r)}]^T$ and polarization $\underline{e}_{(p,s)}$ vectors. The new amplitude $\underline{\widetilde{E}}^{(r)}_{(-X,Y)} = [-\widetilde{E}_X^{(r)}, \widetilde{E}_Y^{(r)}]^T$ and polarization $\underline{e}_{(X,Y)}$ vectors, defined in the interface frame $OXYZ$, can be obtained by the rotation (7.5)-(7.6) and

inversion $\underline{\underline{R}}_I$; $-\underline{\underline{R}}_{I,XX} = 1 = \underline{\underline{R}}_{I,YY}$, transformations applied in the appropriate order, or equivalently, by projection of $\underline{\widetilde{E}}^{(r)}_{(p,s)}$ on the plane $X - Z$ [5,24],

$$\underline{\widetilde{E}}^{(r)}_{(-X,Y)} = \underline{\underline{R}}_I \underline{\underline{R}}_Z(\varphi) \underline{\underline{R}}_Y(\vartheta^{(r)}) \underline{\underline{R}}_I \underline{\widetilde{E}}^{(r)}_{(p,s)}, \tag{7.15}$$

$$\begin{bmatrix} -\widetilde{E}^{(r)}_X \\ \widetilde{E}^{(r)}_Y \end{bmatrix} = (k^{(r)} k_\perp)^{-1} \begin{bmatrix} k_X k^{(r)}_Z & k_Y k^{(r)} \\ -k_Y k^{(r)}_Z & k_X k^{(r)} \end{bmatrix} \begin{bmatrix} \widetilde{E}^{(r)}_p \\ \widetilde{E}^{(r)}_s \end{bmatrix}. \tag{7.16}$$

The reflection matrix $\underline{\underline{r}}_{(-X,Y)}$ can be then evaluated from the local or Fresnel (diagonal) reflection matrix $\underline{\underline{r}}_{(p,s)}$, with its diagonal elements $r_p \equiv r_p(\vartheta^{(i)})$ and $r_s \equiv r_s(\vartheta^{(i)})$, by the application of the inversion and rotation matrices in appropriate order. This transformation yields the definition of the reflection matrix in the frame $\underline{e}_{(X,Y)}$ [5],

$$\underline{\underline{r}}_{(-X,Y)} = \underline{\underline{R}}_I \underline{\underline{R}}_Z(\varphi) \underline{\underline{R}}_Y(\vartheta^{(r)}) \underline{\underline{R}}_I \underline{\underline{r}}_{(p,s)} \underline{\underline{R}}^{-1}_Y(\vartheta^{(i)}) \underline{\underline{R}}^{-1}_Z(\varphi), \tag{7.17}$$

$$\underline{\underline{r}}_{(-X,Y)} = k_\perp^{-2} \begin{bmatrix} r_p k_X^2 - r_s k_Y^2 & (r_p + r_s) k_X k_Y \\ -(r_p + r_s) k_X k_Y & -r_p k_Y^2 + r_s k_X^2 \end{bmatrix}, \tag{7.18}$$

where $\underline{\widetilde{E}}^{(r)}_{(-X,Y)} = \underline{\underline{r}}_{(-X,Y)} \underline{\widetilde{E}}^{(i)}_{(X,Y)}$.

Next, introduction of the polarization parameter $\widetilde{\chi}^{(i)}_{(X,Y)}$ makes the matrix $\underline{\underline{r}}_{(-X,Y)}$ diagonal [24]

$$\underline{\underline{r}}_{(-X,Y)} = \begin{bmatrix} r_{TM} & 0 \\ 0 & r_{TE} \end{bmatrix} = \begin{bmatrix} r_p - \Delta_{TM} & 0 \\ 0 & r_s + \Delta_{TE} \end{bmatrix}, \tag{7.19}$$

where $r_{TM} \equiv r_{TM}(\vartheta^{(i)}, \varphi, \widetilde{\chi}^{(i)}_{(X,Y)})$ and $r_{TE} \equiv r_{TE}(\vartheta^{(i)}, \varphi, \widetilde{\chi}^{(i)}_{(X,Y)})$ mean the coefficients r_p and r_s modified by the terms Δ_{TM} and Δ_{TE} (7.12)-(7.13). Eqs. (7.12) for transmission and (7.19) for reflection, together with definition (7.13) of the beam spectra modifications, explicitly show differences between 3D beam and 2D beam cases. The terms Δ_{TM} and Δ_{TE} disappear for plane waves and 2D beams. Such effects as XPC, interrelations between

beam spin and orbital angular momenta, transverse modifications of the beam profile, phase and polarization are specific only to the 3D case.

Note that the transmission (7.11) and reflection (7.19) matrices are exact for any plane wave of which the incident beam is composed. They are dependent on each other and interrelated through the continuity of the field components tangent to the interface [24]:

$$1 - r_p = \eta t_p, \qquad 1 + r_s = t_s, \tag{7.20}$$

$$1 - r_{TM} = \eta t_{TM}, \qquad 1 + r_{TE} = t_{TE}. \tag{7.21}$$

Eq. (7.21) is given in the main plane of incidence, for $\varphi = 0$, and Eq. (7.21) is given in the local plane of incidence, in general for $\varphi \neq 0$.

7.3 Normal versus critical incidence of beams

The Fresnel coefficients defined for plane-waves are interrelated through the field continuity relations (7.20) at the interface or equivalently by

$$\tfrac{1}{2}(\eta t_p + t_s) = 1 - \tfrac{1}{2}(r_p - r_s), \tag{7.22}$$

$$\tfrac{1}{2}(\eta t_p - t_s) = -\tfrac{1}{2}(r_p + r_s). \tag{7.23}$$

For normal incidence Eqs. (7.22) and (7.23) read $\eta t_p = t_s = 1 - r_p = 1 + r_s$ and $0 = 0$, respectively. Moreover, they read $1 = 1$ for critical incidence of TIR. That suggests that Eq. (7.22) can be associated with normal incidence and Eq. (7.23) with critical incidence of one separate spectral component of the beams. This form of the field continuity relations leads to a special type of beam field decomposition, particularly suitable in treatment of beams at the interface.

7.3.1 Field decomposition in the linear polarization basis

The transmission (7.12) and reflection (7.19) matrices can be decomposed in such a way that the separate terms of the relations (7.22) and (7.23) stand for the amplitudes of separate parts of the decomposition of these matrices. In the TM/TE polarization basis $\underline{e}_{(X,Y)}$, this decomposition takes the following form:

$$\underline{\underline{t}}_{(X,Y)} = +\tfrac{1}{2}(\eta t_p + t_s)\begin{bmatrix}1 & 0\\ 0 & 1\end{bmatrix} + \tfrac{1}{2}(\eta t_p - t_s)k_\perp^{-2}\begin{bmatrix}k_X^2 - k_Y^2 & 2k_Xk_Y\\ 2k_Xk_Y & -k_X^2 + k_Y^2\end{bmatrix}, \tag{7.24}$$

$$\underline{\underline{r}}_{(-X,Y)} = -\tfrac{1}{2}(r_p - r_s)\begin{bmatrix}-1 & 0\\ 0 & 1\end{bmatrix} + \tfrac{1}{2}(r_p + r_s)k_\perp^{-2}\begin{bmatrix}k_X^2 - k_Y^2 & 2k_Xk_Y\\ -2k_Xk_Y & k_X^2 - k_Y^2\end{bmatrix}, \tag{7.25}$$

now explicitly dependent on the azimuthal angle φ through the relations $k_X^2 - k_Y^2 = k_\perp^2\cos 2\varphi$ and $2k_Xk_Y = k_\perp^2 \sin 2\varphi$. The matrix decomposition (7.24) and (7.25), together with a Z-component of the field

$$\widetilde{E}_Z^{(b)} = -(\widetilde{E}_X^{(b)}k_X + \widetilde{E}_Y^{(b)}k_Y)/k_Z^{(b)} \tag{7.26}$$

describe explicitly characteristic properties of beam transmission and reflection. They depend on the beam incidence angle, polarization and transverse field structure, and on the type of media of which the interface is composed.

The diagonal part of the transmission (7.24) matrix is proportional to the identity matrix. Therefore it does not change the polarization state of the beam and remains common for any polarization base used in the beam field representation. The same concerns, up to the sign changes, the reflection matrix (7.25). For critical incidence of TIR the amplitudes of the diagonal ingredients amount $\frac{1}{2}(\eta t_p + t_s) = 1$ and $\frac{1}{2}(r_p - r_s) = 0$, respectively. They correspond to the total transmission of the beams. On the contrary, the amplitudes of the second, XPC parts of the matrices (7.24) and (7.25) yield $\frac{1}{2}(\eta t_p - t_s) = -1$ and $\frac{1}{2}(r_p + r_s) = 1$ for critical incidence of TIR. For normal incidence both of them equal zero. Therefore, the first part in Eqs. (7.24) and (7.25) can be associated with normal incidence and the second - with critical incidence of TIR. For incidence other than normal and critical, all amplitudes in the decompositions in (7.24) and (7.25) take non-zero values.

7.3.2 Field decomposition in the circular polarization basis

In the circular polarization frame $\underline{e}_{(R,L)} = [\underline{e}_R, \underline{e}_L]$, composed of CR and CL polarization vectors $\underline{e}_R$ and $\underline{e}_L$, respectively, defined here in the interface plane $X - Y$, not in the transverse planes $x - y$ of the beams. The

basis $\underline{e}_{(R,L)}$ and the field amplitudes $\underline{\widetilde{E}}^{(b)}_{(R,L)} = [\widetilde{E}^{(b)}_R, \widetilde{E}^{(b)}_L]^T$ in this basis are obtained from the linear basis $\underline{e}_{(X,Y)}$ and the field amplitudes $\underline{E}^{(b)}_{(\pm X,Y)}$ by the unitary transformation $\underline{\underline{U}}$: $U_{RX} = 2^{-1/2} = U_{LX}$ and $-U_{RY} = i2^{-1/2} = U_{LY}$; $\underline{e}_{(R,L)} = \underline{e}_{(X,Y)}\underline{\underline{U}}^+$, $\underline{\widetilde{E}}^{(t)}_{(R,L)} = \underline{\underline{U}}\,\underline{E}^{(t)}_{(X,Y)}$ and $\underline{\widetilde{E}}^{(b)}_{(R,L)} = \underline{\underline{U}}\,\underline{E}^{(b)}_{(-X,Y)}$ (the superscripted plus sign means Hermitian conjugate). This yields (b=t,r):

$$\underline{\widetilde{E}}^{(b)} = \widetilde{E}^{(b)}_R \underline{e}_R + \widetilde{E}^{(b)}_L \underline{e}_L , \tag{7.27}$$

$$\underline{e}_{(R,L)} = 2^{-1/2}\left[\underline{e}_X + i\underline{e}_Y, \quad \underline{e}_X - i\underline{e}_Y\right], \tag{7.28}$$

with transverse and longitudinal field components expressed by:

$$\underline{\widetilde{E}}^{(t)}_{(R,L)} = 2^{-1/2}\left[\widetilde{E}^{(t)}_X - i\,\widetilde{E}^{(t)}_Y \quad \widetilde{E}^{(t)}_X + i\,\widetilde{E}^{(t)}_Y\right]^T , \tag{7.29}$$

$$\underline{\widetilde{E}}^{(r)}_{(R,L)} = 2^{-1/2}\left[-\widetilde{E}^{(r)}_X - i\,\widetilde{E}^{(r)}_Y \quad -\widetilde{E}^{(r)}_X + i\,\widetilde{E}^{(r)}_Y\right]^T , \tag{7.30}$$

$$\widetilde{E}^{(b)}_Z = \mp 2^{-1/2}\left[\widetilde{E}^{(b)}_R \exp(\pm i\varphi) + \widetilde{E}^{(b)}_L \exp(\mp i\varphi)\right]\tan\vartheta^{(b)} . \tag{7.31}$$

The upper (lower) signs in (7.31) pertain the transmitted (b=t) (reflected; b=r) beam. Note that $\exp(\pm i\varphi) = (k_X \pm ik_Y)k_\perp^{-1}$ and $\tan\vartheta^{(b)} = k_\perp (k_Z^{(b)})^{-1}$. The winding number of the Z-components of all beams - incident, transmitted and reflected - is larger (lower) by one than that of the transverse field component of the CR (CL) polarization.

The transmission $\underline{\underline{t}}_{(R,L)} = \underline{\underline{U}}\;\underline{\underline{t}}_{(X,Y)}\;\underline{\underline{U}}^+$ and reflection $\underline{\underline{r}}_{(R,L)} = \underline{\underline{U}}\;\underline{\underline{r}}_{(-X,Y)}\;\underline{\underline{U}}^+$ matrices

$$\underline{\underline{t}}_{(R,L)} = \tfrac{1}{2}(\eta t_p + t_s)\begin{bmatrix}1 & 0\\ 0 & 1\end{bmatrix} + \tfrac{1}{2}(\eta t_p - t_s)\begin{bmatrix}0 & \exp(-2i\varphi)\\ \exp(+2i\varphi) & 0\end{bmatrix}, \tag{7.32}$$

$$\underline{\underline{r}}_{(R,L)} = \tfrac{1}{2}(r_p - r_s)\begin{bmatrix}0 & 1\\ 1 & 0\end{bmatrix} + \tfrac{1}{2}(r_p + r_s)\begin{bmatrix}\exp(+2i\varphi) & 0\\ 0 & \exp(-2i\varphi)\end{bmatrix}, \tag{7.33}$$

can be then decomposed into two parts - diagonal and antidiagonal, with distinct polarization properties.

The diagonal part of the transmission matrix $\underline{\underline{t}}_{(R,L)}$ does not change the beam polarization. It modifies only the amplitudes of beam spectral components by the factor $\frac{1}{2}(\eta t_p + t_s)$. The antidiagonal part of $\underline{\underline{t}}_{(R,L)}$, with its amplitude $\frac{1}{2}(\eta t_p - t_s)$, represents the pure XPC effect of the beam-interface interaction; the CR polarization of the incident beam is replaced by the CL polarization under beam transmission and vice versa. Moreover, this part of the transmission matrix changes, in the beam centre, a topological charge of the beam by two. For the incident CR (CL) polarization, the topological charge is increased (decreased) by two in the CL (CR) polarization of the transmitted beam.

For the beam reflection, due to the inversion $\underline{\underline{R}}_I$, the diagonal and antidiagonal components of the reflection matrix are replaced with respect to their roles in the beam transmission. The first part of $\underline{\underline{r}}_{(R,L)}$, this with the amplitude $\frac{1}{2}(r_p - r_s)$, changes the beam polarization state to the opposite one, but without changes in the beam topological charge. On the contrary, the second part of $\underline{\underline{r}}_{(R,L)}$, this with the amplitude $\frac{1}{2}(r_p + r_s)$, does not change the beam polarization. Instead, due to the XPC effect at the interface, it increases (decreases) the topological charge of the reflected beam by two for the CR (CL) polarization of the incident beam.

The transmission $\underline{\underline{t}}_{(R,L)}$ (7.32) and reflection $\underline{\underline{r}}_{(R,L)}$ (7.33) matrices in the circular CR/CL basis are equivalent to their counterparts $\underline{\underline{t}}_{(X,Y)}$ (7.24) and $\underline{\underline{r}}_{(-X,Y)}$ (7.25) in the linear TM/TE basis. All of them describe completely, in the spectral domain, the transmission and reflection phenomena of 3D beams of arbitrary shape and polarization, incident upon the interface at an arbitrary incidence angle.

7.4 Action of the interface in a spatial domain

Consider now characteristic features of the beam-interface interactions in the spatial domain. With where harmonic dependence on time $\exp(-i\omega t)$ assumed and suppressed, 3D beams of finite cross-sections are usually expressed by their spectral representation, what in the reference frame $OXYZ$ yields

$$\begin{aligned}\underline{E}^{(b)}(X,Y,Z) &= (w_w/2\pi)^2 \exp(\pm ik^{(b)}z) \\ &\times \int dk_X \int dk_Y \underline{\widetilde{E}}^{(b)}(k_X,k_Y,Z)\exp[i(k_X X + k_Y Y)],\end{aligned} \tag{7.34}$$

Note that, although the representation (7.34) is exact, for clarity of further considerations the beam vector amplitudes $\underline{\widetilde{E}}^{(b)}$ are now defined as dependent on Z, the convention typical for paraxial beams [27]. In this way the rep-resentation (7.34) is valid for paraxial and non-paraxial beams, provided that in the second choice the paraxial beam profile and phase distribution are im-posed only in one transverse plane, for instance, as taken below, in the inter-face plane $Z = 0$.

The representation (7.34) translates characteristic features of beams from the spectral domain to the spatial domain. In general, the integration can be accomplished only numerically. Sometimes however, for some specific incident beam distributions, it can be obtained also directly by analytical evaluation of the beam fields in some specific polarization basis. For HG or LG beams of arbitrary order, this evaluation is possible under fulfilment of some additional conditions, as it will be evident from further considerations.

The analysis will be restricted only to a single interface. However, due to the diagonal form of matrices (7.12) and (7.19), the results can be directly generalised to the case of beams at isotropic layered structures [25]. The derivations are exact in the spectral domain and approximate in the spatial domain, with really high accuracy obtained for paraxial beams. Direct integration of Maxwell equations [28] serves as a numerical illustration of the analytical expressions derived. In numerical simulations, a dielectric constant equal two is assumed at the interface for the case of internal reflection. Only beam transmission of normal incidence will be analysed (cf. also [29]); beam reflection and arbitrary incidence can be treated on the same footing [28].

7.4.1 The fundamental Gaussian beam

Let us start from the incident beam with its transverse field distribution $\underline{E}^{(i)}_{(x,y)} = \underline{e}_{(x,y)} G$ and $\underline{\widetilde{E}}^{(i)}_{(x,y)} = \underline{e}_{(x,y)} \widetilde{G}$ at the plane $z = const.$ in a form of the fundamental Gaussian function:

$$G(x,y,z) = (w_w/v)^2(z)\exp\left[-(1/2)(x^2+y^2)v^{-2}(z)\right], \tag{7.35}$$

$$\widetilde{G}(k_x,k_y,z) = 2\pi\exp\left[-(1/2)(k_x^2+k_y^2)v^2(z)\right], \tag{7.36}$$

with the complex beam half-width (radius)

$$v^2(z) = w_w^2(1+izz_D^{-1}). \tag{7.37}$$

The beam is specified by a position of the waist centre, here at $(x,y)=(0,0)$, a beam complex half-width (radius) v and a diffraction length of the beam $z_D = k^{(i)}w_w^2$, w_w being a beam (real) half-width at the waist. The complex half-width v, $v^{-2} = w^{-2} - iR^{-1}$, defines two real quantities: the beam half-width (radius) squared $w^2 = w_w^2(1+z^2z_D^{-2})$ and the radius of the phase-front curvature $R = w_w^2(z^{-1}z_D + zz_D^{-1})$. Unit amplitude of the beam field at the beam centre is assumed as a normalisation condition for the fundamental, as well as for all higher-order, HG and LG beams. Note also that in all field expressions in (7.35)-(7.37), the longitudinal z-coordinate can be normalised to z_D and the two, x and y, transverse coordinates can be normalised to w_w, respectively.

Higher-order HG and LG beams are considered here in their elegant version [11] and thus are hereafter referred to as the EHG and ELG beams. The beams are defined in the spatial domain by appropriate differentiation of the fundamental Gaussian field distribution (7.35)-(7.37). For the discussion of such definitions of the EHG and ELG beams the reader is referred to a recent report [30], where definitions of the, standard and elegant, HG and LG beams were rederived and compared. However, meanwhile the fundamental mode may be here conventionally defined in its transverse plane $(x-y)$, the higher order modes, together with the fundamental, are defined here in the interface plane $X-Y$. In other words, the projected definitions of the elegant beams will be used. For this reason we also hereafter use the replacements $G(x,y,z) \to G(X,Y,Z)$ and $\widetilde{G}(k_x,k_y,z) \to \widetilde{G}(k_X,k_Y,Z)$ in the notation in (7.34). All expressions for these beam modes are explicitly derived below.

7.4.2 Elegant Hermite-Gaussian modes at the interface

Define the EHG mode $G_{m,n}^{(EH)}$ of the order $m+n$ by the partial X and Y derivatives of the order m and n, respectively, applied to the fundamental Gaussian [30]:

$$\widetilde{G}_{m,n}^{(EH)}(k_X,k_Y,Z)=(iw_w)^{m+n}k_X^m k_Y^n \widetilde{G}(k_X,k_Y,Z), \tag{7.38}$$

$$G_{m,n}^{(EH)}(X,Y,Z)=(w_w)^{m+n}\partial_X^m \partial_Y^n G(X,Y,Z). \tag{7.39}$$

The definitions (7.38) and (7.39) are given here up to arbitrary normalization constant factor and imply a unit amplitude of the fundamental Gaussian beam at its waist centre (cf. Eqs. (7.35)-(7.37)). Hence, the partial derivatives ∂_X and ∂_Y increase the EHG mode indices m and n along the X and Y directions, respectively,

$$w_w\partial_X G_{m,n}^{(H)}(X,Y,Z)=G_{m+1,n}^{(EH)}(X,Y,Z), \tag{7.40}$$

$$w_w\partial_Y G_{m,n}^{(H)}(X,Y,Z)=G_{m,n+1}^{(EH)}(X,Y,Z), \tag{7.41}$$

and the transmission matrix (7.24) can be directly applied.

For the incident EHG beam of the TM polarization $\underline{E}^{(i)}=\widetilde{E}_X^{(i)}\underline{e}_X$, with its spectral amplitude $\widetilde{E}_X^{(i)}=\widetilde{G}_{m,n}^{(EH)}$, or for the incident EHG beam of the TE polarization $\underline{E}^{(i)}=\widetilde{E}_Y^{(i)}\underline{e}_Y$, with its spectral amplitude $\widetilde{E}_Y^{(i)}=\widetilde{G}_{m,n}^{(EH)}$, the transmitted beams become:

$$\begin{bmatrix}\widetilde{E}_X^{(t)}\\ \widetilde{E}_Y^{(t)}\end{bmatrix}_{TM}=\tfrac{1}{2}(\eta t_p+t_s)\begin{bmatrix}\widetilde{G}_{m,n}^{(EH)}\\ 0\end{bmatrix}-(\eta t_p-t_s)(k_\perp w_w)^{-2}\begin{bmatrix}0\\ \widetilde{G}_{m+1,n+1}^{(EH)}\end{bmatrix}+\begin{bmatrix}\widetilde{\delta}_X\\ \widetilde{\delta}_Y\end{bmatrix}_{TM}, \tag{7.42}$$

$$\begin{bmatrix}\widetilde{E}_X^{(t)}\\ \widetilde{E}_Y^{(t)}\end{bmatrix}_{TE}=\tfrac{1}{2}(\eta t_p+t_s)\begin{bmatrix}0\\ \widetilde{G}_{m,n}^{(EH)}\end{bmatrix}-(\eta t_p-t_s)(k_\perp w_w)^{-2}\begin{bmatrix}\widetilde{G}_{m+1,n+1}^{(EH)}\\ 0\end{bmatrix}+\begin{bmatrix}\widetilde{\delta}_X\\ \widetilde{\delta}_Y\end{bmatrix}_{TE}, \tag{7.43}$$

respectively. In Eqs. (7.42) and (7.43) the labels TM and TE indicate the type of polarization of the incident beam and the last, correction terms read:

$$\begin{bmatrix} \widetilde{\delta}_X \\ \widetilde{\delta}_Y \end{bmatrix}_{TM} = -\tfrac{1}{2}(\eta t_p - t_s)(k_\perp w_w)^{-2} \begin{bmatrix} \widetilde{G}^{(EH)}_{m+2,n} - \widetilde{G}^{(EH)}_{m,n+2} \\ 0 \end{bmatrix}, \tag{7.44}$$

$$\begin{bmatrix} \widetilde{\delta}_X \\ \widetilde{\delta}_Y \end{bmatrix}_{TE} = +\tfrac{1}{2}(\eta t_p - t_s)(k_\perp w_w)^{-2} \begin{bmatrix} 0 \\ \widetilde{G}^{(EH)}_{m+2,n} - \widetilde{G}^{(EH)}_{m,n+2} \end{bmatrix}. \tag{7.45}$$

As for the normal, or close to normal, incidence the term $\eta t_p - t_s$ is much less than $\eta t_p + t_s$, the contributions $\underline{\widetilde{\delta}}_{TM}$ and $\underline{\widetilde{\delta}}_{TE}$ in Eqs. (7.42) and (7.43), will be further neglected. This approximation is quite reasonable under paraxial approximation assumption, that is roughly for $k^{(i)} w_w > 2\pi$. Eqs. (7.44) and (7.45) indicate that the transmitted beams attain finite values also in the polarization components opposite to those of the incident beam. They are approximately EHG beams with their indices being increased, with respect to the incident beam, by one along both, X and Y, transverse directions.

On the grounds of the divergence Eq. (7.26), one index (in X or Y direction) is further increased by one in the longitudinal field component

$$\widetilde{E}^{(t)}_Z|_{TM} \cong i(2w_w k^{(t)}_Z)^{-1}\left[(\eta t_p + t_s)\widetilde{G}^{(EH)}_{m+1,n} - 2(\eta t_p - t_s)(k_\perp w_w)^{-2}\widetilde{G}^{(EH)}_{m+1,n+2}\right], \tag{7.46}$$

$$\widetilde{E}^{(t)}_Z|_{TE} \cong i(2w_w k^{(t)}_Z)^{-1}\left[(\eta t_p + t_s)\widetilde{G}^{(EH)}_{m,n+1} - 2(\eta t_p - t_s)(k_\perp w_w)^{-2}\widetilde{G}^{(EH)}_{m+2,n+1}\right]. \tag{7.47}$$

For normal or close to normal incidence in the paraxial range, the longitudinal field components in Eqs. (7.46) and (7.47) are approximately proportional to the term $\eta t_p + t_s$. Therefore, the spatial shape of the Z-component of the transmitted beam follows the spatial shape of the Z-component of the incident beam. Moreover $\widetilde{E}^{(t)}_Z|_{TM} \cong t^{(EH)}_Z \widetilde{E}^{(i)}_Z|_{TM}$ and $\widetilde{E}^{(t)}_Z|_{TE} \cong t^{(EH)}_Z \widetilde{E}^{(i)}_Z|_{TE}$, where $t^{(EH)}_Z = \tfrac{1}{2}(\eta t_p + t_s)k^{(i)}_Z / k^{(t)}_Z$ may be regarded as the transmission coefficient of the Z component of the EHG beam.

Beam field distribution in the spatial domain can be now obtained by analytical evaluation, after substitution of Eqs. (7.42) and (7.43) to the repre-

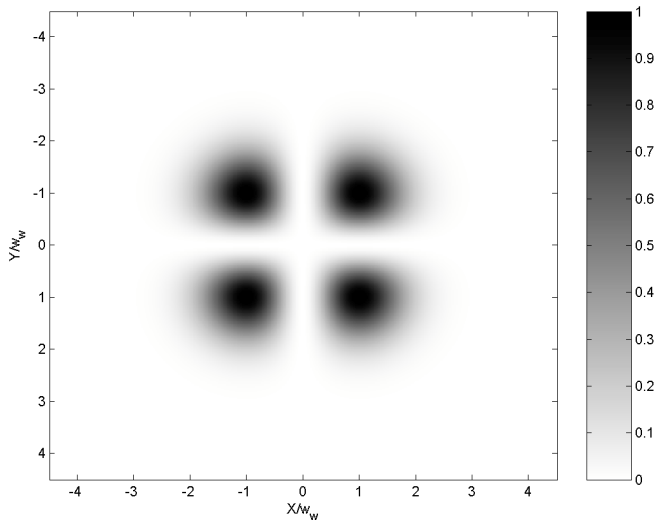

(a)

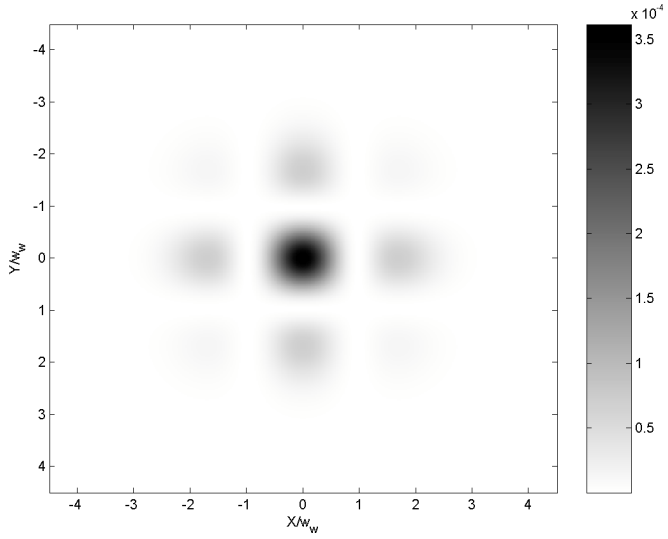

(b)

Figure 7.2. Beam intensity transverse distribution of the EHG beam at the interface; the incident beam of the $EHG_{1,1}$ pattern and of TM polarization (a), the transmitted beam TE component of the $EHG_{2,2}$ pattern (b); X and Y coordinates normalized to w_w, normal incidence.

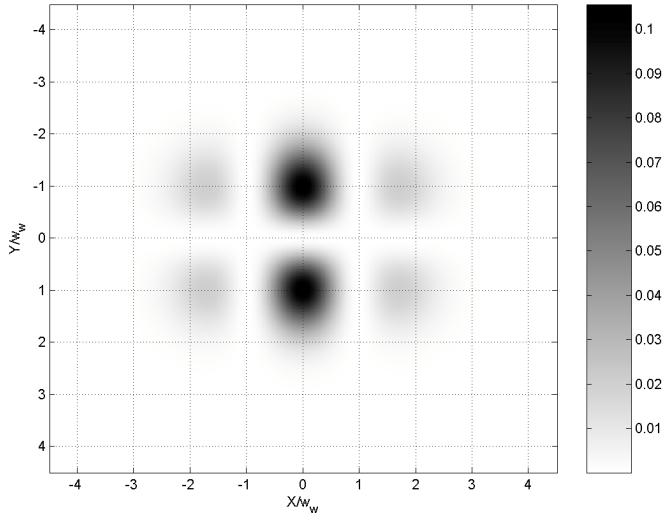

(a)

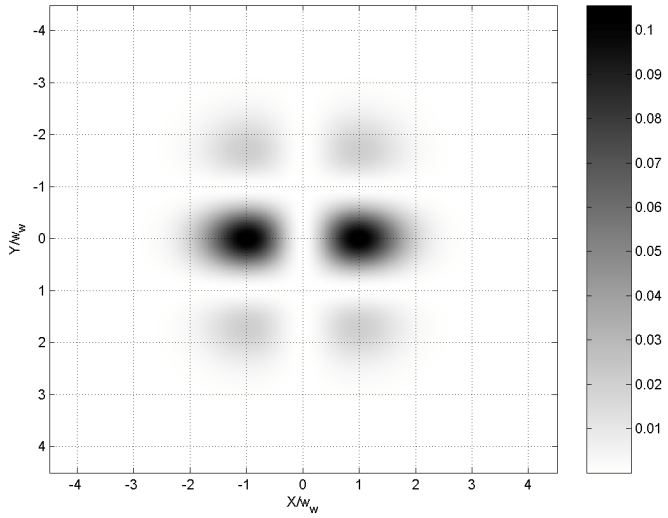

(b)

Figure 7.3. Beam intensity transverse distribution of the EHG beam at the interface; the Z-component of the transmitted beam of the $EHG_{2,1}$ pattern for the incident $EHG_{1,1}$ beam of TM polarization (a) and the Z-component of the transmitted beam of the $EHG_{1,2}$ pattern for the incident $EHG_{1,1}$ beam of TE polarization (b); normal incidence. The central position of the beam is shown by the grid.

sentation (7.34), or simply by direct numerical integration of Maxwell equations. The numerical approach was described and demonstrated in [28] for critical incidence of TIR. In analytic evaluation of (7.34), for normal incidence of paraxial beams, the Fresnel coefficients can be evaluated at $\vartheta^{(i)} = 0$. Field intensity plots are presented in Figs. 7.2 and 7.3 for two wavelengths in the beam diameter at its waist, that is for $k^{(i)} w_w = 2\pi$. The case of normal incidence of the $\mathrm{EHG}_{1,1}$ beam, with the indices in the X and Y directions equal one, is considered.

The incident beam of the $\mathrm{EHG}_{1,1}$ spatial pattern and of TM polarization is shown in Fig. 7.2(a), the pattern of the transmitted beam component of the opposite, TE polatization is shown in Fig. 7.2(b). The plots clearly confirm predictions of Eq. (7.42); the pattern of the TE transmitted field component is of the $\mathrm{EHG}_{2,2}$ spatial shape. For normal incidence of the beam the problem is symmetric in X and Y coordinates. For the TE polarization of the incident beam, the TM component of the transmitted beam possesses the same $\mathrm{EHG}_{2,2}$ pattern as that of the TE component of the transmitted beam for the TM polarization of the incident beam.

The interface, however, still differentiates these two cases in the longitudinal, Z-components of the transmitted beams as it is shown in Fig. 7.3. The Z-component of the transmitted beam exhibits the $\mathrm{EHG}_{2,1}$ pattern for incident TM polarization, as shown in Fig. 7.3(a), and the $\mathrm{EHG}_{1,2}$ pattern for incident TE polarization, as shown in Fig. 7.3(b). Figure 3 entirely confirms theoretical predictions of Eqs. (7.46) and (7.47).

7.4.3 Elegant Laguerre-Gaussian modes at the interface

Let us turn now to the case of beams of a cylindrical symmetry and describe them in the cylindrical reference frames $Or_\perp \psi Z$ and $Ok_\perp \varphi k_Z^{(b)}$ in the spatial and spectral domains, respectively, where $X = r_\perp \cos\psi$, $Y = r_\perp \sin\psi$, $k_X = k_\perp \cos\varphi$ and $k_Y = k_\perp \sin\varphi$. Action of the interface on the incident beams can be then described more compactly in new frames $O\varsigma\bar{\varsigma}Z$ and $O\kappa\bar{\kappa}Z$ of complex coordinates and their complex conjugates (denoted by the overbear). These coordinates are defined in the spatial domain:

$$\varsigma = 2^{-1/2}(X + iY),$$

$$\partial_{\varsigma} = 2^{-1/2}(\partial_X - i\partial_Y), \tag{7.48}$$

where $\varsigma\bar{\varsigma} = 2^{-1} r_{\perp}^2$ and $\partial_{\varsigma}\partial_{\bar{\varsigma}} = 2^{-1}(\partial_X^2 + \partial_Y^2)$, and in the spectral domain:

$$\kappa = 2^{-1/2}(k_X + ik_Y),$$

$$\partial_{\kappa} = 2^{-1/2}(\partial_{k_X} - i\partial_{k_Y}), \tag{7.49}$$

where $\kappa\bar{\kappa} = 2^{-1} k_{\perp}^2$ and $\partial_{\kappa}\partial_{\bar{\kappa}} = 2^{-1}(\partial_{k_x}^2 + \partial_{k_y}^2)$. Note that in cylindrical coordinates $\varsigma = 2^{-1/2} r_{\perp} \exp(i\psi)$, $\kappa = 2^{-1/2} k_{\perp} \exp(i\varphi)$. The fundamental Gaussian (7.35) and (7.36) now reads $G(\varsigma, \bar{\varsigma}, Z) = (w_w / v)^2 \exp(-\varsigma\bar{\varsigma} v^{-2})$ and $G(\kappa, \bar{\kappa}, Z) = 2\pi \exp(-\kappa\bar{\kappa} v^2)$ and the beam representation (7.34), with new dependence on the new complex coordinates, yields

$$\begin{aligned} &\underline{E}^{(b)}(\varsigma, \bar{\varsigma}, Z) = (w_w / 2\pi)^2 \exp(\pm ik^{(b)} z) \\ &\times \int dk_{\perp} \int d\varphi k_{\perp} \underline{\widetilde{E}}^{(b)}(\kappa, \bar{\kappa}, Z) \exp[i(\varsigma\bar{\kappa} + \bar{\varsigma}\kappa)], \end{aligned} \tag{7.50}$$

where $\varsigma\bar{\kappa} + \bar{\varsigma}\kappa = k_{\perp} r_{\perp} \cos(\psi - \varphi)$.

Next, define, at the interface plane $X - Y$ and in the spectral domain, the ELG beam of the order $2p + l$ in the similar manner as it has been done for the EHG beams of the order $m + n$:

$$\widetilde{G}_{p,l}^{(EL)}(\kappa, \bar{\kappa}, Z) = (iw_w)^{2p+l} \kappa^{p+l} \bar{\kappa}^{p} \widetilde{G}(\kappa, \bar{\kappa}, Z), \tag{7.51}$$

where integers p and l are the radial and azimuthal nonnegative indices of the ELG beam [30]. In the spatial domain, the definition (7.51) yields

$$G_{p,l}^{(EL)}(\varsigma, \bar{\varsigma}, Z) = w_w{}^{2p+l} \partial_{\varsigma}^{p} \partial_{\bar{\varsigma}}^{p+l} G(\varsigma, \bar{\varsigma}, Z). \tag{7.52}$$

For negative values of l Eqs. (7.51) and (7.52) can be obtained by appropriate change of the coordinate system; $\widetilde{G}_{p,l}^{(EL)}(\kappa, \bar{\kappa}, Z) = \widetilde{G}_{p,-l}^{(EL)}(\bar{\kappa}, \kappa, Z)$ and $G_{p,l}^{(EL)}(\varsigma, \bar{\varsigma}, Z) = G_{p,-l}^{(EL)}(\bar{\varsigma}, \varsigma, Z)$. Note also that, because $\kappa^{p+l}\bar{\kappa}^{p} = (2^{-1/2} k_{\perp})^{2p+l} \exp(il\varphi)$, the definition (7.51) directly implies changes in the indices of the ELG beams under transmission:

$$\widetilde{G}_{p,l}^{(EL)}(\kappa, \bar{\kappa}, Z) \exp(\pm 2i\varphi) = \widetilde{G}_{p\mp 1, l\pm 2}^{(EL)}(\kappa, \bar{\kappa}, Z), \tag{7.53}$$

$$\widetilde{G}^{(EL)}_{p,l}(\kappa,\overline{\kappa},Z)\exp(\pm i\varphi)=\widetilde{G}^{(EL)}_{p\mp 1/2,l\pm 1}(\kappa,\overline{\kappa},Z)\,, \tag{7.54}$$

including also fractional values admitted in the radial indices of the ELG beams. Eqs. (7.53) and (7.54) are central results of this section. They lead to exact description of the LG beams of circular polarization interacting with the interface, as will be shown below.

Let the incident beam be of the ELG shape with its spectral amplitude $\widetilde{E}^{(i)}_R=\widetilde{G}^{(EL)}_{p,l}$ for the CR polarization, i.e. for $\underline{E}^{(i)}=\widetilde{E}^{(i)}_R\,\underline{\hat{e}}_R$, or with its spectral amplitude $\widetilde{E}^{(i)}_L=\widetilde{G}^{(EL)}_{p,l}$ for the CL polarization, i.e. for $\underline{E}^{(i)}=\widetilde{E}^{(i)}_L\,\underline{\hat{e}}_L$, respectively. Then the rules (7.53) and (7.54), together with the definition of the transmission matrix (7.32), lead in the spectral domain to exact evaluation of the transmitted ELG beams at the interface, with the following outcome:

$$\begin{bmatrix}\widetilde{E}^{(t)}_R\\ \widetilde{E}^{(t)}_L\end{bmatrix}_{CR}=\tfrac{1}{2}(\eta t_p+t_s)\begin{bmatrix}\widetilde{G}^{(EL)}_{p,l}\\ 0\end{bmatrix}+\tfrac{1}{2}(\eta t_p-t_s)\begin{bmatrix}0\\ \widetilde{G}^{(EL)}_{p-1,l+2}\end{bmatrix}, \tag{7.55}$$

$$\begin{bmatrix}\widetilde{E}^{(t)}_R\\ \widetilde{E}^{(t)}_L\end{bmatrix}_{CL}=\tfrac{1}{2}(\eta t_p+t_s)\begin{bmatrix}0\\ \widetilde{G}^{(EL)}_{p,l}\end{bmatrix}+\tfrac{1}{2}(\eta t_p-t_s)\begin{bmatrix}\widetilde{G}^{(EL)}_{p+1,l-2}\\ 0\end{bmatrix}, \tag{7.56}$$

for the CR and CL polarization of the incident beam, respectively.

Similarly, the longitudinal components of the incident beams are of the form $\widetilde{E}^{(i)}_Z=-2^{-1/2}\widetilde{G}^{(EL)}_{p-1/2,l+1}\tan\vartheta^{(i)}$ for the CR polarization and $\widetilde{E}^{(i)}_Z=-2^{-1/2}\widetilde{G}^{(EL)}_{p+1/2,l-1}\tan\vartheta^{(i)}$ for the CL polarization and this yields for the transmitted beam, respectively:

$$\widetilde{E}^{(t)}_Z|_{CR}=-2^{-1/2}\eta t_p\tan\vartheta^{(t)}\widetilde{G}^{(EL)}_{p-1/2,l+1}\,, \tag{7.57}$$

$$\widetilde{E}^{(t)}_Z|_{CL}=-2^{-1/2}\eta t_p\tan\vartheta^{(t)}\widetilde{G}^{(EL)}_{p+1/2,l-1}\,. \tag{7.58}$$

Therefore, the Z-components of the transmitted beams, i.e., $\widetilde{E}^{(t)}_Z=t^{(EL)}_Z\widetilde{E}^{(i)}_Z$, with the transmission coefficient $t^{(EL)}_Z=\eta\ \ t_p\tan\vartheta^{(t)}/\tan\vartheta^{(i)}$, possesses the same topological charge $l\pm 1$ as the incident beam (cf. also Eq. (7.31)). Note

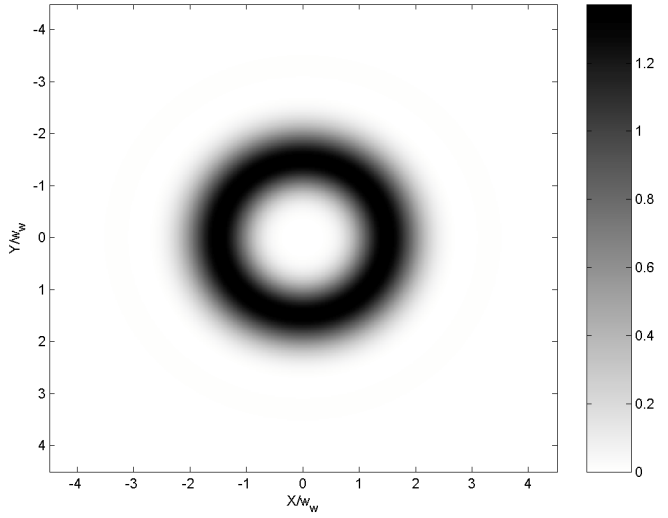

(a)

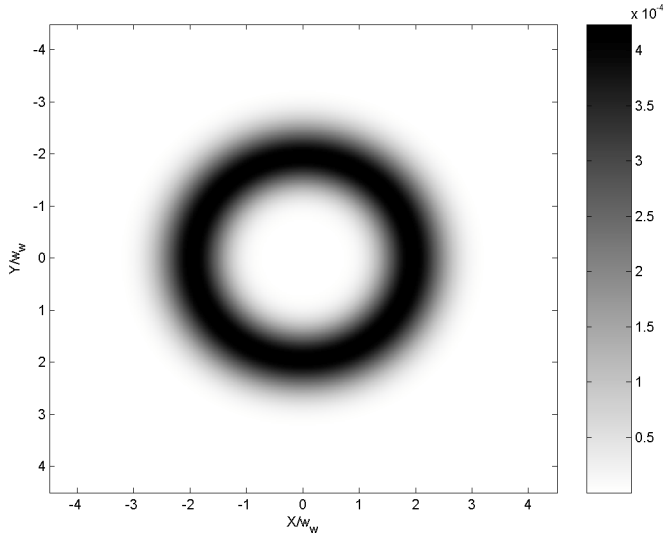

(b)

Figure 7.4. Beam intensity transverse distribution of the ELG beam at the interface; the incident beam of the $ELG_{1,3}$ pattern and of CR polarization (a) and the transmitted beam CL component of the $ELG_{0,5}$ pattern (b); normal incidence.

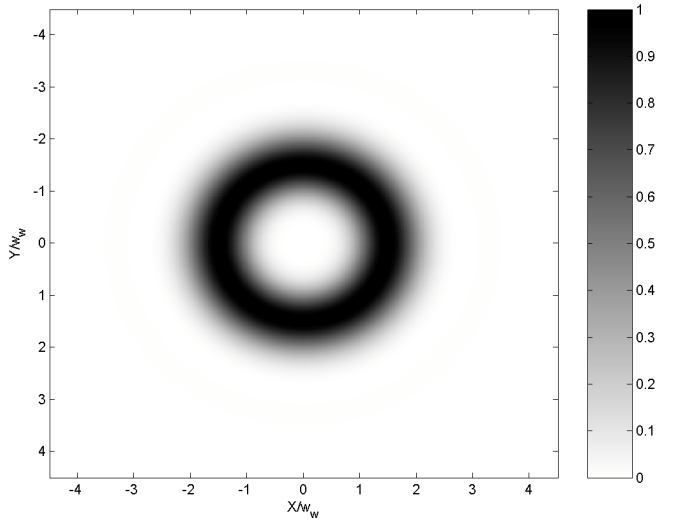

(a)

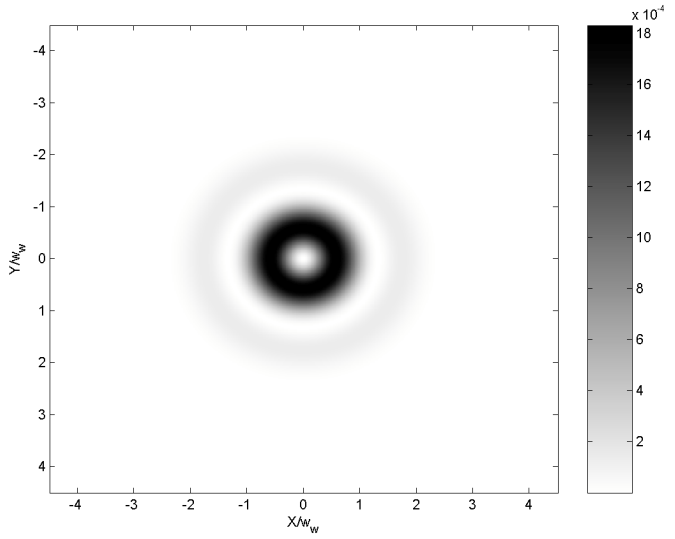

(b)

Figure 7.5. Beam intensity transverse distribution of the ELG beam at the interface; the incident beam of the $ELG_{1,3}$ pattern and of CL polarization (a) and the transmitted beam CR component of the $ELG_{2,1}$ pattern (b); normal incidence.

that, contrary to the EHG beam case, all expressions derived above in the spectral domain for ELG beams are exact and the longitudinal field component resolves into *one* ELG beam function with fractional value $p = 1/2$ of the radial index.

The interface changes indices of the incident ELG beam in the opposite transverse field component. For the incident CR (CL) polarization the radial index of the beam mode decreases (increases) by one and the azimuthal index increases (decreases) by two in the CL (CR) polarization component of the transmitted beam. In (7.55)-(7.56) the radial index of the longitudinal field component decreases (increases) by half and the azimuthal index increases (decreases) by one with respect to the indices of the transverse component of the incident ELG beam of the CR (CL) polarization. Examples of the ELG beam transverse field distribution at the interface is presented in Figs. 7.4-7.8 for narrow beams of $k^{(i)} w_w = 2\pi$. Incidence always is normal and the incident beam always has a pattern of the $ELG_{1,3}$ function.

Figures 7.4 and 7.5 display intensity profiles of the ELG beams. The profile of the incident beam of the $ELG_{1,3}$ pattern and of CR polarization is displayed in Fig. 7.4(a) and that of the CL component of the $ELG_{0,5}$ pattern of the transmitted beam is shown in Fig. 7.4(b). The profile of the incident beam of the $ELG_{1,3}$ pattern and of CL polarization is displayed in Fig. 7.5(a) and that of the CR component of the $ELG_{2,1}$ pattern of the transmitted beam is shown in Fig. 7.5(b). Dependence of a number and radii of the beam annular rings on the incident beam polarization and azimuthal index l is clearly vivid. However a value of the radial index remains uncertain due to a limited accuracy of the numerical integration for points of diminishing intensity of the beams. Also, nothing specific can be inferred from Figs. 7.4 and 7.5 about the azimuthal indices of the beams. The intensity profiles are not sufficient to describe beams of complex structure, especially the beams with singularities in their phase fronts.

In order to complete these figures, phase patterns of the incident and transmitted beams are drawn in Figs. 7.6, 7.7 and 7.8. Values of the azimuthal index are counted as the number of 2π cycles in phase around the beam axis. This number distinguishes the ELG phase patterns of the beams shown in these figures. The phase transverse distribution of the incident $ELG_{1,3}$ beam of CR polarization is shown in Fig. 7.6(a), the phase of the

transmitted beam component of the opposite, CL polatization is shown in Fig. 6(b) - its pattern is of the $ELG_{0,5}$ function. On the other hand, even for normal incidence this case is not symmetric with respect to the replacement of CR polarization by CL polarization in the incident beam - values of the SAM about the Z-axis have opposite signs in these two cases. Therefore, the beam incidence of CL polarization is also described in Fig. 7.7. The phase of the incident $ELG_{1,3}$ beam is shown in Fig. 7.7(a) and the phase of the CR component of the transmitted beam of the $ELG_{2,1}$ shape is shown in Fig. 7.7(b).

Figures 7.6 and 7.7 confirm predictions of Eqs. (7.55) and (7.56) concerning the phase distribution of the beams. However, Figs. 7.6(b) and 7.7(b) display additional ring of zero field amplitude far away from the beam axes. This discrepancy between numerical results and theoretical predictions might be originated by the approximation assumed in evaluation of the Fresnel coefficients (at the beam mean direction) in the field representation (7.34). This may also be caused by limited accuracy of the numerical evaluation of this equation for points of diminishing intensity of the beams. However, the beam phase or the azimuthal index l, not the beam magnitude or radial index p, is used in sorting the beam modes [21].

Figure 7.8 shows the phase distribution of the longitudinal field components predicted by Eqs. (7.57) and (7.58). For the CR polarization of the incident beam of the $ELG_{1,3}$ shape, Fig. 7.8(a) displays the phase distribution for the longitudinal field component of the transmitted beam - this of the pattern of the $ELG_{1/2,4}$ function. For CL polarization of the incident beam of the same shape $ELG_{1,3}$ the phase of the transmitted beam changes to the $ELG_{3/2,2}$ function as shown in Fig. 7.8(b). For both these polarization states of the incident ELG beam the phase structure of the Z-components of the transmitted, and the reflected as well, beams appears the same as that of the incident beams.

The numerical simulations applied in this section are based on direct integration of Maxwell equations [28]. The examples of beam intensity and phase distribution at the interface shown in Figs. 7.2-7.8 evidently confirm theoretical predictions given by analytical expressions (7.42)-(7.47) for EHG beams and (7.55)-(7.58) for ELG beams, evaluated in the interface plane. The XPC effect is fundamental in generation of higher-order modes at the

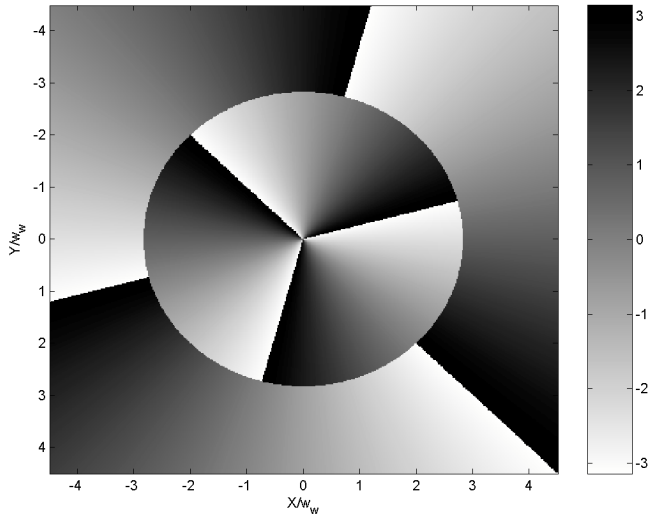

(a)

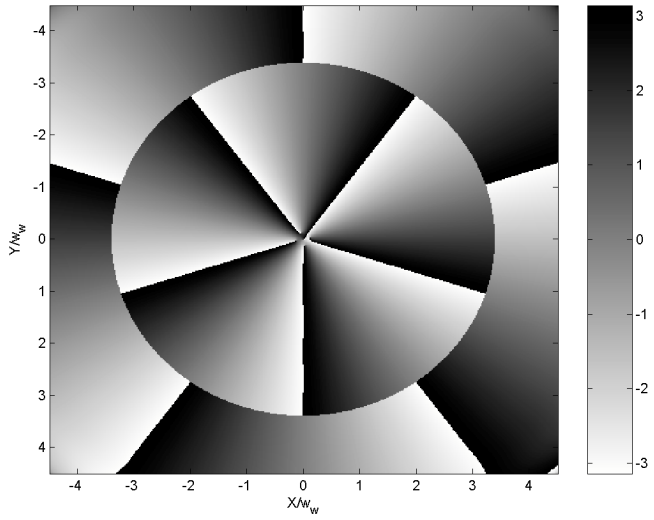

(b)

Figure 7.6. Phase transverse distribution of the ELG beam at the interface; the incident $ELG_{1,3}$ beam of CR polarization (a) and the transmitted beam CL component of the $ELG_{0,5}$ pattern (b); normal incidence.

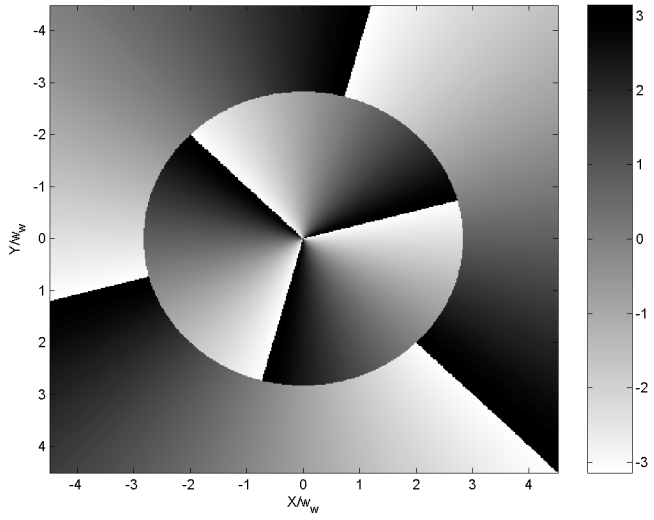

(a)

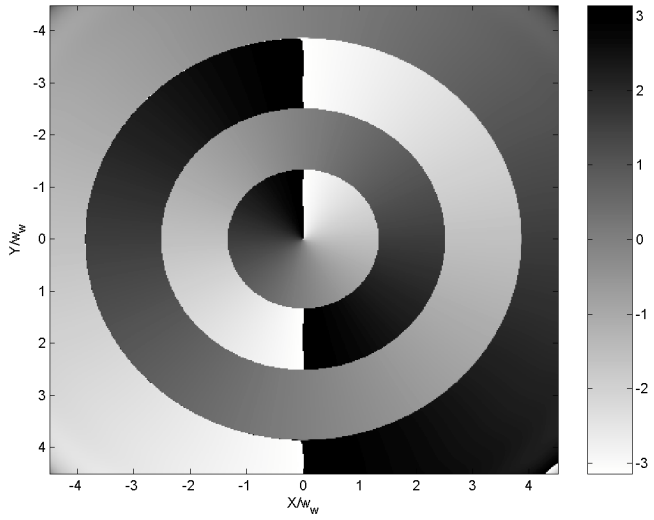

(b)

Figure 7.7. Phase transverse distribution of the ELG beam at the interface; the incident $ELG_{1,3}$ beam of CL polarization (a) and the transmitted beam CR component of the $ELG_{2,1}$ pattern (b); normal incidence.

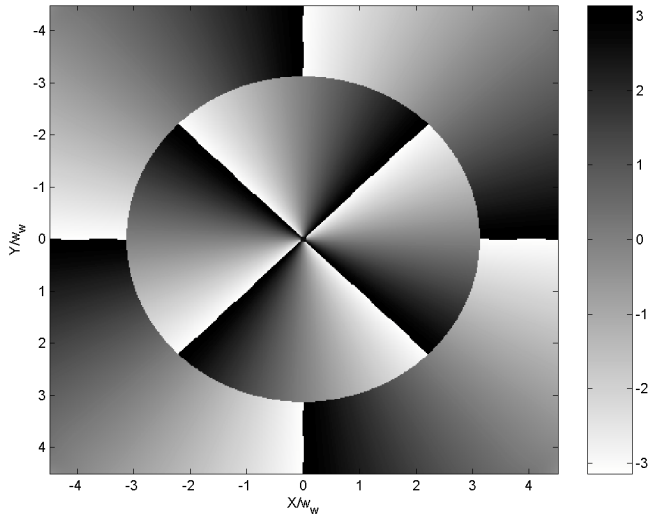

(a)

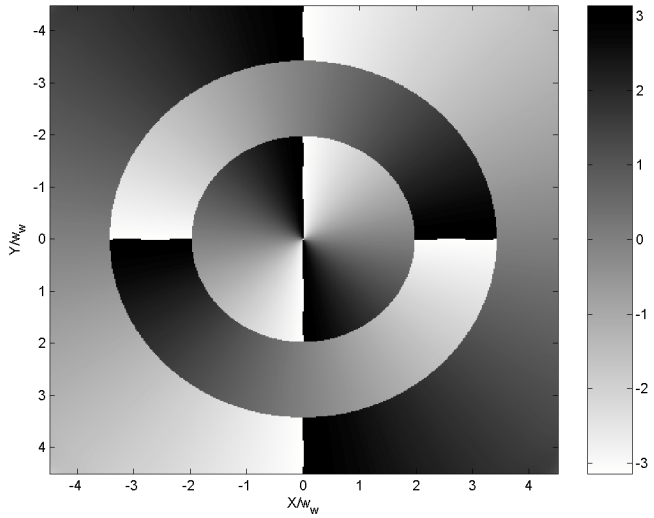

(b)

Figure 7.8. Phase transverse distribution of the ELG beam at the interface; the transmitted beam Z-component of the $ELG_{1/2,4}$ pattern for the incidence of the $ELG_{1,3}$ beam of CR polarization (a), the transmitted beam Z-component of the $ELG_{3/2,2}$ pattern for the incidence of the $ELG_{1,3}$ beam of CL polarization (b); normal incidence.

dielectric interface. Its efficiency can be estimated from the expressions (7.24)-(7.25) and (7.32)-(7.33) for the beam field and its amplitudes (7.22)-(7.23) in the spectral domain. In these expressions, the standard (2D) Fresnel coefficients are replaced by their 3D counterparts:

$$t_{(p,s)}^{(DP)} = \tfrac{1}{2}(\eta t_p + t_s), \tag{7.59}$$

$$r_{(p,s)}^{(DP)} = \tfrac{1}{2}(r_p - r_s), \tag{7.60}$$

for the case of the direct polarization (DP), the same as of the incident beam, and

$$t_{(p,s)}^{(XP)} = \tfrac{1}{2}(\eta t_p - t_s), \tag{7.61}$$

$$r_{(p,s)}^{(XP)} = \tfrac{1}{2}(r_p + r_s), \tag{7.62}$$

for the case of the opposite (cross) polarization (XP), produced by the XPC effect. The DP and XP coefficients do not depend on the incident beam polarization. They are interrelated by the continuity relations at the interface:

$$t_{(p,s)}^{(DP)} = 1 - r_{(p,s)}^{(DP)}, \tag{7.63}$$

$$t_{(p,s)}^{(XP)} = -r_{(p,s)}^{(XP)}, \tag{7.64}$$

separately for the beam components of opposite polarization of the transmitted beams - TM or TE for EHG beams and CR or CL for ELG beams.

The efficiency of the XPC effect is determined by the ratio $t_{(p,s)}^{(XP)} / t_{(p,s)}^{(DP)}$, here given for beam transmission. For normal incidence this ratio is small - of the order 10^{-2}. On the other hand, for beam reflection at critical incidence, magnitude of the ratio $t_{(p,s)}^{(XP)} / t_{(p,s)}^{(DP)}$ is about two orders greater, as expected. However, the case of critical incidence does not seem satisfactory for the ELG beam incidence, as the cylindrical symmetry of the beam-interface configuration becomes then broken and the beams become deformed. Therefore the problem of efficiency of the XPC effect for beam normal incidence still remains to be solved. It seems that a planar boundary between

artificial materials of some sort [31-33] might appear to be a proper solution to this problem.

7.4.4 Beam normal modes at the interface

Within the paraxial approximation the scalar HG and LG functions are solutions of the scalar wave equation. The vector HG and LG beams are paraxial solutions of the Maxwell equations and build two orthogonal basis sets for any paraxial beam mode of free propagation. In the analysis presented in this section these sets comply with four additional conditions. The vector (HG and LG) Gaussian beam should be

(i) considered in their elegant version

and defined:

(ii) in the linear (TE/TM) basis for the EHG beams,

(iii) in the circular (CR/CL) basis for the ELG beams,

(iv) with respect to the interface plane.

The condition (iv) means that, at least for beams other than the fundamental Gaussian, the beam field spatial and polarization structures should be defined in the interface plane $X-Y$ and not, as usual, in the beam transverse plane $x-y$.

The HG and LG beams which obey the conditions (i)-(iv) are named here as the projected EHG and ELG beams. They may be regarded as normal modes of vector beams at the interface. For any member of one from these two sets incident upon the interface, the reflected and transmitted beams also belong to this set. The beams are defined by one pair of their spatial indices - m and n for the EHG beam or p and l for the ELG beam, in each of the two opposite beam polarizations - TM and TE or CR and CL for the EHG or ELG beam, respectively. The interface acts almost exactly in this manner. For ELG beams only oneapproximation necessary in the derivations above was assumed in the spatial domain, concerning mean values of the Fresnel coefficients. Still even this assumption can be neglected if nonuniform polarization of the beams is admitted.

The interface redistributes the incident energy, momentum and angular momentum into a pair of beams of two orthogonal polarization states, one pair for each of the transmitted and reflected beams. One element of this pair

possesses the same polarization and spatial structure as those of the incident beam. The spatial structure of the second element, that of the opposite polarization, appears alsospatially biorthogonal to the first element. This process may be understood as creation and annihilation of beam modes at the planar interface. For ELG beams it also means creation and annihilation of optical vortices placed on axes of these beams.

Having defined the biorthogonal sets of normal modes defined above, any field with arbitrary complex amplitude and polarization distribution can be readily expanded in a standard manner in terms of these modes. Till now EHG and ELG beams have been used mainly in the context of propagation in the free-space, infinite bulk material or non-self-adjoint optical systems [34,35]. This contribution provides, to the best of my knowledge, the first analytical and exact derivation of the decomposition of an arbitrary 3D beam field at the planar interface in terms of the (projected) elegant HG and LG normal beam modes.

7.5 Angular momentum of beams at the interface

Let us now look into the beam transmission from a slightly different point of view. It is well known that beams carry the TAM composed, in general, of SAM and OAM components [1]. The spin component is associated with beam polarization and the orbital component results from azimuthal transverse distribution of the beam phase. For the circularly polarized beams the SAM component is equal to $\sigma\hbar$ per photon, where $\sigma = \pm 1$ for the CR and CL polarization, respectively. Since the LG beams are angular momentum eigenstates, their OAM component, associated with the beam phase dependence of the form $\exp(il\psi)$ is equal to $l\hbar$ per photon. Both the SAM and OAM contribute to the Z-component of TAM per photon:

$$j_Z^{(b)} = (\sigma + l)\hbar\,, \tag{7.65}$$

separately for the incident (b=i), transmitted (b=t) and reflected (b=r) beam, where for any beam the angular momentum is measured with respect to the normal to the interface (the Z-axis). Eqs. (7.55)-(7.56) show that TAM per photon is conserved for ELG beam transmission at the interface, and similarly also for ELG beam reflection. For any photon, transmitted or reflected at the interface, its TAM is conserved:

$$j_Z^{(i)} = j_Z^{(t)} \qquad \text{or} \qquad j_Z^{(i)} = j_Z^{(r)}, \tag{7.66}$$

respectively. Therefore the SAM and OAM components of TAM per photon depend of the polarization of the transmitted beam.

For example, for a single photon of the incident beam $\underline{\widetilde{E}}_R^{(i)} = \widetilde{G}_{p,l}^{(EL)} \underline{\hat{e}}_R$, of the topological charge l and of *the CR polarization* ($\sigma = 1$), its TAM amounts to $j_Z^{(i)} = l + 1$ (cf. eq. (7.55)). The transmitted (or the reflected) photon possess the same TAM $j_Z^{(t)} = l + 1$ independently of its polarization. For the transmitted photon of *the CR polarization* its spin and orbital components are the same as those of the incident photon. However, for *the opposite, CL polarization* of the transmitted beam, the OAM of the photon is increased by two (from l to $l + 2$) as its SAM is decreased at the same time by two (from $\sigma = 1$ to $\sigma = -1$).

Similar rules are also valid for the incident ELG beams $\underline{\widetilde{E}}_L^{(i)} = \widetilde{G}_{p,l}^{(EL)} \underline{\hat{e}}_L$ of *the CL polarization* ($\sigma = -1$). The TAM $j_Z^{(t)} = l - 1$ per photon, as well the SAM $\sigma = -1$ and OAM l per photon, of the transmitted beam of *the same, CL polarization* appears the same as the TAM, SAM and OAM of the incident photon. For the transmitted photon of *the opposite, CR polarization* its OAM is decreased by two (from l to $l - 2$) as its SAM is increased at the same time also by two (from $\sigma = -1$ to $\sigma = 1$). Therefore its TAM per photon $j_Z^{(i)} = l - 1$ remains equal to that of the photon of the incident ELG beam.

Equations (7.55)-(7.56), together with their counterparts for beam reflection, may be regarded as equivalent to the conservation principle of TAM for a single photon at the flat interface. With the continuity relations (7.22)-(7.23) they correspond also to the conservation of integrated TAM $J_Z^{(b)} = j_Z^{(b)} N^{(b)}$ of any set of the (incident, refracted and reflected) projected ELG beams at the interface:

$$J_Z^{(i)} = J_Z^{(t)} + J_Z^{(r)}, \tag{7.67}$$

where $N^{(b)} = U^{(b)} / \hbar\omega$ stands for a number of photons in a monochromatic beam of time averaged energy U per unit length of the beam [14]. Moreover, for the ELG beam incidence, the conservation of TAM of these

beams follows directly from the conservation of TAM of each photon of which these beams are composed.

The above considerations pertain to the LG beams in their projected elegant version and of the circular polarization. In this case the interface is acting, through the transmission matrices (7.32) within the complete set of such beams and produces pure eigenmodes with specified indices (p and l) of the beam spatial structure in each one of the two (CR and CL) states of circular polarization. For beams of other spatial distribution of its complex amplitude and/or polarization - like the standard LG beams of arbitrary polarization - the action of the interface may be understood as creating an appropriate superposition of pure projected ELG beams of circular polarization. In such cases one has to consider mean values of TAM and OAM of these beams [19]. Still the conservation principles of TAM for a single photon (7.66) and for the total beam (7.67) remain valid.

The derivation of the conservation principle (7.55)-(7.56) for TAM of beams at the interface was possible due to the exact form of the transmission and reflection coefficients (7.32)-(7.33) or (7.12), (7.13) and (7.19). Both, the first-order and the second-order transverse corrections (in k_Y; see Eq. (13)) to the standard Fresnel coefficients ηt_p, t_s, r_p and r_s are necessary to obtain this result. The first-order corrections to the Fresnel coefficients, as well as these coefficients by themselves, are not sufficient to guarantee exactly the TAM conservation. Still, the TAM conservation (7.66) for a single photon was also approximately applied, instead of the field continuity relations, in the treatment of beams at a dielectric interface within a geometrical optics approach [36].

Note also that the ELG beams considered here possess cylindrical symmetry in the interface frame $OXYZ$. For incidence angles $\theta^{(i)}$ different from zero, such beams are elliptic and astigmatic in their intensity and phase distribution in their beam frames $Oxyz$. Moreover, the polarization parameters of the beams $\lambda^{(b)}_{(X,Y)} = \pm i$ in the frame $OXYZ$ read $\lambda^{(b)}_{(X,Y)} \cos\theta^{(b)} = \pm i \cos\theta^{(b)}$ for the same beams in their beam frames $Oxyz$ [5]. However, when the orientation of the beam astigmatism and ellipticity are the same, the OAM of the beams is originated only in the helical singularities of beam phase [37].

This is not so for beams of different orientation of their intensity and phase astigmatism. More general astigmatic beam modes may carry OAM not originated exclusively in the beam phase singularities [37]. Such beams also form complete sets of Gaussian solutions of the paraxial wave equation and may serve as another basis for treatment the problem of 3D beams impinging at the interface.

7.6 Comments and conclusions

Beam-interface interactions have been described within a frame of the complete, biorthogonal sets of the projected EHG beams of linear TM/TE uniform polarization and the projected ELG beams of circular CR/CL uniform polarization. It was shown that such beams are normal modes at the interface and thus, in general, at any planar layered structure. The beam transverse spatial profile, phase and polarization are interrelated through the XPC effect present at the interface. These relations differentiate normal and critical incidence of the beams and can be described by generalized Fresnel coefficients of transmission and reflection, specific to the incidence of beams of 3D structure and arbitrary polarization.

Rigorous analytical description of beam fields at the isotropic interface in terms of the projected EHG and ELG vector beam modes has been given. The interface redistributes incident beam energy between beam components of opposite polarization and modifies spatial distribution of their intensity and phase. This process is quantitatively described through changes of indices of transverse spatial distribution of complex beam fields or, for ELG beams of circular polarization, in terms of conservation of their TAM. In the latter case changes of SAM are compensated by changes of OAM, or vice versa. For incidence of beams of general phase and intensity distribution and general polarization, the interface discriminates the beam field in favor of EHG beam modes of linear polarization and of ELG beam modes of circular polarization. The process has been described by derivation of exact analytical expressions for spectral components of the beam field at the interface plane.

Results of this chapter indicate that the dielectric interface, or, in general, any planar multilayered structure, can be used as a mean of control the interplay between the beam field distribution, in its magnitude and phase, and the beam field polarization. The control process is based on the XPC

effect acting at the interface and depends on the incident beam parameters like the beam polarization, shape and angle of incidence [5,28,29]. The ability to control the beam shape and polarization may appear useful in many applications in contemporary optics, provided that the efficiency of the XPC effect can be sufficiently strong. It seems that application of the presented approach to the cases of beams at layered structures, composed of anisotropic, photonic or meta-materials, may reveal such a possibility.

Note that for normal incidence the first-order shifts of the beams disappear and due to this fact they have not been discussed in this chapter. However, the expressions of the transmission and reflection matrices derived in this chapter are also valid in the case of arbitrary beam incidence and the whole formalism presented above can be directly extended into this case. Then, for the oblique incidence of beams, these transmission and reflection matrices can serve as a starting point in the discussion of the beam shifts [28]. Although these shifts have been already defined in Chapter 3, their main characteristics will be discussed, from a slightly different point of view, in Appendix being a final part of this chapter and this book.

Appendix: One more note on the beam shifts

In this appendix, basic relations describing the shifts of the transmitted and reflected beams will be put together, with a few additional comments and final conclusions enclosed. These relations will be given, contrary to the analysis of Chapter 3, with respect to the interface coordinate frame $OXYZ$. It should be noted that the case of oblique beam incidence has been examined in Ref. [28] by the method described in this chapter. This method employs the XPC effect in evaluation of the two opposite, TM and TE or CR and CL, components of the reflected and transmitted fields. As both these field components are evaluated at the same time, they suffer only from the longitudinal shift independent of the incident beam polarization. The transverse shifts are replaced by a superposition of the beam field, represented by the two transverse beam components (see Figure 9). In spite of the presence of the longitudinal shift, the beam field reshaping relations (42)-(43) and (55)-(56) remain valid.

Still, these shifts remain different for each one of the two beam components and, in addition, these components show different transverse field

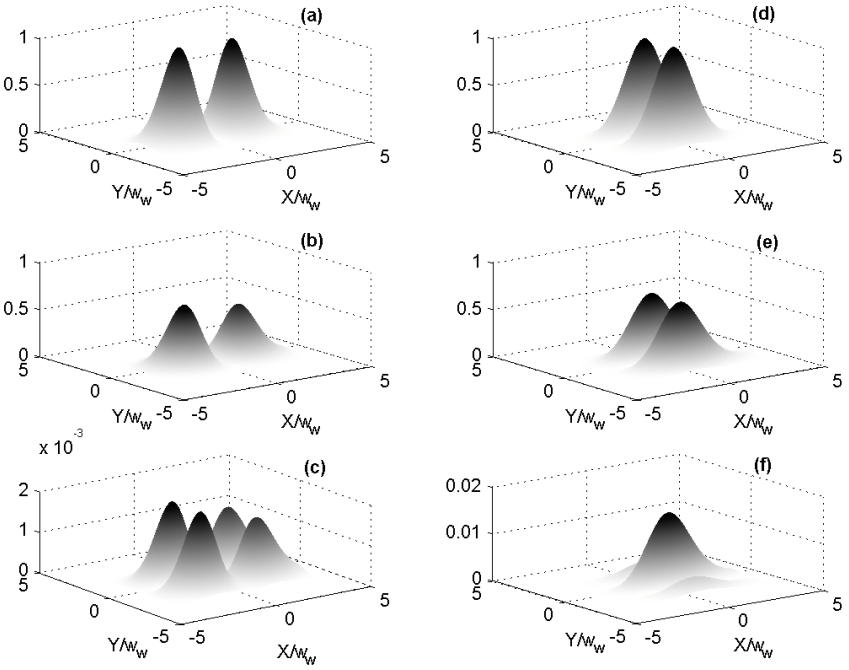

Figure 7.9. Reflection of the EHG beam at the critical incidence of TIR with the incidence angle $\theta_c = 45^o$. Incidence of a $G_{10}^{(EH)}$ beam is presented in (a)-(c), incidence of a $G_{01}^{(EH)}$ beam is presented in (d)-(f). Intensity distributions of the incident beam of TE polarization (a) and (d), reflected beam TE component (b) and (e) and reflected beam TM component (c) and (f) are shown in the interface plane. The first-order longitudinal beam shifts (along X -direction) are clearly visible in (b)-(c) and (e)-(f) (after [28]).

distributions. However, one might expect to have in the analysis of the beam-interface interactions a more convenient, although less accurate, approach, within which the beam components are assumed to be at least of the same field distribution. The approach of this sort was proposed in Chapter 3. In

order to specify more closely this approach, its main relations will be also collected in this Appendix.

The relations describing beam transmission and reflection given in this chapter remain valid for oblique incidence as well, after taking into account the nonzero beam incidence by an angle $\theta_0^{(i)}$. In this case the principal beam frame $Oxyz$ does not coincide with the interface frame $OXYZ$ (cf. Fig. 1). Both frames are related by the rotation $\underline{\underline{R}}_Y(\theta_0^{(i)})$ through the incidence angle $\theta_0^{(i)}$ of the incidence plane $X-Z$ about the Y-axis, given here in the 3D version in the direct domain:

$$\begin{bmatrix} X \\ Y \\ Z \end{bmatrix} = \begin{bmatrix} \cos\theta_0^{(i)} & 0 & \sin\theta_0^{(i)} \\ 0 & 1 & 0 \\ -\sin\theta_0^{(i)} & 0 & \cos\theta_0^{(i)} \end{bmatrix} \begin{bmatrix} \pm x \\ y \\ \pm z \end{bmatrix}, \tag{A.7.1}$$

and in the spectral domain:

$$\begin{bmatrix} k_X \\ k_Y \\ k_Z \end{bmatrix} = \begin{bmatrix} \cos\vartheta_0^{(i)} & 0 & \sin\vartheta_0^{(i)} \\ 0 & 1 & 0 \\ -\sin\vartheta_0^{(i)} & 0 & \cos\vartheta_0^{(i)} \end{bmatrix} \begin{bmatrix} \pm k_x \\ k_y \\ \pm k_z \end{bmatrix}, \tag{A.7.2}$$

respectively, with upper (lower) signs corresponding to the frames of the incident and transmitted (reflected) beams. In (A.7.2), the same value $\vartheta_0^{(i)} = \theta_0^{(i)}$ of the incidence angle is taken in both the direct and spectral domains, thus $\underline{\underline{R}}_Y(\vartheta_0^{(i)}) = \underline{\underline{R}}_Y(\theta_0^{(i)})$. Then, the spectral representation of the beam field can be expressed alternatively in the two frames, in the frame $Oxyz$:

$$\begin{aligned} \underline{E}_{(x,y)}^{(b)}(x,y,z) &= (w_w/2\pi)^2 \exp[\pm ik^{(b)}z] \\ &\times \int dk_x \int dk_y \, \underline{\widetilde{E}}_{(x,y)}^{(b)}(k_x,k_y,z)\exp[i(k_x x + k_y y)], \end{aligned} \tag{A.7.3}$$

or, alternatively, in the frame $OXYZ$:

$$\begin{aligned} \underline{E}_{(\pm X,Y)}^{(b)}(X,Y,Z) &= (w_w/2\pi)^2 (\cos\theta_0^{(i)})^{-1} \exp[\pm ik^{(b)} Z/\cos\theta_0^{(i)}] \\ &\times \int dk_X \int dk_Y \, \underline{\widetilde{E}}_{(\pm X,Y)}^{(b)}(k_X,k_Y,Z)\exp[i(k_X X + k_Y Y)], \end{aligned} \tag{A.7.4}$$

where the upprer (lower) signs correspond to the incident (b=i) or transmitted
(b=t) (reflected; t=r) beams. As both field representations are related by the rotation $\underline{\underline{R}}_Y(\theta_0^{(i)})$:

$$\underline{E}^{(b)}_{(\pm X,Y)}(X,Y,Z) = \underline{E}^{(b)}_{(x,y)}(x,y,z), \tag{A.7.5}$$

the initial condition for the incident beam evolution (with respect to z) can be postulated in any beam transverse plane $x-y$, alternatively in one of the two frames $OXYZ$ or $Oxyz$. It can be accomplished, for example, by postulating the beam field distribution $\underline{E}^{(b)}_{(\pm X,Y)}(X,Y,Z)$ at $Z=-x\sin\theta_0^{(i)}$ or, alterna-tively, by $\underline{E}^{(b)}_{(x,y)}(x,y,0)$ at $z=0$, that is in the beam waist plane. Note that for oblique incidence, any circular cross-section of the beam in the plane $x-y$ corresponds to an elliptic cross-section of the beam in the interface plane $X-Y$.

The beam fields $\underline{\widetilde{E}}^{(i)}_{(X,Y)}$, $\underline{\widetilde{E}}^{(t)}_{(X,Y)}$ and $\underline{\widetilde{E}}^{(r)}_{(-X,Y)}$ have been defined in Section 2 in the linear polarization basis $\underline{e}_{(X,Y)} = [\underline{e}_X, \underline{e}_Y]$ with respect to the interface plane $X-Y$ and interrelated:

$$\underline{\widetilde{E}}^{(t)}_{(X,Y)} = \underline{\underline{t}}_{(X,Y)}\underline{\widetilde{E}}^{(i)}_{(X,Y)}, \tag{A.7.6}$$

$$\underline{\widetilde{E}}^{(r)}_{(-X,Y)} = \underline{\underline{r}}_{(-X,Y)}\underline{\widetilde{E}}^{(i)}_{(X,Y)}, \tag{A.7.7}$$

by the transmission and reflection diagonal matrices:

$$\underline{\underline{t}}_{(X,Y)} = \begin{bmatrix} \eta t_{TM} & 0 \\ 0 & t_{TE} \end{bmatrix}, \tag{A.7.8}$$

$$\underline{\underline{r}}_{(-X,Y)} = \begin{bmatrix} r_{TM} & 0 \\ 0 & r_{TE} \end{bmatrix}, \tag{A.7.9}$$

with their elements in the form of the transmission and reflection coefficients:

$$\eta t_{TM} = \eta t_p + \Delta_{TM} = \eta t_p + (\eta t_p - t_s)k_\perp^{-2}k_Y[\widetilde{\chi}^{(i)}_{(X,Y)}{}^{-1}k_X - k_Y],$$

$$t_{TE} = t_s + \Delta_{TE} = t_s + (\eta t_p - t_s) k_\perp^{-2} k_Y [\tilde{\chi}_{(X,Y)}^{(i)}{}^{+1} k_X + k_Y], \tag{A.7.10}$$

$$r_{TM} = r_p - \Delta_{TM} = r_p + (r_p - r_s) k_\perp^{-2} k_Y [\tilde{\chi}_{(X,Y)}^{(i)}{}^{-1} k_X - k_Y],$$

$$r_{TE} = r_s + \Delta_{TE} = r_s - (r_p - r_s) k_\perp^{-2} k_Y [\tilde{\chi}_{(X,Y)}^{(i)}{}^{+1} k_X + k_Y], \tag{A.7.11}$$

where $\underline{k}_\perp = [k_X, k_Y]^T$ and $\eta = n^{(i)} k_Z^{(t)} / n^{(t)} k_Z^{(i)}$. Note that $\eta t_p - t_s = -(r_p - r_s)$ at the interface.

The coefficients are given in (A.7.10)-(A.7.11) by means of the linear polarization parameter $\tilde{\chi}_{(X,Y)}^{(i)} = \tilde{E}_X^{(i)} / \tilde{E}_Y^{(i)}$, where $\tilde{\chi}_{(X,Y)}^{(i)}{}^{-1} = 0$ and $\tilde{\chi}_{(X,Y)}^{(i)} = 0, -i, i$ for TM, TE, CR and CL polarization states of the incident beam, respectively. The subsequent components in the definitions (A.7.10)-(A.7.11) correspond to the zero-order (Fresnel), first-order and second-order (with respect to k_Y) effects of nsp transmission and reflection. Only the first-order effects are created by the XPC effect at the interface and only these effects are dependent on the polarization state of the incident beam field through the polarization parameter $\tilde{\chi}_{(X,Y)}^{(i)}$, as shown in Eqs. (A.7.10)-(A.7.11). Note that minus sign in the subscript $(-X, Y)$ indicates that the sense of the TM polarization of the beam field, defined in the interface frame $OXYZ$, corresponds to the sense of the actual beam polarization defined in the beam frame $Oxyz$ (cf. Fig. 7.1).

The expressions (A.7.6)-(A.7.11) for the transmission $\underline{\underline{t}}_{(X,Y)}$ and reflection $\underline{\underline{r}}_{(-X,Y)}$ matrices are given in the spectral domain. Their elements are changing, in general, from one local incidence plane $\varphi = \arctan(k_Y / k_X) = const.$ to another local incidence plane. However, the geometrical first- and second-order effects of the nonspecular (nsp) beam transmission and reflection are expected to be known in the direct domain. To define these effects in this domain, the matrices (A.7.8)-(A.7.9) are first approximately evaluated in one plane – the incidence plane $k_Y = k_y = 0$ for $\vartheta = \theta_0$, that is for $\underline{k}_\perp = \underline{k}_{\perp 0} = [k_{X_0}, 0]^T$, where $k_{X_0} = k \sin\theta_0^{(i)}$. After that they can be treated approximately as the shifts of the beams in the direct domain

or can be transferred to this domain by more accurate methods as, for example, the MIG method described in Chapter 4.

Let us first concentrate first on the first-order effects. In this case, the complex in general TM and TE elements of the diagonal matrices for beam transmission (b=t) and reflection (b=r) are expressed by a scalar product of the complex shift vectors $\underline{L}_{TM}^{(b)}$, $\underline{L}_{TE}^{(b)}$ and transverse wave vectors $\underline{k}_{\perp}$ [28]. They can be alternatively defined in the interface plane $X-Y$ or in the plane transverse to the beam axis $x-y$ plane, respectively:

$$\underline{\underline{t}}_{(X,Y)} = \begin{bmatrix} \eta t_p \exp(-i\underline{L}_{TM}^{(t)} \circ (\underline{k}_{\perp} - \underline{k}_{\perp 0})) & 0 \\ 0 & t_s \exp(-i\underline{L}_{TE}^{(t)} \circ (\underline{k}_{\perp} - \underline{k}_{\perp 0})) \end{bmatrix}, \tag{A.7.12}$$

$$\underline{\underline{r}}_{(-X,Y)} = \begin{bmatrix} r_p \exp(-i\underline{L}_{TM}^{(r)} \circ (\underline{k}_{\perp} - \underline{k}_{\perp 0})) & 0 \\ 0 & r_s \exp(-i\underline{L}_{TE}^{(r)} \circ (\underline{k}_{\perp} - \underline{k}_{\perp 0})) \end{bmatrix}, \tag{A.7.13}$$

where

$$\underline{L}_{TM}^{(b)} \circ (\underline{k}_{\perp} - \underline{k}_{\perp 0}) = L_{TMX}^{(b)} (k_X - k_{X_0}) + L_{TMY}^{(b)} k_Y = L_{TMx}^{(b)} k_x + L_{TMy}^{(b)} k_y \,, \tag{A.7.14}$$

$$\underline{L}_{TE}^{(b)} \circ (\underline{k}_{\perp} - \underline{k}_{\perp 0}) = L_{TEX}^{(b)} (k_X - k_{X_0}) + L_{TEY}^{(b)} k_Y = L_{TEx}^{(b)} k_x + L_{TEy}^{(b)} k_y \,. \tag{A.7.15}$$

Next, the complex first-order shifts can be evaluated approximately in the spectral domain by first two (zero-order and fist-order) terms in Taylor expansions of $\ln \eta t_{TM}$, $\ln t_{TE}$, $\ln r_{TM}$ and $\ln t_{TE}$. For beam transmission, the longitudinal first-order complex shifts (along the X-axis) of the TM and TE components of the transmitted beam are:

$$L_{TMX}^{(t)} = i\partial_{k_X} \ln(\eta t_{TM}) \,|_{k_x=k_{x0},k_y=0} = i\partial_{k_X} \ln(\eta t_p) \,|_{k_x=k_{x0},k_y=0} \,,$$

$$L_{TEX}^{(t)} = i\partial_{k_X} \ln t_{TE} \,|_{k_x=k_{x0},k_y=0} = i\partial_{k_X} \ln t_s \,|_{k_x=k_{x0},k_y=0} \,, \tag{A.7.16}$$

and the transverse first-order complex shifts (along the Y-axis) of the TM and TE components of the transmitted beam are:

$$L_{TMY}^{(t)} = i\partial_{k_Y} \ln(\eta t_{TM}) \,|_{k_x=k_{x0},k_y=0} = i(\eta t_p)^{-1} \partial_{k_Y} \Delta_{TM} \,|_{k_x=k_{x0},k_y=0} \,,$$

$$L_{TEY}^{(t)} = i\partial_{k_Y} \ln t_{TE} \mid_{k_x=k_{x0},k_y=0} = it_s^{-1}\partial_{k_Y}\Delta_{TE} \mid_{k_x=k_{x0},k_y=0}, \tag{A.7.17}$$

where $k_{X0} = k\sin\theta_0$. Similarly, for beam reflection one gets:

$$L_{TMX}^{(r)} = i\partial_{k_X} \ln r_{TM} \mid_{k_x=k_{x0},k_y=0} = i\partial_{k_X} \ln r_p \mid_{k_x=k_{x0},k_y=0},$$

$$L_{TEX}^{(r)} = i\partial_{k_X} \ln r_{TE} \mid_{k_x=k_{x0},k_y=0} = i\partial_{k_X} \ln r_s \mid_{k_x=k_{x0},k_y=0}, \tag{A.7.18}$$

and the transverse first-order complex shifts of the TM and TE components of the reflected beam are:

$$L_{TMY}^{(r)} = i\partial_{k_Y} \ln r_{TM} \mid_{k_x=k_{x0},k_y=0} = -ir_p^{-1}\partial_{k_Y}\Delta_{TM} \mid_{k_x=k_{x0},k_y=0},$$

$$L_{TEY}^{(r)} = i\partial_{k_Y} \ln r_{TE} \mid_{k_x=k_{x0},k_y=0} = +ir_s^{-1}\partial_{k_Y}\Delta_{TE} \mid_{k_x=k_{x0},k_y=0}. \tag{A.7.19}$$

Until now all the entities discussed were complex. However, on the grounds on simple geometrical considerations (see Chapter 3), all these complex entities can be interpreted in terms of real geometrical shifts $\delta_{TMX}^{(b)}$, $\delta_{TMY}^{(b)}$, $\delta_{TEX}^{(b)}$, $\delta_{TEY}^{(b)}$ and angular deviations $\delta_{TM\vartheta_X}^{(b)}$, $\delta_{TM\vartheta_Y}^{(b)}$, $\delta_{TE\vartheta_X}^{(b)}$, $\delta_{TE\vartheta_Y}^{(b)}$ of the TM components,

$$\begin{aligned} L_{TMX}^{(b)} &= -L_{TMx}^{(b)}/\cos\theta_0^{(i)} \cong \delta_{TMX}^{(b)} + iz_{Dx}\delta_{TM\vartheta_X}^{(b)} \\ &= -(\delta_{TMx}^{(b)} + iz_{Dx}\delta_{TM\vartheta_x}^{(b)})/\cos\theta_0^{(i)} \\ L_{TMY}^{(b)} &= L_{TMy}^{(b)} \cong \delta_{TMY}^{(b)} + iz_{Dy}\delta_{TM\vartheta_Y}^{(b)} = \delta_{TMy}^{(b)} + iz_{Dy}\delta_{TM\vartheta_y}^{(b)}, \end{aligned} \tag{A.7.20}$$

and TE components,

$$\begin{aligned} L_{TEX}^{(b)} &= -L_{TEx}^{(b)}/\cos\theta_0^{(i)} \cong \delta_{TEX}^{(b)} + iz_{Dx}\delta_{TE\vartheta_X}^{(b)} \\ &= -(\delta_{TEX}^{(b)} + iz_{Dx}\delta_{TE\vartheta_X}^{(b)})/\cos\theta_0^{(i)} \\ L_{TEY}^{(b)} &= L_{TEy}^{(b)} \cong \delta_{TEY}^{(b)} + iz_{Dy}\delta_{TE\vartheta_Y}^{(b)} = \delta_{TEy}^{(b)} + iz_{Dy}\delta_{TE\vartheta_y}^{(b)}, \end{aligned} \tag{A.7.21}$$

of beams, respectively. where z_{Dx} and z_{Dy} are diffraction lengths of the incident beam in the $y=0$ and $x=0$ planes, respectively. The subscripts X and x indicate the longitudinal nsp shifts present in the incidence plane $X-Z$ or $x-z$ in the directions of the X-axis and x-axis, respectively (cf. Fig. 7. 1). The subscripts Y and y indicate the transverse nsp shifts present in

the plane transverse to the incidence plane $x-z$ in the (same) directions of the Y- and y- axes (cf. Fig. 7.1). The subscripts TM and TE indicate the TM or TE component of the transmitted (b=t) or reflected (b=r) beam suffered from the shifts in the directions specified by the X, x, Y or y subscripts.

Now the complex and real first-order beam shifts are specified by (A.7.16)-(A.7.21) and can be applied to the beam field description. For the incident beam expressed in its plane-wave decomposition (A.7.3), the beams acquires, on the grounds of the relations (A.7.6)-(A.7.15), the complex shifted representation in the following form for the transmitted beam:

$$\begin{aligned} &E_X^{(t)}(X,Y,Z) \\ &= (w_w/2\pi)^2(\cos\theta_0^{(i)})^{-1}\eta t_p \exp[ik^{(t)}(-L_{TMX}^{(t)}\sin\theta_0^{(i)} + Z/\cos\theta_0^{(i)})] \\ &\times \int dk_X \int dk_Y \widetilde{E}_X^{(i)}(k_X,k_Y,Z)\exp\{i[(k_X(X-L_{TMX}^{(t)}) + k_Y(Y-L_{TMY}^{(t)})]\}\,, \end{aligned} \tag{A.7.22}$$

$$\begin{aligned} &E_Y^{(t)}(X,Y,Z) \\ &= (w_w/2\pi)^2(\cos\theta_0^{(i)})^{-1} t_s \exp[ik^{(t)}(-L_{TEX}^{(t)}\sin\theta_0^{(i)} + Z/\cos\theta_0^{(i)})] \\ &\times \int dk_X \int dk_Y \widetilde{E}_Y^{(i)}(k_X,k_Y,Z)\exp\{i[(k_X(X-L_{TEX}^{(t)}) + k_Y(Y-L_{TEY}^{(t)})]\}\,, \end{aligned} \tag{A.7.23}$$

and for the reflected beam:

$$\begin{aligned} &E_X^{(r)}(X,Y,Z) \\ &= -(w_w/2\pi)^2(\cos\theta_0^{(i)})^{-1} r_p \exp[ik^{(r)}(-L_{TMX}^{(r)}\sin\theta_0^{(i)} + Z/\cos\theta_0^{(i)})] \\ &\times \int dk_X \int dk_Y \widetilde{E}_X^{(i)}(k_X,k_Y,Z)\exp\{i[(k_X(X-L_{TMX}^{(r)}) + k_Y(Y-L_{TMY}^{(r)})]\}\,, \end{aligned} \tag{A.7.24}$$

$$\begin{aligned} &E_{Y.}^{(r)}(X,Y,Z) \\ &= (w_w/2\pi)^2(\cos\theta_0^{(i)})^{-1} r_s \exp[ik^{(r)}(-L_{TEX}^{(r)}\sin\theta_0^{(i)} + Z/\cos\theta_0^{(i)})] \\ &\times \int dk_X \int dk_Y \widetilde{E}_Y^{(i)}(k_X,k_Y,Z)\exp\{i[(k_X(X-L_{TEX}^{(r)}) + k_Y(Y-L_{TEY}^{(r)})]\}\,. \end{aligned} \tag{A.7.25}$$

The definitions (A.7.16)-(A.7.21) of the first-order shifts applied in the beam representations (A.7.22)-(A.7.25) are completely equivalent to the definitions (A.7.5), (A.7.7) and (3.13) given in Chapter 3 and in previous publications [9] and [5]. Moreover, by complete analogy to the definitions (A.7.6), (A.7.8), (A.7.19), (A.7.21) and (3.13) in Chapter 3, one can also define in this way the entire set of the second-order complex and real beam shifts. The second-order complex shift vectors $\underline{F}_{TM}^{(b)}$ and $\underline{F}_{TE}^{(b)}$ and their real counterparts – longitudinal and transverse focal shifts $\delta_{TMz_x}^{(b)}$, $\delta_{TEz_X}^{(b)}$, $\delta_{TMz_x}^{(b)}$, $\delta_{TEz_y}^{(b)}$ and waist radius modifications $\delta_{Twz_x}^{(b)}$, $\delta_{TEw_x}^{(b)}$, $\delta_{TMw_x}^{(b)}$, $\delta_{TEw_y}^{(b)}$ - are then evaluated in the beam frame $Oxyz$ from the second-order terms in Taylor expansions of $\ln\eta t_{TM}$, $\ln t_{TE}$, $\ln r_{TM}$ and $\ln t_{TE}$ (cf. Eqs. (A.3.3), (A.3.4), (A.3.6) and (A.3.8) in Chapter 3). In effect, the second-order complex shifts $F_{TMx}^{(b)}$, $F_{TMy}^{(b)}$, $F_{TEx}^{(b)}$ and $F_{TMy}^{(b)}$, b=t,r, appear in the form of the second order derivatives with respect to x and y of $\ln\eta t_{TM}$, $\ln t_{TE}$, $\ln r_{TM}$ and $\ln t_{TE}$, in addition multiplied by a factor $-ik^{(b)}$. That was explicitly given for the reflected beam in (A.3.6) and (A.3.8) in Chapter 3.

The beam-field representation (A.7.22)-(A.7.25) seems rather accurate, as it has been derived under only a few clearly defined approximations. One of them concerns the beam polarization, two other concern the beam field distribution. The beam polarization is assumed to be uniform in each transverse cross-section of the beam. That corresponds to most experimental data, as the uniform polarization is enforced by polarizator elements usually included into an optical system. Still this assumption can, if necessary, be removed from the presented formalism.

The second assumption concerns evaluation of the transmissions and reflection coefficients. They are evaluated up to the first-order in (A.7.22)-(A.7.25) or even up to the second-order, if the second-order shifts are included in the analysis [5, 9]. The third assumption is inhibited in the choice of only one plane, where this evaluation is applied. Usually the incidence plane is preferred. It is assumed that the incident 3D beam field can be factorised in this plane into two 2D factors. They are defined in the two mutually orthogonal planes - the incidence plane $X-Z$ and the transverse plane $Y-Z$ [5, 9]. Such cases were considered in Chapter 3 and in this

chapter, by considering incidence of the fundamental and higher-order HG beams.

In the general case, however, the incident beam-field distribution $E^{(i)}(X,Y,Z)$ cannot be represented by such a factorised form and should be expanded first into the 2D beam modes $E^{(i)}_{1,j}(X,Z)$ and $E^{(i)}_{2,j}(Y,Z)$, usually in a form of 2D HG beams [5] (cf. (A.3.10) from Chapter 3):

$$\begin{aligned}&\underline{E}^{(i)}(X,Y,Z)\\&=\underline{s}^{(i)}\exp[ik^{(i)}(Z/\cos\theta_0^{(i)})]\sum_j E^{(i)}_{1,j}(X,Z)E^{(i)}_{2,j}(Y,Z)\,.\end{aligned}\tag{A.7.26}$$

Then the transmitted (b=t) and reflected (b=r) beams can be also expressed by the beam mode expansion, shifted this time by the (here) first-order complex shifts (cf. (A.3.11) from Chapter 3):

$$\begin{aligned}E^{(b)}_X(X,Y,Z)=s^{(b)}_X\exp[ik^{(b)}(-L^{(b)}_{TMX}\sin\theta_0^{(i)}+Z/\cos\theta_0^{(i)})]\\\times\sum_j E^{(b)}_{1,j}(X-L^{(b)}_{TMX},Z)E^{(b)}_{2,j}(Y-L^{(b)}_{TMY},Z)\,,\end{aligned}\tag{A.7.27}$$

$$\begin{aligned}E^{(b)}_Y(X,Y,Z)=s^{(b)}_Y\exp[ik^{(b)}(-L^{(t)}_{TEX}\sin\theta_0^{(i)}+Z/\cos\theta_0^{(i)})]\\\times\sum_j E^{(b)}_{1,j}(X-L^{(b)}_{TEX},Z)E^{(b)}_{2,j}(Y-L^{(b)}_{TEY},Z)\,,\end{aligned}\tag{A.7.28}$$

with the polarization vectors $\underline{s}^{(b)}$ determined by predictions of geometrical optics:

$$\begin{bmatrix}s^{(t)}_X\\s^{(t)}_Y\end{bmatrix}=\begin{bmatrix}\eta t_p & 0\\0 & t_s\end{bmatrix}\begin{bmatrix}s^{(i)}_X\\s^{(i)}_Y\end{bmatrix},\tag{A.7.29}$$

$$\begin{bmatrix}s^{(r)}_X\\s^{(r)}_Y\end{bmatrix}=\begin{bmatrix}-r_p & 0\\0 & r_s\end{bmatrix}\begin{bmatrix}s^{(i)}_X\\s^{(i)}_Y\end{bmatrix}.\tag{A.7.30}$$

Certainly, for beams factorised in $X-Z$ and $Y-Z$ planes, the expansion (A.7.27)-(A.7.28) reduces into only one term with $j=1$.

The second-order complex shifts $F^{(b)}_{TMx}$, $F^{(b)}_{TMy}$, $F^{(b)}_{TEx}$ and $F^{(b)}_{TEy}$, b=t,r, can also be directly included in (A.7.27)-(A.7.28), as well as in (A.7.22)-

(A.7.25). For example, for transmitted beams, it can be accomplished by the substitution in (A.7.27), as well as in (A.7.22)-(A.7.23) (cf. (A.7.1)):

$$X = x\cos\theta_0^{(i)} + (z - F_{TMx}^{(t)})\sin\theta_0^{(i)},$$

$$Z = -x\sin\theta_0^{(i)} + (z - F_{TMx}^{(t)})\cos\theta_0^{(i)}, \tag{A.7.31}$$

in the factors $E_{1,j}^{(t)}(X - L_{TMX}^{(t)}, Z)$, and

$$X = x\cos\theta_0^{(i)} + (z - F_{TMy}^{(t)})\sin\theta_0^{(i)},$$

$$Z = -x\sin\theta_0^{(i)} + (z - F_{TMy}^{(t)})\cos\theta_0^{(i)}, \tag{A.7.32}$$

in the factors $E_{2,j}^{(t)}(Y - L_{TMY}^{(t)}, Z)$. Per analogy, similar substitutions can be accomplished in (A.7.28), as well as in (A.7.24)-(A.7.25), with the subscripts TM replaced by TE in (A.7.31)-(A.7.32). The same sequence of substitutions can be also repeated for reflected beams, provided that x and z are replaced by $-x$ and $-z$ in (A.7.31)-(A.7.32) (cf. (A.7.1)).

Note that the first-order and the second-order shifts are expressed by the logarithmic derivatives of the transmission and reflection coefficients and as such, their definitions can be divergent at same points corresponding, for example, to the critical or Brewster angles of incidence. Therefore, in accomplishment of the integration in (A.7.22)-(A.7.25), more refined methods of integration, like those described in Chapter 4 or just direct numerical procedures of integration, should be applied. In this way the method described appears quite accurate up to the lower limit of the paraxial approximation and covers general cases of incident beams of arbitrary polarization and with arbitrary field distribution.

Basic characteristics of the first-order shifts defined by (A.7.16)-(A.7.28) have been discussed in Chapter 3. Contrary to the transverse first-order complex beam shifts, the longitudinal first-order complex beam shifts $L_{TMX}^{(b)}$ and $L_{TEX}^{(b)}$, as well as their real counterparts $\delta_{TMX}^{(b)}$, $\delta_{TM\vartheta_X}^{(b)}$, $\delta_{TEX}^{(b)}$ and $\delta_{TE\vartheta_X}^{(b)}$, do not depend on the state of the incident beam polarization. This means that they do not depend on the polarization parameter $\chi_{(X,Y)}^{(i)}$ in both, TM and TE, components of the beam fields. Their magnitudes are proportional to the

logarithmic derivatives of the Fresnel transmission and reflection coefficients evaluated in the incidence plane at the incidence angles of the beam axes. Usually, magnitudes of the TM shifts are larger than their TE counterparts.

Magnitudes of the transverse shifts are proportional to the difference between Fresnel coefficients of transmission or, equivalently, to the sum of the Fresnel coefficients of reflection. Therefore, they are the strongest at the critical incidence of TIR. Contrary to the longitudinal first-order shifts, the transverse shifts depend on beam polarization. For the circular, right-handed or left-handed, polarization of the incident beam, the transverse shifts $L_{TMY}^{(b)}$ and $L_{TEY}^{(b)}$ are of finite magnitude. Their real counterparts $\delta_{TMY}^{(b)}$, $\delta_{TM\vartheta_Y}^{(b)}$ and $\delta_{TEY}^{(b)}$, $\delta_{TE\vartheta_Y}^{(b)}$ are of different directions for the opposite circular polarization states of the incident beam.

The beam shifts for TM and TE beam components are different, in general. Therefore the beams, as composed of the TM and TE components, are not uniformly shifted. That means that, in addition to the geometrical shifts, the beams are, in general, also deformed. Moreover, for the linear, TM or TE, polarization of the incident beam, the transverse shifts (A.7.16)-(A.7.19) of the reflected and transmitted beams - with the same polarization as that for the incident beam and of a finite field magnitude - disappear altogether. In addition, the transverse shifts of the components of the opposite polarization and with zero amplitude are divergent. This is the consequence of the implicit assumption, translated into the diagonal form of (A.7.8)-(A.7.9), that for the pure TM or TE polarization of the incident beam, the transmitted (reflected) beam possesses the same, pure TM or TE, polariza-tion.

All of that confirms the fact that the transmitted and reflected beams do not exactly follow the polarization and shape of the incident beam. This also indicates that the method of the beam description in terms of the (longitudinal and transverse) beams shifts is approximate. However, the alternative analyti-cal method described in this chapter, in Sections 2-5, does not need any assumption on the polarization state of the transmitted and reflected beams, with respect to the polarization state of the incident beam. In other words, the method is independent of the polarization state of the

incident beam as both polarization components of the beam field are treated simultaneously. Therefore, the method remains exact in the spectral domain.

On the other hand, in the direct domain and for oblique incidence of beams, the method needs in addition only the definitions of the longitudinal beam shifts. Introduction of the approximate definitions of the transverse shifts is necessary in this approach. This opens a new path of further research on the beam interactions with the interface or, more generally, with multilayers, supported by more accurate analytical considerations and more precise theoretical predictions.

*Main content of this chapter has been published in the Physical Review E **74**, 056613; 1-16, 2006.*

References

[1] L. Allen, M. W. Beijersbergen, R. J. C. Spreeuw, and J. P. Woerdman, „Orbital angular momentum of light and the transformation of Laguerre-Gaussian laser modes", Phys. Rev. A **45**, 8185-8189 (1992).

[2] P. Yeh, *Optical Waves in Layered Media* (Wiley, New York, 1976).

[3] M. W. Beijerrsbergen, L. Allen, H. E. L. O. van der Veen and J. P. Woerdman, „Astigmatic laser mode converters and transfer of orbital angular momentum", Opt. Commun. **96**, 123-132 (1993).

[4] L. Allen, J. Courtial and M. J. Padgett, "Matrix formulation for the propagation of light beams with orbital and spin angular momenta", Phys. Rev. E **60**, 7497-7503 (1999).

[5] W. Nasalski, "Three-dimensional beam reflection at dielectric interfaces", Opt. Commun. **197**, 217-233 (2001).

[6] J. Lekner, *Theory of Reflection* (Kluwer, Dordrecht, 1978).

[7] M. S. Soskin and M. V. Vasnetsov, "Singular optics", Progress in Optics **42**, 220-276 (2001).

[8] J. P. Hugonin and R. Petit, "Étude générale des déplacements à la réflexion totale", J. Optics (Paris), **8**, 73-87 (1977).

[9] W. Nasalski, "Longitudinal and transverse effects of nonspecular reflection", J. Opt. Soc. Am. A, **13**, 172-181 (1996).

[10] F. I. Baida, D. Van Labeke, and J.-M. Vigoureux, "Numerical study of the displacement of a three-dimensional Gaussian beam transmitted at total internal reflection. Near field applications", J. Opt. Soc. Am. A **17**, 858-866 (2000).

[11] A. E. Siegman, "Hermite-Gaussian functions of complex argument as optical beam eigenfunctions", J. Opt. Soc. Am. **63**, 1093-1995 (1973).

[12] T. Takenaka, M. Yokota, and O. Fukumitsu, "Propagation of light beams beyond the paraxial approximation", J. Opt. Soc. Am. A **2**, 826-829 (1985).

[13] S. Saghafi and C. J. R. Sheppard, "Near field and far field of elegant Hermite-Gaussian and Laguerre-Gaussian modes", J. Mod. Opt. **45**, 1999-2009 (1998).

[14] L. Allen, M. J. Padgett and M. Babiker, "The orbital angular momentum of light", Progress in Optics **39**, 291-372 (1999).

[15] A. T. O'Neil, I. Mac Vicar, L. Allen, and M. J. Padgett, "Intrinsic and extrinsic nature of the orbital angular momentum of a light beam", Phys.Rev. Lett. **88**, 053601-1-4 (2002).

[16] R. Zambrini and S. M. Barnett, "Quasi-intrinsic angular momentum and the measurement of its spectrum", Phys. Rev. Lett. **96**, 113901-1-4 (2006).

[17] *The Physics of Quantum Informatio*n, edited by D. Bouwmeester, A. Ekert, and A. Zeilinger (Springer, New York, 2000).

[18] J. Leach, M. J. Padgett, S. M. Barnett, S. Franke-Arnold, and J.Courtial, "Measuring the orbital angular momentum of a single photon", Phys. Rev. Lett. **88**, 257901-1-4 (2002).

[19] G. Molina-Terriza, J. P. Torres, and L. Torner, "Management of the angular momentum of light: preparation of photons in multidimensional vector states of angular momentum", Phys. Rev. Lett. **88**, 013601-1-4 (2002).

[20] A. Vaziri, G. Weihs, and A. Zeilinger, "Experimental two-photon, three-dimensional entanglement for quantum communication", Phys. Rev. Lett. **89**, 240401-1-4 (2002).

[21] J. Leach, J. Courtial, K. Skeldon, S. M. Barnett, S. Franke-Arnold, and M. J. Padgett, "Interferometric methods to measure orbital and spin, or the total angular momentum of a single photon", Phys. Rev. Lett. **92**, 013601-1-4 (2004).

[22] M. Padgett, S. M. Barnett, and R. Loudon, "The angular momentum of light inside a dielectric", J. Mod. Opt. **50**,1555-1562 (2003).

[23] R. Loudon, S. M. Barnett, and C. Baxter, "Radiation pressure and momentum transfer in dielectrics: the photon drag effect", Phys. Rev. A **71**,063802-1-11 (2005).

[24] W. Nasalski, "Amplitude-polarization representation of three-dimensional beams at a dielectric interface", J. Opt. A: Pure Appl. Opt. **5**, 128-136 (2003).

[25] W. Nasalski, "Three-dimensional beam scattering at multilayers: formulation of the problem", J. Tech. Phys. **45**, 121-139 (2004).

[26] M. Born and E. Wolf, *Principles of Optic*s, 7th ed. (CambridgeUniversity Press, Cambridge, England, 1999).

[27] M. Lax, W. H. Louisell, and W. B. McKnight, "From Maxwell to paraxial wave optics", Phys. Rev. A **11**, 1365-1370 (1975).

[28] W. Nasalski and Y. Pagani, "Excitation and cancellation of higher-order beam modes at isotropic interfaces", J. Opt. A: Pure Appl. Opt. **8**, 21-29 (2006).

[29] W. Nasalski and Y. Pagani, "Cross-polarization coupling of Laguerre-Gaussian beam modes at isotropic interfaces", Proc. SPIE **6195**, 6195L-1-12 (2006).

[30] J. Enderlein and F. Pampaloni, "Unified operator approach for deriving Hermite-Gaussian and Laguerre-Gaussian laser modes", J. Opt. Soc. Am. A **21**, 1553-1558 (2004).

[31] J. B. Pendry, "Negative refraction makes a perfect lens", Phys. Rev. Lett. **85**, 3966-3969 (2000).

[32] M. Notomi, "Theory of light propagation in strongly modulated photonic crystals: refractionlike behavior in the vicinity of the photonic band gap", Phys. Rev. B **62**, 10696-10705 (2000).

[33] R. W. Ziolkowski and E. Heyman, "Wave propagation in media having negative permittivity and permeability", Phys. Rev. E **64**, 056625-1-15 (2001).

[34] A. E. Siegman, *Lasers* (University Science Books, Mill Valley, CA, 1986).

[35] A. Kostenbauer, Y. Sun, and A. E. Siegman, "Eigenmode expansions using biorthogonal functions: complex-valued Hermite-Gaussians", J. Opt. Soc. Am. A **14**, 1780-1790 (1997).

[36] M. Onoda, S. Murakami, and N. Nagaosa, „Hall effect of light", Phys. Rev. Lett. **93**, 083901-1-4 (2004).

[37] J. Visser and G. Nienhuis, "Orbital angular momentum of general astigmatic modes", Phys. Rev. A **70**, 013809-1-12 (2004).

Subject Index

Q

R

S

T

Author Index

Z